



Brett, Natasha June Maria (2025) *The role of mRNA capping enzyme CMTR1 in hepatocellular carcinoma and the innate immune response*. PhD thesis.

<https://theses.gla.ac.uk/84921/>

Copyright and moral rights for this work are retained by the author

A copy can be downloaded for personal non-commercial research or study, without prior permission or charge

This work cannot be reproduced or quoted extensively from without first obtaining permission from the author

The content must not be changed in any way or sold commercially in any format or medium without the formal permission of the author

When referring to this work, full bibliographic details including the author, title, awarding institution and date of the thesis must be given

Enlighten: Theses

<https://theses.gla.ac.uk/>
research-enlighten@glasgow.ac.uk

**The Role of mRNA capping enzyme CMTR1 in Hepatocellular
Carcinoma and the Innate Immune Response**



**University
of Glasgow**

Natasha June Maria Brett

Supervisor: Professor Victoria Cowling

Submitted in fulfilment of the requirements for the degree of Doctor of Philosophy

School of Cancer Sciences

College of Medical, Veterinary and Life Sciences

University of Glasgow

September 2024

Abstract

mRNA capping is essential for the efficient translation and processing of transcripts generated by RNA polymerase II (RNAPII) in eukaryotes. Cap methyltransferase 1 (CMTR1) is responsible for the generation of the mature Cap-1 structure (m⁷G(5')ppp(5')Nm, by the addition of a methyl group at the 2'-O-ribose position of the first transcribed nucleotide. This modification acts as a means for the innate immune system to differentiate “self” and “non-self” RNA species and appears to regulate the expression of specific genes implicated in proliferation, ribosomal biogenesis and histone synthesis. In murine models of liver cancer, where oncogenes *Cttnb1* and *MYC* were dysregulated, conditional knock out of CMTR1 accelerated tumorigenesis. To enrich understanding of the role of CMTR1 in Hepatocellular carcinoma (HCC), characterisation of CMTR1 and relevant binding partners was undertaken in mouse models and Huh-7 cell lines. Following this, the CMTR1 interactome was analysed in wild type (WT) and *Cttnb1*^{ex3/WT}; R26^{-LSL-Myc} mouse liver to determine if CMTR1 interacting proteins influence the role of this capping enzyme in liver cancer. Of the proteins identified as potential interacting partners of CMTR1, Argininosuccinate synthetase (ASS1) and PGAM family member 5, mitochondrial serine/threonine protein phosphatase (PGAM5) were selected for validation. This has laid initial foundations for further investigation into the biological ramifications of these interactions, particularly in regard to hepatocellular carcinoma.

CMTR1 is phosphorylated at 15 sites within the N-terminus of the protein, which promotes binding between CMTR1 and RNAPII to enhance capping activity. CMTR1 has been previously identified as an interferon stimulated gene (ISG) and promotes expression of fellow ISGs, in part by preventing Interferon induced proteins with tetratricopeptide repeats (IFIT) mediated translational inhibition. To determine the role of CMTR1 phosphorylation in the innate immune response mouse embryonic fibroblasts (MEFs) expressing WT CMTR1 and a phosphodeficient mutant were treated with immunostimulatory agents, followed by analysis of ISG expression. In the absence of CMTR1 phosphorylation expression of various ISGs was attenuated, particularly at earlier stages of the interferon response. Despite this, follow up experiments involving infection of MEF cells with Influenza A virus (IAV) uncovered that CMTR1 phosphorylation promotes IAV infection.

Contents

Chapter 1: Introduction	15
1.1 mRNA capping	17
1.2 Eukaryotic gene expression	20
1.2.1 mRNA Transcription.....	20
1.2.2 Translation initiation.....	23
1.2.3 Splicing	25
1.2.4 Nuclear export.....	25
1.2.5 Polyadenylation.....	26
1.2.6 mRNA turnover	27
1.3 Regulation of mRNA capping	30
1.3.1 Decapping and recapping	30
1.3.2 c-Myc.....	31
1.3.3 DHX15 (DEAH-Box Helicase 15).....	32
1.3.4 Post translational modifications	32
1.3.5 Conclusion.....	33
1.4.1 Roles for the Cap-1 structure/CMTR1 in innate immunity.....	34
1.4.2 CMTR1 in Transcription and Translation of mRNA	35
1.4.3 CMTR1 in development and mRNA processing.	36
1.5 CMTR1 structure	38
1.6 Putative CMTR1 interacting proteins	41
1.6.1 ASS1.....	41
1.6.2 PGAM5.....	42
1.7 Roles of CMTR1 in disease and pathology	46
1.7.1- CMTR1 in cancer	46
1.7.2- CMTR1 in inflammatory diseases and viral infection	47
1.8 Hepatocellular carcinoma	48
1.8.1 Molecular drivers HCC.....	48
1.8.2 Outcome, Prevention, and Treatment.....	50
1.9 Innate immune responses to uncapped RNA	52
1.9.1 RLRs.....	52
1.9.2 RNA sensing and IFN signalling.....	55
1.9.3 ISGs (with specific focus on IFIT proteins, CMTR1 and ISG15).....	58
1.9.4 Viral mechanisms of capping	61
1.10 Aims	66

Chapter 2: Materials and Methods	67
2.1 Cell culture, maintenance, and treatment	68
2.1.1 Cell line culture	68
2.1.2 Cryopreservation and recovery of cell lines	68
2.1.3 DNA vector transduction.....	69
2.1.4 DNA vector transfection	69
2.1.5 Poly (I:C) transfection.....	69
2.1.6 Drug treatments.....	70
2.1.7 MitoSpy staining	70
2.2 Protein analysis	71
2.2.1 Whole cell lysis.....	71
2.2.2 Organ lysis.....	71
2.2.3 Immunoprecipitation (IP)	71
2.2.4 SDS-PAGE western blotting	72
2.2.5 Mass spectrometry and data analysis.....	75
2.2.6 BS3 cross linking.....	76
2.2.7 Immunofluorescence	76
2.3 RNA analysis	78
2.3.1 RNA extraction	78
2.3.2 cDNA synthesis.....	78
2.3.3 qPCR.....	78
2.4 Viral infection and Flow cytometry	80
2.4.1 Infection	80
2.4.2 Flow cytometry	80
2.5 Statistical analysis	81
2.5.1 Statistical analysis	81
2.5.2 Generation of Kaplan-Meier curves	81
Chapter 3: Characterisation of CMTR1 in liver	82
3.1- Introduction	83
3.2- Results	84
3.2.1 Expression of capping enzymes CMTR1 and RNMT increases when β -catenin and c-Myc are dysregulated in the murine liver.....	84
3.2.2 Dysregulation of c-Myc in the liver results in elevated expression and phosphorylation of RNA Pol II.	85
3.2.3 The Interaction between DHX15 and CMTR1 is preserved in WT and <i>Ctnnb1</i> ^{ex3/WT} ; R26 ^{-LSL-Myc} mouse liver	86
3.2.4 Phospho-CMTR1 cannot be detected in murine liver lysate.	90

3.2.5 CMTR1 expression is predominantly nuclear in Huh-7, an HCC derived cell line.	92
3.2.6 CMTR1 antibodies purified from different sheep bleeds bind to CMTR1 equivalently in liver lysate.....	92
3.2.7 Use of BS3 cross-linking agent substantially reduces CMTR1 retrieval from murine Liver	93
3.2.8 DTT does not substantially impact CMTR1 retrieval but does reduce the number of binding partners identified in proteomic analysis.	96
3.3- Discussion	99
3.3.1 Expression of CMTR1 and RNAPII in WT and <i>Ctnnb1</i> ^{ex3/WT} ; R26- ^{LSL-Myc} liver.....	99
3.3.2 CMTR1-DHX15	101
3.3.3 Phosphorylation of CMTR1.....	102
3.3.4 CMTR1 localisation in Huh-7 cell lines	103
3.3.5 Optimisation of CMTR1 IP/MS.....	104
Chapter 4: Identifying novel CMTR1 interacting proteins in the liver.	105
4.1- Introduction	106
4.2- Results	107
4.2.1 Identification of CMTR1 interacting proteins in liver	107
4.2.2 Proteins identified in CMTR1 complexes are enriched for GO terms relating to metabolic biological processes.....	108
4.2.3 Survival is more favourable in HCC patients with high expression of ASS1 and PGAM5, two proteins identified as potential CMTR1 binding partners.	114
4.2.4 Binding partners identified by IP/MS visualised by IP/WB performed on organ and Huh-7 cell extract.	116
4.2.5 PGAM5 and CMTR1 are ubiquitously expressed amongst organs and cell lines, however the extent of PGAM5-CMTR1 interaction varies.....	118
4.2.6 Determining if FCCP treatment in Huh-7 cell lines induces PGAM-5 cleavage. .	119
4.2.7 PGAM5 and CMTR1 both localise to the nucleus in Huh-7 cells, treatment with FCCP does not substantially alter co-localisation	121
4.3- Discussion	127
4.3.1 Characteristics of CMTR1 binding partners and differences from previous interactome studies.....	127
4.3.2 Validating interactors	129
4.3.3 Localisation of CMTR1-PGAM5 interactions.....	130
Chapter 5: Determining the role of CMTR1 phosphorylation in the innate immune response and Influenza A viral infection	133
5.1 Introduction	134
5.2 Results	136
5.2.1 Pharmacological inhibition of CK2, a kinase responsible for CMTR1 phosphorylation results in decreased levels of ISG mRNA transcripts.....	136

5.2.2 Deletion of endogenous CMTR1 complemented by expression of a phosphodeficient CMTR1 mutant results in delayed expression of IFIT3 and ISG15 in MEF cell lines	138
5.2.3 Stimulation of RNA sensing pathways by HWM poly I:C treatment results in delayed ISG expression when CMTR1 cannot be phosphorylated	141
5.2.4 CMTR1 phosphorylation is upregulated during the IFN response	144
5.2.5 P-CMTR1 is a pro-viral factor during IAV infection	146
5.3- Discussion	150
5.3.1 CK2 mediated phosphorylation of CMTR1.....	150
5.3.2 Regulation of ISG expression by CMTR1	151
5.3.3 Potential mechanisms of CMTR1 anti and pro-viral activity	153
Chapter 6: Discussion	156
6.1 Summary	157
6.2 CMTR1 mediated immune responses in Hepatocellular Carcinoma	159
6.3 The potential role of CMTR1 regulated gene expression in Hepatocellular Carcinoma	163
6.4 Biological relevance of models used in this work	165
6.5 Biological implications of putative CMTR1 protein interactions	166
6.6 The role of CMTR1 in viral infection and implications for treatment	169
6.7 Future work	174
6.8 Conclusions	176
Chapter 7: Appendices.....	177
Chapter 8: References	216

List of Figures

Figure 1.1-The Structure of the mRNA cap.	18
Figure 1.2-mRNA capping occurs via interaction between capping enzymes and RNAPII during proximal promoter pausing or early elongation stages.	22
Figure 1.3-The role of the mRNA cap.	29
Figure 1.4-The Domain Structure of Human CMTR1.	40
Figure 1.5-Human domain structures of putative CMTR1 binding proteins, ASS1 and PGAM5.	45
Figure 1.6-Summary of development, aetiology and drivers of Hepatocellular Carcinoma.	50
Figure 1.7-The Immune response to uncapped RNA.	57
Figure 1.8- A proposed role for CMTR1 phosphorylation in the innate immune response.	60
Figure 1.9-Cap snatching and Immune evasion strategies of IAV.	64
Figure 1.10- Capping and Immune evasion strategies of SINV.	65
Figure 3.1-Expression of capping enzymes CMTR1 and RNMT is significantly increased in B/M liver compared to WT controls.	87
Figure 3.2-Expression and phosphorylation of RNAPII is on average high in liver extract where MYC alone is dysregulated.	88
Figure 3.3-The interaction between DHX15 and CMTR1 is preserved in WT and B/M liver.	89
Figure 3.4-Phospho-CMTR1 cannot be detected in murine liver extract.	91
Figure 3.5-CMTR1 expression is predominantly nuclear in Huh-7 cancer cell lines.	94
Figure 3.6-CMTR1 antibodies purified from different sheep bleeds bind to CMTR1 equivalently in liver extract.	95
Figure 3.7-Use of BS3 cross-linking agent appears to substantially reduce antigen retrieval of CMTR1 in murine liver.	97
Figure 3.8-DTT does not appear to substantially impact antigen retrieval but does reduce the number of binding partners identified in proteomic analysis.	98
Figure 4.1-Proteins identified via CMTR1 IP/MS are enriched for GO terms relating to metabolic biological processes.	112
Figure 4.2-Proteins identified as CMTR1 binding partners in both WT and B/M liver lysate are predominantly localised in cytoplasmic, nuclear and mitochondrial compartments.	113
Figure 4.3-Survival probability is more favourable in HCC patients with high expression of ASS1 and PGAM5.	115

Figure 4.4-Binding partners identified via mass spectrometry can be visualised by IP/WB performed on liver extract.	117
Figure 4.5-CMTR1 interacts with PGAM5 but not ASS1 in Huh-7 cells.	118
Figure 4.6-PGAM5 and CMTR1 are ubiquitously expressed amongst organs and cell lines, however the extent of PGAM5-CMTR1 interaction varies.	120
Figure 4.7-Determining if FCCP treatment in Huh-7 cell lines induced PGAM5 cleavage. .	122
Figure 4.8- PGAM5 and CMTR1 Immunostaining in Huh-7 cells.	125
Figure 4.9- Results of Co-localisation assay for CMTR1 and PGAM5 signal in mock and FCCP treated Huh-7 cell lines.	126
Figure 5.1-Pharmacological inhibition of CK2, a kinase responsible for CMTR1 phosphorylation results in decreased levels of mRNA transcripts for various ISGs.	137
Figure 5.2-Generation of MEF cell lines expressing HA-15A-CMTR1, a phosphodeficient mutant of CMTR1.	138
Figure 5.3-Deletion of endogenous CMTR1 complemented by expression of a phosphodeficient CMTR1 mutant results in delayed protein expression of IFIT3 and ISG15 in MEF cell lines.	140
Figure 5.4-Expression of ISG proteins following stimulation with HWM Poly I:C is delayed when CMTR1 cannot be phosphorylated.	143
Figure 5.5-Stimulation of RNA sensing pathways with HMW Poly I:C results in decreased expression of IFIT3 transcripts.	144
Figure 5.6-CMTR1 phosphorylation is upregulated during the IFN response	145
Figure 5.7-The phosphorylation status of CMTR1 impacts IAV infection.....	148

Acknowledgments

Firstly, I would like to thank my supervisor Prof Victoria Cowling for all her support, none of this would be possible without her guidance and I will always be grateful for the time and effort she has invested in me.

I would also like to thank every single member of the Cowling lab past and present, Alison, Kaisa, Rajaei, Shang, Jacquie, Lydia, Dimi, Veronica, Garry, Luke, Radek and Fiona. Special thanks to Lydia for her support and friendship during the good and the bad, her detailed protocols, and wonderful chit-chat. Thanks to Rajaei for his very stimulating discussion on extraterrestrials. Alison for her boundless patience when re-explaining something to me for the 15th time, and Dimi for her wonderful company and for checking over so much of my thesis. Thanks to all of you as a lab for putting up with my awful sense of humour for the past few years. I am truly lucky to have been given the opportunity to work with such a kind, knowledgeable, and nurturing group of people. I will sorely miss every single one of you.

I am grateful to the MRC for funding all the work I have carried out and providing me with the opportunity to continue my research journey. I would like to extend my gratitude to my examiners Dr Leo Carlin and Dr Leonie Unterholzner for taking time from their busy schedules to wade through my thesis.

Finally, I would like to say thank you to all my loved ones outside the lab. Thank you to my family for all the support and joy they have given me and special thanks to my wonderful husband Adam, for always providing me with a shoulder to lean on.

Author's Declaration

I certify that the thesis presented here for examination for a PhD degree of the University of Glasgow is solely my own work other than where I have clearly indicated that it is the work of others (in which case the extent of any work carried out jointly by me and any other person is clearly identified in it) and that the thesis has not been edited by a third party beyond what is permitted by the University's PGR Code of Practice.

I declare that the thesis does not include work forming part of a thesis presented successfully for another degree

I declare that this thesis has been produced in accordance with the University of Glasgow's Code of Good Practice in Research.

Abbreviations

ALDH2	Aldehyde dehydrogenase 2
ALK	Anaplastic lymphoma kinase protein
AMPK	5' AMP-activated protein kinase
ARID1A	AT-rich interactive domain-containing protein 1A
ASS1	Argininosuccinate synthetase 1
ATP	Adenosine triphosphate
BCL-xL	B-cell lymphoma-extra large
BS3	Bis(sulfosuccinimidyl)suberate
CAPAM	mRNA cap adenosine N6-methyltransferase
CAP-MAP	Cap analysis protocol with minimal analyte processing
CARDS	Caspase activation and recruitment domains
CBC	Cap binding complex
CCDC115	Coiled-Coil Domain Containing 115
CCND1	Cyclin D1
CDK	Cyclin dependent kinase
cGAS	Cyclic GMP-AMP synthase
chIP	Chromatin immunoprecipitation
CII	Checkpoint inhibitor immunotherapy
CK2	Casein Kinase II
cKO	Conditional knock-out
CMTR1	Cap methyltransferase 1
CMTR2	Cap methyltransferase 2
Co-IP	Co-Immunoprecipitation
CPSF	Cleavage and polyadenylation specificity factor
CRC	Colorectal cancer
CRISPR	Clustered regularly interspaced short palindromic repeats
CstF	Cleavage stimulation factor
CTD	C-terminal domain
DAN	Deadenylating nuclease
DCP2	Decapping enzyme 2

DDX58	DEAD (Asp-Glu-Ala-Asp) box polypeptide 58
DEN	Diethylnitrosamine
DHX15	DExH-Box helicase 15
DHX58	DExH-Box helicase 58
DMP	Dimethyl pimelimidate
DSIF	DRB sensitivity inducing factor
DSTT	Division of signal transduction therapy, University of Dundee
dsRNA	Double stranded RNA
DTT	Dithiothreitol
eIF	Elongation initiation factor
EML4	Echinoderm microtubule-associated protein-like 4
ESC	Embryonic stem cells
ETS/TCF	E26 transformation specific transcription factor family
FABP1	Fatty acid binding protein 1
FCCP	Carbonylcyanide-p-trifluoromethoxyphenylhydrazone
GAPDH	Glyceraldehyde 3-phosphate dehydrogenase
GO	Gene ontology
GTP	Guanosine Triphosphate
GTF	General transcription factor
HA	Haemagglutinin
HBV	Hepatitis B virus
HCV	Hepatitis C virus
HCC	Hepatocellular carcinoma
HIV	Human immunodeficiency virus
IAP	Inhibitor of apoptosis
IAV	Influenza A virus
IBV	Influenza B virus
IFIT	Interferon induced proteins with tetratricopeptide repeats
IFITM1	Interferon induced transmembrane protein 1
IFN	Interferon
IFNAR	Interferon-alpha/beta receptor subunit
IgG	Immunoglobulin G
IKK	Inhibitor of nuclear factor- κ B kinase

IL6	Interleukin 6
IP	Immunoprecipitation
IP/MS	Immunoprecipitation/Mass spectrometry
IP/WB	Immunoprecipitation/Western blotting
IRES	Internal ribosome entry site
IRF	Interferon regulatory factor
ISG	Interferon stimulated genes
ISGF	Interferon stimulated gene factor
ISRE	Interferon stimulated response elements
IV	Invitrogen
JAK	Janus kinase
KEAP1	Kelch-like ECH associated protein 1
KD	Knock down
LGP2	Laboratory of genetics and physiology 2
MAPK	Mitogen activated protein kinase
MAVS	Mitochondrial antiviral signalling protein
MEF	Mouse embryonic fibroblasts
MDA5	Melanoma differentiation associated protein 5
MHV	Mouse hepatitis virus
MOI	Multiplicity of infection
MX1	Mx dynamin like GTPase 1
NADH	Nicotinamide adenine dinucleotide
NAFLD	Non-alcoholic fatty liver disease
NDUFS2	NADH:ubiquinone oxidoreductase core subunit 2
NEFL	Neurofilament light polypeptide
NEMO	NF- κ B essential modulator
NFE2L2	Nuclear factor erythroid-derived 2-like 2
NF- κ B	Nuclear factor kappa-light-chain-enhancer of activated B cells
NPC	Nuclear pore complex
NSCLC	Non-small cell lung cancer
NSP	Non-structural protein
NVL2	Nuclear VCP-like 2

OB	Oligonucleotide/oligosaccharide binding
OMM	Outer mitochondrial membrane
P53	Tumour protein 53
PARL	Presenilin associated rhomboid like protein
PD-1	Programmed cell death protein 1
PDL1	Programmed cell death ligand 1
PIC	Pre-initiation complex
PGAM5	PGAM family member 5, mitochondrial serine/threonine protein phosphatase
Poly I:C	Polyinosinic:polycytidylic acid
PA	Polymerase acidic protein
PB1/2	Basic polymerase ½
PRD	Proline rich domain
PRMT7	Protein arginine methyltransferase 7
PRR	Pattern recognition receptors
PTM	Post translational modification
QZ	Quinalizarin
RAF-1	RAF proto-oncogene serine/threonine protein kinase
RAM	RNMT activating miniprotein
RB	Retinoblastoma protein
RFM	Rossmann fold motif
RFP	Red fluorescent protein
RIG-I	Retinoic acid inducible gene-1
RLR	RIG-I like receptor
RNGTT	RNA guanylyltransferase
RNMT	RNA guanine-7 methyltransferase
RNP II	RNA polymerase II
RNP III	RNA polymerase III
ROS	Reactive oxygen species
Rpb1	DNA-directed RNA polymerase II subunit RPB1
RT-qPCR	Quantitative reverse transcription polymerase chain reaction
SAH	S-adenosylhomocysteine
SAHH	S-adenosylhomocysteine hydrolase

SAM	S-adenosylmethionine
siRNA	Small interfering RNA
SINV	Sindbis virus
SNP	Single nucleotide polymorphism
ssRNA	Single stranded RNA
STAT	Signal transducer and activator of transcription
TBK1	TANK binding kinase 1
TCGA	The cancer genome atlas
TCGA-LIHC	The cancer genome atlas-liver hepatocellular carcinoma
TERT	Telomerase reverse transcriptase
TLR	Toll like receptor
TMEM199	Transmembrane protein 199
TNF- α	Tumour necrosis factor- α
TOM20	Translocase of outer mitochondrial membrane 20
TOP	Terminal oligopyrimidine tract
TRAF	TNF receptor associated factors
TREX	Transcription and export
TSS	Transcription start site
TYK2	Tyrosine kinase 2
UTR	Untranslated region
vRNA	Viral RNA
VSV	Vesicular stomatitis virus
WDR7	WD repeat-containing protein 7

Chapter 1: Introduction

This thesis focuses on the role and status of Cap methyltransferase 1 (CMTR1) in both the initiation of liver cancer and innate immune responses. Characterisation of CMTR1 within wild type (WT) liver and liver where oncogenes *Ctnnb1* and *MYC* were dysregulated was undertaken. This resulted in the discovery of novel CMTR1 interacting proteins, Argininosuccinate synthetase (ASS1) and PGAM Family Member 5, Mitochondrial Serine/Threonine Protein Phosphatase (PGAM5), as described in chapter 3 and 4. Previous work conducted in the Cowling lab uncovered a cluster of phosphorylation sites within CMTR1 which promote CMTR1-dependent gene expression. The data presented in chapter 5 of this thesis is based on following up these initial findings to uncover the biological relevance of CMTR1 phosphorylation in the induction of interferon stimulated genes (ISG) and Influenza A virus (IAV) infection.

This introduction subsequently covers:

- The process of mRNA capping
- Eukaryotic gene expression and the function of mRNA capping
- Regulation of mRNA capping
- Specific functions and structure of CMTR1
- Description of putative interacting proteins of CMTR1
- Aetiologies, molecular drivers, and treatment of Hepatocellular Carcinoma (HCC)
- The innate immune response to viral RNA
- Viral capping mechanisms
- Overall aims

1.1 mRNA capping

mRNA capping is a co-transcriptional modification that occurs on RNA species transcribed by RNA Polymerase II (RNAPII) (Ramanathan *et al.*, 2016). The process of mRNA capping is mediated by the RNA triphosphatase and guanylyltransferase activity of RNA guanylyltransferase and 5'-phosphatase (RNGTT, also referred to as capping enzyme/CE). RNGTT cleaves the terminal phosphate of the triphosphate bridge adjacent to the first transcribed nucleotide, adding an inverted guanosine monophosphate moiety in its place, by utilising guanosine triphosphate (GTP) as a substrate. This forms the intermediate cap structure (G(5')ppp(5')N), resulting in the release of pyrophosphate (Shatkin, 1976).

RNA guanine-7 methyltransferase (RNMT) in conjugation with an activating subunit RNMT-activating miniprotein (RAM), directs methyltransferase activity towards the N7 position of the inverted cap guanosine, yielding the Cap-0 structure (m7G(5')ppp(5')N, also referred to as m7G) (Gonatopoulos-Pournatzis *et al.*, 2011). Additional modification occurs at the 2'-O-ribose of the first transcribed nucleotide via methylation at this position by Cap methyltransferase 1 (CMTR1), forming the Cap-1 structure (m7G(5')ppp(5')Nm) (Furuichi *et al.*, 1975, Bélanger *et al.*, 2010). These methyltransferase reactions use S-adenosylmethionine (SAM) as a methyl-donor substrate, resulting in the release of S-adenosylhomocysteine (SAH) as a by-product (Sun *et al.*, 2021, Perveen *et al.*, 2024).

2'-O-ribose methylation of the first transcribed nucleotide was previously characterised as a universal feature to all RNA transcribed by RNAPII (Smietanski *et al.*, 2014). However, emerging data has suggested a degree of variation in the extent of this modification amongst cell lines (Culjkovic-Kraljacic *et al.*, 2020, Kruse *et al.*, 2011, Wang *et al.*, 2019).

Methylation of the second transcribed nucleotide at the 2'-O-ribose generates the Cap-2 structure (m7G(5')ppp(5')NmNm) and is enabled by the activity of an additional methyltransferase enzyme, cap methyltransferase 2 (CMTR2) (Werner *et al.*, 2011). The N6 position of the first nucleotide is also subject to methylation, providing this nucleotide is adenosine (Fan *et al.*, 2003). Methylation at this site yields m7G(5')ppp(5')m6Am and is undertaken by cap-specific adenosine methyltransferase (CAPAM, also known as PCIF1) (Fan *et al.*, 2003, Akichicka *et*

al., 2019). The proportion of cap-2 methylation present within the transcriptome differs amongst mammalian cell lines, with only 25% of mouse embryonic stem cell transcripts possessing this modification compared to 56% of MCF-7 cells transcripts (a human breast cancer cell line) (Despic and Jaffrey, 2023). Methylation at the N6 position of the first transcribed adenosine nucleotide is noted to occur in 20-30% of mRNA transcripts within HeLa cells (Wei *et al.*, 1975) (Figure 1.1)

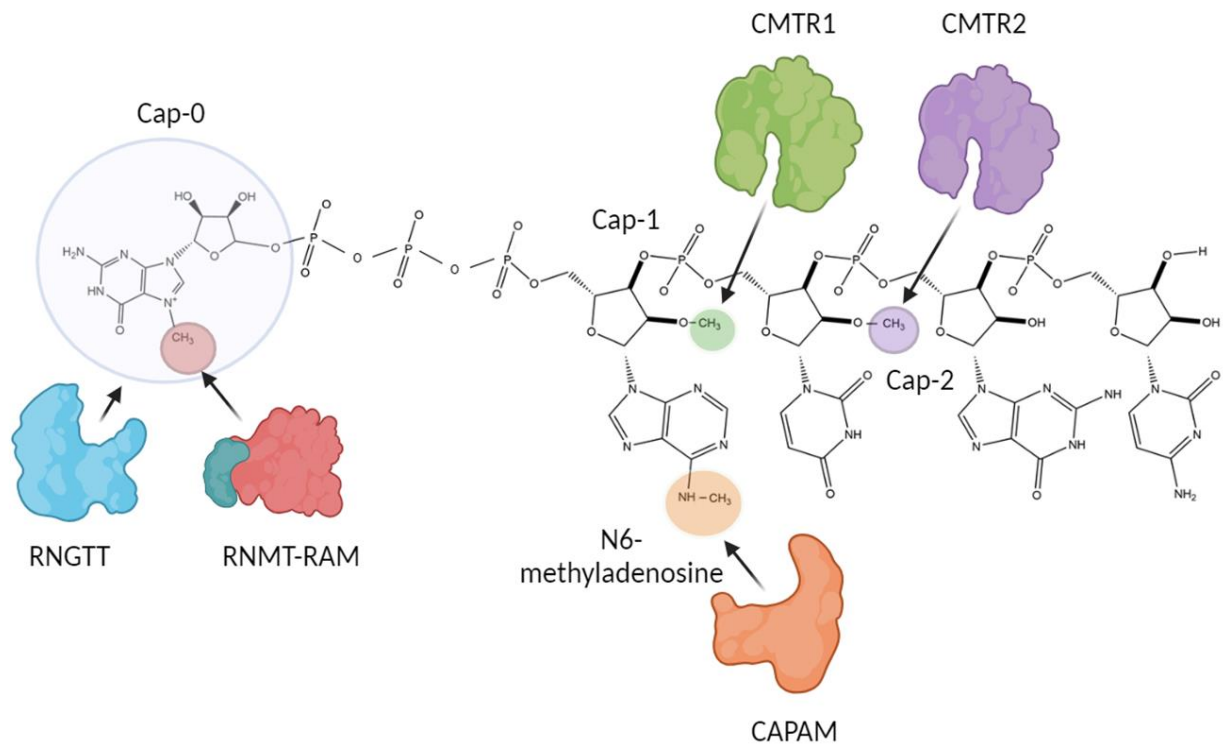


Figure 1.1-The Structure of the mRNA cap.

Addition of the N7-methylguanosine (Cap-0) structure is mediated by the triphosphatase and guanylyltransferase activity of RNGTT, which forms an intermediary cap structure (G(5')ppp(5')N). The mature Cap-0 structure (m7G(5')ppp(5')N) is formed by the addition of a methyl group to the N7 position of guanosine via methyltransferase RNMT. Cap-1 (m7G(5')ppp(5')Nm) and Cap-2 structures (m7G(5')ppp(5')NmNm) are produced on the 2'-O-ribose of the first and second transcribed nucleotide by the activity of methyl transferase enzymes CMTR1 and CMTR2, respectively. Methylation of adenosine on the N-6 position (providing adenosine is the first transcribed nucleotide) to form m7G(5')ppp(5')m6Am, is achieved by the activity of an additional methyltransferase, CAPAM. Figure made in BioRender. RNGTT (RNA Guanylyltransferase and 5'-Phosphatase), RNMT (RNA Guanine-7 Methyltransferase) CMTR1 (Cap Methyltransferase 1), CMTR2 (Cap Methyltransferase 2), CAPAM (Cap-specific Adenosine Methyltransferase).

Capping enzymes exert their activity via recruitment to the 5' end of nascent mRNA, concurrent with transcription. In the case of RNGTT, CMTR1 and CAPAM (McCracken *et al.*, 1997, Inesta-Vaquera *et al.*, 2018, Fan *et al.*, 2003) this is enabled by interaction with the C-terminal domain (CTD) of RNAPII. This interaction is further enhanced when RNAPII is phosphorylated on serine 5 (S5P) at YSPTSPS heptad repeats by cyclin-dependent kinase 7 (CDK7) (Ho *et al.*, 1998). The sequence of events necessary to generate mature cap structures is yet to be fully elucidated. However, as m7G methylation requires the presence of an inverted guanosine monophosphate within its RNA target (Shuman *et al.*, 1995), it is logical to assume RNMT exerts methyltransferase activity after RNGTT. Furthermore, it has been demonstrated that the presence of m7G is dispensable for human CMTR1 enzymatic activity *in-vitro*, suggesting that 2'-O-ribose methylation of the first nucleotide may occur prior to methylation by RNMT (Bélanger *et al.*, 2010, Werner *et al.*, 2011). CMTR2 can recognise both Cap-0 and Cap-1 structures, with a slight preference for binding to the latter. This suggests methylation of nucleotides may occur sequentially (Werner *et al.*, 2011). Addition of m6Am on mRNA via CAPAM enzymatic activity *in-vitro* requires recognition of the m7G cap structure, with CAPAM displaying further preference for binding to mRNA which already possess a Cap-1 structure (Akichika *et al.*, 2019). This permits for the conclusion to be drawn that CAPAM mediated methylation likely occurs subsequent to the activity of RNMT and CMTR1.

1.2 Eukaryotic gene expression

1.2.1 mRNA Transcription

mRNA transcription refers to the initial stage of protein coding gene expression, by which DNA is transcribed into mRNA via RNAPII. This process is initiated at a defined transcription start site (TSS), within the 5' end of the gene. Present within the TSS is the promoter sequence, which encompasses a short base pair sequence and serves as a locale for the binding of transcriptional machinery (Haberle and Stark, 2018).

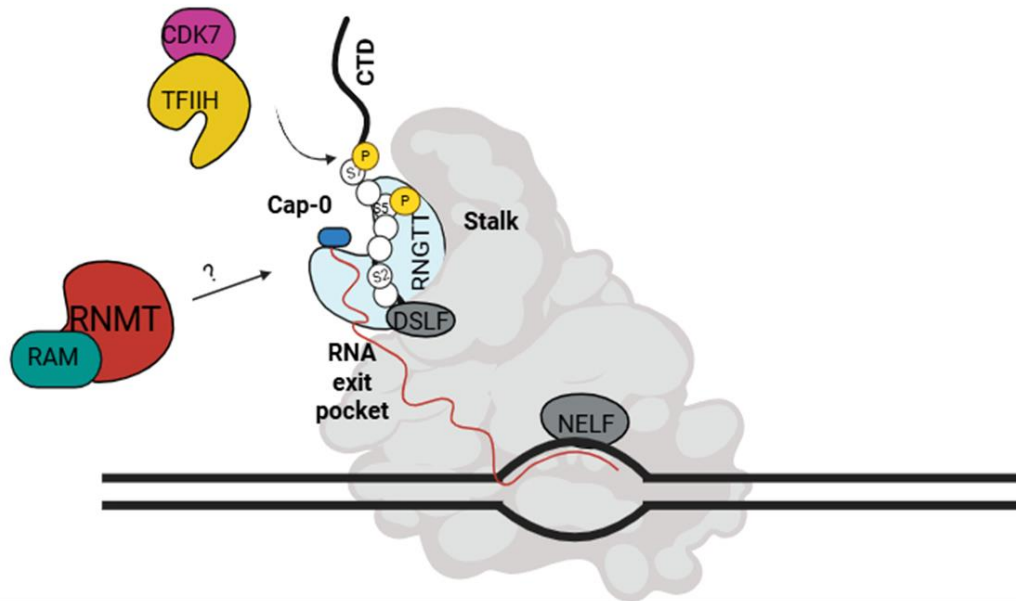
Transcription begins with the formation of the pre-initiation complex (PIC) at the promoter, mediated by a variety of general transcription factors (GTF) including, Transcription factor IIA (TFIIA), TFIIB, TFIID, TFIIIE, TFIIIF, and TFIIH. Initially, TFIID recognises the TATA box or other core elements within promoter sequences, permitting for subsequent association with TFIIA and TFIIB (Kim *et al.*, 1993). The resultant TFIID-TFIIA-TFIIB complex recruits TFIIIF in conjugation with RNAPII, alongside TFIIIE (Imbalzano *et al.*, 1994, Hampsey *et al.*, 1998). TFIIH exerts helicase activity in the presence of adenosine triphosphate (ATP) to unwind DNA adjacent to the TSS (Schaeffer *et al.*, 1993), opening this site for subsequent transcriptional activity. To then proceed downstream of the gene for transcription elongation, RNAPII must disassociate from GTFs in a process termed “promoter escape.” Promoter escape requires phosphorylation of the C-terminal domain (CTD) of RNAPII at serine 5 and 7 via TFIIH in association with Cyclin-dependent kinase 7 (CDK7) (Spangler *et al.*, 2001). RNAPII then proceeds to synthesise a small section of mRNA 30-50 base pairs in length, prior to transcriptional pausing. RNAPII pausing is mediated by DRB sensitivity-inducing factor (DSIF) and negative elongation factor (NELF) (Yamaguchi *et al.*, 1999). RNAPII pausing provides an opportunity for early-stage mRNA processing, including capping, whilst sustaining accessibility of upstream promoter elements to transcription factors (Shopland *et al.*, 1995, Moteki and Price, 2002).

RNGTT, CMTR1 and CAPAM all bind directly to the CTD of RNAPII, with enhanced specificity for the CTD when the latter is phosphorylated at S5P (Ho and Shuman, 1999, Inesta-Vaquera *et al.*, 2018, Hirose *et al.*, 2008). Phosphorylation of the S5P site within the CTD of RNAPII occurs during the early stages of transcription to

enable transcription initiation and promoter escape, coupling mRNA capping to the transcriptional process. The checkpoint model of mRNA capping states that recruitment of capping enzymes to RNAPII occurs during transcriptional pausing (Rasmussen and Lis, 1993, Mandal *et al.*, 2004). Despite this, other structural and biochemical studies have indicated that mRNA capping may occur during early elongation stages, during active transcription (Kim *et al.*, 2004, Garg *et al.*, 2023).

Localisation of RNGTT to the CTD of RNAPII is enabled via interaction with multiple S5P RNAPII CTD heptads, which stimulates activity of the guanylyltransferase domain (GTase) via an allosteric mechanism (Bage *et al.*, 2021) This interaction permits RNGTT to dock to the RNAPII stalk and position its triphosphatase domain adjacent to the RNA exit pocket. Upon completion of the triphosphatase reaction catalysis of guanylyltransferase activity takes place, as the pre-mRNA substrate reaches a length of at least 22 nucleotides and encounters the active site of the GTase domain (Garg *et al.*, 2023). This process is potentially aided via displacement of the triphosphatase domain by the GTase domain in a manner which likely involves DSIF (Garg *et al.*, 2023). CMTR1 and CAPAM interact with the CTD of RNAPII via their WW domains, which recognises the phosphorylated serine/threonine-proline in RNAPII heptapeptide repeats (Gavva *et al.*, 1997). G-patch domains, such as the one identified in CMTR1 typically function as an RNA binding motif, leading to the proposal that the WW and G-patch regions may function in tandem to bridge CMTR1 to RNAPII and nascent mRNA (Haline-Vaz *et al.*, 2008). This would then leave the methyltransferase domains accessible to conduct subsequent capping activity (Haline-Vaz *et al.*, 2008). As is the case with RNGTT, CMTR1 docks to the stalk of RNAPII and exiting pre-mRNA, displacing RNGTT in the process (Garg *et al.*, 2023). As the pre-mRNA substrate reaches a length of at least 29 nucleotides, methylation of the first transcribed nucleotide by CMTR1 takes place (Garg *et al.*, 2023). Interaction between RNMT and RNAPII has not been directly demonstrated and hence the mechanism by which RNMT is recruited to promoter elements for capping remains unknown. It is postulated this may be due to the transiency of binding between RNAPII and RNMT or facilitated by interaction between RNMT and RNA (Aregger and Cowling, 2013) (Figure 1.2).

Cap 0 formation



Cap 1 formation

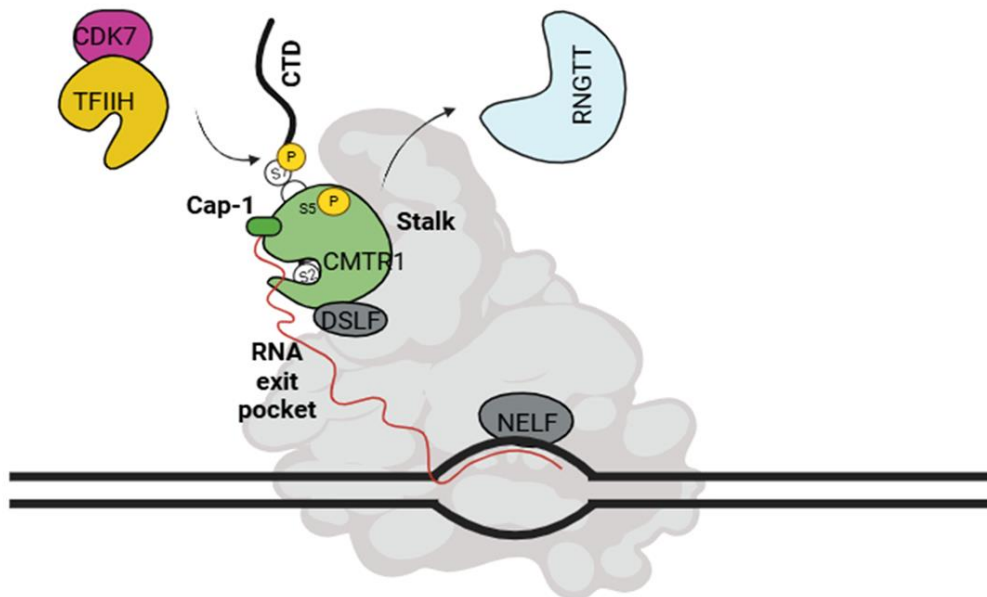


Figure 1.2-mRNA capping occurs via interaction between capping enzymes and RNAPII during proximal promoter pausing or early elongation stages.

Promoter escape requires phosphorylation of the CTD at serine 5 and 7 by CDK7 in association with TFIIF. After an initial round of transcription, transcriptional pausing is induced via the activity of DSIF and NELF. Upon or just after transcriptional pausing, RINGTT binds to multiple S5P sites within RNAPII CTD heptads, permitting RINGTT to dock at the stalk structure of RNAPII adjacent to the RNA

exit pocket. RNGTT initially exerts triphosphatase activity towards the nascent pre-mRNA as it escapes from the RNA exit pocket. Pre-mRNA then encounters the GTase domain of RNGTT to form the immature Cap-0 structure. RNMT in conjugation with activating subunit RAM catalyses formation of the mature Cap-0 structure through an unknown mechanism, as direct interaction between RNAPII and RNMT-RAM has not been demonstrated. CMTR1 binds to 5'P sites via its WW domain and docks to the RNAPII stalk structure in a similar manner to RNGTT. This is followed by displacement of RNGTT by CMTR1 in a manner which likely involves cooperation with the SPT5 subunit of DSIF. Methylation of the first transcribed nucleotide takes place via the activity of CMTR1 to form the Cap-1 structure. Figure made in BioRender. CTD (C-terminal domain), CDK7 (Cyclin dependent kinase 7), TFIIH (Transcription factor II H), DSIF (DRB sensitivity-inducing factor), NELF (negative elongation factor), RNGTT (RNA Guanylyltransferase and 5'-Phosphatase), RNAPII (RNA Polymerase II), GTase (Guanylyltransferase), RNMT (RNA Guanine-7 Methyltransferase), RAM (RNMT Activating Mini-protein), CMTR1 (Cap Methyltransferase 1), SPT5 (Transcription elongation factor SPT5)

For pause-release to occur and meaningful continuation of the elongation process, cyclin dependent kinase 9 (CDK9) a subunit of positive transcription elongation factor B (P-TEFB), phosphorylates DSIF and NEFL alongside RNAPII at the serine 2 position of the CTD (S2P). These modifications promote dissociation of NEFL alongside DSIF, permitting for the continuation of the transcriptional process (Cheng and Price, 2007, Marshall *et al.*, 1996). Initial transcription of the subsequent kilobase tends to be inefficient until optimum phosphorylation of RNAPII at S2P, which additionally functions as a marker of termination (Buratowski 2009). As transcription and 3' end mRNA processing are also coupled, cleavage and polyadenylation of transcripts at the 3' end occurs concurrently during pausing and elongation (Ahn *et al.*, 2004). Polyadenylation permits recruitment of both human cleavage and polyadenylation specificity factor (CPSF) and cleavage stimulatory factor (CstF) to the elongation complex and CTD, respectively. CPSF and CstF work in tandem to stall RNAPII and cleave nascent transcripts at the Poly A site, permitting for release of RNAPII from the DNA template (Schul *et al.*, 1996, Hirose and Manley 1998).

1.2.2 Translation initiation

The presence of the m7G cap (Cap-0) in mRNA structures is indispensable for canonical cap-dependent translation of mRNA to protein in eukaryotic cells (Muthukrishnan *et al.*, 1975). Translation initiation is facilitated by formation of two complexes in parallel, the 43S pre-initiation complex (43S) and the 48S pre-

initiation complex (48S). The 43S complex consists of proteins eukaryotic translation initiation factor 1 (eIF1), eIF1A, eIF3, and eIF5, alongside a tertiary complex composed of eIF2 bound to GTP and methionine initiator transfer RNA (tRNA) (Merrick and Pavitt, 2018). In conjunction with formation of the 43S complex, interaction between the 5' cap structure and cap binding protein eIF4E occurs; the latter of which is one component of the larger eIF4F complex, comprised of RNA helicase eIF4A and scaffold protein eIF4G (Kumar *et al.*, 2016). Upon binding of the eIF4F complex to the 5' cap, recruitment of the 43S complex occurs to generate the complete 48S complex. Once formed, the 48S complex then scans the 5' untranslated region (UTR) of the transcript until it encounters the start codon for methionine, which is enabled by unwinding of secondary RNA structures via the ATPase helicase activity of eIF4A (Brito Querido *et al.*, 2024). Upon recognition of the start codon, the majority of eIF components dissociate from the complex, this enables interaction between the complex and the 60s large ribosomal subunit via eIF5b catalytic activity. This step marks the end of translation initiation and the beginning of the elongation phase of protein synthesis (Brito Querido *et al.*, 2024, Hinnebusch and Lorsch, 2012).

In the context of translation initiation, the m7G cap functions as a binding site to bridge interactions between mRNA and initiation factors (Tahara *et al.*, 1981), enabling downstream recognition of codons by tRNAs. The importance of the m7G cap in enabling translation has been well established, with experiments conducted in the 1970s initially reporting abrogation of translation upon removal of the Cap structure within mRNA transcripts (Muthukrishnan *et al.*, 1975). Work conducted subsequently reported significant increases in translational efficiency upon m7G capping in *Xenopus* oocytes (Drummond *et al.*, 1985, Gillian-Daniel *et al.*, 1998). Since then, it has been established that cKO of RNMT and reductions in Cap-0 formation negatively impacts T-cell activation, with these cells failing to express terminal polypyrimidine tract (TOP) mRNAs, which are required to promote ribosome biogenesis and facilitate metabolic reprogramming (Galloway *et al.*, 2021). Furthermore, depletion of the RNMT activating subunit RAM in mammalian systems resulted in poorer incorporation of labelled amino acids into proteins and loss of actively translating polysomes (Gonatopoulos-Pournatzis *et al.*, 2011).

1.2.3 Splicing

The nuclear cap binding complex (CBC), composed of nuclear cap binding protein subunit 1 and 2 (CBP80 and CBP20 respectively) , enables assembly of mRNA and small nuclear riboproteins (snRNPs) for formation of the spliceosome complex (Izaurralde *et al.*, 1994, Wilkinson *et al.*, 2020). Splicing is a crucial step within mRNA processing which involves the excision of introns and ligation of exons for complete maturation of mRNA. The splicing process introduces diversity within the transcriptome by producing alternative transcripts. This is achieved via intron retention, exon splicing and the utilisation of alternate splice sites, the result of which is the generation of varied proteins for differential function (Wang *et al.*, 2015).

Spliceosome assembly to pre-mRNA involves recognition of intronic 5' and 3' splice sites by U1 and U2 snRNPs, followed by recruitment of U4, U5 and U6 snRNPs. Subsequent to this, displacement of U1 occurs in a manner which forms an intronic "lariat" and permits ligation of 5' and 3' exons via nucleophilic attack (Wilkinson *et al.*, 2020, Wang *et al.*, 2015). U1, U2, U4, U5 and U6 snRNP proteins have been found to co-purify with the CBC on mRNA. Upon depletion of the CBC, association of snRNPs with intronic sites is negatively impacted without alteration of total snRNP levels (Pabis *et al.*, 2013). The biological impact of this is inhibition of cellular proliferation, a phenomenon attributed to the resultant defects in splicing (Narita *et al.*, 2007, Pabis *et al.*, 2013).

1.2.4 Nuclear export

Nuclear export of mRNA into the cytoplasm regulates translation by impacting the availability of mRNA for ribosome binding. The CBC, via synergistic binding of two component subunits (CBP80 and CBP20), recognises the m7G cap of nascent mRNA (Izaurralde *et al.*, 1994, Nojima *et al.*, 2007) permitting CBP80 to act as a platform for assembly of the transcription export (TREX) complex. The TREX complex consists of UAP56, Aly/Ref proteins and a multimeric THO complex (Cheng *et al.*, 2006). Assembly of the TREX complex results in the processing of mRNA into export competent messenger ribonucleoprotein (mRNP), mRNP is then targeted to the nuclear pore complex (NPC) via the export receptor, permitting for movement through the NPC (Xie and Ren, 2019, Köhler and Hurt, 2007). Once mRNP has

entered the cytoplasm, binding of various protein factors occurs to promote dissociation and remodelling (Tran *et al.*, 2007, Lund and Guthrie, 2005). One key component of mRNP remodelling at this stage is the replacement of the CBC with eIF4E to promote ribosome binding and subsequent translation (Daneshmandi, 2001).

Whilst being predominantly associated with promotion of translation initiation, eIF4E, a cap binding factor, has been demonstrated to increase export of specific transcripts. Most notably those of capping enzymes *RNMT*, *RNGTT*, and *RAM* when eIF4E is localised to the nucleus (Culjkovic-Kraljacic *et al.*, 2020). Overexpression of eIF4E increased nuclear export of *RNMT*, *RNGTT*, *RAM* alongside oncogenes *MYC* and *CCND1* by a factor of 2-fold, subsequently leading to enhancements in *RNMT* and *RNGTT* translation (Culjkovic-Kraljacic *et al.*, 2020). This involves a pathway of export distinct from the bulk pathway described above, with specificity of eIF4E for export of m7G capped transcripts being dependent on the presence of eIF4E sensitivity elements within the RNA structure (Culjkovic *et al.*, 2005).

Inhibition of interactions between cap binding proteins and the m7G cap have been shown to interfere with nuclear export and splicing in eukaryotic systems. Pre-injection of anti-CBP20 antibodies in xenopus oocytes followed by microinjection of U snRNA both impacted splicing and prevented export of select U snRNAs from the nucleus (Izaurralde *et al.*, 1995). Whilst heterozygous KO of cap-binding protein eIF4E in U2OS cell lines negatively impacts protein expression of targets for nuclear export (Culjkovic-Kraljacic *et al.*, 2020).

1.2.5 Polyadenylation

The poly(A) tail adjacent to the 3' UTR of mRNA, contributes to nuclear export, stability, and translation. Hence, deadenylated transcripts are prone to repression to limit expression of their respective genes (Brawerman, 1981, Saguez *et al.*, 2008). A role has been highlighted for the 5' cap in mediating both adenylation and deadenylation of transcripts. The presence of the cap structure promotes efficient cleavage and polyadenylation at downstream 3'UTR sites (Hart *et al.*, 1985), with this being mediated via physical interaction between the CBC and polyadenylation factors at the extreme ends of the transcript (Flaherty *et al.*, 1997). Conversely, binding between the cap structure and deadenylating nuclease (DAN) has been noted to occur to promote shortening of the poly(A) tail, with decreases in binding

between DAN and the cap via eIF4E, or elements in the 5'UTR inhibiting the deadenylation processes (Gao *et al.*, 2000).

1.2.6 mRNA turnover

A crucial component of gene expression regulation involves turnover of RNA transcripts, which is enabled by mRNA decay pathways (Adijibade and Mazroui, 2014). In general, degradation of mRNA in eukaryotes begins with deadenylation and subsequent shortening of the 3' poly(A tail) (Chen and Shyu, 2011). The main cytoplasmic deadenylase complexes which enables this to occur consist of the Pan2-Pan3 complex and the Ccr4-Not complex (Uchida *et al.*, 2004, Lau *et al.*, 2009). Following deadenylation, mRNA may be degraded in the 3' to 5' direction within exosomes; alternatively, deadenylated transcripts can be subjected to decapping (elaborated on in section 1.3.1), permitting for degradation to occur in the 5' to 3' direction via the activity of Xrn1 alongside other exonucleases (Chen and Shyu, 2011, Adijibade and Mazroui, 2014). Preference for the direction of degradation is determined by motifs within the transcript sequence, alongside the profile of RNA-binding proteins interacting with the sequence being targeted for degradation (Stoecklin *et al.*, 2006, Grochowski *et al.*, 2024, Adijibade and Mazroui, 2014).

Nonsense mediated decay (NMD) allows for the degradation of mRNA containing premature stop codons (PTC), preventing translation of truncated proteins. PTC are detected during by ribosomes during the scanning process at the start of translation, as the presence of PTC leads to ribosome stalling and a failure to remove downstream exon-exon junction complexes (EJC) (Le Hir *et al.*, 2001, Nickless *et al.*, 2017). Following this event, up-frameshift protein 1 (UPF1) associates with the EJC via UPF2 and UPF3 to trigger NMD. Subsequent mRNA decay requires phosphorylation of UPF1 at ST/Q motifs within the C-terminus by Serine/threonine protein kinase (SMG1) (Kashima *et al.*, 2006), enabling phosphospecific interactions with fellow nonsense mediated decay factors SMG5, SMG6 and SMG7 (Okada-Katsuhata *et al.*, 2012). SMG5 and SMG7 aid in the degradation process by promoting the recruitment of decapping and deadenylation proteins including mRNA decapping enzyme 2 (DCP2) and Poly(A) ribonuclease (POP2), generating unprotected RNA ends which are accessible to exonucleases (Loh *et al.*, 2013, Cho *et al.*, 2013). SMG6 meanwhile contributes to mRNA decay

by displaying endonuclease activity, resulting in cleavage of mRNA transcripts internally, adjacent to the PTC (Eberle *et al.*, 2009, Huntzinger *et al.*, 2008). Despite, the process of decapping itself being crucial for end stage mRNA degradation within the NMD pathway, the cap itself may contribute indirectly to NMD via recruitment of CBP80. CBP80 interacts with UPF1 as demonstrated via Co-IP, with disruption of this interaction significantly enhancing expression of LacZ mRNA containing PTC. Mechanistically, this observation can be attributed in part to the role of CBP80 in ensuring interaction of SMG1 and UPF1 to the EJC, alongside its role in PTC recognition during initiation of NMD (Hwang *et al.*, 2011).

Processing-bodies (P bodies) are discrete cytoplasmic granules comprised of mRNA alongside proteins enriched for molecular functions relating to 5' to 3' mRNA decay and translational repression (Luo *et al.*, 2018). P bodies are primarily believed to act as a site of mRNA decay, although others postulate that they may also function as a storage site for repressed transcripts and inactive decay enzymes (Hubstenberger *et al.*, 2017, Standart and Weil, 2018). One piece of evidence which implicates a role for P bodies in RNA degradation comes from the observation that depletion of exonuclease XRN1 results in an increase in the number of P-body foci, suggesting accumulation of decay intermediates at this site (Teixiera *et al.*, 2005, Cougot *et al.*, 2004, Sheth and Parker 2003). Additionally, various exonucleases, decapping enzymes and factors, alongside components of the NMD pathway (e.g. UPF proteins and SMG7) are found to localise within P-body granules (Ingelfinger *et al.*, 2002, Sheth and Parker 2003, Van Dijk *et al.*, 2002, Unterholzner and Izaurralde, 2004).

Overall, efficient degradation of mRNA (at least in the 5' to 3' direction) is dependent on the removal of the 5' cap structure, as this permit accessibility to exonucleases (Adijibade and Mazroui, 2014). Conversely, binding of CBP80 to the 5' cap of mRNA transcripts appears to play a role in ensuring NMD, by facilitating interaction between NMD factors and the EJC downstream of the PTC (Hwang *et al.*, 2011). These observations thus indicate a role for mRNA capping in conferring both mRNA stability and ensuring decay (albeit indirectly in the case of the latter), which further ensures appropriate regulation of gene expression.

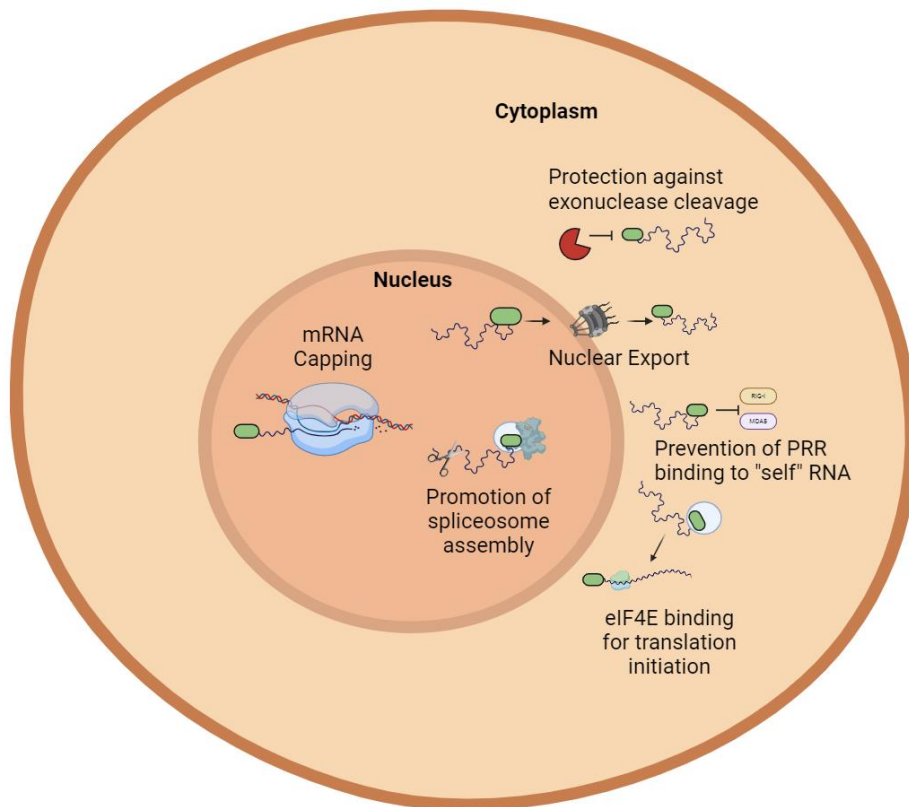


Figure 1.3-The role of the mRNA cap.

The presence of N7-methylguanosine structure allows for interaction between mRNA and interacting proteins such as the CBC and eIF4E, this being crucial for canonical cap-dependent translation of most cellular mRNAs. Beyond this, binding between the cap and CBC within the nucleus allows for the initiation of splicing via interaction with snRNPs, culminating in the formation of the mature spliceosome. Nuclear export of mRNAs is permitted by interaction of the CBC to the cap alongside various nuclear export factors. The presence of an mRNA cap offers protection against exonuclease cleavage and degradation, owing to the specificity of exonucleases towards unmethylated mRNA species. The Cap-1 structure meanwhile, has been primarily recognised for its role in allowing the innate immune system to differentiate between host and foreign mRNA species. This is achieved by preventing binding between host transcripts and pattern recognition receptors (PRR), such as MDA5 and RIG-I. Figure made in BioRender. CBC (Cap binding complex), eIF4E (eukaryotic translation initiation factor 4E), snRNPs (small nuclear riboproteins), MDA5 (Melanoma differentiation associated protein 5), RIG-I (Retinoic acid inducible gene-1).

1.3 Regulation of mRNA capping

Given that gene expression is a highly regulated process to permit for adaption in response to stimuli and stressors, it stands to reason that capping too is subject to external regulation. Process such as decapping, expression of external capping enzyme interactors, the presence of inhibitory by-products, and post translational modifications (PTM) have all been demonstrated to regulate capping activity.

These are elaborated on below.

1.3.1 Decapping and recapping

Once capped, mRNA transcripts are subject to decapping as a quality control and regulatory mechanism, marking transcripts for degradation via exonuclease cleavage at the end of their lifecycle (Muhlrad *et al.*, 1994, Badis *et al.*, 2004). The decapping process removes the m7G moiety to generate transcripts with 5' monophosphate ends, which permits the necessary conformational changes to occur for binding within the active site of cytoplasmic exonucleases (Jinek *et al.*, 2011). A substantial number of decapping reactions within the cell are catalysed by mRNA decapping enzyme 2 (DCP2) (Wurm and Sprangers, 2019). To prevent global deficits in transcript capping, DCP2 displays low basal activity and is dependent on accessory factors to stimulate hydrolytic catalytic activity (Piccirillo *et al.*, 2003, Beelman *et al.*, 1996, He and Jacobson, 2015, Tharun *et al.*, 2000). The most important of these accessory factors, is the cofactor DCP1, which generates the decapping holoenzyme when in complex with DCP2 (Beelman *et al.*, 1996). The mechanism by which DCP2 recognises and cleaves m7G structures is yet to be elucidated. However, it is known that DCP2 is capable of targeting transcripts for decapping regardless of 2'-O-ribose methylation status. The presence of methylation at the m6A site however, via the enzymatic activity of CAPAM, negatively regulates decapping by DCP2 and promotes mRNA stability (Mauer *et al.*, 2017). The enzyme decapping exoribonuclease (DXO) possesses pyrophosphohydrolase, decapping and exoribonuclease activity, with specificity for improperly capped mRNA, as it is unable to bind transcripts methylated at the 2'-O-ribose position of the first nucleotide. This suggests a putative role for the Cap-1 structure as a marker of transcript quality and may aid in the expression of specific genes (Picard-Jean *et al.*, 2018).

Recapping refers to the process of re-adding cap structures to transcripts localised in the cytoplasm, particularly upon decapping or internal endonuclease cleavage (Mercer *et al.*, 2010, Grudzien-Nogalska and Kiledjian 2017). This process is enabled by the presence of capping enzymes RNMT, RAM and RNGTT in the cytoplasm (Mukherjee *et al.*, 2012). As previously mentioned, the decapping process when mediated by DCP2, generates 5' monophosphate ends on transcripts, which are incompatible for catalysis of guanylyltransferase reactions by RNGTT (Jinek *et al.*, 2011). A yet unidentified kinase has been found to exist in complex with RNGTT within the cytoplasm and enables conversion of 5' monophosphate to 5' diphosphate. This provides RNGTT with a suitable substrate for recapping (Otsuka *et al.*, 2009). This data demonstrates molecular distinction between nuclear capping and cytoplasmic recapping, representing additional regulatory layers for modulation of gene expression via this mechanism.

1.3.2 c-Myc

c-Myc is a potent regulator of gene expression within cell lines, contributing to its status as a proto-oncogene (Menssen and Hermeking, 2002). In addition to directly promoting gene expression as a transcription factor, c-Myc positively regulates formation of the m7G cap. Positive regulation of capping by c-Myc occurs by facilitating increases in RNAPII phosphorylation alongside conversion of SAH, an inhibitory byproduct of methyltransferase reactions. Myc stimulates RNAPII phosphorylation by increased recruitment of TFIIH to the TSS, leading to enhancements in cap formation (Cowling and Cole, 2007, Posternak *et al.*, 2017). Most methyltransferase reactions utilise SAM as a methyl donor and produce SAH as a by-product, SAH consequently competes against SAM for binding in the active site of methyltransferases as part of a negative feedback loop (Cantoni and Chiang, 1980, Fukumoto *et al.*, 2022). This negative feedback loop can be interrupted by the activity of S-adenosyl homocysteine hydrolase (SAHH), which converts inhibitory SAH to homocysteine and adenosine. SAHH is a target gene of c-Myc and can be transcriptionally upregulated via binding of c-Myc at its gene promoter (Fernandez-Sanchez *et al.*, 2009), further augmenting the pro-capping function of c-Myc alongside increases in RNAPII phosphorylation.

It has been demonstrated that whilst overexpression of c-Myc results in modest increases in m7G capping across the transcriptome, a more substantial enrichment of cap formation occurs within c-Myc target genes (Cole and Cowling, 2009). Increased capping of Wnt signalling pathway genes has also been observed upon c-Myc overexpression. This can be attributed to c-Myc dependent recruitment of RNMT to Wnt component gene promoters, alongside induction of CDK7 kinase activity (Posternak *et al.*, 2017).

1.3.3 DHX15 (DEAH-Box Helicase 15)

DHX15, is a DEAH (Asp-Glu-Ala-His) box RNA helicase primarily characterised by its role in unwinding complex RNA structures to facilitate splicing and maturation of mRNA (Semlow *et al.*, 2016). Beyond functions in general RNA processing, a role for DHX15 has been highlighted in the activation of NF- κ B and mitogen activated protein kinase (MAPK) pathways in response to RNA virus infection, via binding to mitochondrial anti-viral signalling protein (MAVS) (Mosallanejad *et al.*, 2014). CMTR1 has been demonstrated to directly interact with DHX15, with this occurring specifically between the G-patch of CMTR1 and the oligonucleotide/oligosaccharide-binding (OB) domain of DHX15 (Inesta-Vaquera *et al.*, 2018, Toczydlowska-Socha *et al.*, 2018). The functional consequence of this interaction is inhibition of CMTR1 methyltransferase activity and repressed translation of CMTR1-dependent genes. Furthermore, interactions between CMTR1, RNAPII and DHX15 are mutually exclusive, suggesting DHX15 may prevent recruitment of CMTR1 to mRNA targets for capping (Inesta-Vaquera *et al.*, 2018).

1.3.4 Post translational modifications

As is the case with many proteins, post translational modifications (PTM) in capping enzymes can occur to modulate function (Mann and Jensen, 2003, Aregger *et al.*, 2016, Lukoszek *et al.*, 2024). Phosphorylation sites have been identified in both RNMT and CMTR1 methyltransferase capping enzymes, the biological relevance of which is discussed below.

Phosphorylation of RNMT at the T77 position by CDK-1-cyclin B1 occurs during the G2/M phase of the cell cycle, resulting in enhanced capping at the G1 phase to enable a “transcriptional burst”, which occurs after the completion of mitosis. Phosphorylation at T77 promotes RNMT activity by interfering with interactions

between RNMT and Importin α -1 (KPNA2), an inhibitor of RNMT-RAM methyltransferase activity. Additionally, phosphorylation of the T77 site likely alters RNMT conformation in a manner which promotes accessibility of the SAM binding domain. Abrogation of RNMT phosphorylation via conversion of threonine to alanine results in proliferative defects in transformed mammary epithelial cells, due to disruption in gene expression (Aregger *et al.*, 2016). Phosphorylation of CMTR1 occurs at 15 sites within the N-terminal domain, denoted as the Phosphorylation-patch (P-patch). These sites are targeted for phosphorylation by casein kinase 2 (CK2) (Lukoszek *et al.*, 2024), a pleiotropic kinase with fundamental roles in cell survival, metabolism, proliferation, inflammation and DNA repair (Pinna and Meggio, 1997, Kato *et al.*, 2003, Gibson *et al.*, 2017, Loizou *et al.*, 2004). Whilst phosphorylation of the P-patch does not lead to a direct enhancement of methyltransferase activity, it does promote interaction between RNAPII CTD and CMTR1. Upon mutation of phosphorylated residues within the P-patch to alanine, significant decreases in mature Cap-1 structures across the transcriptome are noted, leading to suppression of CMTR1 dependent gene expression (Lukoszek *et al.*, 2024).

1.3.5 Conclusion

Overall, the m7G cap is able to influence a multitude of processes to permit and promote gene expression for cell function and survival. Unfortunately, it is hard to dissect which specific process fundamentally governs this role, as many previous studies regarding the necessity of cap binding proteins and hence the cap itself are based on depletion of proteins with multifactorial roles in gene expression. For example, the CBC and eIF4E. It is also of import to note that both CBC and eIF4E are capable of efficiently binding to the cap structure in the absence of 2'-O-ribose methylation, suggesting CMTR1 activity is dispensable in these processes. This leaves an open question as to the exact relevance of the Cap-1 structure and other modifications in regulation of mRNA processes and gene expression. Current evidence suggests that CMTR1 does not have global influences in modulating gene expression, at least not to the same extent as RNMT. Rather, CMTR1 functions to ensure expression of specific genes, particularly those implicated in metabolism, mRNA processing and innate immunity (Williams *et al.*, 2020, Liang *et al.*, 2022, Dohnalkova *et al.*, 2023, Inesta-Vaquera *et al.*, 2018, Lee *et al.*, 2020).

1.4 CMTR1 function

1.4.1 Roles for the Cap-1 structure/CMTR1 in innate immunity.

The Cap-1 structure is well-characterised as a means by which the innate immune system differentiates between RNA of self and non-self-origin. Various pattern recognition receptors (PRRs), including MDA5 (gene name: *IFIH1*) and RIG-I (gene name: *DDX58*) recognise viral RNA species due to the absence of 2'-O-ribose methylation at the first transcribed nucleotide (Züst *et al.*, 2011, Schuberth-Wagner *et al.*, 2015). Furthermore, effectors of the Interferon (IFN) response downstream to PRRs such as Interferon induced proteins with tetratricopeptide repeats (IFITs) , selectively bind to transcripts lacking Cap-1 structures. Sequestering these from translation initiation factors (Habjan *et al.*, 2013).

Knockdown (KD) of CMTR1 in both monocyte and liver cell lines results in a significant reduction of IFN stimulated gene 15 (ISG15), Mx dynamin like GTPase 1 (MX1) and Interferon induced transmembrane protein 1 (IFITM1) expression upon IFN treatment. However, this is not attributable to transcriptional deficits and is restored upon depletion of translational repressor protein IFIT1 (Williams *et al.*, 2020). CMTR1-dependent interferon stimulated genes (ISGs) contain elements in their 5'UTR which predispose them for IFIT mediated repression in the absence of the complete cap structure (Williams *et al.*, 2020). These translational deficits which are induced upon depletion of CMTR1 are thought to contribute to an observed increase in the infectivity of Dengue, Zika and Vesicular stomatitis (VSV) viruses, highlighting a role for CMTR1 as an anti-viral factor (Williams *et al.*, 2020). These findings have been replicated in mouse embryonic fibroblasts (MEF), where suppression of ISGs in response to IFN is observed upon expression of a phosphodeficient CMTR1 mutant or depletion of WT CMTR1 (Lukoszek *et al.*, 2024). In contrast to the findings of Williams *et al.*, suppression of ISG expression in these MEF models was noted to occur transcriptionally and translationally (Lukoszek *et al.*, 2024), suggesting CMTR1 promotes IFN responses through mechanisms other than IFIT evasion in the MEF model.

Given that 2'-O-ribose methylation serves to prevent PRR recognition, an immune response to self RNA may be expected to occur upon CMTR1 depletion. However, several studies have generated contradictory findings in this regard and suggest

variation in responses to improperly capped host transcripts amongst tissues. Conditional KO (cKO) of CMTR1 within the liver of adult mice resulted in significant upregulation of ISG transcript expression in the absence of additional stimuli, when measured 6- and 22-days post induction of cre-recombinase (Dohnalkova *et al.*, 2023). Moreover, unpublished observations from the Sansom lab have noted that cKO CMTR1 mice develop chronic fibrosis of the liver within the first year of life, subsequent to chronic hepatitis (Sansom lab, personal communication). Despite these findings it should be stated that a link between differential CMTR1 function and hepatitis in human patients has yet to be uncovered. Primary human fibroblasts and A549 (lung adenocarcinoma) cells display upregulation of IFN- β in response to CMTR1 KD, which is attenuated upon inhibition of PRRs (Schuberth-Wagner *et al.*, 2015). Contrastingly, induction of either IFN or ISG expression was not noted upon CMTR1 depletion in Huh-7 (hepatoma) cell lines (Williams *et al.*, 2020), however, this may be due to maintenance of low-level methyltransferase activity or oncogenic factors. Additionally, CMTR1 KD in neurones results in no detectable alterations in expression for type I IFN signalling genes, implicating other factors in the detection of improperly capped RNA in the brain (Lee *et al.*, 2020).

1.4.2 CMTR1 in Transcription and Translation of mRNA

Unlike fellow methyltransferase RNMT, CMTR1 activity is dispensable for ensuring canonical translation in cells, as the cap binding proteins essential for enabling translation are capable of recognising m7G moieties alone (Tahara *et al.*, 1981). Despite this, CMTR1 has been described to enhance translation in *Xenopus* oocyte models (Kuge *et al.*, 1998). Furthermore, whilst Cap-1 formation on select nucleotides only modestly promoted protein expression in 3T3-L1 or HeLa cell lines, it dramatically increased expression of transcripts starting with adenosine, cytosine, or uracil nucleotides in JAWS II cells (a murine dendritic cell line). Cap-1 formation specifically enhanced translation of mRNAs where adenosine was the first transcribed nucleotide in the JAWS II model, as additional methylation at the N6 site via CAPAM provided a synergistic effect (Sikorski *et al.*, 2020). Together, these data highlight that CMTR1 may further enhance translation of genes in conjunction with RNMT and even CAPAM methyltransferase activity. However, the

mechanism behind this remains elusive and cannot be attributed to differences in affinity for translation initiation factors between Cap-0 and Cap-1 structures.

Specific expression of genes implicated in metabolism, cell cycle progression and development have been found to be regulated by CMTR1 in a variety of works. Inhibition of binding between CMTR1 and negative regulator DHX15 resulted in significant enrichment of 59 transcripts within polysomes, most of which were associated with cell cycle and metabolic processes. The consequence of this being increased growth in mammary epithelial tumours (Inesta-Vaquera *et al.*, 2018). Work conducted in embryonic stem cells (ESC) demonstrated upregulation of CMTR1 during neural differentiation, with CMTR1 KD in ESC resulting in a failure to proliferate and widespread apoptosis upon differentiation. These observations were tied to a dependency on CMTR1 for expression of histones and ribosomal proteins. Chromatin immunoprecipitation-DNA sequencing (ChIP) analysis conducted on ESCs showed RNAPII recruitment to the TSS of histone and ribosomal genes was regulated by CMTR1, with CMTR1 KD repressing binding of RNAPII at these sites (Liang *et al.*, 2022).

Recent work from the literature has shown that mutations in the G-patch of CMTR1 rescues *general anaesthetic sensitivity abnormal 1 (gas-1)* mutant nematode models from hyperoxia and mitochondrial stress (Meisel *et al.*, 2024).

NADH:ubiquinone oxidoreductase core subunit S2 (Ndufs2), the human homologue of *gas-1* is a component of mitochondrial complex 1 required for oxidation of nicotinamide-adenine dinucleotide (NADH) (Pujo *et al.*, 2013), complete loss of which results in mitochondrial complex I deficiency in human patients (Scheffler, 2015, Loeffen *et al.*, 2001). Rescue of *gas-1* mutant phenotypes was enabled by ectopic localisation of CMTR1 to P-bodies, resulting in translation of *nduf-2.2*, a *gas-1* paralogue normally restricted to expression in dopaminergic neurones (Meisel *et al.*, 2024).

1.4.3 CMTR1 in development and mRNA processing.

In mice deletion of CMTR1 results in arrested development by embryonic day 7.5 alongside lethality, in the absence of IFN induction due to the presence of improperly capped transcripts. However, this phenomenon has not yet been described in human patients. Analysis into the transcriptome of this model found

specific downregulation of small nucleolar RNA (snoRNA) host genes, required for ribosomal and small nuclear RNA (snRNA) modification, although no deficits were noted in the intronic splicing of snoRNA host genes (Dohnalkova *et al.*, 2023). One paper currently available in preprint has described reduced transcription of snoRNA host genes, ribosomal proteins and 5'TOP-RNAs in CMTR1 KO HEK293T cell lines. Whilst CMTR1 KO did not mediate global alterations in either splicing or transcript stability in this study, transcription of ribosomal proteins was specifically affected (Wolter *et al.*, 2023, preprint). The protein NVL2 is a crucial ribosome biogenesis factor, responsible for maturation of the 60S ribosomal subunit (Nagahama *et al.*, 2004). Upon depletion of CMTR1, protein expression of NVL2 was abrogated due to alterations in splicing which favour excision of exon 8. This resulted in expression of the NVL2- Δ 8 transcript possessing a premature stop codon which was subjected to nonsense mediated decay, impacting downstream ribosome maturation (Wolter *et al.*, 2023, preprint).

Knock-down (KD) of CMTR1 in neurones resulted in reductions of dendritic length and number, suggesting CMTR1 may regulate developmental processes in the brain. Neurones possess an intact innate immune response and express components of RNA sensing pathways; however, no immune response was induced in this model upon CMTR1 KD (Lee *et al.*, 2020). Knock out of CMTR1 in neurones was found to reduce transcript levels of calcium/calmodulin-dependent protein kinase (Camk2 α) (Lee *et al.*, 2020), a kinase responsible for long term potentiation at synapses (Miller *et al.*, 2002). Implying that CMTR1 contributes to brain development by ensuring expression of specific neural factors.

1.5 CMTR1 structure

The characterised regions of the CMTR1 protein include a nuclear localisation signal (NLS), phosphorylation patch (P-patch), G-patch, Rossmann-fold methyltransferase domain, guanylyltransferase like domain and WW protein binding domain, in order of the N to C terminus (Lukoszek *et al.*, 2024, Smietanski *et al.*, 2014) (Figure 1.4).

The P-patch at the N-terminal domain of CMTR1 contains a cluster of serine and threonine residues to facilitate phosphorylation across this region, mediated by the activity of CK2 (Lukoszek *et al.*, 2024). Phosphorylation within the P-patch occurs on at least 15 confirmed residues including: S26, S28, T30, S31, S46, S49, S51, S53, S55, T57, S63, S64, S66, S75 and S89. The presence of phosphoryl groups at these sites does not impact methyltransferase activity nor interaction with negative regulator DHX15 but promotes binding between CMTR1 and the CTD of RNAPII. It is thought that the disordered P-patch may be capable of interacting with positively charged regions in the WW domain, in a manner which stimulates RNAPII binding via intramolecular interaction (Lukoszek *et al.*, 2024).

The G-patch of CMTR1 is a glycine rich region comprised of approximately 50 amino acids with the following consensus motif hhxxxGaxxGxGhGxxxxG (where G=glycine, h= hydrophobic residues, a= aromatic residues), associated with functions in RNA processing and binding (Aravind and Koonin 1999, Bohnsack *et al.*, 2021). The G-patch of CMTR1 contains hydrophobic leucine at residues 94, 106 and 128, a feature which it shares with other DHX15 interacting proteins. Mutation of leucine specifically at residues L94 and L106 are sufficient to eliminate interaction between CMTR1 and DHX15. The functional consequence of G-patch mediated interaction with DHX15 is inhibition of methyltransferase activity and suppression of CMTR1 regulated genes (Inesta-Vaquera *et al.*, 2018). Thus far, DHX15 is the only known interactor of the CMTR1 G patch (to the authors knowledge), which is mediated by the OB domain. Given that OB domains are a specific feature of DEAH/RHA helicases (He *et al.*, 2010, Ozgur *et al.*, 2015, Silverman *et al.*, 2004, Walbott *et al.*, 2010) it is possible that CMTR1 exerts additional gene regulatory functions via interaction with other members of this protein family.

The catalytic activity of CMTR1 is confined to amino acid residues 126-550, comprising the Rossmann fold methyltransferase (RFM) domain (Smietanski *et al.*, 2014). The RFM domain consists of a seven stranded β -sheet surrounded by six α -helices (Bujnicki 1999, Byszewska *et al.*, 2014). Catalysis of methyltransferase reactions requires the methyl donor SAM, which binds at a pocket between strands 2, 3 and 4 of the β -sheet (Anantharaman *et al.*, 2002). Upon interaction with CMTR1, the RNA phosphodiester backbone binds and curves around the protein, with the 1st nucleotide being located at the periphery of the RNA curve, adjacent to SAM. The m7G Cap-0 structure can be accommodated in a binding pocket, which is mediated by interaction with the side chain K203 and the 2'-OH on the ribose of the m7G cap, alongside side chain E373 and the m7G aromatic ring (Smietanski *et al.*, 2014). Although human CMTR1 can accommodate the m7G cap it has not shown to be necessary for enabling CMTR1 methyltransferase activity (Belanger *et al.*, 2010). It is of interest to note that viral analogues of CMTR1 share a great degree of conservation in terms of positioning for methyl donor and substrate targets (Benarroch *et al.*, 2004, Egloff *et al.*, 2002, Krafcikova *et al.*, 2020) but differ in regard to how they accommodate m7G structures (Hodel *et al.*, 1998, Bollati *et al.*, 2009), suggesting a unique dependency for Cap-0 formation prior to methylation of the first nucleotide in certain viral species.

The guanylyltransferase like (GT-like) domain of CMTR1 is catalytically inactive and the exact purpose served by this region is unclear. Despite this, it has been demonstrated that the GT-like sequence promotes CMTR1 methyltransferase activity in a non-essential manner (Smietanski *et al.*, 2014). Furthermore, structural work conducted by Garg *et al* indicates that the GT-like domain facilitates binding between CMTR1 and the OB fold within the RPB7 subunit of RNAPII, enhancing recruitment of CMTR1 to nascent RNA (Garg *et al.*, 2023).

WW domains are primarily characterised by their function in facilitation of protein-protein interactions, these typically consist of 35-40 amino acids which fold into a three stranded anti-parallel β -sheet, forming binding groves for ligand interaction (Bork and Sudol, 1994, Macias *et al.*, 1996, Verdecia *et al.*, 2000). This domain displays preference for binding with motifs rich in proline residues alongside phosphorylated serine/threonine/proline sites (Chen and Sudol, 1995, Lu *et al.*,

1999), the latter of which is found within the CTD of RNAPII upon initiation of eukaryotic transcription (Komarnitsky *et al.*, 2000, Haline-Vaz *et al.*, 2008).

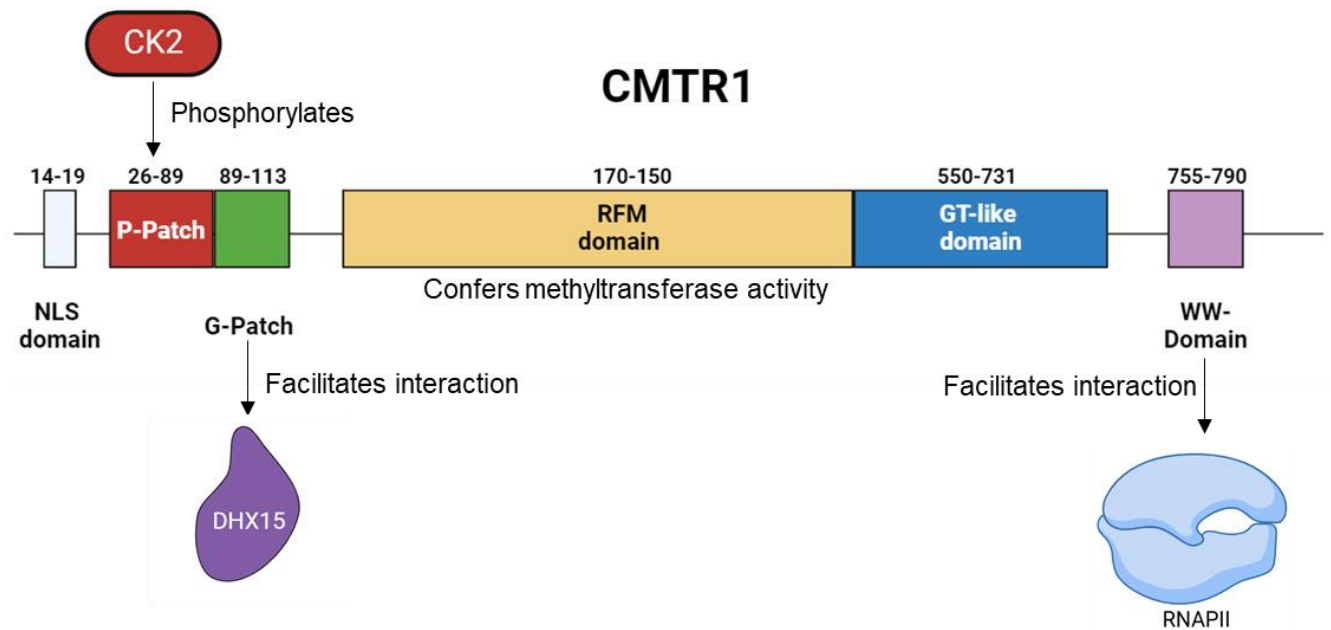


Figure 1.4-The Domain Structure of Human CMTR1.

A diagram depicting individual characterised domains of human CMTR1, and corresponding number of amino acids found within each domain. The P-Patch is phosphorylated via the activity of kinase CK2, the G-patch domain facilitates interaction between CMTR1 and protein DHX15, whilst the WW domain facilitates interaction between CMTR1 and RNAPII. The RFM domain confers methyltransferase catalytic activity. NLS (Nuclear localisation signal), P-Patch (Phosphorylation Patch), G-Patch(Glycine Rich Patch), RFM (Rossmann Fold Methyltransferase), GT-like (guanylyltransferase-like), WW (protein binding domain, contains 2 conserved tryptophans (W), CK2 (Casein Kinase II), DHX15 (DExH-Box helicase 15), RNAPII (RNA Polymerase II).

Figure made in BioRender and Microsoft PowerPoint. Figure adapted from Lukoszek *et al.*, 2024.

1.6 Putative CMTR1 interacting proteins

The interactome of CMTR1 is relatively poorly characterised, thus far only RNAPII and DHX15 have been extensively validated as CMTR1 binding proteins (Haline-Vaz *et al.*, 2008, Inesta-Vaquera *et al.*, 2018). Study into the CMTR1 interactome of HEK293 cells has identified putative binding partners of CMTR1 with implicated functions in modulating gene expression and mRNA processing. (Simabuco *et al.*, 2018). Argininosuccinate synthetase (ASS1) and PGAM Family Member 5, Mitochondrial Serine/Threonine Protein Phosphatase (PGAM5) were identified as CMTR1 interactors in murine liver, the data for which is presented further on in this body of work (Chapter 4).

1.6.1 ASS1

Argininosuccinate synthetase (ASS1) is a key component of the urea cycle, which involves 5 separate enzymatic reactions to convert toxic ammonia to urea (Matsumoto *et al.*, 2019). Deficiency or impairment of ASS1 function results in citrullinemia type 1, a potentially life-threatening metabolic disorder characterised by hyperammonaemia (Beaudet *et al.*, 1986). The reaction catalysed by ASS1 is the conversion of citrulline and aspartate to argininosuccinate via ATP hydrolysis, which is a rate limiting step in arginine biosynthesis (Ghose and Raushel, 1985).

Human ASS1 is composed of a nucleotide-binding, synthetase and C-terminal helix domain (Figure 1.5) and is assembled into a functional homotetramer composed of two identical dimer units (Karlberg *et al.*, 2008). The nucleotide binding domain permits for ATP binding, a co-substrate for the reaction mediated by the catalytic synthetase domain (Goto *et al.*, 2003). Simultaneously, the C-terminal helix enables oligomerisation of the protein structure to ensure the required conformation for enzymatic activity (Karlberg *et al.*, 2008). Interestingly, interaction between ASS1 and another methyltransferase, protein arginine methyltransferase 7 (PRMT7) has been demonstrated and occurs at a site between the synthetase domain and C-terminal helix of ASS1 (Verma *et al.*, 2017).

Although the urea cycle involves the activity of mitochondrial proteins (Matsumoto *et al.*, 2019), ASS1 is localised to the cytosol with expression of this protein being highest in periportal hepatocytes (Halpern *et al.*, 2017). Despite initial

characterisation as a metabolic enzyme recent work has contributed to a growing appreciation for a role of ASS1 in modulating immune responses (Mao *et al.*, 2022, Tarasenko *et al.*, 2015). Expression of ASS1 is found to be dysregulated in a variety of tumours, where it may play either tumour suppressor or pro-oncogenic roles (Kim *et al.*, 2021, Tao *et al.*, 2019, Keshet *et al.*, 2020).

In cell lines derived from hepatocellular carcinoma (HCC) patients, high expression of ASS1 correlates positively with survival. This is attributed to ASS1 mediated activation of the PERK/eIF2 α /ATF4/CHOP pathway, cumulating in ER-stress related apoptosis of tumour cells (Kim *et al.*, 2021). Furthermore, overexpression of ASS1 was found to inhibit phosphorylation of proto-oncogenic transcription factor signal transducer and activator of transcription 3 (STAT3) in HCC cell lines (Tao *et al.*, 2019). Complementing the above findings further are molecular studies which show p53 positively regulates ASS1 to destabilise chromatin remodelling, in a manner which halts gene transcription following DNA damaging (Lim *et al.*, 2024). Contrastingly, ASS1 expression is found to be upregulated in mammalian breast, colorectal and lung carcinoma cell lines, particularly following glucose deprivation. In these models, ASS1 was found to promote purine synthesis, inhibition of which promoted anti-tumour T-cell responses upon anti-PD-1 therapy (Keshet *et al.*, 2020).

1.6.2 PGAM5

PGAM Family Member 5, Mitochondrial Serine/Threonine Protein Phosphatase (PGAM5), is a mitochondrial Ser/Thr/His phosphatase and member of the phosphoglycerate mutase family. Phosphoglycerate mutase proteins catalyse conversion of 3-phosphoglycate to 2-phosphoglycate to facilitate glycolysis and gluconeogenesis (Fothergill-Gilmore and Watson, 1989). However, unlike fellow family members PGAM5 lacks mutase activity due to poor conservation of a phospho-histidine signature motif in the PGAM domain (Lo and Hannink, 2006). PGAM5 has numerous functions in regulating mitochondrial dynamics and has been implicated to play roles in mitochondrial biogenesis, fission, motility, mitophagy, and cell death processes (Sugo *et al.*, 2018, Bernkopf *et al.*, 2018, Xu *et al.*, 2015, O'Mealey *et al.*, 2017, Sekine *et al.*, 2012, Lu *et al.*, 2016).

PGAM5 exists in human cell lines as two distinct isoforms, PGAM5-L and PGAM5-S, which arise due to alternative splicing at the 3' end of the mRNA transcript. Both isoforms share the initial 239 amino acid sequence, with the longer isoform (PGAM5-L) possessing an additional 50 amino acids after the conserved sequence, whilst the short isoform (PGAM5-S) contains 16 hydrophobic amino acids subsequent to the conserved sequence (Lo and Hannink, 2006). The C-terminal tail of the protein, which is altered in the PGAM-S isoform is crucial for dimeric assembly of PGAM5 monomers (Chaikuad *et al.*, 2017). The characterised domains of PGAM5 include a transmembrane domain (Sekine *et al.*, 2012), a neo-IAP binding motif (Zhuang *et al.*, 2013), a WDXNWD motif (Wilkins *et al.*, 2014), a NXESGE motif (Lo and Hannink, 2006), a PGAM domain (Takeda *et al.*, 2009) and a C-terminal tail (Chaikuad *et al.*, 2017) (Figure 1.5).

Cleavage of the transmembrane domain of PGAM5 via presenilin-associated rhomboid-like protein (PARL) occurs upon loss of mitochondrial potential or rupture of the outer mitochondrial membrane, enabling greater motility of PGAM5 to coordinate cellular responses to mitochondrial stress (Sekine *et al.*, 2012, Bernkopf *et al.*, 2018, Yamaguchi *et al.*, 2019, Baba *et al.*, 2021). Upon cleavage and subsequent release into the cytosol, PGAM5 dephosphorylates Axin, a scaffold protein of the β -catenin destruction complex, to mediate upregulation of Wnt signalling and facilitate mitochondrial biogenesis (Bernkopf *et al.*, 2018). Additionally, cleavage of PGAM5 has also been demonstrated to promote localisation into the nucleus, where dephosphorylation of serine/arginine rich proteins with roles in mRNA processing occurs (Baba *et al.*, 2021).

The neo-IAP binding motif, which is accessible upon cleavage, permits PGAM5 to interact with inhibitors of apoptosis protein (IAP) and regulate cell death processes (Zhuang *et al.*, 2013). The WDXNWD domain is required for multimeric assembly of PGAM5 by mediating protein-protein interaction and serves to promote phosphatase activity via allosteric activation of the adjacent monomer's PGAM domain within the dimer complex (Wilkins *et al.*, 2014). The NXESGE motif of PGAM5 enables binding to the Kelch domain of Keap1, a protein sensor of oxidative stress which facilitates metabolic rewiring (Lo and Hannink, 2006). The PGAM domain enables removal of phospho-groups from substrates and is the centre of

PGAM5 catalytic activity. Upon binding, phosphate molecules interact with the catalytic centre held together by a β -sheet core structure aligned with a charged cluster of amino acids. These positively charged amino acids include two histidine (H105 and H230) and two arginine residues (R104 and R152), which adopt the 2H-phosphatase arrangement necessary for catalytic activity upon phosphate binding (Chaikuad *et al.*, 2017). PGAM5 displays a preference for dephosphorylating negatively charged substrates containing phosphorylated serine/threonine residues and fails to exert enzymatic activity upon tyrosine phospho-peptides (Taked *et al.*, 2009, Wilkins *et al.*, 2014).

Considering the role of PGAM5 in regulating mitochondrial dynamics and cell death programmes it is unsurprising that this protein has been implicated in tumorigenesis. Significantly higher expression of PGAM5 has been noted in HCC tumour tissues compared to non-tumour matched controls and correlated with poorer patient survival. These observations were attributed to binding between PGAM5 and anti-apoptotic protein B-cell lymphoma-extra large (Bcl-xL), which conferred protection of the latter against proteasomal degradation, inhibiting apoptosis (Cheng *et al.*, 2018). Additional work has also demonstrated KO of PGAM5 attenuated liver tumour cell growth via downregulation of fatty Acid Binding Protein 1 (FABP1) expression, a protein implicated in long chain fatty acid uptake and the promotion of HCC angiogenesis (Muthusamy *et al.*, 2023). Conversely, in the context of colorectal cancer (CRC), ratios of kelch-like ECH-associated protein 1 (Keap1) and PGAM5 expression are dysregulated in a manner which favours degradation of PGAM5, with this predicting CRC tumour metastasis (Chang *et al.*, 2017).

1.7 Roles of CMTR1 in disease and pathology

1.7.1- CMTR1 in cancer

Preliminary experiments conducted in the Sansom lab have implicated CMTR1 in liver cancer oncogenesis. Conditional knock-out (cKO) of CMTR1 in murine models resulted in chronic inflammation and fibrosis of the liver within the first year of life. When cKO of CMTR1 is induced in conjunction with dysregulation of oncogenes β -catenin and c-Myc, tumorigenesis is accelerated compared to WT controls. This suggests CMTR1 possesses a tumour suppressive role in the preliminary stages of liver cancer initiation (Sansom lab, personal communication).

Analysis conducted on datasets from the cancer genome atlas (TCGA) indicates significant increases in CMTR1 expression occur in CRC tumour tissue compared to normal matched controls. Knock down of CMTR1 in CRC cell lines coincides with reduced expression of cell cycle genes *CDK6* and *CCND1* (You *et al.*, 2023), which are implicated in promoting cancer cell proliferation (Obaya *et al.*, 2002).

Furthermore, CMTR1 KD cell lines displayed a lower extent of oncogenic STAT3 expression and phosphorylation, mediated by inhibition of RNAPII recruitment to the TSS of the STAT3 promoter by CMTR1 (You *et al.*, 2023). Rearrangement and generation of fusion proteins containing anaplastic lymphoma kinase protein (ALK) occurs in around 0.8% of cancer cases (Ross *et al.*, 2017). The majority of ALK fusion events in non-small cell lung carcinoma (NSCLC) involve the generation of EML4-ALK fusion proteins (Takeuchi *et al.*, 2009), however, a CMTR1-ALK fusion has been reported in a single case of NSCLC in a 75-year-old male patient. The authors of this case report identified that the CMTR1-ALK gene consisted of the first two exons of CMTR1 fused to exon 20-29 of ALK, inducing a frameshift mutation which prevented ALK translation and conferred resistance to ALK inhibitor therapy (Du *et al.*, 2018). Additionally, a multi-omics study currently in preprint has identified that mRNA, protein, and phosphoprotein levels of CMTR1 are significantly higher in multiple cancers when compared to normal adjacent tissues, with mRNA expression of CMTR1 being enriched in liver cancer patients (Campeanu *et al.*, 2024, preprint).

1.7.2- CMTR1 in inflammatory diseases and viral infection

Genome wide association studies analysing occurrence of asthma exacerbation in patients taking inhaled corticosteroids identified the SNP rs2395672 in CMTR1 as a risk factor for asthma-related hospitalisation. Further experimentation determined that CMTR1 was over-expressed in nasal lavage samples of patients during picornavirus induced asthma exacerbation. Although the authors of this study did not perform mechanistic follow up experiments, they postulated that CMTR1's role in regulating viral immune responses was likely to influence asthma pathogenesis (Dahlin *et al.*, 2015).

As alluded to above, CMTR1's role in innate immunity permits it to function as an anti-viral factor in the context of Dengue, ZIKA and VSV infection. Depletion of CMTR1 resulted in increased expression of viral RNA relative to cellular Glyceraldehyde-3-phosphate dehydrogenase (GAPDH) alongside immunostaining of viral proteins; a phenotype which was maintained upon depletion of STAT1 in isolation, suggesting anti-viral activity is facilitated by CMTR1 mediated regulation of ISGs (Williams *et al.*, 2020). Contrasting these findings is the observation that CMTR1 functions as a pro-viral factor in the context of influenza A virus (IAV) and influenza B virus (IBV) infection (Li *et al.*, 2020, Tsukamoto *et al.*, 2023), which may be attributed to dependency on CMTR1 to conduct cap-snatching. Cap-snatching refers to a process by which viruses cleave the mature Cap-1 structure from host mRNAs and utilise these to prime viral mRNA synthesis (Decroly and Canard, 2017). Genome-wide CRISPR/Cas9 screening initially identified WDR7, CCDC115, TMEM 199 and CMTR1 as IAV host factors. Depletion of CMTR1 in both A549 and normal human lung fibroblasts conferred strong protection against IAV infection, reflected by decreased staining of viral hemagglutinin protein within these cell lines. Viral RNA luciferase constructs exhibit decreased activity upon CMTR1 KO, with these cells simultaneously displaying reductions in capped viral RNAs (Li *et al.*, 2020). Additional study demonstrates IAV and IBV replication is inhibited in CMTR1 KO A549 cells, with specific defects occurring in IAV cap snatching from U2 spliceosomal snRNA. Curiously, replication of other orthomyxoviruses and bunyaviruses which also perform cap-snatching were not altered upon CMTR1 KO (Tsukamoto *et al.*, 2023).

1.8 Hepatocellular carcinoma

Primary liver cancer, of which hepatocellular carcinoma (HCC) is the most common type, is the 4th leading cause of cancer-related death worldwide (Villanueva, 2019). The 5-year survival rate proceeding diagnosis in Europe stands at only 12% (Lepage *et al.*, 2015), highlighting the need to enhance current understanding of HCC pathology and pioneer new treatment regimes. A figure summarising aetiology, molecular drivers and typical progression of HCC can be found below (Figure 1.6).

Hepatocellular carcinoma is typically preceded by liver diseases with an underlying inflammatory component, progressing from hepatitis to cirrhosis and the eventual development of HCC (Yu *et al.*, 2018). The incidence of HCC is highest in East Asia, Sub-Saharan Africa and Northern Africa, which is in part attributed to the burden of hepatitis B virus (HBV) infection in these regions (Rumgay *et al.*, 2022). Despite this, a recent epidemiological shift has been noted, with rates of HCC increasing in Western countries alongside incidence of non-alcoholic fatty liver (NAFLD) and alcohol-related liver disease (Singal *et al.*, 2023, Estes *et al.*, 2018, Huang *et al.*, 2022). The remainder of HCC cases which cannot be attributed to viral infection, obesity, or alcohol abuse can stem from autoimmune and genetic disorders (Valean *et al.*, 2019), with aflatoxin exposure contributing further to the epidemiology of HCC in less developed regions (Liu and Wu, 2010).

1.8.1 Molecular drivers HCC

The most common molecular drivers of HCC oncogenesis involve mutations and alterations in *TERT*, *TP53*, *CTNNB1*, *MYC* and *ARID1A* genes (Ally *et al.*, 2017, Totoki *et al.*, 2014, Schulze *et al.*, 2015, Nault *et al.*, 2013). The *TERT* gene encodes for telomerase reverse transcriptase, an enzyme which catalyses telomere lengthening to enable unrestrained proliferative capacity and self-renewal in cancerous cells (Shay and Wright, 2019). *TERT* mutations in liver cancer are often centred within promoter sequences, inducing formation of atypical ETS/TCF binding motifs which drive *TERT* expression (Nault and Zucman-Rossi, 2015, Huang *et al.*, 2013). Mutations in *TERT* are found in preneoplastic macro nodules within cirrhotic liver, prior to development of full-fledged HCC, suggesting *TERT*

mutations are a key component of HCC tumour initiation (Nault *et al.*, 2013). Interplay is thought to exist between *TERT* and fellow oncogene *CTNNB1* in a manner which promotes oncogenesis. *TERT* mutations co-occur with those in *CTNNB1* and other WNT signalling genes to a significant extent (Totoki *et al.*, 2014). Furthermore, β -catenin binds to the *TERT* promoters, with expression of stable β -catenin enhancing expression of *TERT* in human carcinoma cells (Hoffmeyer *et al.*, 2012).

The *CTNNB1* gene encodes the transcription factor β -catenin and is found to be mutated in a number of cancers (Zehir *et al.*, 2017, Gao *et al.*, 2017). Mutations in *CTNNB1* are often associated with HCC arising from excessive alcohol and tobacco use (Schulze *et al.*, 2015). Mechanistically, phosphorylation of β -catenin by members of the destruction complex permit for ubiquitination and degradation of the protein in the absence of appropriate signalling ligands (Stamos and Weis, 2013). Tumour promoting mutations in β -catenin tend to be concentrated within or nearby phosphorylation sites at exon 3, preventing degradation of β -catenin and enabling continuous oncogenic Wnt signalling (Provost *et al.*, 2003, He and Tang, 2020). Interestingly, expression of a stable β -catenin mutant alone is not sufficient to induce liver tumorigenesis in mouse models (Harada *et al.*, 2002, Tripathy *et al.*, 2018).

Overexpression of c-Myc via focal amplification is abundant in HCC tumours of both viral and alcohol related aetiologies (Schlaeger *et al.*, 2008, Schaub *et al.*, 2018, Lin *et al.*, 2010). Amplification of *MYC* in isolation is not sufficient to induce HCC, as is the case with stable β -catenin mutant expression (Molina-Sánchez *et al.*, 2020, Beer *et al.*, 2004, Harada *et al.*, 2002). Myc functions as a transcription factor with activating and repressor functions, dysregulation of which contributes to unconstrained proliferation and growth in cancers (Daksis *et al.*, 1994, Van Riggelen *et al.*, 2010). The Hepatitis B viral protein HBx is noted to promote stability of c-Myc by blocking ubiquitin mediated degradation in hepatoma cell lines (Kalra and Kumar, 2006). Additionally, β -catenin has been identified to bind to elements in the *MYC* promoter, further enhancing overexpression (He *et al.*, 1998), these findings highlight the role of cooperation between these two oncogenes in HCC carcinogenesis.

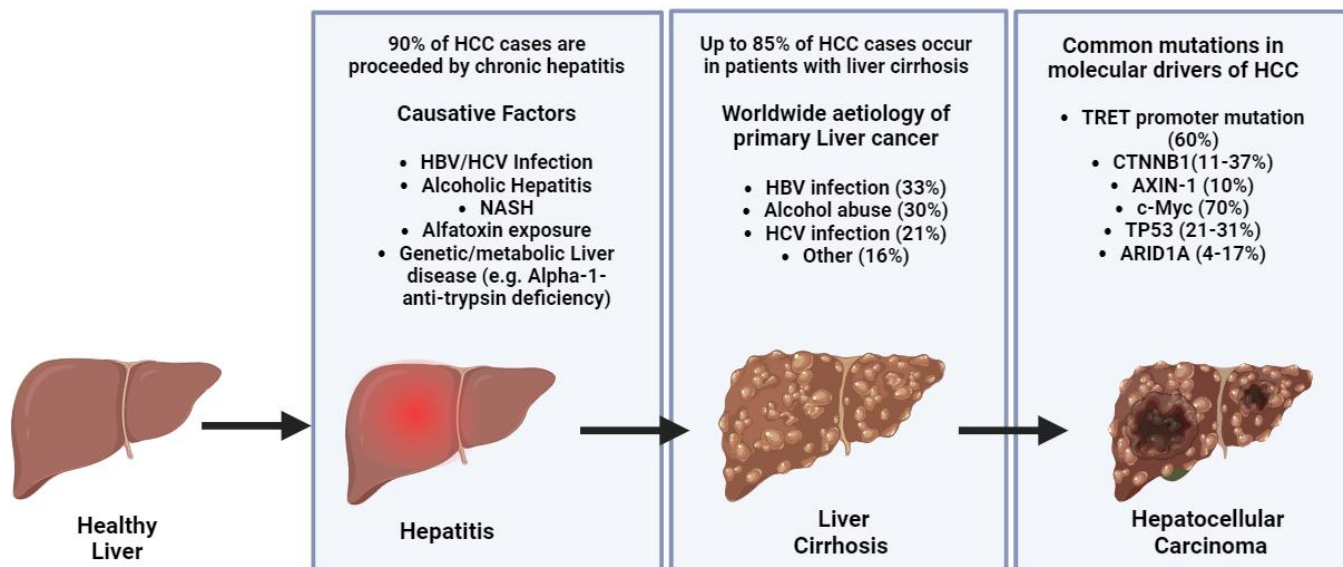


Figure 1.6-Summary of development, aetiology and drivers of Hepatocellular Carcinoma.

Progression to HCC from healthy liver is typically preceded by chronic inflammation of the liver (hepatitis) and cirrhosis. Causative factors and common molecular drivers of HCC are highlighted above. Figure made in BioRender. HCC (hepatocellular carcinoma), HBV (Hepatitis B virus), HCV (Hepatitis C virus), NASH (Non-alcoholic steatohepatitis).

1.8.2 Outcome, Prevention, and Treatment

Outcomes for HCC tend to be poor, with 5-year relative survival rates reaching only 12% for primary liver cancer in a European study (Lepage *et al.*, 2015). The most successful prevention strategy for reducing HCC incidence thus far has been the implementation of HBV vaccination programs. Analysis of HCC rates in Taiwanese children between 1981 and 1994 demonstrated a significant and potent reduction in HCC incidence upon vaccination (Chang *et al.*, 1997), indicating efficacy. Treatment of underlying viral aetiologies after infection has also been demonstrated to reduce HCC incidence, particularly if administered prior to liver cirrhosis (Kanwal *et al.*, 2017).

Resection, ablation, and transplantation of the liver can be curative but are typically dependent on diagnosis at an early stage of disease progression. Sorafenib is a pleiotropic protein kinase inhibitor and constitutes the first line of treatment in cases of advanced HCC (Llovet *et al.*, 2008). Inhibition of Raf-1 and vascular endothelial growth factor receptors permit sorafenib to exert an anti-angiogenic

effect and promote tumour cell-apoptosis in mouse xenograft models (Liu *et al.*, 2006). Administration of Sorafenib in a cohort of East-Asian patients improved overall median survival to 6.5 months, compared to 4.2 months in the placebo control group (Cheng *et al.*, 2009). Recombinant IFN therapy is used in cases of HCC relating to Hepatitis C virus (HCV) infection. Treatment with IFN prior to development of HCC in HCV patients reduces subsequent incidence and may decrease rates of reoccurrence in HCC patients who have undergone surgical resection (Hsu *et al.*, 2015, Ishikawa 2008, Kubo *et al.*, 2001). Additionally, mouse xenograft models treated with type I IFN display reductions in cancer proliferation and angiogenesis, alongside increases in tumour cell apoptosis. The anti-cancer effect of type I IFN is further enhanced when sorafenib is co-administered (Enomoto *et al.*, 2017). Checkpoint immune inhibitors (CII) offer an alternative avenue for HCC treatment, particularly in those with advanced disease who are resistant to sorafenib (Huang *et al.*, 2020). These inhibitors specifically target programmed cell death protein 1 ligand and its cognate receptor (PDL1), activation of which attenuates anti-tumour T-cell responses (Wang *et al.*, 2019). A phase 1b clinical study analysing the efficacy of CII pembrolizumab in conjunction with kinase inhibitor Lenvatinib demonstrated efficacy of this treatment in exerting anti-tumour activity (Kudo *et al.*, 2023).

1.9 Innate immune responses to uncapped RNA

Unlike DNA, host RNA is localised to both cytoplasm and nucleus under normal physiological conditions, meaning detection of specific motifs is required to differentiate between endogenous and non-self RNA. Prominent nucleic acid sensors of DNA or RNA include endosomal Toll-like receptors (TLR), cyclic GMP-AMP synthase (cGAS) and retinoic acid-inducible gene 1-like receptors (RLRs) (Alexopoulou *et al.*, 2001, Wu *et al.*, 2013, Yoneyama *et al.*, 2004, Yoneyama *et al.*, 2005). Retinoic acid-inducible gene 1 (RIG-I, gene name: *DDX58*), melanoma differentiation-associated protein 5 (MDA5, gene name: *IFIH1*) and laboratory of genetics and physiology 2 (LGP2, gene name: *DHX58*) make up the 3 members of the RLR protein family, which mediate RNA sensing within the cytosol (Rehwinkel and Gack, 2020). These RLR proteins (particularly MDA5) predominantly mediate sensing of dsRNA species (Wu *et al.*, 2013, Kato *et al.*, 2008) which can be derived from both viruses which possess dsRNA genomes and as an intermediary of ssRNA virus replication (Triantafilou *et al.*, 2012). Additionally, RLR proteins have been specifically demonstrated to respond to mRNA lacking methylation at the 2'-O-ribose position of the first nucleotide (Schuberth-Wagner *et al.*, 2015, Devarkar *et al.*, 2016, Züst *et al.*, 2011). This implicates the cap-1 structure as a means by which the innate immune system differentiates “self” and “non-self”.

1.9.1 RLRs

Structurally, RIG-I consist of two caspase activation and recruitment domains (CARDS) at the N-terminus, flanked by a central DExD/H-Box RNA helicase core, followed by a regulatory Zn²⁺ domain at the C-terminal end of the protein. This general domain structure is shared with fellow RLR family member MDA5 and to an extent LGP2 (Yoneyama *et al.*, 2005, Luo *et al.*, 2011). RIG-I sensing of viral RNAs is dependent on possession of unique biochemical features which are not expected to occur naturally in host RNAs. RNAs containing blunt 5'triphosphate ends, uncapped 5' diphosphate groups, and those which lack methylation at the 2'-O-ribose position are prone to detection via RIG-I (Schlee *et al.*, 2009, Goubau *et al.*, 2014, Schuberth-Wagner *et al.*, 2015). The Cap-1 structure of mRNA prevents recognition by RIG-I via steric hindrance, dependent on a specific histidine residue at the 830 amino acid position of RIG-I. The presence of the m7G cap alone on RNA

is not sufficient to negatively impact RIG-I stimulation (Schuberth-Wagner *et al.*, 2015).

In the absence of an appropriate ligand the N-terminal CARD domains of RIG-I are folded back, mediating interaction between these regions and the central helicase domain which sequesters RIG-I from immune response adaptor proteins (Kowalinski *et al.*, 2011, Luo *et al.*, 2011, Saito *et al.*, 2007). Upon ligand binding, the helicase domain wraps around viral RNA in a ringlike structure. This mediates the conformational changes required in conjunction with ATP to open CARD domains for downstream signalling (Jiang *et al.*, 2011, Rehwinkel and Gack, 2020). The freeing of these CARD domains upon ligand binding permits for oligomerisation of RLRs and is thought to be required to further facilitate downstream signalling. Exactly how this oligomerisation occurs is highly debated, proposed mechanisms of RIG-I oligomerisation include non-destructive polyubiquitination (Jiang *et al.*, 2012), and ATP driven translocation (Peisley *et al.*, 2013), with some researchers suggesting functionality for RLRs as monomers (Louber *et al.*, 2014). Upon activation, RIG-I interacts with a single CARD domain in the mitochondrial anti-viral signalling protein (MAVS), which is tethered to the outer mitochondrial membrane (Seth *et al.*, 2005). This interaction facilitates filament formation and MAVS aggregation, which is indispensable for recruitment of TNF receptor associated factor (TRAF) proteins, dimerization of Interferon regulatory factor 3 (IRF3) and activation I κ B kinase (IKK) complexes (Hou *et al.*, 2011). Following activation of these immune factors, NF- κ B is freed from its inhibitory complex and is able to induce expression of pro-inflammatory cytokines via translocation into the nucleus, simultaneously, entry of dimerised IRF3 into the nucleus induces expression of type I IFNs (Seth *et al.*, 2005). Type I IFNs are then able to act on their cognate receptor, inducing downstream formation of the transcription factor complex Interferon-stimulated gene factor 3 (ISGF3), which results in the induction of numerous interferon stimulated genes (ISGs) (Kessler *et al.*, 1988, Levy *et al.*, 1989). Expression of these ISGs results in the cell entering an anti-viral state, as these factors are able to directly interfere with viral function and further augment pathogen sensing (Schneider *et al.*, 2014).

Given the high degree of similarity in structure, it is believed that MDA5 adopts similar mechanisms of innate immune activation upon binding with nucleic acid as RIG-I (Rehwinkel and Gack, 2020). Where RIG-I and MDA5 are believed to differ functionally is primarily on their choice of activating ligand. Both RLRs are able to respond to double stranded RNA (dsRNA) species lacking 2'-O-ribose methylation of the first nucleotide but favour RNA ligands of differing lengths, with MDA5 preferentially binding to polyinosinic-polycytidylic acid (Poly I:C) over 2Kbp (Kato *et al.*, 2008). This is reflected in the utility of these two proteins within the context of infection with specific RNA viruses, as RIG-I is critical for IFN production in response to paramyxovirus species whereas expression of MDA5 is essential for detection of long dsRNA replicative intermediates of picornaviruses (Kato *et al.*, 2006, Feng *et al.*, 2012). AU elements within viral RNA are also thought to factor into ligand binding of RLR family members, with MDA5 appearing to favour binding to AU rich RNA species, as opposed to those enriched for GC elements (Runge *et al.*, 2014). The exact biochemical mechanism of how the Cap-1 structure is able to abrogate MDA5 signalling is yet to be elucidated. Despite this it has been shown that RNA from recombinant mouse hepatitis virus (MHV) lacking 2'-O-methylation activity is prone to activating MDA5 mediated IFN- β production, which is rescued upon restoration of MHV capping enzyme activity (Züst *et al.*, 2011). Unlike RIG-I, MDA5 is unable to form extensive intra-molecular interactions and hence adopts an open conformation even in the absence of an appropriate ligand. Once bound to ligand, multiple MDA5 monomers form filaments on dsRNA via cooperative binding between helicase and CTD ring like structures, these are then able to promote aggregation of MAVS for downstream signalling (Zheng *et al.*, 2015).

LGP2 is the third and most poorly characterised member of the RLR family, appearing to exert both positive and negative regulatory roles on innate immune responses to viral RNA (Rodriguez *et al.*, 2014). LGP2 contains a central helicase similar to that of RIG-I and MDA5 and is able to bind to dsRNA with greater affinity than fellow RLRs but lacks CARD domains required for inducing aggregation of MAVS (Murali *et al.*, 2008, Rothenfusser *et al.*, 2005, Rodriguez *et al.*, 2014). Overexpression models of LGP2 display reductions in IFN signalling mediated by RIG-I in response to Sendai and Newcastle disease viral infection, potentially due to LGP2 “mopping up” excess dsRNA as part of a negative feedback mechanism

(Rothenfusser *et al.*, 2005). Aggregation of MAVS via RLR CARD domains is necessary for recruitment of IKKi (an inducible form of IKK) to then mediate phosphorylation of IRF3. LGP2 has been demonstrated to interact with MAVS and compete with IKKi for binding, thus diminishing activation of IRF3 to negatively regulate IFN signalling (Komuro and Horvath, 2006). Conversely, depletion of LGP2 in mice was shown to result in susceptibility to encephalomyocarditis virus infection, dependent on abrogation of LGP2's ATPase activity. The authors of the study postulate this may be attributable to LGP2 facilitating the unwinding and mis-localisation of viral RNAs, improving ease of detection by RIG-I and MDA5 (Sato *et al.*, 2010).

1.9.2 RNA sensing and IFN signalling.

In response to RNA sensing by PRRs such as the RLR family members, aggregation of MAVS is achieved. This facilitates maturation of the MAVS signalosome for recruitment of TRAF proteins and phosphorylation of downstream factors (Seth *et al.*, 2005, Hou *et al.*, 2011). As previously mentioned, the N-terminal CARD domain enables activation via binding of RIG-I and MDA5 oligomer structures (Kowalinski *et al.*, 2011). Additionally, MAVS possesses a C-terminal transmembrane domain which maintains localisation to the outer mitochondrial membrane and contains a central proline-rich domain (PRD) (Hou *et al.*, 2011). MAVS is able to interact with TNF receptor associated factor proteins 2, 3, 5 or 6 (TRAF2/3/5/6), which then proceed to promote activation of both TANK binding kinase 1 (TBK1) and I κ B kinase (IKK) complexes through mechanisms involving E3 ligase activity (Liu *et al.*, 2013, Fang *et al.*, 2017). Activation of TBK1 is mediated by both autophosphorylation and the extrinsic kinase activity of IKKB (Clark *et al.*, 2011), enabling downstream phosphorylation of Interferon regulatory factors 3 and 7 (IRF3 and IRF7). Phosphorylation of IRF induces dimerization of these proteins, resulting in translocation to the nucleus and binding to inflammatory gene promoters with IRF-binding elements, including those of IFN α and IFN β (Hiscott *et al.*, 1999, Fitzgerald *et al.*, 2003). The activated IKK complex consists of two kinase subunits, IKK α and IKK β (Mercurio *et al.*, 1997) alongside noncatalytic protein NEMO, which then proceed to phosphorylate inhibitory I κ B subunits within the NF- κ B complex to promote ubiquitin degradation (Karin, 1999). Once liberated from this complex, canonical NF- κ B protein family members are free to translocate to the nucleus and

modulate expression of pro-inflammatory factors (Beinke and Ley, 2004) (Figure 1.7).

Once expressed, all type I Interferons bind to a heterodimeric transmembrane receptor consisting of subunit chains IFNAR1 and IFNAR2. Type I IFNs can be expressed by the majority of cells within the human body, in contrast, type II IFN (consisting of IFN- γ only) is exclusively produced by leukocytes (McNab *et al.*, 2015). Within humans type I IFN can be divided into IFN- α (which can further be divided into 13 subtypes), IFN- β , IFN- ϵ , IFN- κ and IFN- ω , although the former two subtypes are the most well characterised (Platanias *et al.*, 2005). Despite sharing a cognate receptor, expression of distinct type I IFNs is believed to result in differential outcomes during infection by specific pathogens, perhaps due to differences in the potency of the induced immune responses (Foster *et al.*, 2009, Fox *et al.*, 2020), which may be owed to variance in affinity for the type I IFN receptor (Lavoie *et al.*, 2011, Moraga *et al.*, 2008).

Interaction between type I IFNs and the type I IFN receptor permits for closer association between the two chains and cross-phosphorylation of tyrosine kinase 2 (TYK2) bound to INFAR1, and Janus kinase 1 (JAK1) bound to INFAR2. Cross-phosphorylation of TYK2 and JAK1 enables these proteins to act as a platform for subsequent phosphorylation of multiple STAT family protein members, including key drivers of the IFN response STAT1 and STAT2 (Piehler *et al.*, 2012, Schindler *et al.*, 2007). These actions generate the formation of ISGF3, composed of STAT1, STAT2 and IRF9, which is then able to promote expression of IFN stimulated genes (ISG) (Fu *et al.*, 1990, Schindler *et al.*, 2007). Expression of ISGs occur on the basis of IFN-stimulated regulatory elements (ISRE) within gene promoters, canonically consisting of a TTTCNNTTTC motif (where N= any nucleotide) (Leviyang, 2021, Shemesh *et al.*, 2021).

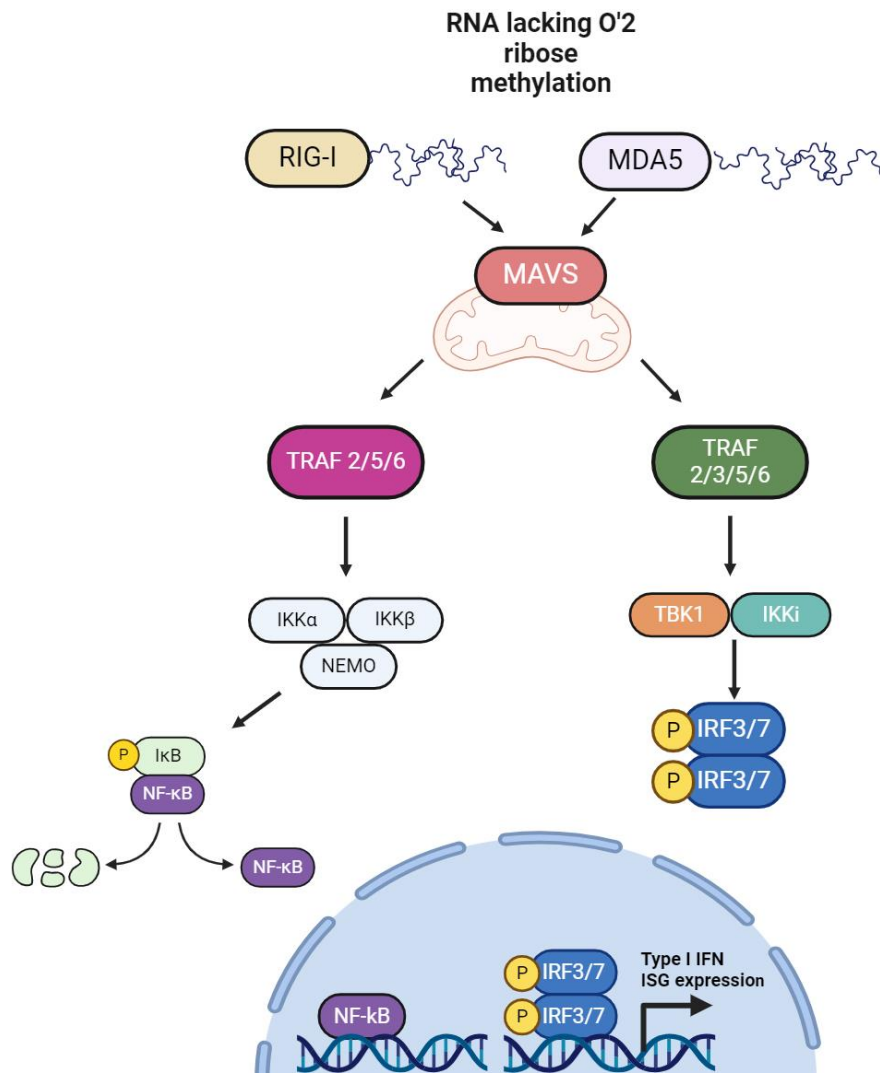


Figure 1.7-The Immune response to uncapped RNA.

RIG-I and MDA5 serve as PRRs for detection of viral RNA. Both RIG-I and MDA5 bind to mRNA lacking methylation at the 2'-O ribose position (Cap-1 structure). Interaction between RNA and these PRRs results in binding to adaptor protein MAVS, which triggers oligomerisation to form the MAVS signalosome. TRAF proteins are then recruited, which initiate downstream phosphorylation of IRF3 and 7 transcription factors, for IFN and ISG production. TRAF proteins are also capable of activating NF-κB via activation of IKK (composed of IKKβ/IKKα and NEMO) which phosphorylate inhibitor IκB, leading to the ubiquitination and degradation of the latter. This enables NF-κB to carry out its function as a transcription factor for production of various pro-inflammatory mediators. Figure made in BioRender. PRR (Pattern recognition receptor) RIG-I (Retinoic acid inducible gene-1), MDA5 (Melanoma differentiation associated protein 5), MAVS (Mitochondrial antiviral signalling protein), TRAF (TNF receptor associated factors), TBK1 (TANK binding kinase 1), IKK (Inhibitor of nuclear factor-κB kinase), NEMO (NF-κB essential modulator) IRF (IFN regulatory factor), NF-κB (Nuclear factor kappa-light-chain-enhancer of activated B cells), IFN (Interferon), ISG (Interferon stimulated gene).

1.9.3 ISGs (with specific focus on IFIT proteins, CMTR1 and ISG15)

The end result of IFN signalling is the induction of ISG expression to mediate anti-viral responses and further potentiate the IFN response (Schoggins and Rice, 2011, Schneider *et al.*, 2014). The exact number and profile of ISGs induced by IFN varies amongst organism and cell type, with around 200-500 ISGs being expressed by most non-haematopoietic cells (De Veer *et al.*, 2001, Schoggins *et al.*, 2011).

Multiple ISGs exert anti-viral activity by directly interfering with the viral lifecycle. For example, MX1 has been found to disrupt interaction between IAV viral polymerase basic protein 2 (PB2) and nucleoprotein (NP), resulting in a decrease in viral polymerase activity and thus viral transcription (Verhelst *et al.*, 2012). Another ISG, cholesterol-25-hydroxylase (CH25H) converts cholesterol into 25-hydroxycholesterol, a product which induces biochemical changes in the host cellular membrane changes to impair viral membrane fusion, effectively preventing enveloped viral entry (Liu *et al.*, 2013). Beyond direct anti-viral effectors, many ISGs function to sustain and intensify IFN responses. For example, PRRs including RIG-I, MDA5 and IRF1/7 mediate viral RNA sensing upstream of ISG transcription and are further upregulated upon IFN induction as ISGs in a positive feedback loop (Pine, 1992, Honda *et al.*, 2005, Kang *et al.*, 2002, Yoneyama *et al.*, 2004). Other ISGs function to sustain the IFN response by augmenting the function of PRRs and other IFN signalling pathway factors, DDX60 for example promotes the binding of dsRNA to RIG-I, enhancing activation of RLR signalling pathways upstream of ISG induction (Miyashita *et al.*, 2011). In turn, as chronic activation of IFN signalling is detrimental to human host cells, there are also ISGs which function as negative regulators of the IFN response, such as ubiquitin specific peptidase 18 (USP18). USP18 specifically binds to the INFA2 subunit of the type I IFN receptor and prevents this from phosphorylating JAK1, inhibiting further inflammatory signalling (Honke *et al.*, 2016).

Interferon-induced proteins with tetratricopeptide repeats (IFITs) are a class of anti-viral proteins induced by expression of IFN. Humans possess 5 IFIT genes: *IFIT1*, *IFIT1B*, *IFIT2*, *IFIT3* and *IFIT5*, whilst mice possess 6: *Ifit1*, *Ifit1b*, *Ifit1c*, *Ifit2*, *Ifit3*, *Ifit3b* (Daugherty *et al.*, 2016). IFIT1 selectively binds to the 5'UTR of RNA species lacking the Cap-1 structure and inhibit these from interacting with

translation initiation factors to halt viral protein production (Daffis *et al.*, 2010, Hui *et al.*, 2003). Interestingly, one recently published study has implicated that methylation at the N6 position of adenosine mediated by CAPAM may also be of importance in conferring protection for host mRNAs against IFIT repression (Geng *et al.*, 2024). IFITs have been implicated in ensuring robust immune responses towards a variety of viral species, including HCV, IAV and VSV (Raychoudhuri *et al.*, 2011, Pichlmair *et al.*, 2011). IFIT2 and IFIT3 promote IFIT1 mediated inhibition of viral protein translation by stabilising binding between IFIT1 and viral RNA (Fleith *et al.*, 2018).

The methyltransferase CMTR1 responsible for formation of the mature Cap-1 structure is induced by IFN, giving rise to its alternative moniker, interferon stimulated gene 95 (ISG95) (Haline-Vaz *et al.*, 2008, Su *et al.*, 2002, Guerra *et al.*, 2003). Exactly how CMTR1 exerts anti-viral functions are still in the process of being elucidated. However, Williams *et al.*, uncovered a role for CMTR1 in ensuring expression of fellow ISGs including ISG15, MX1, and IFITM1 by negatively regulating IFIT mediated translational inhibition (Williams *et al.*, 2020). Findings by Lukoszek *et al.*, which make up a component of Chapter 5 in this work, uncovered that abrogation of CMTR1 phosphorylation results in significantly reduced expression of a number of ISGs on both the protein and transcript level. Combined with the observation that phosphorylation of CMTR1 promotes interaction with RNAPII, it may be proposed that CMTR1 functions as an ISG by ensuring protein expression of fellow ISGs via capping activity. This activity is likely to be of particular importance when the cell enters an anti-viral state, as IFIT and other protein factors display an enhanced capacity to inhibit improperly capped host mRNA (Figure 1.8) (Lukoszek *et al.*, 2024, Daffis *et al.*, 2010, Züst *et al.*, 2011).

ISG15 is another example of a protein produced in response to IFN, with recent data suggesting expression of this protein is regulated by CMTR1 activity (Williams *et al.*, 2020, Lukoszek *et al.*, 2024). This protein is a member of the ubiquitin-like protein family and exerts activity once conjugated to target proteins via a process termed ISGylation, which involves the participation of E3 ligases. (Loeb and Haas, 1992, Fan *et al.*, 2015). The functional consequences of ISGylation on host proteins is not well characterised but it appears to negatively regulate turnover of

ubiquitylated proteins upon the formation of mixed chains (Fan et al., 2015). Targeting of viral proteins for ISGylation has been documented, with this contributing to restriction of Ebola and Influenza virus infection (Lai et al., 2009, Okumura et al., 2008, Lenschow et al., 2007). Furthermore, free ISG15 displays cytokine like properties by stimulating lymphocyte proliferation (D’Cunha et al., 1996) and interacts with other IFN pathway components to regulate innate immune responses (Du et al., 2017, Shi et al., 2010).

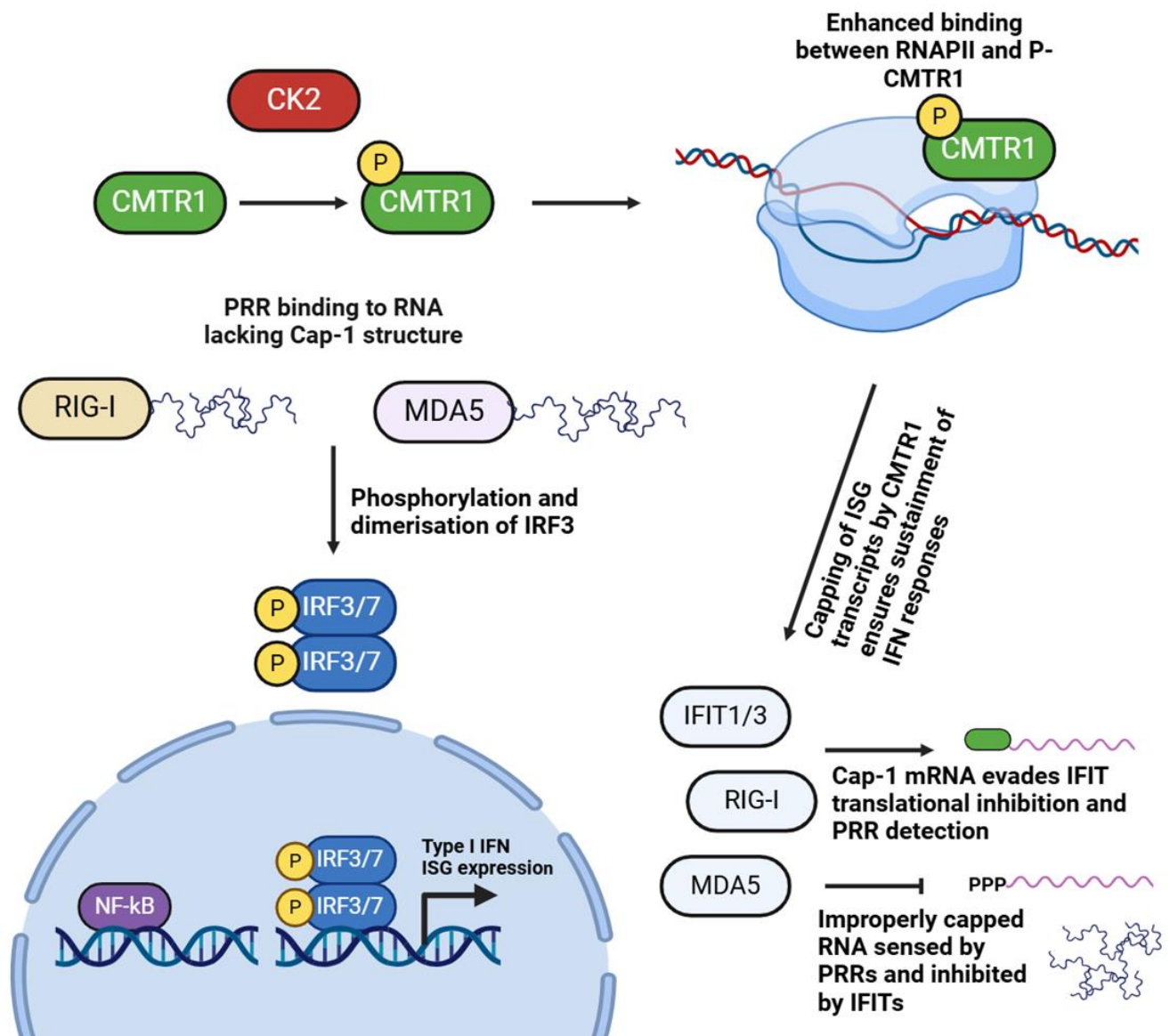


Figure 1.8- A proposed role for CMTR1 phosphorylation in the innate immune response. CMTR1 is phosphorylated at 15 sites within the N-terminal domain of the protein, via the activity of CK2. Phosphorylation of CMTR1 enables enhanced interaction with RNAPII at 5SP, increasing overall capping efficiency. 5’PPP RNA, dsRNA, and RNA which lacks 2’-O-ribose methylation are capable of being recognised by innate immune PRRs (e.g. RIG-I and MDA5).

Recognition of “non-self” RNA by PRR’s cumulates in activation of pro-inflammatory transcription factors IRF3/7 and NF- κ B, inducing expression of ISGs. Various ISGs, such as IFIT proteins and MDA5 bind to RNA species which lack 2’-O-ribose methylation (Cap-1 structure) and inhibit their translation. Thus, in a pro-inflammatory state, the cell possesses a lower tolerance for improperly capped transcripts. For this reason, there is a greater need for the cell to ensure host transcripts encoding ISGs are properly capped by CMTR1 to sustain the immune response. Figure made in BioRender. CMTR1 (Cap Methyltransferase 1), CK2 (Casein Kinase 2), RNAPII (RNA Polymerase II), dsRNA (Double stranded RNA), PRR (Pattern recognition receptor), RIG-I (Retinoic acid inducible gene-1), MDA5 (Differentiation-associated protein 5), IRF (Interferon regulatory factor), NF- κ B (Nuclear factor kappa-light-chain-enhancer of activated B cells), IFIT (Interferon-induced proteins with tetratricopeptide repeats), ISG (IFN stimulated gene).

1.9.4 Viral mechanisms of capping

Viruses have evolved a diverse range of mechanisms to prevent sensing of viral RNA by PRRs. These primarily consist of utilisation of host capping machinery, production of their own viral capping machinery, or cap-snatching from host mRNAs. Capping of viral mRNA that occurs via the same process employed by eukaryotes are classified as “conventional capping mechanisms” (Decroly *et al.*, 2012). Examples of viruses which possess these conventional capping mechanisms include RNA viruses such as Human immunodeficiency virus (HIV) and rotavirus family members, alongside DNA viruses such as HBV and Vaccinia (Chiu *et al.*, 2001, Reinisch *et al.*, 2000, Urushibara *et al.*, 1975).

Manipulation of host capping machinery by HIV is enabled by production of viral Tat protein. HIV does not encode its own polymerase and instead employs host RNAPII for transcription, hence capping enzymes are recruited as they would be under normal physiological conditions. To ensure preferential capping of viral transcripts the viral protein Tat promotes phosphorylation of RNAPII at S5P and directly stimulates host capping enzyme activity (Chiu *et al.*, 2001, Zhou *et al.*, 2003). Vaccinia virus meanwhile encodes a single enzyme termed D1, which exerts the same enzymatic activity as RNGTT and RNMT to facilitate production of the m7G cap (De la Peña *et al.*, 2007). Maturation of the cap structure on vaccinia RNA is then enabled by viral protein 39, which displays 2’-O-ribose methyltransferase activity and stimulates formation of a poly(A) tail (Schnierle *et al.*, 1992).

Unconventional viral capping mechanisms include cap snatching (a feature of Orthomyxoviridae viral RNA transcription) (Figure 1.9), incomplete formation of

the cap structure as performed by alphaviruses (Figure 1.10), and the Mononegavirales RNA capping pathway (Decroly *et al.*, 2011).

In the case of IAV infection, cap snatching involves the intrinsic endonuclease and polymerase activity of the IAV polymerase complex, consisting of three subunits including the polymerase acidic subunit (PA) and two separate polymerase basic subunits (PB1 and PB2). The IAV polymerase complex enables both transcription and replication of the viral genome. IAV possesses a negative single strand RNA (-ssRNA) genome, composed of 8 segmented genes associated with the IAV polymerase complex (Dadonaite *et al.*, 2019). The PB2 subunit of the IAV polymerase has been demonstrated to bind with high affinity to the m7G structure present on pre-mRNA (Xie *et al.*, 2016, Guilligay *et al.*, 2008), with it being postulated via structural modelling that Cap-1 methylation further increases this affinity, by establishing additional interactions with hydrophobic amino acids in the alpha helix of PB2 (Tsukamoto *et al.*, 2023). Interaction between the PB2 subunit and the cap is believed to be followed by rotation of PB2 in a manner which directs the transcript towards the active site of the PA subunit (Reich *et al.*, 2014). The PA subunit is then able to carry out endonuclease activity and cut host mRNA 10-13 nucleotides downstream of the cap structure. Cleavage at these sites allows the host mRNA nucleotides to be fed into IAV polymerase PB1 subunit, which then uses these additional nucleotides for priming of viral mRNA synthesis from the -ssRNA genomic template (Reich *et al.*, 2014). This process results in transcription of viral mRNA containing mature cap structures, which can bind to cap binding proteins for facilitation of canonical translation whilst avoiding detection by the innate immune system (Tsukamoto *et al.*, 2023). Additionally, this mechanism may act as another means by which influenza induces host-translational shutoff, as decapped host mRNA is targeted for degradation (Hopkins *et al.*, 2015). The majority of biochemical and structural studies demonstrate cap snatching mechanisms occurring on free capped primers. However, it is postulated that cap snatching *In-vivo* is directed towards pre-mRNA during early stages of active transcription initiation by RNPII, likely in the immediate aftermath of mRNA capping. This assumption is based on the observation that the IAV polymerase co-purifies with the S5P CTD of RNAPII but not the S2P CTD (Martínez-Alonso *et al.*,

2016), the latter of which indicates entry into the elongation and termination steps of transcription (Buratowski 2009) after capping has occurred.

In contrast to IAV, SINV is a positive single stranded RNA (+ssRNA) virus which possesses a genome containing 2 open reading frames and encodes its own m7G capping machinery but lacks the ability to carry out 2'-O-ribose methylation, yielding immature caps (Ahola and Kääriäinen, 1995) (Figure 5.9). Capping of SINV RNA occurs on the genomic and subgenomic vRNA strands co-transcriptionally, with SINV encoding its own RNA-dependent RNA polymerase (NSP4) (LaPointe et al., 2018, Rubach et al., 2009). Four non-structural viral proteins (NSP1, NSP2, NSP3 and NSP4) form the replicative enzyme complex in conjugation with host factors to enable replication of both the viral genome and transcription of the subgenomic RNA from a negative sense intermediate (Singer et al., 2021). The viral NSP1 protein, encoded by the genomic vRNA; possesses both methyltransferase and guanylyltransferase activity (Mi and Stollar, 1991). This results in conversion of GTP to m7GMP, by use of S-adenosyl methionine as a substrate. Followed by addition of m7GMP to viral RNA (vRNA); subsequent to cleavage of the terminal phosphate located at the 5' end of the RNA structure, enabled by the triphosphatase activity of viral NSP2 (Vasiljeva et al., 2000, Ahola and Kääriäinen, 1995). The end product of this series of reaction is viral RNA with a cap-0 structure (m7G(5')ppp(5')n). This structure permits for binding of translation initiation factors (LaPointe et al., 2018) but is still in theory subject to identification by PRRs (Züst et al., 2015, Devarkar et al., 2016). Rather than undertaking ribose methylation of the first transcribed nucleotide to obfuscate viral RNA from PRRs, SINV is dependent on host transcriptional shut off via RNAPII degradation to prevent induction of the IFN response. This is achieved through binding between the Rpb1 subunit of RNAPII and NSP2 resulting in Rpb1 ubiquitination and degradation (Akhrymuk et al., 2018, Akhrymuk et al., 2012). The mechanism of NSP2 mediated degradation of Rpb1 has not yet been fully characterised and it is unknown whether conformational changes are induced which promote ubiquitination or if NSP2 allows for direct binding of ubiquitin ligases.

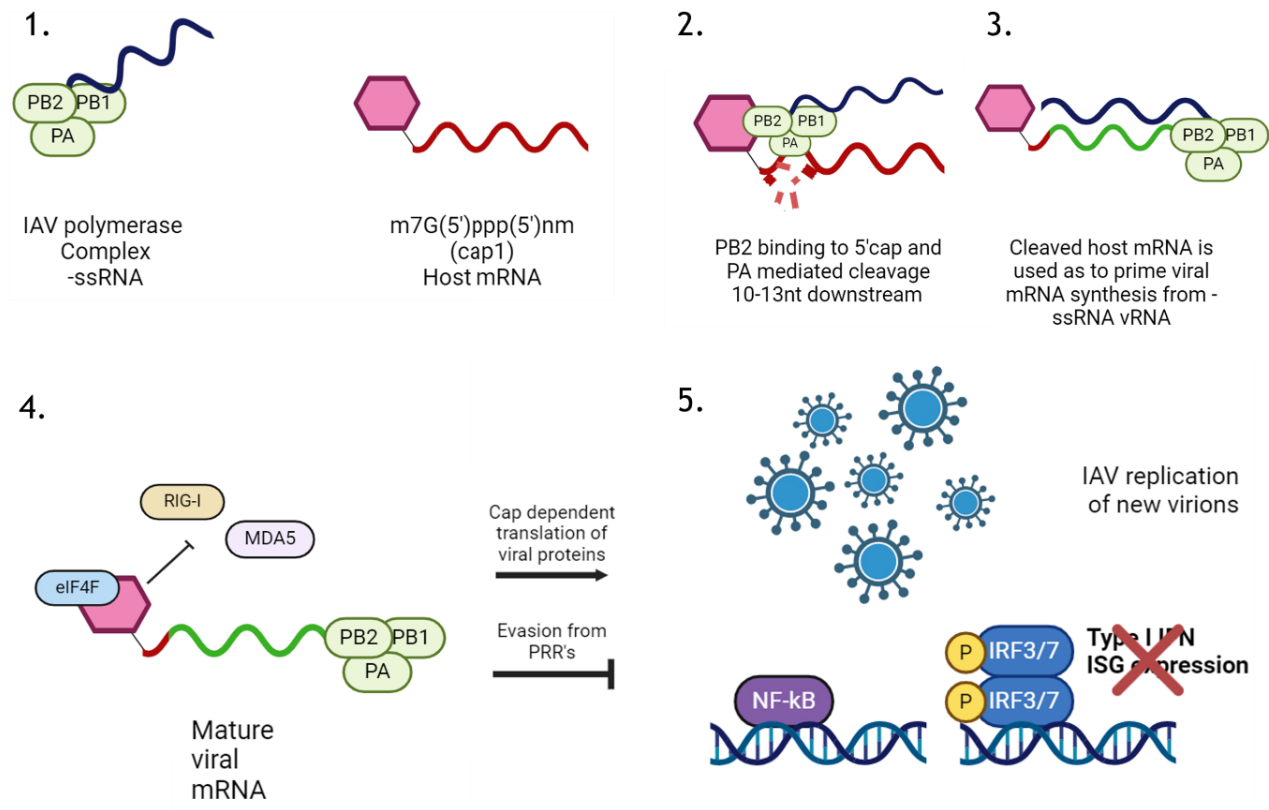


Figure 1.9-Cap snatching and Immune evasion strategies of IAV

IAV possesses a -ssRNA genome, consisting of 8 segmented genes, each of which is associated with the IAV polymerase complex (1). The IAV polymerase complex's PB2 subunit binds to capped host mRNA (m7G(5')ppp(5')nm), with cleavage occurring 10-13 nucleotides downstream of the cap, via the endonuclease activity of the viral PA subunit (2). After successful cleavage of host mRNA, the remaining nucleotides are used to prime viral mRNA synthesis. (3). This gives rise to the formation of mature viral mRNA with a Cap-1 structure. Due to the Cap-1 structure, this mature viral mRNA is able to evade PRR's and hijack cap-dependent translation machinery (4). The result of this being viral propagation, alongside repression of the FN response (5). Figure made in BioRender. vRNA (viral RNA), -ssRNA (negative single stranded RNA), PB1/2 (polymerase basic subunit), PA (polymerase acidic subunit).

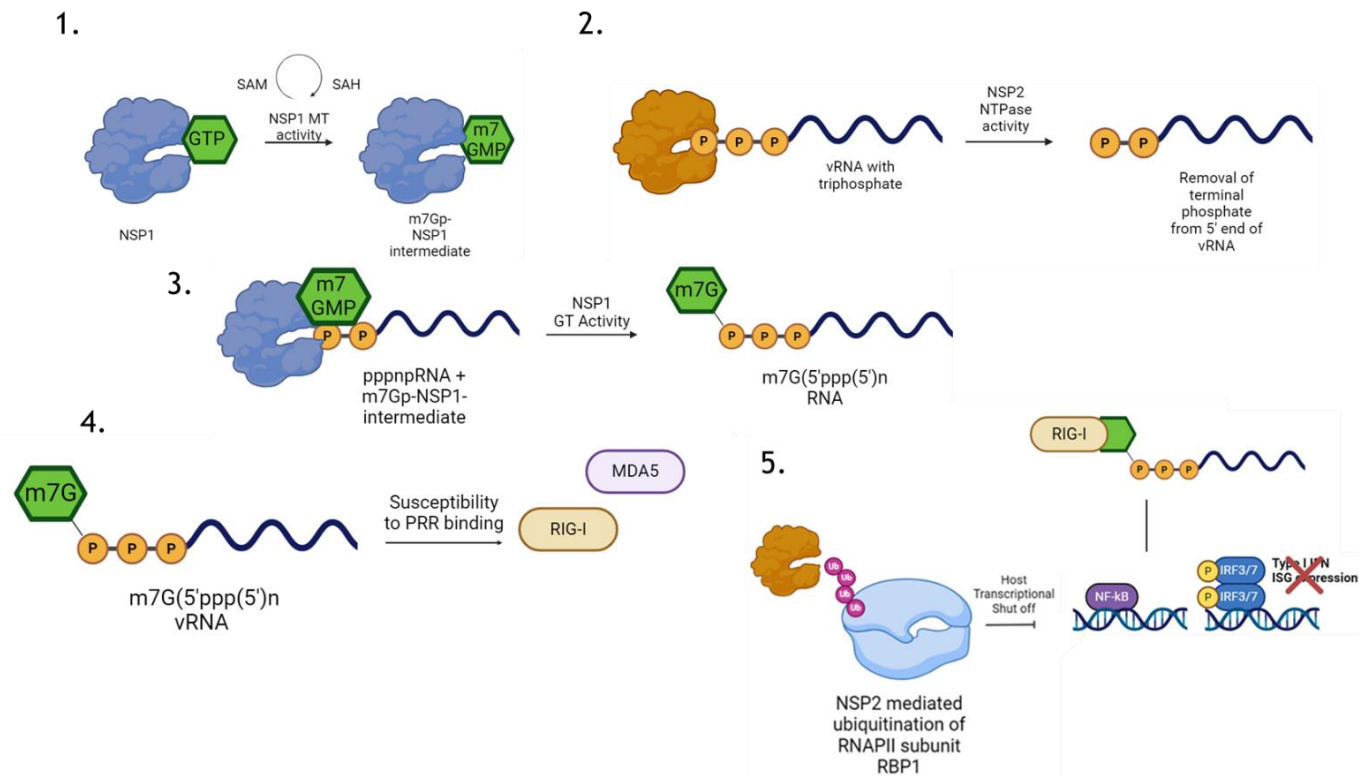


Figure 1.10- Capping and Immune evasion strategies of SINV

A m7G(5')ppp(5')n structure is added co-transcriptionally to alphavirus RNA. The MT and GT domain of NSP1 generates m7Gp. This is achieved via a series of reactions involving SAM as a substrate, alongside release of SAH and pyrophosphate (1,2). An additional viral protein NSP2, removes the terminal phosphate from the 5' end of vRNA (3). This enables NSP1 to exert GT activity, resulting in formation of the Cap-0 structure (m7G(5')ppp(5')n) (4). Due to the absence of Cap-1, SINV mRNA can still be detected by PRR's (5). Despite this being the case, the IFN response fails to be mounted against SINV due to NSP2 mediated degradation of RNAPII RBP1 subunit (6). Figure made in BioRender. SINV (Sindbis virus), MT (methyltransferase), GT (guanylyltransferase), NSP1/2 (non-structural protein 1), SAM (S-Adenosyl methionine), SAH (S-Adenosyl homocysteine), vRNA (viral RNA), RBP1 (RNA polymerase II subunit RPB1).

1.10 Aims

Formation of the Cap-1 structure is dispensable for canonical translation and mRNA processing, which is mediated by interaction between the m7G/Cap-0 structure and cap binding factors. Despite this, a growing appreciation has emerged of a role for CMTR1 in facilitating recognition of host mRNA as self and regulating expression of specific genes implicated in immunity, metabolism, and growth. Work conducted several years ago in the Cowling lab identified that expression of certain pro-growth genes was dependent on CMTR1 activity and that this contributed to proliferation in cancer cell lines (Inesta-Vaquera *et al.*, 2018). Contrastingly, data from the Sansom lab found cKO of CMTR1 results in unchecked inflammation and fibrosis of the liver, fostering subsequent tumour formation, especially when combined with dysregulation of β -catenin and c-Myc (Sansom Lab, personal communication). This suggests a putative but differential role for CMTR1 in specific stages of liver oncogenesis which warrants further investigation.

Phosphorylation of CMTR1 at 15 residues within the N-terminus promotes capping activity via interaction with RNAPII, enabling CMTR1 to regulate expression of specific genes (Lukoszek *et al.*, 2024). Whilst CMTR1 is a noted interferon stimulated gene (Haline-Vaz *et al.*, 2008), relatively little is known about its participation in innate immunity. Previous literature has demonstrated that CMTR1 is needed to sustain protein expression of select ISGs and exerts anti-viral activity against Dengue and Zika viruses (Williams *et al.*, 2020). This leads to the question as to what the exact biological consequences of CMTR1 phosphorylation are and if this has any impact on anti-viral immunity. This being the case, the main aims of this thesis are as follows:

- Characterisation of CMTR1 and established protein interactors in mouse models of HCC (Chapter 3)
- Identification and validation of novel hepatic CMTR1 protein interactors (Chapter 4)
- Determination of the impact of CMTR1 phosphorylation on ISG expression (Chapter 5)
- Investigation into how CMTR1 phosphorylation influences outcomes of viral infection (Chapter 5)

Chapter 2: Materials and Methods

2.1 Cell culture, maintenance, and treatment

2.1.1 Cell line culture

Cell lines were incubated at 37°C, in the presence of 5% CO₂. Culturing of cell lines was carried out in Dulbecco's Modified Eagle Medium (DMEM) (Gibco) media supplemented with 10% foetal calf serum (FCS) (Gibco), 2 mM L-Glutamine (Gibco), 100 U/ml Penicillin, and 0.1 mg/ml Streptomycin (Pen-Strep) (Gibco). A549 and mouse embryonic fibroblast (MEF) cell lines expressing exogenous vectors for WT-HA-CMTR1, 15A-HA-CMTR1, or an empty vector control were cultured with the addition of 0.5 mg/ml G418 (Formedium) to maintain selection pressure. Mouse embryonic fibroblasts were extracted from pregnant female mice floxed at exon 3 of *Cmtr1*, who had been crossed with male mice of the same genetic background and subsequently immortalised by serial passage (*Cmtr1*^{fl/fl} MEFs). Extraction of MEFs was undertaken by Dr Radoslaw Lukoszek. Passaging of adherent cells was carried out by washing with phosphate-buffered saline (PBS) prior to addition of dissociation agent 0.05% trypsin-EDTA phenol red (Thermo-Fisher Scientific). Trypsin was neutralised and cells resuspended with DMEM media prior to replating.

2.1.2 Cryopreservation and recovery of cell lines

Cells were cultured in a 10 cm dish until 80-90% confluency was achieved, washed, and dissociated as previously mentioned. Freezing media was made up with FCS supplemented with 10% Dimethyl sulfoxide (DMSO) (Sigma-Aldrich) by volume. After dissociation, cells were resuspended in DMEM, pelleted by centrifugation at 300 x g for 5 mins, and resuspended in freezing media. 1 ml of cell suspension was transferred into a 2 ml cryovial which was subsequently placed into a Mr. Frosty™ Freezing Container (Thermo-Fisher Scientific), to achieve a cooling rate of 1°C per minute in a -80°C freezer. 24 hrs post freezing, cryovials were transferred to liquid nitrogen. Cells were recovered from liquid nitrogen by warming cryovials in a 37°C incubator, followed by pelleting, removal of freezing media and addition of fresh DMEM.

2.1.3 DNA vector transduction

Generation of retroviral vectors was achieved by transfection of Phoenix-Ampho packaging cells with a customised pBMN-I-GFP (Addgene, #1736) based vector (cloning and *invitro* mutagenesis was conducted by the division of signal transduction therapy, University of Dundee and the Cowling lab) expressing HA-WT CMTR1, HA-15A CMTR1, or an empty vector control (EV), using Lipofectamine 2000 (Thermo Fisher Scientific). 48 hrs post transfection, supernatant was extracted from packaging cells and passed through a 0.45 µm filter. The resulting filtrate was transferred to cells in the presence of 5 µg/ml of polybrene (Sigma-Aldrich). 4 days after exposure to lentivirus, fresh DMEM culture media supplemented with 0.5 mg/ml G418 was added to cells to provide selection pressure. Transduction of MEF cells were carried out by Dr Radoslaw Lukoszek, transduction of A549 cells was conducted by the author of this work.

2.1.4 DNA vector transfection

MEFs were transfected with 7 µg (per 15 cm dish) of a custom DNA vector where an expression cassette derived from a pBS598 EF1alpha-EGFPcre plasmid (Addgene, #11923) was subcloned into a pBABE-Puro (Addgene, #1764) vector backbone (vector designed and cloned by Dr Radoslaw Lukoszek), using 21 µl (per 15 cm dish) of GenJet™ In Vitro DNA Transfection Reagent for MEFs (SignaGen Laboratories). Nucleic acid-lipid complexes were prepared with DMEM media in the absence of FCS and left to incubate at room temperature for 15 mins prior to addition to cells. Once nucleic acid-lipid complexes were added to cells, these were left to incubate for 20 mins at 37°C prior to plating. Selection pressure was induced by the addition of 2 µg/mL of puromycin 24 hrs post transfection for a period of 48 hrs.

2.1.5 Poly (I:C) transfection

High molecular weight polyinosinic-polycytidylic acid (HMW poly(I:C)) (Invivogen) was transfected into MEF cell lines plated in a 10 cm dish at a concentration of 5 µg/ml using 40 µl (per 10 cm dish) of Lipofectamine™ 2000 (Invitrogen). Nucleic acid-lipid complexes were prepared with DMEM media containing no FCS and left to incubate at room temperature for 5 mins prior to addition to cells. A negative control consisting of cells treated with lipofectamine™ 2000 only was also

generated. Cells were harvested for either protein or nucleic acid 17 or 24 hrs post transfection.

2.1.6 Drug treatments

MEF or A549 cell lines plated within a 10 cm dish were treated with 400 U/ml IFN (Universal Type I IFN) (PBL Assay Science), diluted in DMEM. IFN treated cells were harvested for protein or nucleic acid at multiple intervals over a maximum period of 24 hrs, as stated in figure legends. A 0 hr untreated control was generated where cells were exposed to DMEM only and harvested immediately upon commencement of the time course. MEF cell lines were pre-treated with 10 μ M of selective CK2-inhibitor quinalizarin (QZ) diluted in DMSO (Sigma-Aldrich) for 0.5-3 hrs. Carbonyl cyanide-p-trifluoromethoxyphenylhydrazone (FCCP) (Abcam), a mitochondrial oxidative phosphorylation uncoupler diluted in DMSO, was applied to Huh-7 and A549 cell lines to induce PGAM5 cleavage. FCCP was used at a concentration of 5-10 μ M for a maximum of 4 hrs. Negative controls were generated for QZ and FCCP treated cells, where cells were exposed to DMSO only.

2.1.7 MitoSpy staining

Mitochondrial labelling was carried out using MitoSpy Green FM and MitoSpy Red CMXRos (BioLegend). Cells were treated with 25 nM MitoSpy Green FM and MitoSpy Red CMXRos diluted in DMSO for 30 mins, prior to processing and downstream analysis by Flow cytometry.

2.2 Protein analysis

2.2.1 Whole cell lysis

To perform lysis, culture media was aspirated from a 10 cm dish, and cells washed with cold PBS, on ice. Cells were scraped into Radioimmunoprecipitation assay (RIPA) buffer (50 mM Tris-HCl pH 8, 150 mM NaCl, 1% NP-40, 0.1% SDS, 0.5% Sodium Deoxycholate) supplemented with Aprotinin (1% by volume) (Sigma-Aldrich), Leupeptin (10 μ m) (Sigma-Aldrich), Pepstatin (1 μ m) (Sigma-Aldrich), Phosphatase inhibitor cocktail 2 (PI2) (1% by volume) (Sigma- Aldrich), and Phosphatase inhibitor cocktail 3 (PI3) (1% by volume) (Sigma-Aldrich). After which, lysate was centrifuged at 16,000 x g for 10 mins at 4°C to pellet the insoluble fraction. The soluble fraction was then transferred to a fresh microcentrifuge tube. Protein concentration was determined using the Pierce bicinchoninic acid assay (BCA) Protein Assay Kit (Thermo Scientific). Absorbance was measured using a Sunrise plate reader (Tecan).

2.2.2 Organ lysis

A small section of whole frozen organ was extracted using metal forceps and a scalpel, after transfer of the whole organ into a 10 cm dish containing PBS on ice. This organ section was placed into a tissue homogenizing kit tube (Precellys) containing ceramic beads with 1ml of RIPA buffer. This tube was transferred to a Precellys Evolution Touch Homogeniser (Precellys) and spun at 2516 x g for 20 seconds, followed by a 20 second pause for 6 cycles. Lysate was left to rest on ice for 10 mins and centrifuged at 16,000 x g for 10 mins at 4°C to pellet the insoluble fraction. This was followed by transfer of the soluble fraction into a fresh Eppendorf. Protein concentration determined via BCA as previously described.

2.2.3 Immunoprecipitation (IP)

Protein lysate extracted from cells plated in a 10 or 15 cm dish was made up to the appropriate concentration (2 mg unless stated otherwise in figure legend) in RIPA buffer, to a total volume of 500 μ l. Protein lysate was pre-cleared using 20 μ l of protein G agarose beads (Division of signal transduction therapy, University of Dundee/DSTT) and left to incubate for 1 hr on a spinning rotator to eliminate non-specific interactions. 20 μ l of pre-washed protein G Dynabeads (ThermoFisher

Scientific), alongside 2-3 µg of antibody (IgG) were added to pre-cleared lysate and incubated at 4 °C overnight.

The post IP-input was then generated by taking 20 µl of the IP and flow-through, alongside 10 µl of 4x NuPAGE™ Lithium dodecyl sulphate sample buffer (LB) (Invitrogen) and 25 mM Dithiothreitol (DTT) (Thermo Scientific). Flow-through samples were prepared in the same manner as the post IP-input, after isolation from the bead-antibody complex using a magnetic strip. Both input and flow-through samples were boiled at 100 °C for 5 mins prior to loading for sodium dodecyl sulphate-polyacrylamide gel electrophoresis (SDS-PAGE). After this, beads were washed 3 times with RIPA buffer for at least 5 minutes. Once the final wash was complete, the IP was transferred to a fresh Eppendorf tube. The IP was eluted using 2x LB and 25 mM DTT, then boiled at 100 °C for 5 mins.

2.2.4 SDS-PAGE western blotting

Prior to SDS-PAGE, protein lysate was diluted to a concentration of 10-30 µg in LB supplemented with 25 mM DTT. Samples were then boiled at 100 °C for 5 mins and centrifuged at 16,000 x g for 30 seconds to ensure denaturation of tertiary and secondary protein structures. Electrophoresis was carried out using either home-made gels in Mini-PROTEAN™ tetra cells (Bio-Rad) or a pre-cast NuPAGE™ 4-12% Bis-Tris Protein Gel in a XCell SureLock™ mini cell. Homemade gels were run in 1x Tris-Glycine running buffer (25 mM Tris, 192 mM glycine, 0.1% SDS), whilst pre-cast gels were run in NuPAGE™ MOPS SDS Running Buffer (Life Technologies).

SDS-PAGE gels, Immobilon®-FL polyvinylidene difluoride (PVDF, Merck Millipore) membrane, and Whatman blotting paper (Fisher Scientific) were equilibrated in transfer buffer (20% methanol, 25 mM Tris-HCl, 192 mM glycine), prior to assembly of the transfer stack. Transfer was carried out in a Mini Trans-Blot® Cell (Bio-Rad), either at 70 V for 90 mins on ice, or at 10 V overnight.

Once transfer was complete the PVDF membrane was dried and reactivated with 100% methanol, after which blocking was performed using either 10% fish gelatine (Biotium) or 5% BSA made up in tris buffer saline (TBS), for a minimum of 30 mins. The membrane was left to incubate in the presence of primary antibody either overnight at 4 °C or at room temperature for 2 hrs. After primary antibody incubation was complete the membrane was washed with TBS-0.1% Tween-20

(TBST) 3 times for at least 5 mins, prior to addition of IRDye® 680RD or 800CW (Li-Cor) (Infrared conjugated) secondary antibody (diluted 1:10,000 in TBS). After secondary antibody incubation, a final set of 3 washes were performed with TBST. Imaging of membranes took place using Odyssey CLx imaging system (Li-cor). Analysis of western blot images and quantification of protein signal was conducted using Image Studio Lite™. A list of antibodies used for western blotting and/or immunoprecipitation, catalogue number, dilution/amount used, and species of origin can be found below.

Target Protein/target	Source	Catalogue number/Bleed	Amount (IP) or Dilution (WB)	Stock Conc	Species
Actin	Santa-Cruz	sc-47778	1:2000	0.2mg/ml	Mouse
ASS1	Proteintech	16210-1-AP	1:1000	0.6mg/ml	Rabbit
CMTR1	DSTT	3 rd and 4 th	1:500 (WB), 3µg (IP)	0.33mg/ml	Sheep
CMTR1	Sigma-Aldrich	HPA029954	1:500-1:250	0.5mg/ml	Rabbit
CMTR1	Proteintech	27707-1-AP	3 µg (IP)	0.8mg/ml	Rabbit
CMTR1	Invitrogen	PA5-56316	3 µg (IP)	0.2mg/ml	Rabbit
Phospho-CMTR1	DSTT	3 rd	1:300	0.5mg/ml	Sheep
DHX15	Abcam	ab254591	1:1000	0.08mg/ml	Rabbit
IFIT1	Abcam	ab229083	1:1000	0.08mg/ml	Rabbit
IFIT3	Santa-Cruz	sc-393512	1:500	0.2mg/ml	Mouse
ISG15	Santa-Cruz	sc-166712	1:500	0.2 mg/ml	Mouse
PGAM5	Proteintech	28445-1-AP	1:1000	0.5 mg/ml	Rabbit
RFP	Proteintech	5f8	1:1000	1mg/ml	Rat
Rpb1 (RNA PII)	Cell Signalling	#14958	1:1000	0.1mg/ml	Rabbit
RNA PII S5P	ChromoTek	3E8	1:250	0.2mg/ml	Rat
RNA PII S2P	ChromoTek	3E10	1:250	0.2mg/ml	Rat
RNMT	DSTT	3 rd bleed	1:500	0.5mg/ml	Sheep
SINV Capsid protein	Kindly provided by Dr Alfredo Castello	N/A	1:5000	N/A	Rabbit
TOM20	Proteintech	66777-1-Ig	1:1000	1mg/ml	Mouse
IRDye® 680RD Anti-Mouse IgG	LI-COR Biotechnology	926-68072	1:10000	1mg/ml	Donkey
IRDye® 680RD Anti-Rabbit IgG	LI-COR Biotechnology	926-68073	1:10000	1mg/ml	Donkey
IRDye® 800CW Anti-Rabbit IgG	LI-COR Biotechnology	926-32213	1:10000	1mg/ml	Donkey
IRDye® 680RD Goat anti-Rat IgG	LI-COR Biotechnology	926-68076	1:10000	1mg/ml	Donkey
IRDye® 680RD Anti-Goat IgG (cross reacts with sheep)	LI-COR Biotechnology	926-68074	1:10000	1mg/ml	Donkey

Table 2.1-List of antibodies used in western blotting and immunoprecipitation

A table listing antibodies used in western blotting, target proteins, source, bleed/catalogue number, dilution used, stock concentration, and species of origin. IRDye® 680RD Anti-Goat IgG cross reacts with sheep. DSTT (University of Dundee, Division of signal and transduction therapy), IP (immunoprecipitation), WB (western blot).

2.2.5 Mass spectrometry and data analysis

IP for downstream mass spectrometry analysis was carried out using 2 mg of liver lysate, 3 µg of sheep IgG anti-CMTR1 antibody (from a stock concentration of 0.33 mg/ml), and 20 µl of protein G dynabeads per sample. IP was carried out overnight at 4°C. Washing was carried out using RIPA buffer supplemented with proteinase and phosphatase inhibitors. Upon the final wash, IP samples were eluted in storage buffer (2 M Urea, 100 Mm Ammonium Bicarbonate), then handed over to the CRUK Scotland Institute Proteomics facility for downstream processing and analysis.

On-bead digest was performed by adding 2 M urea in 100 mM ammonium bicarbonate supplemented with 1 mM DTT and 155 ng EndoLysC to the beads, for a 30-minute incubation period at room temperature. This was followed by a second pre-digest step with 155 ng of trypsin under the same conditions. An alkylation step was performed by incubating samples with 5 mM iodoacetamide made up in 2 M urea in 100 mM ammonium bicarbonate for 5 mins at room temperature. A final digest was carried out overnight at 35°C with 150 ng trypsin in 100 mM ammonium bicarbonate and 1 M urea. A stage-tip clean up step was then performed using a C18 empore disk (3M) to remove contaminants. Peptides were run through an Orbitrap Fusion Lumos mass spectrometer (Thermo Scientific) coupled to an EASY-nLC II 1200 chromatography system (Thermo Scientific). Peptides were electrosprayed into the mass spectrometry using a nanoelectrospray ion source (Thermo Scientific). Data was acquired with Xcalibur software (Thermo Scientific) in positive ion detection mode using data dependent acquisition. A full scan mass (MS1) at a range of 350-1550 m/z was undertaken, with the top 10 most intense ions being subject to higher energy collisional dissociation fragmentation for MS2 analysis. Ions that were already selected for MS2 were then dynamically excluded for 30 sec for detection of less abundant peptides.

Raw data was processed using MAXQuant™ version 1.6.3.3 (Cox and Mann, 2008) software and searched against the Uniprot *Mus Musculus* database (Swiss-Prot, 17, 219 entries) using the Andromeda search engine (Cox *et al.*, 2011). Minimum peptide length was set to 7 amino acids and trypsin cleavage was selected to allow for up to 2 missed cleavage sites. False discovery rate was set to 1%. Further processing of the MAXQuant output (e.g. principal component and clustering analysis) was completed using Perseus software version 1.6.15.0. (Tyanova *et al.*, 2016)

2.2.6 BS3 cross linking

Bisulfosuccinimidyl suberate (BS3) (Thermo Fisher) cross linking agent was used to cross link IgG antibody to Protein G dynabeads for immunoprecipitation. Dynabeads were rinsed 2 times in ice-cold PBS prior to incubation with Anti-CMTR1 IgG antibody for 1 hr at room temperature. After this incubation period had elapsed, IgG-coupled dynabeads were washed twice in conjugation buffer (20 mM Sodium phosphate, 0.15 M NaCl (pH 7-9)). 5-0.5 mM of BS3 prepared from a 100 mM stock solution was added to the coupled dynabeads for 30 mins at room temperature. Quenching was carried out by exposing IgG-coupled dynabeads to quenching buffer (1M Tris HCl (pH 7.5)) for 15 mins at room temperature. Beads were then washed a final 3 times with RIPA buffer prior to continuation of IP.

2.2.7 Immunofluorescence

Cells were seeded onto a μ -Slide 8-well chambered coverslip (Ibidi) and left to proliferate for 48 hrs. Fixation was achieved by addition of ice cold 4% Formaldehyde (FA) (Santa-Cruz) diluted in PBS for 20 mins at room temperature, whilst permeabilization was achieved by the addition of 0.5% Triton X-100 (Sigma-Aldrich) diluted in PBS for 5 mins. Blocking was performed by exposing samples to 5% Donkey serum (VWR) diluted in 0.05% PBS-Tween 20 (PBS-T) for 1 hr. Primary antibody was diluted in the same solution used for blocking, and samples incubated overnight at 4°C. After primary antibody incubation 3 washes were performed with PBST for at least 5 mins, followed by a final wash in blocking buffer. Secondary antibodies conjugated to a fluorescent dye were diluted in blocking buffer by a factor of 1:1000 and incubated with the sample for 2 hrs at room temperature. After which, samples were washed 4 times for 5 mins with

PBST and another 3 times with PBS alone. Finally, samples were exposed to Fluoroshield mounting medium with 4',6-diamidino-2-phenylindol (DAPI) (Abcam), to mount and counterstain for DNA as a nuclear marker. Imaging was conducted on a Nikon A1R confocal microscope and processed using the OMERO desktop app. Co-localisation analysis was carried out using the BIOP JACOP (just another co-localization) plugin on ImageJ. Regions of interest were manually selected, and Li's auto-thresholding applied to calculate Mander's and Pearson's correlation coefficient.

Target	Source	Bleed/Catalogue number	Dilution	Stock Conc	Species
CMTR1	DSTT	3 rd bleed	1:100	0.33mg/ml	Sheep
CMTR1	Sigma-Aldrich	HPA029954	1:100	0.5mg/ml	Rabbit
PGAM5	Proteintech	28445-1-AP	1:1000	0.5mg/ml	Rabbit
RNMT	DSTT	3 rd bleed	1:500	0.5mg/ml	Sheep
Anti-rabbit(Alexa 488)	Invitrogen	A-21206	1:1000	2mg/ml	Donkey
Anti-rabbit (Alexa 594)	Invitrogen	A-21207	1:1000	2mg/ml	Donkey
Anti-sheep (Alexa 594)	Invitrogen	A-11016	1:1000	2mg/ml	Donkey

Table 2.2- List of antibodies used in Immunofluorescence

A table listing antibodies used in Immunofluorescence, target proteins, source, bleed/catalogue number, dilution used and species of origin. DSTT= University of Dundee, Division of signal and transduction therapy.

2.3 RNA analysis

2.3.1 RNA extraction

RNA was extracted from cell lines using the GeneJET RNA Purification Kit (Thermo Scientific). For RNA extraction, cells were lysed in buffer supplied in the kit, which was supplemented with 2 M DTT/ml. After addition of 100% ethanol, lysate was transferred to a GeneJet purification column and spun for 1 min at 1200 x g. Wash buffers provided in the kit were then added to the column, with centrifugation being performed at 1200 x g for 1-2 mins between each wash-step. Elution of RNA was achieved using 100 µl of nuclease-free water. Concentration and purity of eluted RNA was determined using a NanoDrop 2000 spectrophotometer (Thermo Scientific). Long term storage of extracted RNA occurred at -80°C.

2.3.2 cDNA synthesis

750 ng of RNA was added to 4 µl of 5x iScript Reaction mix (containing oligo(dT) and random hexamer primers) (BioRad), and 1 µl of iScript Reverse Transcriptase (BioRad), which was made up to a total volume of 20 µl with nuclease-free water. The reaction mix was then incubated in a DNA Engine Dyad PTC0220 Peltier Thermal Cycler (Bio-Rad). The resultant cDNA samples were diluted threefold with nuclease-free water prior to use, or stored at -20°C.

2.3.3 qPCR

For each individual sample analysed by qPCR, 2 µl of a forward and reverse primer mix (10 µM) (Invitrogen) were added to wells, alongside 1 µl of cDNA and 3 µl of SsoFast EvaGreen Supermix (Bio-Rad)). The PCR reaction was performed on a CFX384 Touch Real-Time PCR Detection System (Bio-Rad). Once the reaction was complete, data was exported as cycle threshold (CT) values using CFX manager (Bio-Rad). From the resultant CT values, the relative RNA level of the transcript of interest to the housekeeping gene GAPDH was calculated for normalisation. A list of primer sequences used for qPCR and the target transcripts can be found below. All qPCR experiments within this body of work were performed with cDNA of mouse origin.

Target gene (Mus musculus)	Forward Primer Sequence	Reverse Primer Sequence
IFIT1	GCTACCACCTTTACAGCAACC	GAGGTTGTGCATCCCCAATG
IFIT3	GCAGCACAGAAACAGATCACC	TGGTTGCACACCCTGTCTTC
IFIH1	CTGAGACTGCCCATGACGAG	TACACCTGACTCATTCCCGC
ISG15	ACTCCTTAATTCCAGGGGACCTA	AGTTAGTCACGGACACCAGGA
DHX58	CAAGGTGGTGGTACTGGTCAA	AGAGCTGTTGAGTGCCAAC

Table 2.3- List of primers used in qPCR analysis

A table listing primers used in qPCR analysis, the target gene and forward/reverse sequence of the primers.

2.4 Viral infection and Flow cytometry

2.4.1 Infection

MEF cells were infected with A/Puerto Rico/8/34 (PR8-H1N1) Influenza A virus (IAV) expressing a mCherry reporter gene fused to the viral NS1 gene. mCherry-PR8 IAV colorflu (Fukuyama *et al.*, 2015) was kindly provided by Dr Edward Hutchinson. Cells were seeded the day prior to infection in a 24-well dish, to ensure formation of a confluent monolayer the following day. On the day of infection, a spare well was washed and trypsinised to provide a cell count. This was done to calculate the appropriate volume of virus stock needed to infect cells at a multiplicity of Infection (MOI) of 1. Supplemented DMEM media was removed from cells, followed by washing with PBS. PBS was removed and replaced with serum free DMEM inoculum to prevent FCS mediated inhibition of IAV entry. Cells were incubated for 1 hr at 37°C in the presence of 5% CO₂, after which the inoculum was removed and replaced with supplemented DMEM. Cells were returned to the incubator until 24 hrs had elapsed, then processed for downstream analysis by flow cytometry.

Infection of MEFs with Sindbis virus was conducted using pT7-SvmCherry (SINV-mCherry), kindly provided by Dr Alfredo Castello. pT7-SvmCherry expresses mCherry via insertion of the tag adjacent to a subgenomic promoter in the viral genome. As described above, spare wells were set aside for counting to ensure cells were infected at a multiplicity of infection (MOI) of 0.1, with virus inoculum being prepared in serum free DMEM. Supplemented DMEM was aspirated from cells and replaced with inoculum, with plates being left to incubate for 1hr before removal of the inoculum and re-addition of supplemented DMEM. Cells were then lysed for protein 17 hrs post infection for downstream analysis.

2.4.2 Flow cytometry

Prior to flow cytometry analysis, cells were washed, trypsinised and spun down to create a cell suspension. Cells were resuspended in PBS supplemented with 0.5% w/v BSA and 2 mM EDTA (MACS buffer) containing DAPI (Biolegend) at a concentration of 1 µg/mL. The suspension was filtered through a 70 µm strainer to prevent clumping. Relevant single stained and unstained controls for compensation were also processed. A compensation control for DAPI staining was generated by fixing cells with 4% FA prior to resuspension in PBS supplemented with 1 µg/ml of

DAPI. Once processing was complete, the cell suspension was transferred to either a microcentrifuge tube or a round-bottom polystyrene test tube. Flow cytometry was performed using either a BD LSRFortessa cell analyser (BD Biosciences) or Attune NxT flow cytometer (Invitrogen), the same analyser was used for experimental repeats. FlowJo v 10.9 was used to analyse flow cytometry data.

2.5 Statistical analysis

2.5.1 Statistical analysis

Statistical significance was determined by Student's T-test and statistical testing conducted on GraphPad Prism 10 (Graph Pad Software). Exact P-values are given, where $P < 0.05$ indicates significance and $P > 0.05$ indicates non-significance.

2.5.2 Generation of Kaplan-Meier curves

Clinical data was obtained from the genomic data commons (GDC) data portal, using the cancer genome atlas liver hepatocellular carcinoma (TCGA-LIHC) dataset, comprised of 371 HCC patients. RNA sequencing data counts were extracted, and variance stabilising transformation conducted. The dataset was bifurcated by the median count value to classify patients into those with high or low expression of the protein of interest. Survival curves were compared using a log-rank test.

Chapter 3: Characterisation of CMTR1 in liver

3.1- Introduction

Dysregulation of the inflammatory response, particularly in the context of chronic inflammation has come to the forefront as a driver of tumorigenesis (Correa, 1995, Diao *et al.*, 2001, Ekblom Anders *et al.*, 1990, Coussens & Werb, 2002).

Hepatocellular carcinoma (HCC) is no exception to this, with the majority of HCC cases being preceded by chronic hepatitis (Akinyemiju *et al.*, 2017, Wong *et al.*, 2011, Yu *et al.*, 2018). Regulation and plasticity of gene expression via mRNA translation is a fundamental biological process that underpins survival in all living cells. However, in terms of cancer progression, this is often exploited to promote continuous proliferative and anti-apoptotic signalling (Sager, 1997). Studies conducted in HCC murine models where expression of oncogenes *Myc* (protein name: c-Myc) and *Ctnnb1* (protein name: β -catenin) are dysregulated found that hastening of tumorigenesis occurred upon CMTR1 knock-out (KO) within the liver (Sansom lab, personal communication). Although the underlying mechanism of these observations have yet to be dissected, it can be speculated that the role of CMTR1 in regulation of the innate immune response (Schuberth-Wagner *et al.*, 2015, Habjan *et al.*, 2013, Williams *et al.*, 2020) and gene expression (Liang *et al.*, 2022, Dohnalkova *et al.*, 2023) are of relevance.

To improve understanding of how CMTR1 may influence tumorigenesis, CMTR1 was characterised in models of hepatocyte transformation and liver cancer. This was achieved by determining the expression level of CMTR1 and binding partners, followed by investigation into interactions and phosphorylation status. These experiments were conducted in both organs derived from mouse models of HCC initiation and a human liver cancer cell line (Huh-7). Due to challenges associated with immunoprecipitating CMTR1 from liver extracts, extensive optimisation was performed to produce robust data for downstream mass spectrometry analysis.

3.2- Results

3.2.1 Expression of capping enzymes CMTR1 and RNMT increases when β -catenin and c-Myc are dysregulated in the murine liver

Mutations impacting WNT/ β -catenin signalling pathways are found to occur in 54% of HCC cases (Schulze *et al.*, 2015), whilst aberrant activation of c-Myc is observed in 30-60% of primary HCC patients (Schlaeger *et al.*, 2008). HCC associated mutations in WNT/ β -catenin signalling typically permit for accumulation of β -catenin in the cytoplasm, followed by translocation into the nucleus where the transcription of target genes can occur (Aoki *et al.*, 1999). Target genes of β -catenin include *c-Jun* (Mann *et al.*, 1999), *MYC* (Gekas *et al.*, 2016) and *CCND1* (Cyclin D1) (Shtutman *et al.*, 1999), which encode for oncogenic factors to promote excess proliferation. Over-expression of c-Myc is associated with upregulation of growth signalling pathways alongside inhibition of negative cell cycle regulators, permitting for further contribution towards oncogenic transformation (Dhanasekaran *et al.*, 2022). Genetic aberrations in *Myc* and *Ctnnb1* in isolation are not sufficient to induce HCC without further pro-oncogenic insults but do so over time when dysregulated in tandem (Harada *et al.*, 2002, Tripathy *et al.*, 2018, Molina-Sánchez *et al.*, 2020, Beer *et al.*, 2004).

Samples were obtained from mice of WT, *Ctnnb1*^{ex3/WT} (B), R26-LSL-*Myc* (M), and *Ctnnb1*^{ex3/WT}; R26-LSL-*Myc* (B/M) genetic background (kindly provided by the Sansom lab), 4 and 10 days after induction of cre recombinase expression via an adeno-associated virus vector. *Ctnnb1*^{ex3/WT} mice possess loxP sites flanking exon 3 of *Ctnnb1*, to allow for excision of sequences which permit for protein phosphorylation and mediate β -catenin degradation (Parker and Neufeld, 2020). R26-LSL-*Myc* mice over-express human *MYC* cDNA. Overexpression of human *MYC* in this model is driven by an endogenous Gt(Rosa)26sor promoter and facilitated by removal of a floxed STOP-cassette. These mouse models were selected as they are well-established and possess similar underlying mechanisms of tumour development to human HCC patients (Bisso *et al.*, 2020, Villar *et al.*, 2023, Müller *et al.*, 2022, Preprint).

Western blotting was conducted on WT, *Ctnnb1*^{ex3/WT}, R26-LSL-*Myc*, and *Ctnnb1*^{ex3/WT}; R26-LSL-*Myc* liver lysate 10 days post cre induction with antibodies targeting CMTR1

and RNMT, alongside DHX15 (a negative regulator of CMTR1 (Inesta-Vaquera *et al.*, 2018)). Data obtained from western blotting (Figure 3.1 a) showed that expression of CMTR1 (Figure 3.1 b) and RNMT (Figure 3.1 c) were significantly higher in *Ctnnb1*^{ex3/WT}; R26^{-LSL-Myc} liver lysate compared to WT matched controls. RNMT expression was also significantly higher in R26^{-LSL-Myc} liver. Expression of DHX15 meanwhile was not found to be significantly altered between genotypes (Figure 3.1 d). Although this may be attributed to extensive variation within replicates of the same genotype.

3.2.2 Dysregulation of c-Myc in the liver results in elevated expression and phosphorylation of RNA Pol II.

CMTR1 exerts methyltransferase activity via interaction between its WW domain and the C-terminal domain (CTD) of RNA polymerase II (RNAPII), providing the latter is phosphorylated at YSPTSPS heptad repeats on Serine-5 (S5P) (Inesta-Vaquera *et al.*, 2018). Phosphorylation of S5 occurs during transcription initiation, resulting in recruitment of certain capping enzymes. In most cases, levels of S5P gradually decrease as RNAPII reaches the 3' end of the transcribed gene (Cho *et al.*, 1997). Phosphorylation on Serine 2 (S2P) meanwhile typically occurs during the elongation phase of transcription and is specifically enriched during transcription termination (Cho *et al.*, 2001). Levels of RNAPII expression and phosphorylation status were hence examined in mouse models where *MYC* and *CTNNB1* expression is dysregulated, as these may be indicative of alterations in the extent of CMTR1-RNAPII binding and subsequent capping activity.

Western blotting was conducted on liver protein lysate using antibodies targeting the largest RNAPII subunit Rpb1 (total RNAPII), RNAPII S5P (S5P) and RNAPII S2P (S2P) (Figure 3.2 a). Average expression values for total and phospho-RNAPII at both S5P and S2P sites were approximately 1.5-2-fold higher in R26^{-LSL-Myc} liver lysate where c-Myc alone was dysregulated compared to the WT control.

Meanwhile, in *Ctnnb1*^{ex3/WT}, average expression values of total RNAPII and S5P phosphorylation were comparable to the WT control. The average fold change of signal for S2P phosphorylation in *Ctnnb1*^{ex3/WT}; R26^{-LSL-Myc} liver extract was roughly half the value of the WT control (Figure 3.2 b, c, d). However, none of these differences were found to be statistically significant. To confirm if any trends in

terms of alterations between RNAPII expression and phosphorylation are significant between genotypes, additional replicates may be beneficial.

3.2.3 The Interaction between DHX15 and CMTR1 is preserved in WT and *Ctnnb1*^{ex3/WT}; R26-^{LSL-Myc} mouse liver

DHX15 is a DEAH box helicase and negative regulator of CMTR1, a function which it carries out by inhibiting methyltransferase activity (Inesta-Vaquera et al., 2018). Interaction between CMTR1 and DHX15 is mediated by binding of DHX15's OB fold domain to the G-patch of CMTR1. The biological impact of this interaction has been demonstrated through experiments where G-patch mutations resulted in enhanced translation of CMTR1-dependent genes, particularly those associated with metabolic and cell cycle processes. CMTR1 binding to DHX15 has been demonstrated to occur in HeLa, HCC1806, MCF7 and HEK293 cell lines, but not in cells of liver origin (to the author's knowledge) (Inesta-Vaquera *et al.*, 2018, Toczydlowska-Socha *et al.*, 2018). Although DHX15 expression was not significantly altered in *Ctnnb1*^{ex3/WT}; R26-^{LSL-Myc} liver compared to the WT when determined by western blot (Figure 3.1 a, d), it could not be discounted that the extent of CMTR1-DHX15 interaction was unaltered upon dysregulation of *MYC* or *CTNBB1*.

To determine if this was the case, DHX15 was co-immunoprecipitated (Co-IP'd) from CMTR1 in liver lysate, taken 4 and 10 days after induction of *MYC* and *Ctnnb1* dysregulation via cre recombinase (Figure 3.3 a). These data demonstrated that interaction between CMTR1-DHX15 is preserved in the liver. When this experiment was conducted in biological triplicate using lysate taken 10 days post-induction only, there was no substantial change in the amount of DHX15 being purified with CMTR1 between genotypes, even when accounting for differences in CMTR1 antigen retrieval amongst replicates (Figure 3.3 b).

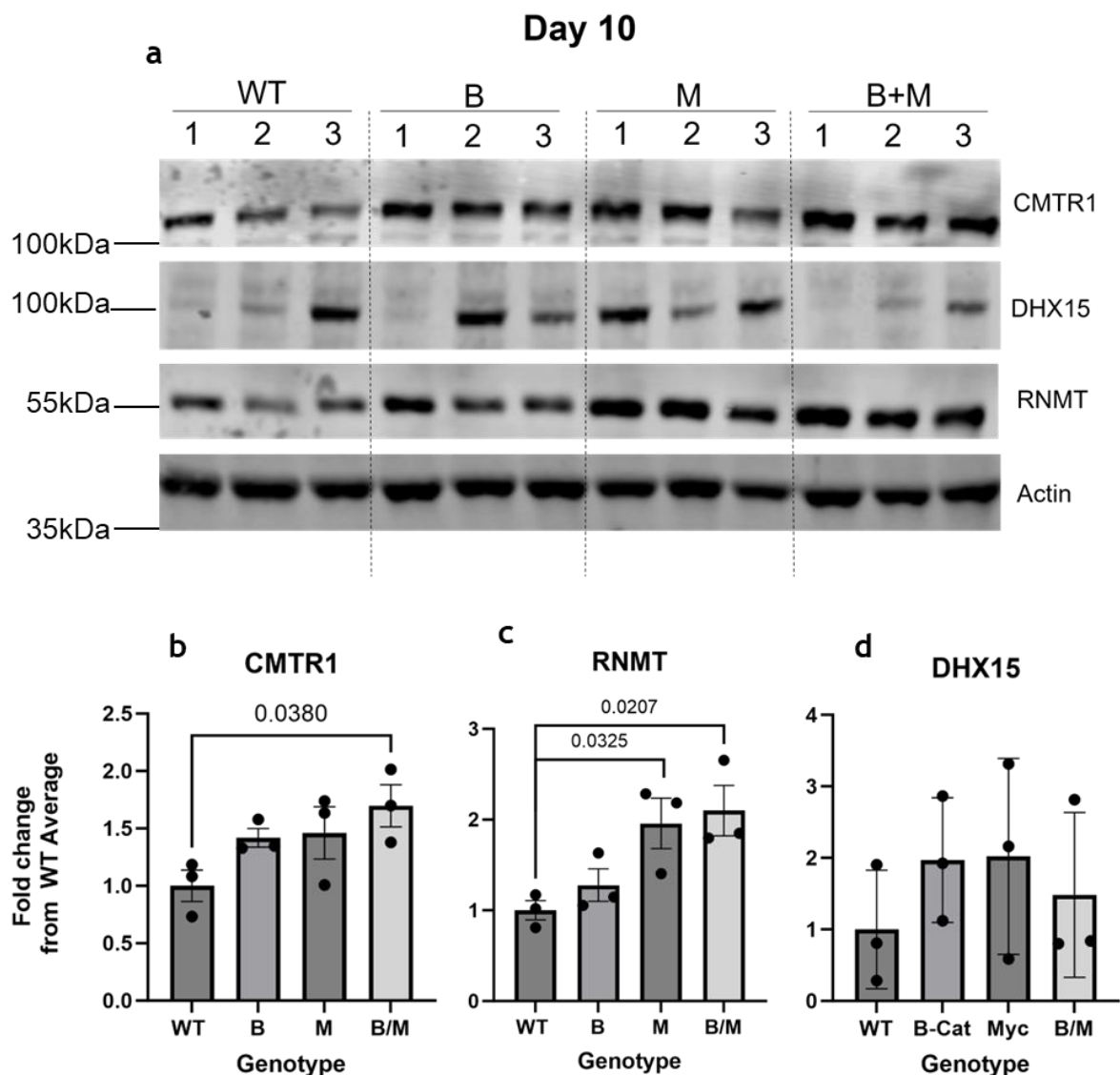


Figure 3.1-Expression of capping enzymes CMTR1 and RNMT is significantly increased in B/M liver compared to WT controls.

Western blotting was conducted using 20 μ g of liver lysate obtained from WT, B, M, and B/M mice, 10 days post induction of oncogenes via AAV-Cre, in triplicate. Western blotting analysis was carried out using antibodies for capping enzymes, RNMT and CMTR1 and CMTR1 binding partner DHX15, as indicated on the right side of the panel. Molecular weight is indicated on the left side of the panel. Actin was used as a loading control (a). Quantification of signal for each sample and protein of interest was normalised in comparison to the average WT signal (b, c, d). Student's t-test was performed to determine significance between genotypes regarding protein expression. Quantification was carried out using Image Studio™ Lite (Li-Cor). N=3. Bars show the mean value, with error bars depicting the SEM, each point represents an individual replicate. WT (Wild type), B (Cttnb1(ex3)), M (R26-LSL-Myc), B/M (Cttnb1(ex3)/R26-LSL-Myc), AAV-Cre (Adeno-associated virus cre), RNMT (RNA Guanine-7 Methyltransferase), CMTR1 (Cap Methyltransferase 1), DHX15 (DEXH-Box helicase 15), SEM (Standard error mean)

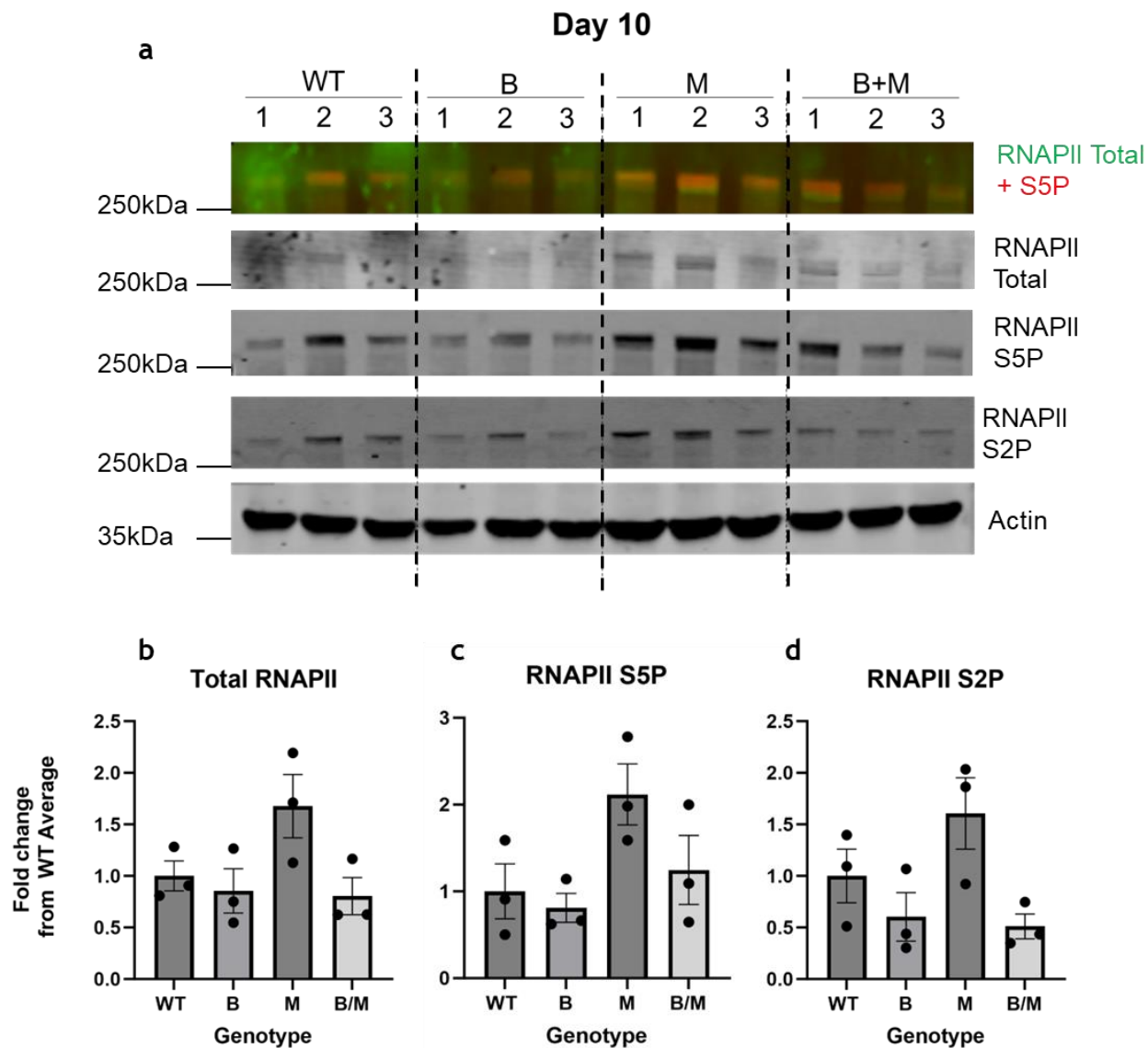


Figure 3.2-Expression and phosphorylation of RNAPII is on average high in liver extract where MYC alone is dysregulated.

Western blotting was conducted using 20 μ g of liver lysate obtained from WT, B, M, and B/M mice, 10 days post induction of oncogenes via AAV-Cre in triplicate. Western blotting analysis was carried out using antibodies for total and phosphorylated RNAPII, as indicated on the right side of the panel. Total and S5P RNAPII were visualised on the same blot using separate channels through use of Li-Cor secondary antibodies conjugated to near-infrared fluorescent dyes of different wavelengths. Primary RPB-1 (total RNAPII) antibody was targeted for detection by IRDye[®] 800CW donkey anti-Rabbit IgG secondary antibody and visualised in green when overlaid, primary 5SP antibody was targeted for detection by IRDye[®] 680RD goat anti-Rat IgG secondary antibody and visualised in red when overlaid (a). Molecular weight is indicated on the left side of the panel. Actin was used as a loading control (a). Quantification of signal for each sample and protein of interest was normalised in comparison to the average WT signal (b, c, d). Students t-test was

performed to determine significance between genotypes regarding protein expression. Quantification was carried out using Image Studio™ Lite (Li-Cor). N=3. Bars show the mean value, with error bars depicting the SEM, each point represents an individual replicate. WT (wild type), B (Ctnnb1(ex3)), M (R26-LSL-Myc), B/M (Ctnnb1(ex3)/R26-LSL-Myc), AAV-Cre (adeno-associated virus), RNAPII (RNA Polymerase II), SEM (standard error mean)

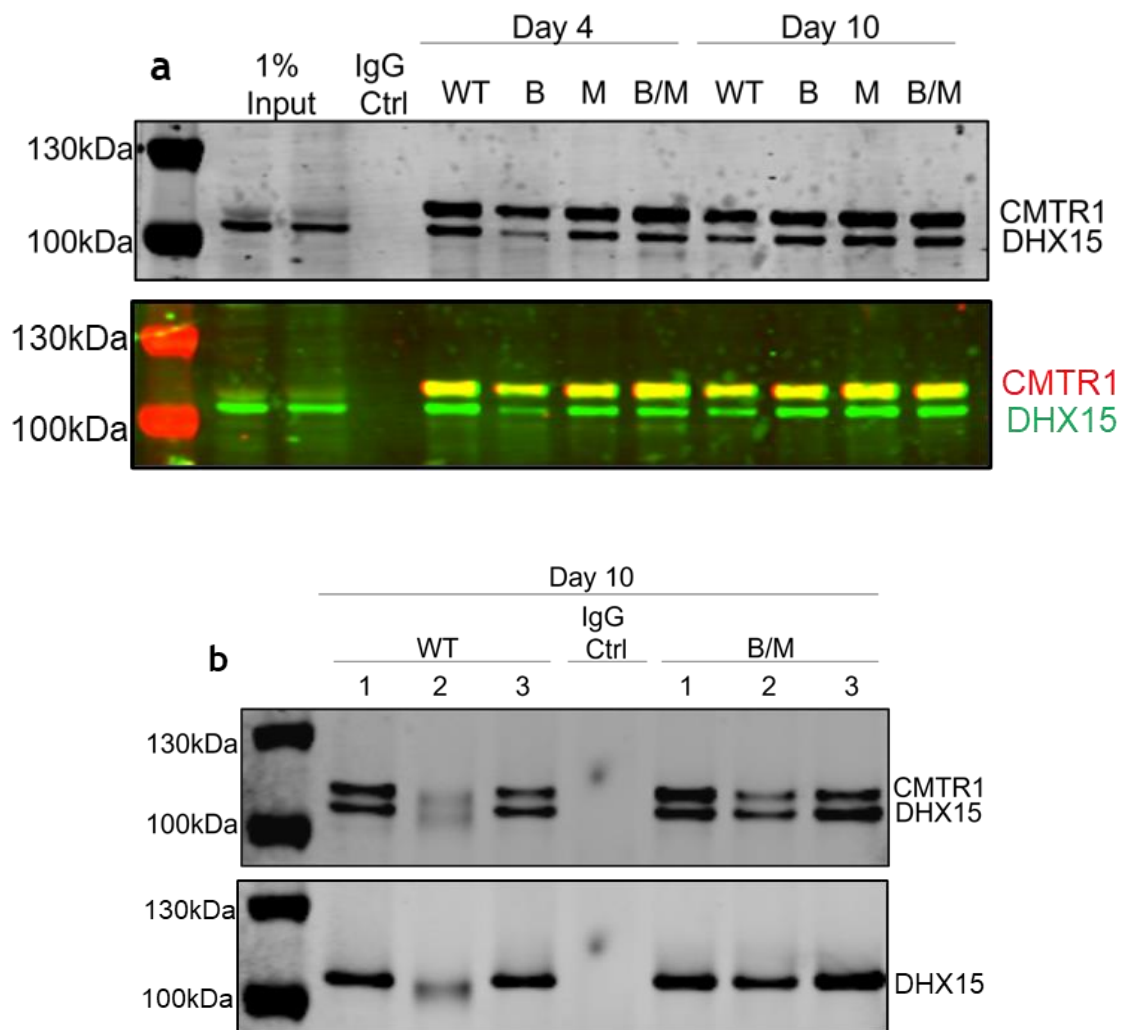


Figure 3.3-The interaction between DHX15 and CMTR1 is preserved in WT and B/M liver.

IIP was carried out using 2 mg of liver lysate and 2 µg of sheep IgG anti-CMTR1 antibody, an isotype and species matched non-specific antibody was used as a control to confirm specificity of the interaction. Liver lysate was obtained from WT, B, M, and B/M mice, both 4- and 10-days (a, b) post induction of oncogenes via AAV-Cre. Post-IP input samples of 10 µg were loaded alongside the IP, with ¼ of the IP being loaded per sample. Western blotting was then conducted for CMTR1 and DHX15. CMTR1 and DHX15 were visualised on the same blot using separate channels through use of Li-Cor secondary antibodies conjugated to near-infrared fluorescent dyes of different wavelengths.

Primary CMTR1 antibody was targeted for detection by IRDye® 680RD donkey anti-rabbit IgG secondary antibody and visualised in red when overlaid, primary DHX15 antibody was targeted for detection by IRDye® 800CW donkey anti-Rabbit IgG secondary antibody and visualised in green when overlaid (a). For Figure 3.3 b, the same secondary antibody (IRDye® 680RD donkey anti-rabbit IgG) was used to visualise DHX15 and CMTR1 (b). Molecular weight is indicated on the left side of the panel. For Figure 3.2 a N=1, for Figure 3.2 b N=3. IP (Immunoprecipitation), CMTR1 (Cap Methyltransferase 1), WT (Wild type), B (Ctnnb1^{ex3/WT}), M (R26^{-LSL-Myc}), B/M (Ctnnb1^{ex3/WT}; R26^{-LSL-Myc}), AAV-Cre (Adeno-associated virus cre), DHX15 (DEAH-Box Helicase 15)

3.2.4 Phospho-CMTR1 cannot be detected in murine liver lysate.

Phosphorylation of CMTR1 (P-CMTR1) is mediated by Casein kinase 2 activity (CK2) and occurs at 15 sites within the N-terminal domain of CMTR1, termed the P-Patch. Binding between CMTR1 and the CTD of RNAPII is enhanced by P-CMTR1, with expression of a phosphodeficient mutant accompanying reductions in CMTR1-dependent gene expression (Lukoszek *et al.*, 2024).

Given the relevance of P-CMTR1 in gene expression, the phosphorylation status of CMTR1 in WT and Ctnnb1^{ex3/WT}; R26^{-LSL-Myc} liver was determined. This was conducted by performing CMTR1-IP, followed by blotting with antibody raised against the S28, T30 and S31 phospho-sites of P-CMTR1. As this antibody had successfully detected P-CMTR1 in HeLa cells previously, these were used as a positive control.

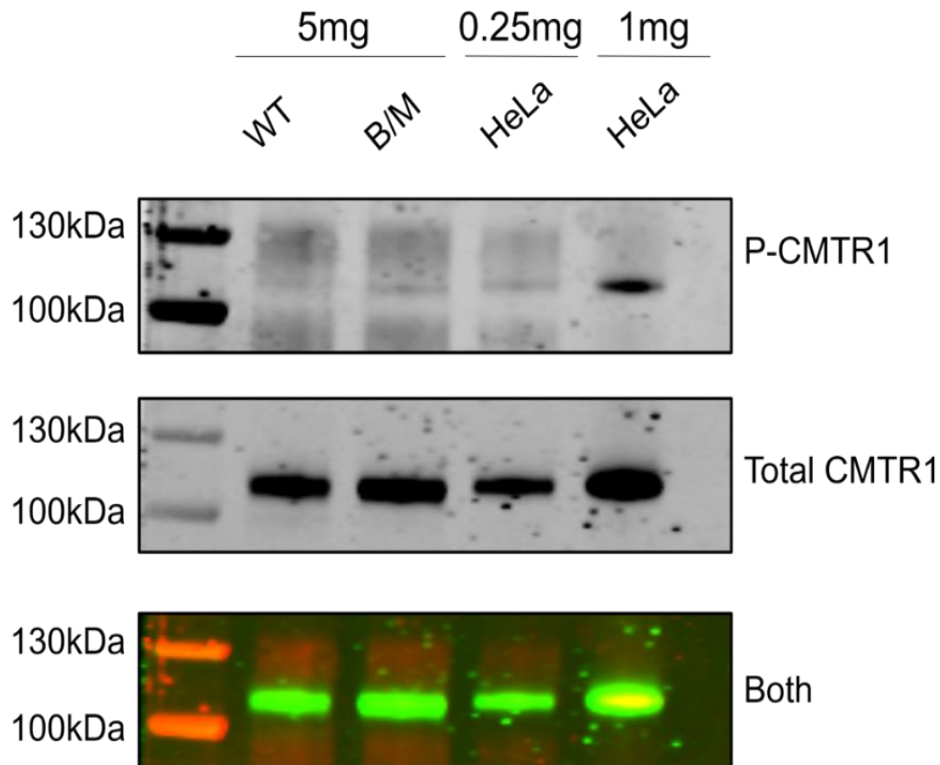


Figure 3.4-Phospho-CMTR1 cannot be detected in murine liver extract

Immunoprecipitation was carried out using 5 mg of liver lysate and 2 μ g of sheep IgG anti-CMTR1 antibody, Liver lysate was obtained from WT and B/M mice 10-days post induction of oncogenes via AAV-Cre. 0.25 and 1 mg of lysate from HeLa cell lines was also used in to produce a comparative signal for CMTR1. Western blotting was then conducted for CMTR1 and P-CMTR1, molecular weight is indicated on the left side of the panel. N=2. IP (Immunoprecipitation), WT (Wild type), B/M (*Ctnnb1^{ex3/WT}; R26^{-LSL-Myc}*), CMTR1 (Cap Methyltransferase 1), AAV-cre (Adeno-associated virus-cre), P-CMTR1 (Phospho-CMTR1)

P-CMTR1 was found to be below the limit of detection when Immunoprecipitation followed by western blotting (IP/WB) of CMTR1 was performed, using 5mg of WT or *Ctnnb1^{ex3/WT}; R26^{-LSL-Myc}* liver lysate. This was despite a distinct band appearing when IP/WB was performed using HeLa cell extract (Figure 3.4). Mass spectrometry performed downstream of CMTR1-IP (IP/MS) also failed to detect any CMTR1 phosphorylation sites consistently (data not shown). Together these data suggest that phosphorylation of CMTR1 is either low or absent in liver.

3.2.5 CMTR1 expression is predominantly nuclear in Huh-7, an HCC derived cell line.

CMTR1 is generally characterised as a nuclear protein, which is unsurprising given that 2'-O-ribose methylation occurs during interaction with RNAPII (Smietanski *et al.*, 2014). Immunostaining conducted on HeLa and embryonic stem (ES) cells demonstrated that CMTR1 is localised to the nucleus, with no signal being detected in cytoplasmic compartments (Dr Joana Silvia, PhD thesis, Liang *et al.*, 2022). Immunostaining performed on cortical mice neurons conducted by Lee *et al.* meanwhile shows that whilst CMTR1 is predominantly localised in the nucleus, a limited degree of cytoplasmic staining can also be noted (Lee *et al.*, 2020).

To ascertain if previous findings on CMTR1 localisation were applicable to liver cells, immunostaining was conducted on Huh-7 (Hepatoma derived) cell lines. Two separate CMTR1 antibodies were used for staining, one purchased from Sigma-Aldrich and one generated by the Division of Signalling Transduction therapy at the University of Dundee (DSTT). Both CMTR1 antibodies display similar patterns of staining, giving confidence to the validity of the results. In accordance with previous findings in mice neurones, CMTR1 displays predominantly nuclear staining in HCC cells, with weak cytoplasmic signal present (Figure 3.5). The data obtained disagrees with findings in HeLa and ES cells, potentially suggesting a distinct biological role for CMTR1 in the cytoplasm of specific cell lines.

3.2.6 CMTR1 antibodies purified from different sheep bleeds bind to CMTR1 equivalently in liver lysate.

Once initial exploration of CMTR1 protein expression and interactions had been conducted, further characterisation of the CMTR1 liver interactome was attempted via mass spectrometry. To meet this goal, optimisation of CMTR1 immunoprecipitation (CMTR1-IP) was implemented. The first step of this optimisation process involved determining the optimal antibody to use for CMTR1-IP, specifically by taking the bleed and affinity ligand used for purification into account.

Production of polyclonal antibodies involves immunizing the chosen host species with the target antigen, followed by bleeding of the animal to obtain antibody. Multiple bleeds are usually taken from the individual animal over time to achieve

peak antibody titre and tend to vary in terms of concentration and specificity (Leenaars & Hendriksen 2005). Purification of antibodies from these bleeds is typically conducted by a process termed antigen-specific affinity purification, where immobilised antigen is used as an affinity ligand attached to a solid matrix (Huse *et al.*, 2002). It should be emphasised that the affinity ligand used for purification is not required to be the same antigen used during the immunization process. In this case, whilst recombinant human full length CMTR1 was used for immunisation, sheep bleeds were purified against both human and mouse recombinant CMTR1.

To determine if antibody bleed and antigen used for purification impacted CMTR1 retrieval in mouse liver, IP/WB was performed. A commercial antibody purchased from Proteintech (PT) was also tested simultaneously. All antibodies, excluding the PT antibody were able to successfully IP CMTR1 from WT mouse liver, and did so to a similar extent. Visually, the antibody obtained from the 3rd bleed which was purified against human CMTR1 antigen (anti-human CMTR1 antibody) produced the strongest signal (Figure 3.6). For this reason, all follow-up CMTR1-IP experiments were carried out using 3rd bleed anti-human CMTR1 antibody.

3.2.7 Use of BS3 cross-linking agent substantially reduces CMTR1 retrieval from murine Liver

Two key issues intrinsic to IP/MS involve contamination of elution fractions with antibody chains and nonspecific protein interaction with the isolation matrix (Jensen *et al.*, 2021). Bissulfosuccinimidyl suberate (BS3) is a crosslinking agent which covalently links the Fc region of Immunoglobulin G (IgG) to protein G beads, by reacting with amines from lysine side chains and protein N-termini (Belsom and Rappsilber 2021). To negate potential issues during data analysis that may arise from antibody contamination, crosslinking of antibody-bead conjugates was attempted with 5 mM of BS3 (the concentration recommended by the manufacturer). This was followed by IP/WB to visualise antigen retrieval. Additionally, another commercial antibody raised against CMTR1 and purchased from Invitrogen (IV) was tested for use in CMTR1-IP concurrently.

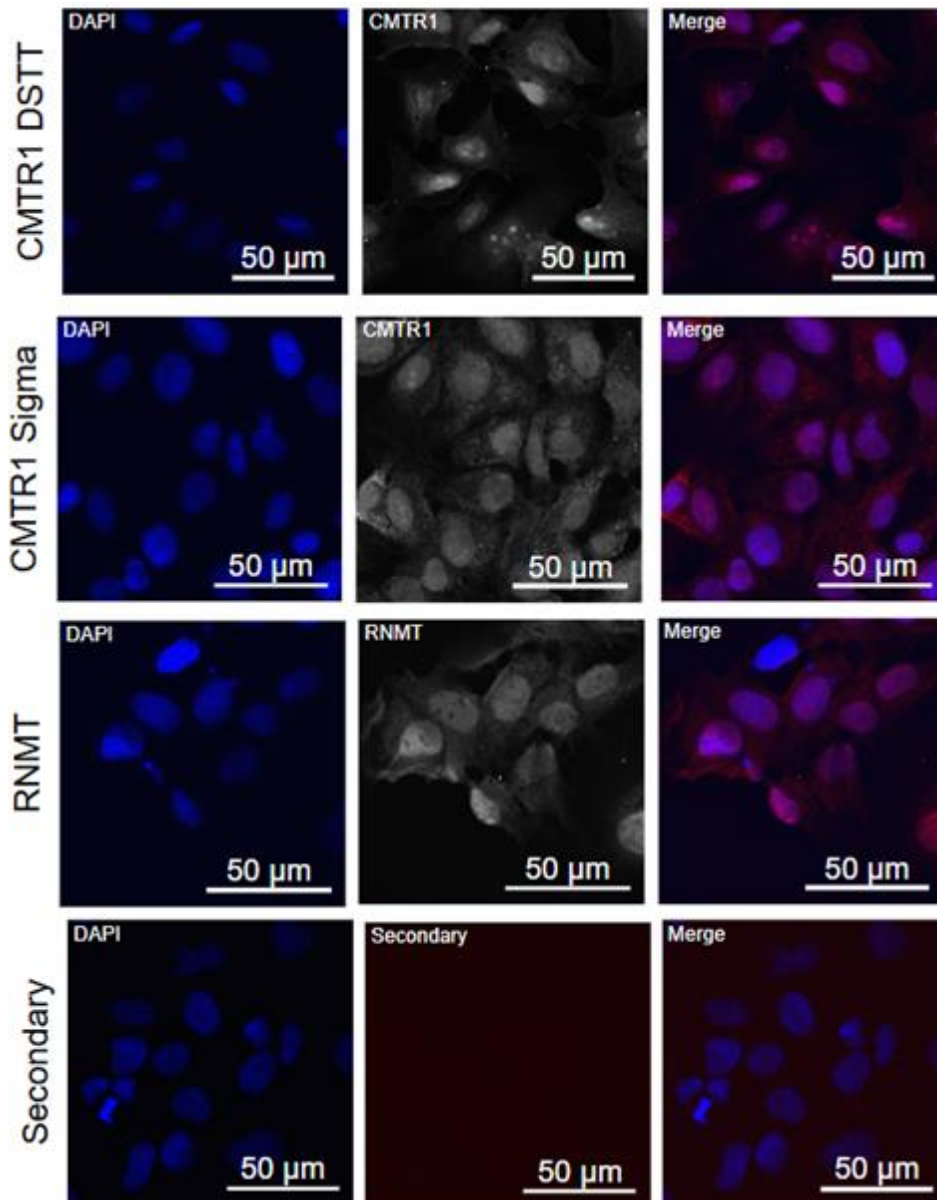


Figure 3.5-CMTR1 expression is predominantly nuclear in Huh-7 cancer cell lines

Huh-7 Cell lines were fixed in 4% FA before subsequently being permeabilised with 0.1% Triton X-100 and stained with antibodies targeting CMTR1 or RNMT as indicated (both shown in red or monochrome). Two separate CMTR1 antibodies, one raised in sheep (DSTT), and another raised in rabbit (Sigma-Aldrich) were used to validate staining specificity. anti-RNMT antibody (DSTT) (IgG, raised in sheep) was used to stain for RNMT. As this RNMT antibody had been extensively used for IF staining previously in the lab, it was used as a positive control. Samples were also DAPI (shown in blue) stained to visualise the nuclear compartment. A secondary only control was generated by treating Huh-7 cells with only anti-sheep and anti-rabbit Alexa 594 secondary antibody. Imaging was performed on the Nikon A1R and analysed with Omero. Scale bars represent a 20µm distance. Images taken on 20 x objective. For CMTR1 DSTT staining N=3. FA (Formaldehyde), CMTR1 (Cap Methyltransferase), RNMT (RNA Guanine-7 Methyltransferase), DSTT (Division of signal transduction therapy, University of Dundee), IF (Immunofluorescence), DAPI (4',6-diamidino-2-phenylindol)

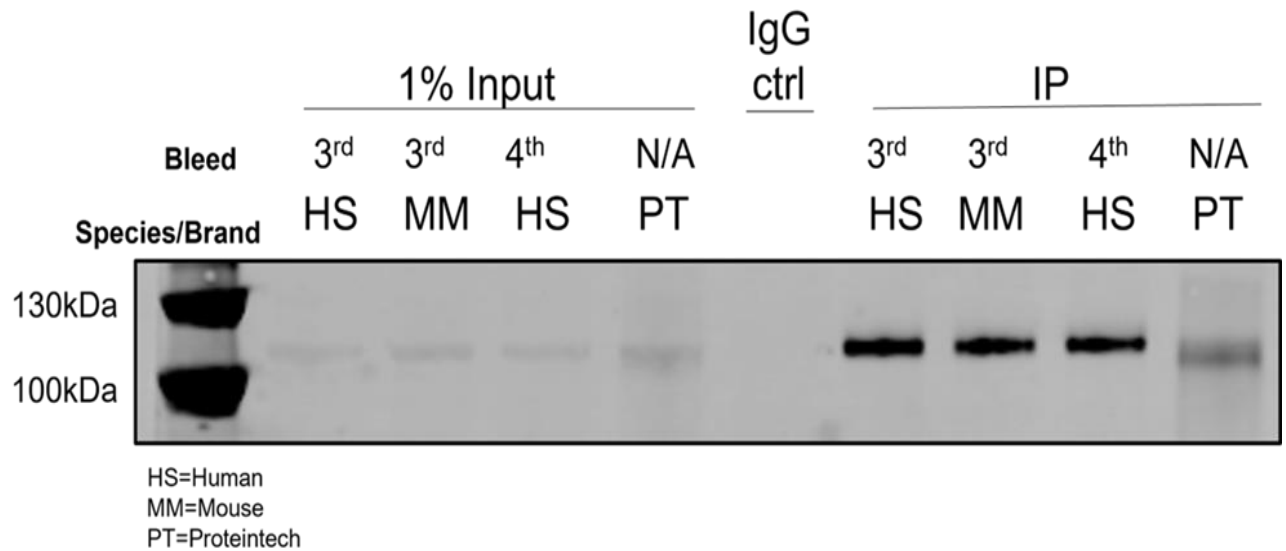


Figure 3.6-CMTR1 antibodies purified from different sheep bleeds bind to CMTR1 equivalently in liver extract

IP was carried out using 2 mg of liver lysate from WT mice and 2µg of sheep IgG anti-CMTR1 antibody obtained from either the 3rd or 4th bleed, which were purified on a column against beads bound to antigen of either human or mouse origin, as indicated. In addition to this, IP was trialed using rabbit anti-CMTR1 antibody purchased from Proteintech . An isotype matched non-specific antibody was used as an IgG control to confirm specificity of the interaction. Post IP-input samples of 10 µg were loaded alongside the IP, with ¼ of the IP being loaded per sample. Western blotting was then conducted for CMTR1, the molecular weight is indicated on the left side of the panel. N=2. IP (Immunoprecipitation), WT (Wild type), CMTR1 (Cap Methyltransferase 1), HS (Human), MM (Mouse), PT (Proteintech)

It was found that the use of 5 mM BS3 dramatically reduced CMTR1 retrieval from WT mouse liver compared to the negative control. The IV antibody also failed to successfully IP CMTR1 from mouse liver and was discarded as a potential candidate for use in CMTR1 IP/MS (Figure 3.7 a). To reduce the impact of cross-linking on CMTR1 retrieval, crosslinking was repeated using 0.5 mM BS3. Whilst CMTR1 retrieval improved when 0.5 mM BS3 was used compared to 5 mM, the resultant signal was still considerably lower than the non-treated control (Figure 3.7 b). IP/MS experiments showed that the number of individual proteins identified fell by almost half when cross-linking was performed with 0.5 mM BS3, with only 30 interactors being identified in the crosslinked dataset compared to 56 in the control. Overlap between the datasets produced by the experimental condition and control was also poor, with only 3 proteins being identified in both.

Data from the literature shows utilisation of BS3 as a crosslinking agent reduces non-specific binding of proteins to the isolation matrix, enhancing specificity (Sousa *et al.*, 2011). This may account for the reduced number of CMTR1 interactors detected in the crosslinked dataset. However, as IP/MS was intended to be carried out only as a method of signposting unique CMTR1 interactors in the liver; extensive validation of binding partners would still be necessary, regardless of any improvement in specificity. Furthermore, despite concerns, it was found that antibody chain contamination in non-crosslinked samples did not significantly impede downstream analysis (Kelly Hodge, personal communication). For these reasons, it was decided that cross linking was dispensable in this scenario and that antigen retrieval would be prioritised. Consequently, all subsequent downstream CMTR1 IP/MS experiments were conducted without BS3.

3.2.8 DTT does not substantially impact CMTR1 retrieval but does reduce the number of binding partners identified in proteomic analysis.

Dithiothreitol is a reducing agent which targets disulphide bonds between cysteines and is commonly used to disrupt higher protein structures for biological analysis (Alliegro, 2000). Previous work carried out in the lab has identified that supplementation of lysis buffer with 5mM DTT is necessary to preserve the interaction between RNAPII and CMTR1 (personal communication, Professor Victoria Cowling). However, manufacturers of protein G dynabeads warn against its use due to off-target effects, such as the denaturation of antibody-bead conjugates and certain protein complexes (Thermo Fisher, Dynabeads® Co-Immunoprecipitation Kit manual).

To ascertain whether DTT had a deleterious effect on CMTR1 retrieval, CMTR1 IP was performed using both RIPA buffer supplemented with 5 mM DTT (RIPA + DTT) and RIPA buffer where no DTT was added (RIPA - DTT). IP/WB showed that the addition of DTT had little effect on the amount of CMTR1 retrieved (Figure 3.8 a). However, when IP/MS was performed a lower number of potential binding partners were identified upon DTT supplementation (Figure 3.8 b), with 52 interactors identified in the RIPA - DTT dataset compared to only 40 in the RIPA + DTT dataset.

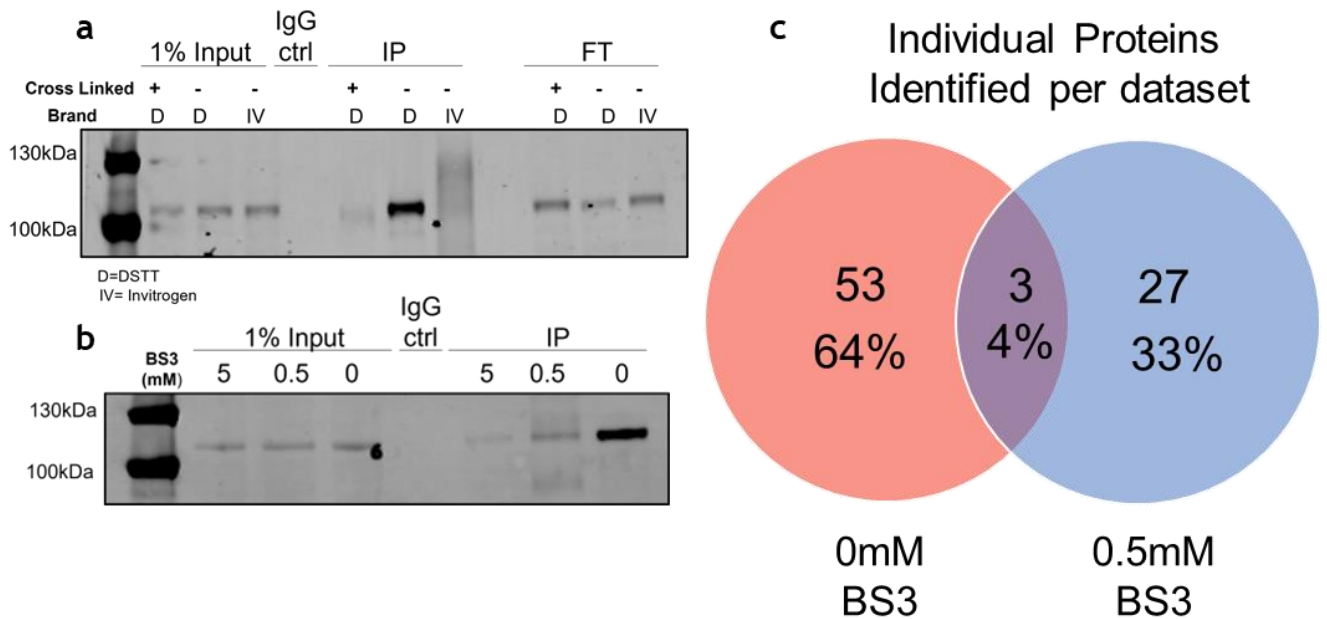


Figure 3.7-Use of BS3 cross-linking agent appears to substantially reduce antigen retrieval of CMTR1 in murine liver.

IP was carried out using 2 mg of liver Lysate obtained from WT mice and 2 μ g of sheep IgG anti-CMTR1 antibody (DSTT, abbreviated as D), in addition to this rabbit IgG anti-CMTR1 antibody purchased from Invitrogen (IV) was also trialled to determine if this could successfully IP CMTR1 (a). Antibody was crosslinked to Protein G magnetic beads using either 5 mM BS3 or the concentration of BS3 stated. Post IP-input samples of 10 μ g were loaded alongside the IP, with $\frac{1}{4}$ of the IP being loaded per sample, 10 μ g of flow through was also loaded (a). Downstream mass spectrometry was conducted on samples treated with sheep IgG anti-CMTR1 antibody cross-linked to Protein G magnetic beads using 0.5 mM BS3 and a non-cross-linked control. A Venn diagram depicts the number of individual proteins identified and the overlap between the two data sets generated by each sample (c). N=2. IP (immunoprecipitation), WT (wild type), DSTT/D (Division of signal transduction therapy, University of Dundee), IV (Invitrogen), FT (flow through), BS3 (Bis(sulfosuccinimidyl)suberate).

These data suggest that whilst DTT supplementation does not affect antigen retrieval of CMTR1, it may interfere with interactions between CMTR1 and other proteins. As this was the case, it was decided that CMTR1-IP should be subsequently performed in the absence of DTT. Adding to this decision was the observation that RNAPII failed to Co-IP with CMTR1 in any dataset, regardless of DTT supplementation (data not shown).

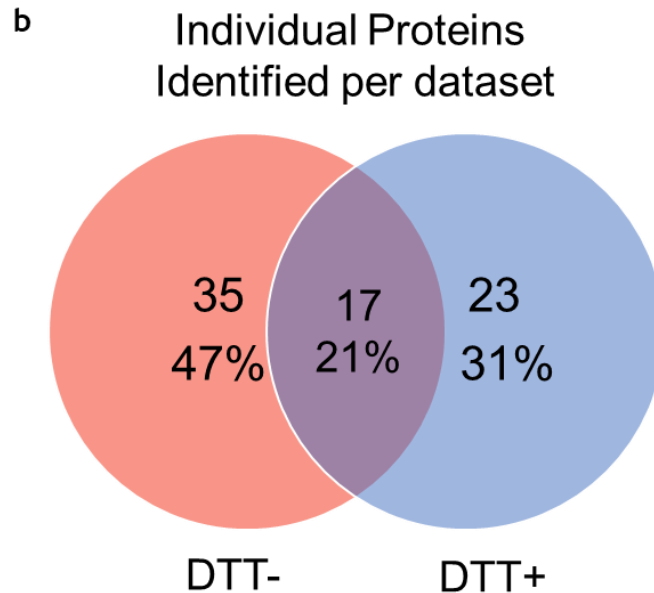
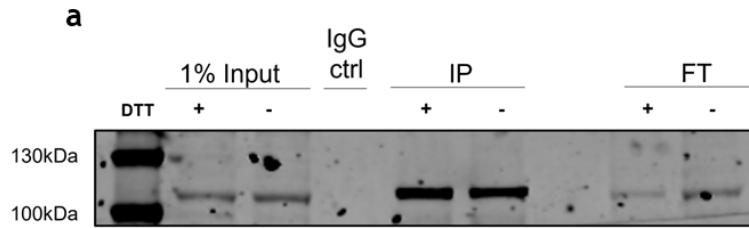


Figure 3.8- DTT does not appear to substantially impact antigen retrieval but does reduce the number of binding partners identified in proteomic analysis.

IP was carried out using 2 mg of liver Lysate obtained from WT mice and 2 μ g of sheep IgG anti-CMTR1 antibody. Liver was either lysed in RIPA buffer supplemented with 5 mM DTT (with washes being carried out with the same buffer), or RIPA buffer where no DTT was added. Post IP-input samples of 10 μ g were loaded alongside the IP, with $\frac{1}{4}$ of the IP being loaded per sample, 10 μ g of flow through was also loaded (a). Downstream mass spectrometry was then conducted on these samples. A Venn diagram depicts the number of individual proteins identified and the overlap between the data sets generated by each condition (b). N=2. IP (Immunoprecipitation), WT (Wild type), CMTR1 (Cap methyltransferase 1), RIPA (Radioimmunoprecipitation assay buffer), DTT (Dithiothreitol), FT (Flow through).

3.3- Discussion

The work described in this chapter sought to investigate CMTR1 expression, interaction, modification, and localisation in the liver. Expression of CMTR1, RNMT and RNAPII were altered in mouse models of HCC, compared to WT controls. However, protein levels of DHX15, a negative regulator of CMTR1 were unchanged. To investigate the presence and extent of CMTR1-DHX15 interaction, IP/WB was performed, which confirmed the occurrence of the interaction in liver. Phosphorylation of CMTR1 P-patch could not be detected in liver lysate by IP/WB or IP/MS, implying it is minimal or absent in hepatic cells. CMTR1 is primarily localised to the nucleus in Huh-7 cells. However, weak staining can be seen in the cytoplasm, which may suggest a specific role for CMTR1 in this compartment. The possible significance of these findings is discussed below.

3.3.1 Expression of CMTR1 and RNAPII in WT and *Ctnnb1*^{ex3/WT}; R26-^{LSL-Myc} liver

As shown in the results section, expression of CMTR1 and RNMT are significantly higher in *Ctnnb1*^{ex3/WT}; R26-^{LSL-Myc} livers compared to WT controls. RNMT protein signal is also considerably increased in R26-^{LSL-Myc} liver, regardless of the status of *Ctnnb1*. It may be the case that these observed increases in capping enzyme expression occur to facilitate and promote translation, particularly of pro-oncogenic transcripts in a manner which promotes initiation and maintenance of tumour cells.

Overexpression of RNMT has been previously demonstrated to enhance cap methylation and translation of Cyclin D1 transcripts (Cowling, 2010). Enhanced expression of Cyclin D1 is associated with poor outcomes in HCC (Nishida *et al.*, 1994), with induction of Cyclin D1 in mouse models being sufficient to initiate liver cancer in the absence of other drivers (Deane *et al.*, 2001). This information suggests that increases in RNMT noted in *Ctnnb1*^{ex3/WT}; R26-^{LSL-Myc} and R26-^{LSL-Myc} liver may contribute to HCC by promoting expression of specific oncogenes such as Cyclin D1. However, interrogation of the transcriptome will be required to confirm this.

CMTR1 has been demonstrated to specifically enhance translation of genes enriched for GO terms associated with the cell cycle, DNA damage responses, metabolic enzymes, and focal adhesion-associated molecules (Inesta-Vaquera *et*

et al., 2019). All of which have functions associated with pro-oncogenic processes (Groelly *et al.*, 2022, Tenen *et al.*, 2021, Murphy *et al.*, 2020). In addition to these observations, siRNA CMTR1 knock-down (KD) has been shown to reduce proliferation in two independent mammary epithelial tumour lines (Inesta-Vaquera *et al.*, 2018). Whilst in Colorectal cancer models KD of CMTR1 was demonstrated to suppress cell proliferation via inhibition of RNAPII recruitment to the STAT3 promoter (You *et al.*, 2023). Beyond the ability of CMTR1 to regulate gene expression, the role of capping in regulation of innate immunity should not be discounted when discussing tumorigenicity. The Cap-1 structure acts as a means for pattern recognition receptors (PRR's) such as RIG-I and MDA5 to differentiate endogenous and exogenous nucleic acid, inhibiting aberrant activation of the IFN response and IFIT mediated translational repression (Züst *et al.*, 2011, Schuberth-Wagner *et al.*, 2015, Williams *et al.*, 2020). Whilst it is true that chronic IFN exposure may exert proliferative effects (Asao & Fu, 2000), it also possesses numerous tumour suppressor functions (Lee *et al.*, 2017, Maeda *et al.*, 2014, Diamond *et al.*, 2011). Hence, it stands to reason that high levels of CMTR1 expression may be exploited by cancer cells to avoid immune activation. The above information provides an explanation as to why we find CMTR1 to be upregulated in HCC models and offers insight into how this may contribute to liver cancer development.

In order to determine if increases in capping enzyme protein levels favour expression of pro-oncogenic transcripts in a liver context, RNA sequencing on liver tissue or HCC cell lines where CMTR1/RNMT is depleted or overexpressed may be beneficial. CMTR1 has been previously found to promote expression of specific genes by recruiting RNAPII to transcription start sites (Liang *et al.*, 2022). Hence, performing CHIP-Seq analysis in the aforementioned models may also be of use in ascertaining if and how CMTR1 influences expression of oncogenic factors.

On average, higher levels of RNAPII expression and phosphorylation are observed in R26-^{LSL-Myc} liver. This may act synergistically when combined with enhancements in CMTR1 expression, as interaction with RNAPII at 5'P is indispensable for cap methylation (Ho & Shuman, 1999). Upregulation of average RNAPII 5'P expression values in the c-Myc dysregulated model is not particularly surprising, given that c-

Myc has been previously demonstrated to promote phosphorylation at this site, as a regulatory mechanism of capping activity. (Cowling & Cole, 2009). Taken together with CMTR1's potential tumorigenic role in promoting expression of specific genes, these data suggest that regulation of 2'O-methylation may act as one of many means by which c-Myc carries out its oncogenic functions.

Another observation of note is the fact that the average value of signal for phosphorylation of RNAPII at S2P was considerably lower in *Cttnb1*^{ex3/WT}; R26-^{LSL-Myc} liver compared to the WT. This is of interest as low levels of RNAPII S2P are associated with transcription termination defects (Collin *et al.*, 2019). Termination defects have been found to correlate with worse outcomes in renal carcinoma patients, by contributing to aberrant transcriptional readthrough in a manner which promotes oncogene expression (Grosso *et al.*, 2015). Thus, it may be the case that low levels of S2P contribute to tumorigenesis in the *Cttnb1*^{ex3/WT}; R26-^{LSL-Myc} model alongside upregulation of CMTR1 and RNMT.

Although speculation can be made regarding the biological relevance of differences in RNAPII expression and phosphorylation, it should be emphasised that none of the differences between *MYC/Cttnb1* dysregulated liver and WT liver extracts were found to be statistically significant. For this reason, it may be beneficial to carry out additional repeats. Alternatively, this experiment could be conducted in hepatic tumour cell lines, as this would permit for synchronisation to be performed and control for variations in RNAPII phosphorylation and capping which result from cell cycle phase (Aregger *et al.*, 2016, Oelgeschläger, 2002).

3.3.2 CMTR1-DHX15

Our data demonstrates that the DHX15-CMTR1 interaction is maintained in the liver and does not appear to be substantially altered in *Cttnb1*^{ex3/WT}; R26-^{LSL-Myc} liver compared to WT controls. Despite being a negative regulator of CMTR1 activity, the extent of CMTR1-DHX15 binding in *Cttnb1*^{ex3/WT}; R26-^{LSL-Myc} liver is unchanged even when CMTR1 expression is increased, when compared to WT controls. This lends further credence to the idea that capping activity of CMTR1 may be enhanced in an HCC context.

DHX15 itself appears to have contradictory roles in promotion and inhibition of cancer, dependent on tumour origin. For example, whilst in prostate cancer DHX15

is associated with progression to castration resistance (Xu *et al.*, 2019); In glioma DHX15 expression suppresses tumour formation in xenograft models, which may be attributed to inhibition of NF- κ B target and splicing gene expression (Ito *et al.*, 2017). Information concerning the role of DHX15 in HCC specifically is by no means extensive, but one study has implicated this protein in the inhibition of cancer cell proliferation via suppression of autophagy (Zhao *et al.*, 2021). The emerging role of CMTR1 and negative regulator DHX15 in cancer makes it somewhat surprising that no differences were found in this interaction between WT and *Ctnnb1*^{ex3/WT}; R26-^{LSL-Myc} liver. However, this may be attributed to the high degree of variation in DHX15 protein levels between biological replicates. It is not clear whether this variation stems from a genuine biological cause or perhaps a technical issue. It may be of note that livers were obtained from non-colony matched cohorts. For this reason, it may be beneficial to repeat western blotting for DHX15, particularly with colony-matched samples.

3.3.3 Phosphorylation of CMTR1

Phosphorylation of CMTR1 within the P-Patch promotes Cap-1 formation and CMTR1 dependent gene expression, including expression of genes implicated in growth and ribosome production (Lukoszek *et al.*, 2024). However, P-CMTR1 could not be detected in the liver by IP/WB nor IP/MS. From this finding it may be concluded that phosphorylation of CMTR1 does not occur in the liver or is at the very least present below the limit of detection. Interaction between RNMT and activating subunit RAM increases RNMT capping activity when SAM substrate availability is poor (Varshney *et al.*, 2016). Previous work conducted by Dr Lydia Hepburn in the Cowling lab uncovered that interaction between RNMT and its RAM is below the limit of detection in the liver. The liver is the predominant site of methionine metabolism in the body and hence the availability of SAM for methyltransferase reactions is high in this organ (Barak *et al.*, 1990, Lu and Mato, 2012). It may be the case that high abundance of SAM in the liver permits CMTR1 and RNMT to carry out methyltransferase activity to the extent necessary for liver function in the absence of additional interactions and modifications such as phosphorylation. Methionine metabolism and SAM availability is often disrupted in HCC (Yang *et al.*, 2015, Liu *et al.*, 2011), which may impact capping and would be of interest to investigate further. It is also worth noting that in terms of direct gene regulation,

CMTR1 specifically enhances expression of transcripts associated with the cell cycle, ribosomal proteins, and histone synthesis (Inesta-Vaquera *et al.*, 2018, Liang *et al.*, 2022, Wolter *et al.*, 2023, Preprint). Whilst healthy hepatocytes do possess regenerative and proliferative capacity, they predominantly exist in a “post-mitotic” state and are for the most part arrested in the G0 phase of the cell cycle. (Sigal *et al.*, 1995, Alva-Medina *et al.*, 2010). This information adds further credence to the assumption that even in the absence of phosphorylation CMTR1 maintains activity to the extent required for normal liver function.

3.3.4 CMTR1 localisation in Huh-7 cell lines

Immunostaining performed on Huh-7 cell lines demonstrated that CMTR1 primarily displays nuclear localisation but is weakly present in the cytoplasm. This finding agrees with work carried out by Lee *et al.*, where staining of CMTR1 in neurones shows a very similar pattern of localisation (Lee *et al.*, 2020). However, it does disagree with the previous data generated in HeLa cell lines, where cytoplasmic immunostaining of CMTR1 was below the limit of detection (Liang *et al.*, 2022, Joana Silva, PhD thesis). Together these findings suggest there may be a unique function of CMTR1 in the cytoplasm, particularly in cells of hepatic and neuronal origin. Information on the role of capping enzymes beyond the nucleus is limited. However, it has been demonstrated that accumulation of RNGTT in the cytoplasm enables “re-capping” to occur (Otsuka *et al.*, 2009). Hence, it can be suggested that CMTR1 is carrying out a similar function at this location. An alternative possibility is that there may be other unknown roles for CMTR1 in the cytoplasm, unrelated to capping. Answering the question as to whether the localisation of CMTR1 is altered in Huh-7 cells when compared to non-transformed cell lines may also be of use to determine a role for CMTR1 in liver oncogenesis.

When performing IF, staining was performed with two separate CMTR1 antibodies to enhance confidence in the findings. To build on this further, it may be beneficial to generate CMTR1 KO Huh-7 cell lines as a negative control when performing future experiments. In terms of the conclusions drawn regarding CMTR1 localisation, fractionation of protein lysate followed by western blotting may also be conducted to reinforce these further.

3.3.5 Optimisation of CMTR1 IP/MS

Optimisation of CMTR1 IP/MS in liver lysate demonstrated that the use of cross-linking agents and DTT are likely to impact specificity and sensitivity. Although it was decided that use of BS3 should not be implemented for liver CMTR1 IP/MS experiments, it may have been beneficial to trial alternate cross-linking agents. BS3 exerts cross-linking activity by targeting primary amine groups but can cross-react with other nucleophilic groups (Kalkhof and Sinz, 2008). This cross-reactivity may interfere with the antibody's antigen binding region and account for the reduction seen in antigen retrieval. Dimethyl pimelimidate (DMP), a common alternative to BS3, lacks this cross-reactivity and may negate loss of CMTR1 retrieval whilst improving specificity (Sousa *et al.*, 2011).

In conclusion, selection of antibody, cross-linking agent, and DTT supplementation should be tailored according to the biological question the experiment is attempting to answer. In this scenario IP/MS was conducted as a method of identifying a large pool of potential binding partners to then validate individually downstream, hence antigen retrieval was prioritised over specificity.

Chapter 4: Identifying novel CMTR1 interacting proteins in the liver.

4.1- Introduction

Recent study has suggested a role for CMTR1 in the oncogenesis of both colorectal (CRC) and liver cancer. Work conducted by You *et al.* implicated a pro-tumorigenic role for CMTR1 in CRC via the promotion of STAT3 expression (You *et al.*, 2023). Conversely, unpublished data from the Sansom lab indicate that CMTR1 plays a protective role against hepatitis and tumorigenesis, subsequent to *Ctnnb1* and *MYC* dysregulation in murine liver. Characterisation of CMTR1 in WT murine and *Ctnnb1*^{ex3/WT}; R26^{-LSL-Myc} liver was undertaken to gain further insight into the role of CMTR1 in cancer, as described in the previous chapter (chapter 3). The CMTR1 interactome has yet to be studied in either a liver or oncogenic context and was hence investigated to enrich understanding of a potential function for CMTR1 in hepatocellular carcinoma (HCC). Mass spectrometry analysis of complexes purified by immunoprecipitation (IP/MS) was undertaken following the optimisation process as detailed in chapter 3. Once data was obtained from IP/MS, individual proteins were selected for downstream validation, based on their relevance to liver function and cancer.

This chapter primarily focuses on validation of two novel CMTR1 interacting proteins, Argininosuccinate synthase 1 (ASS1) and PGAM family member 5, a mitochondrial serine/threonine protein phosphatase (PGAM5). ASS1 is a key component of the arginine synthesis pathway, where it enables conversion of citrulline and aspartate to argininosuccinate (Ghose and Raushel, 1985). Despite classification as a phosphoglycerate mutase, PGAM5 lacks enzymatic activity in this regard, instead utilising phosphatase activity alongside protein-protein interactions for functionality. PGAM5 has been implicated in the regulation of mitochondrial dynamics (Bernkopf *et al.*, 2018, Sugo *et al.*, 2018) and cell death processes (Wang *et al.*, 2012, Lenhausen *et al.*, 2016).

4.2- Results

4.2.1 Identification of CMTR1 interacting proteins in liver

To identify CMTR1 interacting proteins in liver, total cell extract was obtained from WT and *Ctnnb1*^{ex3/WT}; R26-^{LSL-Myc} mouse liver, 10 days after induction of cre expression. 2 mg of protein from this extract was then used to carry out IP overnight by using an IgG antibody of sheep origin raised against recombinant human CMTR1. In total, 5 biological replicates of CMTR1-IP were conducted on both WT and *Ctnnb1*^{ex3/WT}; R26-^{LSL-Myc} liver. Alongside these replicates, controls were generated for both tissue types analysed. This was achieved by undertaking IP with an isotype matched control antibody, which lacks specificity for CMTR1 (referred to from here on as an IgG control). These samples were then submitted for mass spectrometry analysis. From the data obtained in this experiment a final list was compiled of proteins likely to be genuine CMTR1 interactors in WT (Table 4.1) and *Ctnnb1*^{ex3/WT}; R26-^{LSL-Myc} liver (Table 4.2). This list was based on the following criteria: identification of proteins in at least 3 replicates and the presence of at least double the number of unique peptides per protein compared to the IgG control (Table 4.3).

The bait protein CMTR1 was identified in all 5 biological replicates carried out in WT and *Ctnnb1*^{ex3/WT}; R26-^{LSL-Myc} liver but not in either of the IgG controls, suggesting that the antibody used bound to the protein of interest specifically. DHX15, an established interactor of CMTR1 (Inesta-Vaquera *et al.*, 2018) was identified in all 5 replicates of the *Ctnnb1*^{ex3/WT}; R26-^{LSL-Myc} dataset but only in 2 WT replicates. Despite data obtained from IP/WB indicating a similar extent of interaction between these two proteins in WT and *Ctnnb1*^{ex3/WT}; R26-^{LSL-Myc} liver. Additionally, RNAPII, another experimentally verified CMTR1 interacting protein (Haline-Vaz *et al.*, 2008, Inesta-Vaquera *et al.*, 2018) was not found to Co-IP with CMTR1 in either WT or *Ctnnb1*^{ex3/WT}; R26-^{LSL-Myc} liver amongst any of the replicates. This may be attributed to loss of this interaction during sample preparation or differences in underlying methodology compared to other works.

In terms of overlap, 46% of interactors in the *Ctnnb1*^{ex3/WT}; R26-^{LSL-Myc} dataset were also found in the WT dataset (12/26), suggesting a degree of similarity between the CMTR1 interactome in WT and *Ctnnb1*/MYC dysregulated liver. Interestingly,

many proteins identified in these interactome datasets are implicated to have tumour suppressor or promoter functions in HCC (Wang *et al.*, 2021, Teng *et al.*, 2011).

4.2.2 Proteins identified in CMTR1 complexes are enriched for GO terms relating to metabolic biological processes.

Once datasets of CMTR1 interacting proteins were compiled, gene ontology (GO) analysis was conducted to determine enrichment of biological process terms. The top 2 terms enriched in the WT dataset (Figure 4.1 a) were “branched amino acid metabolic process” and “branched amino acid catabolic processes”, which placed 5th and 6th amongst the top 10 enriched terms in the *Cttnb1*^{ex3/WT}; R26-LSL-Myc dataset (Figure 4.1 b). In the *Cttnb1*^{ex3/WT}; R26-LSL-Myc dataset the top 2 most enriched terms related to protein folding. These being “chaperone cofactor-dependent protein refolding” and “De novo post translational protein folding,” which were the 3rd and 4th most enriched terms in the WT dataset respectively. The majority of the top 10 enriched terms were shared amongst the two datasets, again highlighting the similarities of the CMTR1 interactome in WT and *Cttnb1*^{ex3/WT}; R26-LSL-Myc liver. Many of these enriched terms related to metabolism, specifically amino acid metabolism, suggesting a role for CMTR1 in governing this function in liver. One term found only in the top 10 GO enriched terms of the WT dataset included “regulation of chaperone-mediated autophagy,” a process which enables turnover of select cytosolic proteins and is required for lung tumour growth (Kon *et al.*, 2011). The term “response to unfolded protein” was unique to the top 10 enriched terms of the *Cttnb1*^{ex3/WT}; R26-LSL-Myc dataset and is associated with promoting tumour cell survival upon exposure to hypoxia and glucose deprivation (Park *et al.*, 2004).

CMTR1 IP	WT.1		WT.2		WT.3		WT.4		WT.5	
	Gene Names	Intensity	Peptides	Intensity	Peptides	Intensity	Peptides	Intensity	Peptides	Intensity
Acaa2	22.136	2	0	0	23.733	2	20.859	1	22.605	2
Aldh2	20.273	1	0	0	21.082	1	20.326	1	0	0
Ass1	23.841	3	25.389	2	24.276	2	24.568	3	23.702	4
Atp5a1	25.565	8	0	0	23.163	2	23.771	3	23.829	4
Bckdha	28.468	8	27.547	6	28.842	8	28.298	9	27.318	8
Bckdhb	24.665	9	0	0	0	4	24.6305	6	24.363	7
C1qb	0	0	0	0	22.09	1	21.500	1	22.213	1
Cmtr1	25.725	6	25.478	3	25.536	7	23.940	4	26.126	11
Cps1	28.965	23	28.402	8	27.478	12	26.672	11	26.852	18
Dbt	32.028	23	31.539	9	31.83	18	30.973	17	31.078	19
Dld	24.788	3	0	0	23.475	3	20.620	1	21.201	1
Dpsyl3	28.951	1	0	0	0	0	26.842	1	27.659	1
Eef1a1	23.207	2	0	0	23.257	2	22.957	1	23.279	2
Gapdh	0	0	23.975	1	22.174	2	23.087	2	23.274	2
Gpx1	24.608	4	0	0	21.309	1	22.7406	3	23.380	3
Hmgcs2	0	0	0	0	21.751	1	21.307	1	20.980	1
Hspa5	0	0	0	0	22.121	3	21.988	3	21.224	2
Hspa8	20.086	1	0	0	22.068	3	22.589	3	0	1
Hspa9	0	1	0	0	23.570	5	21.641	2	21.387	2
Mgst1	23.134	1	0	0	22.788	1	23.3802	2	22.359	1
Pc	21.376	2	23.317	2	23.044	4	20.899	1	0	1
Psmc1	0	0	23.473	2	20.403	1	0	1	20.688	1
Psmc2	0	0	0	0	21.817	2	21.859	2	22.014	2
Rpl7a	0	0	0	0	21.548	2	20.757	1	19.864	1
Rps8	21.274	2	0	0	20.487	1	22.272	2	0	1
Slc25a5	20.090	1	0	0	0	0	21.924	1	21.153	1

Table 4.1- List of proteins identified as potential CMTR1 interacting partners in WT liver via CMTR1 IP/MS.

This list is composed of proteins identified via CMTR1 IP-M/S, which were found to be present in at least 3 out of 5 biological replicates, using liver lysate from WT mice. Proteins listed were found to have at least double the number of unique peptides identified in at least 3 samples compared to the species and isotype matched IgG control. Rows highlighted in red are hits found in previous studies (Simabuco *et al.*, 2019). CMTR1 (Cap Methyltransferase 1), IP/MS (Immunoprecipitation/Mass spectrometry), WT (Wild type).

CMTR1 IP	B/M.1		B/M.2		B/M.3		B/M.4		B/M.5	
	Intensity	Peptides								
Acaa2	23.541	2	NaN	0	NaN	0	21.514	1	21.134	1
Ass1	25.621	3	21.742	1	23.238	1	24.523	2	20.706	1
Atp5a1	25.680	6	22.358	2	NaN	0	21.945	1	23.166	6
Bckdha	29.515	8	26.763	6	27.244	5	27.354	6	27.737	12
Cfl1	20.620	1	NaN	0	21.608	1	21.599	1	20.402	1
Cmtr1	25.833	2	24.693	8	22.701	3	24.831	6	25.257	8
Cps1	28.717	18	26.610	12	25.051	5	26.370	9	26.379	12
Dbt	32.961	16	31.409	19	31.750	16	31.683	14	31.299	23
Dhx15	26.181	4	22.729	1	21.673	1	23.626	3	24.337	5
Fga	21.795	1	NaN	0	23.166	2	22.703	2	0	0
Fmo5	22.727	2	NaN	0	NaN	0	21.986	1	20.343	1
Gapdh	24.561	2	22.993	1	NaN	0	23.739	3	20.840	1
H1f0	23.524	1	20.048	1	22.542	1	NaN	0	NaN	0
Hist1hd	23.756	3	22.094	1	23.693	3	NaN	0	NaN	0
Hspa5	22.649	4	NaN	1	NaN	0	20.985	2	21.971	3
Hspa8	23.958	3	NaN	1	NaN	1	21.648	3	21.402	4
Pc	23.996	4	20.137	1	NaN	0	21.756	2	NaN	0
Pgam5	22.683	1	22.844	2	22.534	2	23.384	2	20.584	1
Psm2	NaN	0	22.854	3	20.402	1	21.874	1	20.840	2
Ran	20.909	1	20.583	1	20.142	1	19.929	1	NaN	0
Tufm	NaN	0	21.192	1	20.245	1	20.777	1	NaN	0

Table 4.2- List of proteins identified as potential CMTR1 interacting partners in B/M liver via CMTR1 IP/MS.

This list is composed of proteins identified via CMTR1 IP-M/S, which were found to be present in at least 3 out of 5 biological replicates, when using liver lysate from B/M mice. Proteins listed were found to have at least double the number of unique peptides identified in at least 3 samples compared to the species and isotype matched IgG control. Rows highlighted in red are hits found in previous studies (Inesta-Vaquera *et al.*, 2018, Simabuco *et al.*, 2019). CMTR1 (Cap Methyltransferase 1), B/M (*Ctnnb1*^{ex3/WT}; R26-^{LSL-Myc} liver), IP/MS (Immunoprecipitation/Mass spectrometry).

IgG control	WT	
Gene Names	Intensity	Peptides
Acaa2	0	0
Aldh2	0	0
Ass1	0	0
Atp5a1	0	0
Bckdha	0	0
Bckdhb	0	0
C1qb	0	0
Cmtr1	0	0
Cps1	24.079	5
Dbt	0	0
Dld	0	0
Dpsyl3	0	0
Eef1a1	0	0
Gapdh	0	0
Gpx1	0	0
Hmgcs2	0	0
Hspa5	0	0
Hspa8	0	0
Hspa9	0	0
Mgst1	0	0
Pc	0	0
Pgam5	0	0
Psmc1	0	0
Psmd2	0	0
Rpl7a	0	0
Rps8	0	0
Slc25a5	0	0

IgG control	B/M	
Gene Names	Intensity	Peptides
Acaa2	0	0
Ass1	0	0
Atp5a1	21.972	1
Bckdha	0	0
Clf1	0	0
Cmtr1	0	0
Cps1	24.299	4
Dbt	0	0
Dhx15	0	0
Fga	0	0
Fmo5	0	0
Gapdh	0	0
H1f0	0	0
Hist1h1d	0	0
Hspa5	0	0
Hspa8	0	0
Pc	0	0
Pgam5	0	0
Psmd2	0	0
Ran	0	0
Tufm	0	0

Table 4.3- List of proteins identified in IgG control samples

This list is composed of proteins identified via CMTR1 IP-M/S in the IgG control in both WT and B/M liver lysate. Intensity and the number of peptides identified is included. CMTR1 (Cap Methyltransferase 1), IP/MS (Immunoprecipitation/Mass spectrometry), WT (Wild type), B/M (Ctnnb1ex3/WT; R26-LSL-Myc liver).

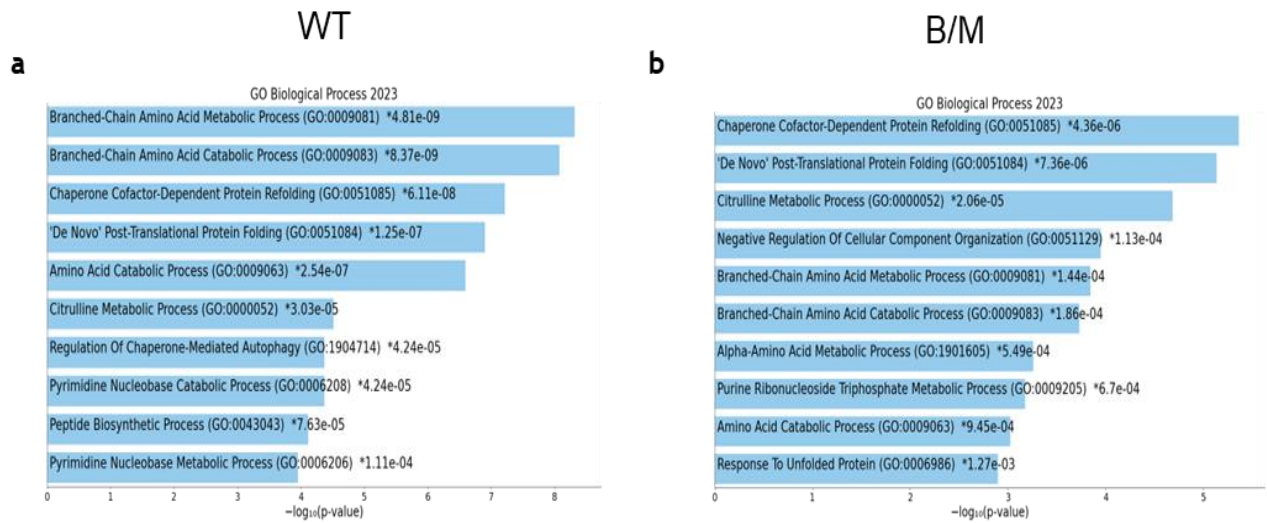


Figure 4.1-Proteins identified via CMTR1 IP/MS are enriched for GO terms relating to metabolic biological processes

CMTR1 IP/MS was carried out on 5 biological replicates of WT and B/M mice liver. A final list of potential binding partners was created based on proteins identified in at least 3 biological replicates which possessed double the number of unique peptides compared to the IgG control. GO analysis was conducted to determine the top 10 GO biological processes biological process terms by significance for WT liver (a) and B/M liver (b). GO analysis was conducted on Enrichr. CMTR1 (Cap Methyltransferase 1), IP/MS (Immunoprecipitation/Mass spectrometry), GO (Gene ontology), WT (Wild type), B/M (*Ctnnb1*^{ex3/WT}; R26-^{LSL-Myc})

In addition to determining enrichment of biological processes amongst the CMTR1-interactome, enrichment of terms relating to interactor localisation was also investigated. Given that CMTR1 is characterised as a nuclear protein it was surprising to find a high extent of enrichment for mitochondrial and vesicular GO terms (Figure 4.2 a, Figure 4.2 b). Once again, top 10 GO localisation terms were highly similar in both datasets, with both sharing “intracellular organelle lumen” and “mitochondrial matrix” as their top 2 enriched terms. In regard to the distribution of individual proteins found in the datasets, 20 and 25% of proteins found in complex with CMTR1 were localised to the nucleus in WT (Figure 4.2 c) and *Ctnnb1*^{ex3/WT}; R26-^{LSL-Myc} (Figure 4.2 d) liver respectively. The vast majority of remaining proteins were found in either the mitochondria or cytoplasm; with endoplasmic reticulum, membrane, cytoskeletal and secreted proteins making up a small fraction of the remaining compartments.

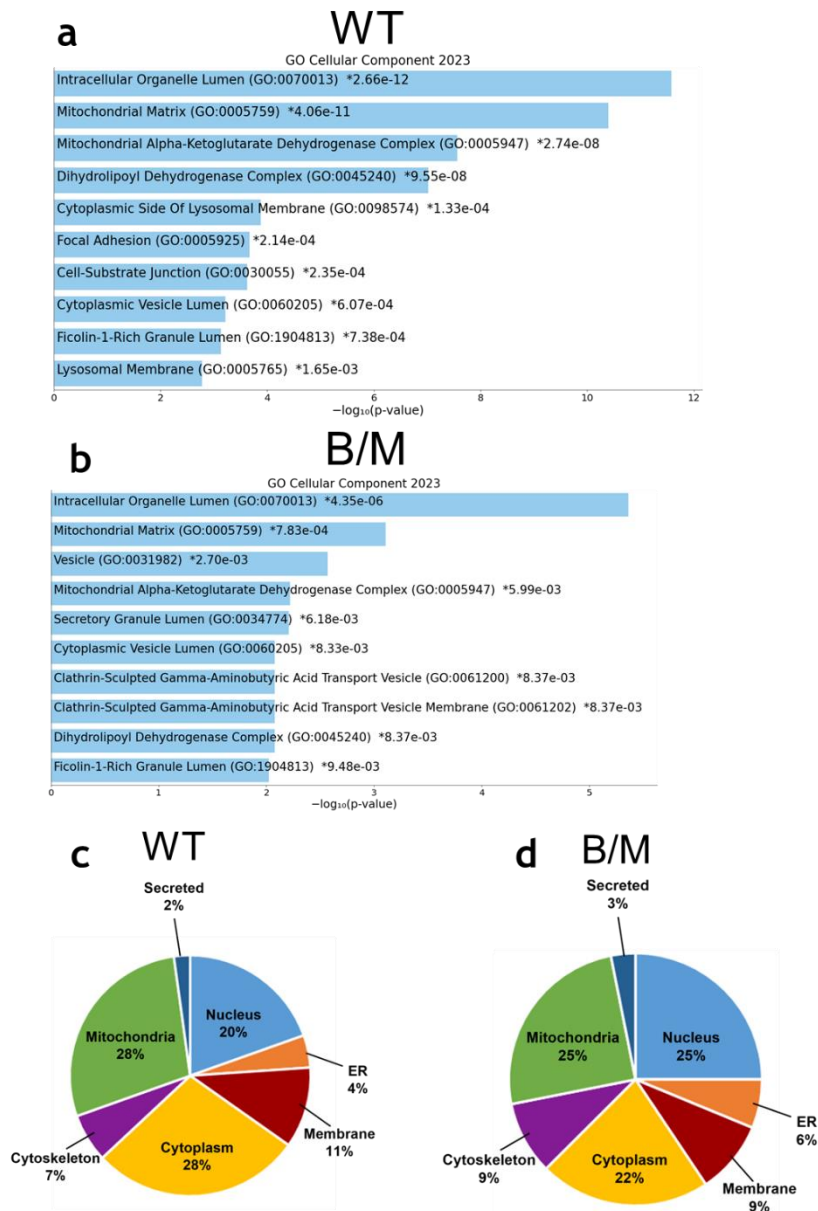


Figure 4.2-Proteins identified as CMTR1 binding partners in both WT and B/M liver lysate are predominantly localised in cytoplasmic, nuclear and mitochondrial compartments

CMTR1 IP/MS was carried out on 5 biological replicates of WT and B/M mice liver. A final list of potential binding partners was created based on proteins identified in at least 3 biological replicates which possessed double the number of unique peptides compared to the IgG control. Gene ontology analysis was conducted to determine the top 10 GO cellular component terms by significance for WT liver (a) and B/M liver (b). Pie charts are displayed to show distribution of individual protein hits amongst nuclear, ER, membrane, cytoplasmic, cytoskeletal, mitochondrial, and secreted compartments for WT (c) and B/M liver (d). GO analysis was conducted on Enrichr. CMTR1 (Cap Methyltransferase 1), WT (Wild type), B/M (*Ctnnb1*^{ex3/WT}; R26-^{LSL-Myc}), GO (Gene ontology), ER (Endoplasmic reticulum).

4.2.3 Survival is more favourable in HCC patients with high expression of ASS1 and PGAM5, two proteins identified as potential CMTR1 binding partners.

After establishing GO enriched biological function and localisation terms in the interactome datasets, individual proteins were selected for validation. Validation of ASS1 as a CMTR1 binding partner was undertaken. ASS1 is crucial for maintaining liver function and possess tumour suppressor effects in HCC (Kim *et al.*, 2021, Tao *et al.*, 2019). PGAM5 was selected for downstream validation as it was previously found to be upregulated in HCC, where it contributes to chemoresistance (Cheng *et al.*, 2018). The interactor PGAM5 is of particular interest for further study as it was found in all 5 replicates of CMTR1-IP carried out in *Ctnnb1*^{ex3/WT}; R26-^{LSL-Myc} liver at relatively high intensity but was only found in a single WT liver replicate, suggesting potential relevance for the CMTR1-PGAM5 interaction in liver oncogenesis specifically.

To better understanding of how ASS1 and PGAM5 contribute to outcomes in liver cancer, Kaplan-Meier curves were generated from a dataset obtained from the cancer genome atlas (TCGA-LIHC), which was comprised of HCC patients. Patients from these datasets were classified into high- or low-level expression groups for either ASS1 (Figure 4.3 a) or PGAM5 (Figure 4.3 b). It was found that patient survival probability was more favourable in those expressing high levels of PGAM5 or ASS1, compared to the low expression group. This finding, regarding ASS1 expression agrees with previous data indicating a suppressive role for ASS1 in tumour progression (Kim *et al.*, 2021). However, the finding that high expression of PGAM5 favoured survival probability was unexpected, given that high levels of PGAM5 expression were previously demonstrated to predict poorer overall survival in a Chinese patient cohort (Cheng *et al.*, 2018).

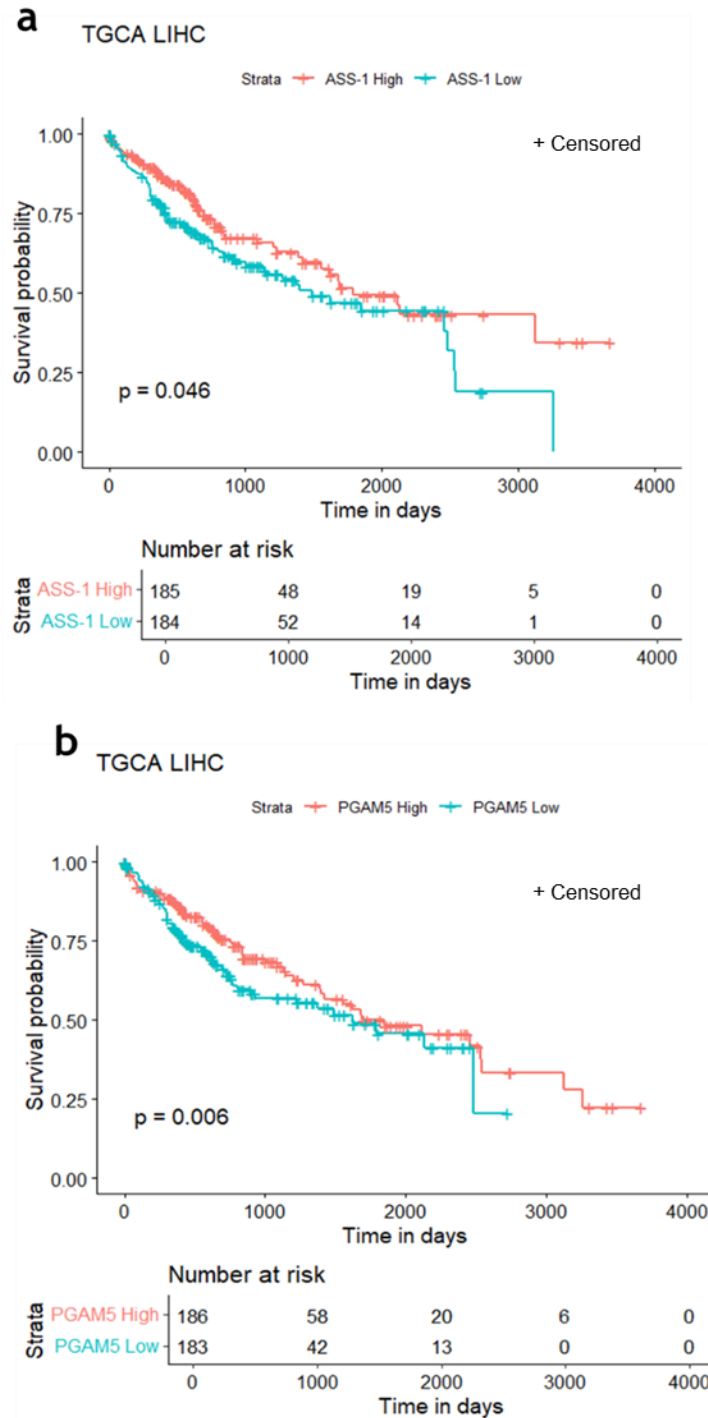


Figure 4.3-Survival probability is more favourable in HCC patients with high expression of ASS1 and PGAM5.

Kaplan-Meier curves generated from a TCGA-LIHC dataset comprised of 371 HCC patients. The dataset was bifurcated by median value of RNA-Seq expression values to determine differences in survival probability between patients with high or low expression of ASS1 (a) or PGAM5 (b). Log-Rank test was performed to determine significance. HCC (Hepatocellular carcinoma), ASS1 (Argininosuccinate synthetase), PGAM5 (PGAM family member 5, mitochondrial serine/threonine protein phosphatase), TCGA-LIHC (The Cancer Genome Atlas-Liver Hepatocellular Carcinoma).

4.2.4 Binding partners identified by IP/MS visualised by IP/WB performed on organ and Huh-7 cell extract.

To confirm CMTR1 IP/MS findings, purification of both ASS1 and PGAM5 via CMTR1 Co-IP was attempted in WT and *Ctnnb1*^{ex3/WT}; R26-^{LSL-Myc} liver extract. In 3 separate biological replicates ASS1 was found to purify with CMTR1 in both WT and *Ctnnb1*^{ex3/WT}; R26-^{LSL-Myc} liver (Figure 4.4 a) by immunoblot. Initially, under normal wash conditions a signal consistent with ASS1 was present in the lane corresponding to the IgG control. However, this was remedied with the implementation of high-salt washes for all samples, suggesting identification of ASS1 in IP/MS was not solely a result of non-specific interactions with the isolation matrix. Purification of PGAM5 from CMTR1-IP was achieved in 3 replicates using *Ctnnb1*^{ex3/WT}; R26-^{LSL-Myc} liver extract but did not appear to occur in all 3 replicates conducted with WT liver extract (Figure 4.4 b), in agreement with the IP/MS data. Additionally, no signal for PGAM5 appeared in the IgG control lane, suggesting interactions occurred specifically between CMTR1 and PGAM5. PGAM5 contains a transmembrane domain which is subject to cleavage by presenilin-associated rhomboid like protein (PARL), generating PGAM5 (Δ 24) (Sekine *et al.*, 2012). Both full length and cleaved PGAM5 can be identified by western blotting and account for the presence of two bands for PGAM5 in the IP lanes. The extent of ASS1 and PGAM5 signal correlated with the degree of CMTR1 retrieved, implying specificity.

To further uncover the biological relevance of CMTR1 interactions, ASS1 and PGAM5 Co-IP was attempted in Huh-7 cells (a hepatoma cell line) (Figure 4.5). When purification of ASS1 was attempted, the resultant signal was below the limit of detection. The interaction between CMTR1 and PGAM5 meanwhile was preserved in Huh-7 cells, with signal being produced for both full length and cleaved PGAM5. These findings indicated that Huh-7 cell lines were an appropriate model for further exploration into CMTR1-PGAM5 but not CMTR1-ASS1 interactions. For this reason, further experiments focused on confirming the validity of PGAM5 binding to CMTR1.

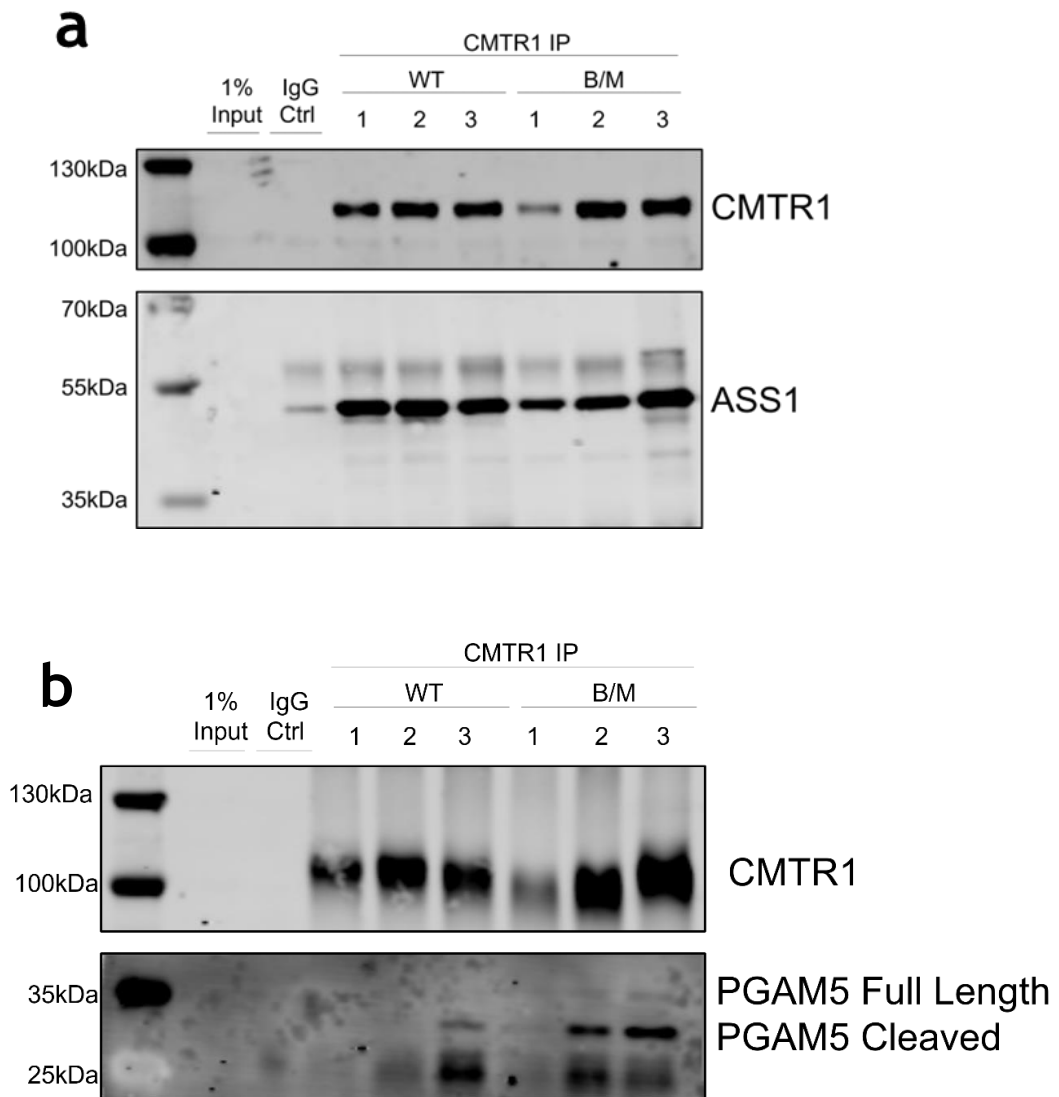


Figure 4.4-Binding partners identified via mass spectrometry can be visualised by IP/WB performed on liver extract.

CMTR1-IP/WB was conducted using 2 mg of liver lysate and 2 µg of sheep IgG anti-CMTR1. Liver lysate was obtained from 3 separate WT and B/M mice. Western blotting was then conducted for CMTR1 and ASS1 (a) or CMTR1 and PGAM5 (b). PGAM5 exists in both a full-length and lower molecular weight cleaved conformation within cells and tissues. Post IP-input samples of 20 µg for liver and were loaded alongside the IP, with ¼ of the IP being loaded per sample. An isotype and species matched non-specific antibody was used as an IgG control to confirm specificity of the interaction. Molecular weight is indicated on the left side of the panel. N=3. CMTR1 (Cap Methyltransferase 1), IP/WB (immunoprecipitation/Western blot), ASS1 (Argininosuccinate synthetase), PGAM5 (PGAM5 family member 5, mitochondrial serine/threonine protein phosphatase), IP (Immunoprecipitation), WT (Wild type), B/M (*Ctnnb1*^{ex3/WT}; R26^{-LSL-Myc}).

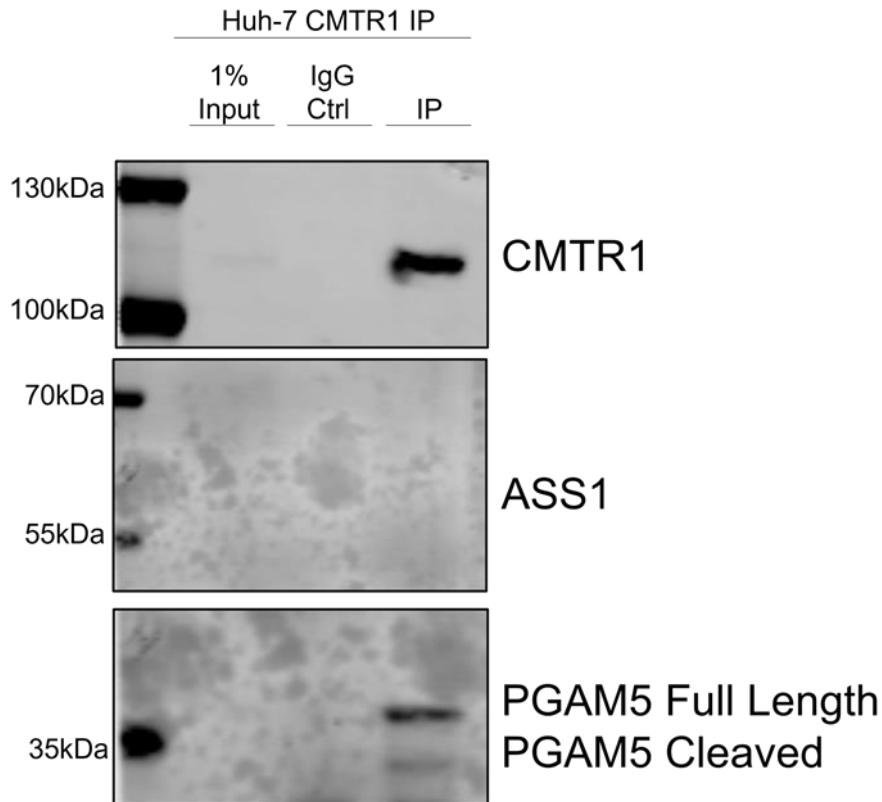


Figure 4.5-CMTR1 interacts with PGAM5 but not ASS1 in Huh-7 cells.

IP was carried out using 1mg of Huh-7 cell lysate alongside 2 μ g of sheep IgG anti-CMTR1. Western blotting was then undertaken for CMTR1, ASS1 and PGAM5. N=2. Post IP-input samples of 10ug were loaded alongside the IP, with $\frac{1}{4}$ of the IP being loaded per sample. An isotype and species matched non-specific antibody was used as an IgG control to confirm specificity of the interaction. Molecular weight is indicated on the left side of the panel. CMTR1 (Cap Methyltransferase 1), PGAM5 (PGAM family member, mitochondrial serine/threonine protein phosphatase, ASS1 (Argininosuccinate synthetase), IP (Immunoprecipitation)

4.2.5 PGAM5 and CMTR1 are ubiquitously expressed amongst organs and cell lines, however the extent of PGAM5-CMTR1 interaction varies.

To determine if interaction between CMTR1 and PGAM5 was unique to liver and HCC cell lines, western blotting of CMTR1 and PGAM5 was undertaken in a panel of organ extract, alongside Co-IP of PGAM5 from CMTR1 in multiple cell lines (Figure 4.6 a). Blotting for CMTR1 and PGAM5 in organs revealed that CMTR1 expression is relatively consistent, which may be unremarkable given its universal role in gene expression and innate immune regulation (Smietanski *et al.*, 2014). Expression of PGAM5 was also consistent amongst organs with a few marked outliers, these being brain, liver and Huh-7 cell line extract, where expression of PGAM5 was highest. Interestingly, in brain extract levels of PGAM5 (Δ 24) were higher than full length

PGAM5, which tends to occur as a response to loss of mitochondrial potential (Sekine *et al.*, 2012). In other organs and the huh-7 cell lines, the ratio of PGAM5 ($\Delta 24$) to full length PGAM5 was similar. Expression of PGAM5 was highest in Huh-7 cell lines, which agrees with previous findings where PGAM5 is noted to be upregulated in HCC.

Once expression of CMTR1 and PGAM5 was determined amongst extract from different organs, CMTR1-IP followed by blotting for PGAM5 was carried out in A549 (lung cancer), HEK293 (embryonic kidney) and Huh-7 cell lines. Signal for both full length and cleaved PGAM5 could be visualised from these extracts. However, a stronger signal was produced for PGAM5 in the lane where the Huh-7 CMTR1 IP was loaded compared to HEK293 and A549 cell lines. This is despite similar levels of retrieval for CMTR1. No signal for PGAM5 nor CMTR1 could be detected in any of the IgG control lanes. Overall, this suggests that whilst interaction between CMTR1 and PGAM5 is preserved in multiple cell lines, it may be occurring to a greater extent in HCC cell lines, such as Huh-7.

4.2.6 Determining if FCCP treatment in Huh-7 cell lines induces PGAM-5 cleavage.

Reports from the literature have indicated that upon cleavage, PGAM5 relocates to the cytosol and nucleus (Bernkopf *et al.*, 2018, Baba *et al.*, 2021). Cleavage via PARL tends to occur in response to mitochondrial stress when accompanied by a loss of mitochondrial potential (Sekine *et al.*, 2012). Loss of mitochondrial potential can be artificially induced by treating cells with Carbonyl cyanide-p-trifluoromethoxyphenylhydrazone (FCCP). As CMTR1 has not been reported to localise to the mitochondria (to the author's knowledge), it can be assumed that interaction between CMTR1 and PGAM5 would primarily occur upon PGAM5 cleavage and subsequent relocation to the nucleus and/or cytoplasm. For this reason, FCCP treatment was optimised in Huh-7 cell lines.

Huh-7 cells were treated with either 5 or 10 μM FCCP, then harvested for protein at 1, 2 and 4 hrs post-treatment (Figure 4.7). Throughout the course of treatment, signal for CMTR1 was unaltered when determined by western blotting. As expected, levels of full length PGAM5 decreased at all time points compared to the vehicle control. In contrast, the signal produced for cleaved PGAM5 increased in a time dependent manner.

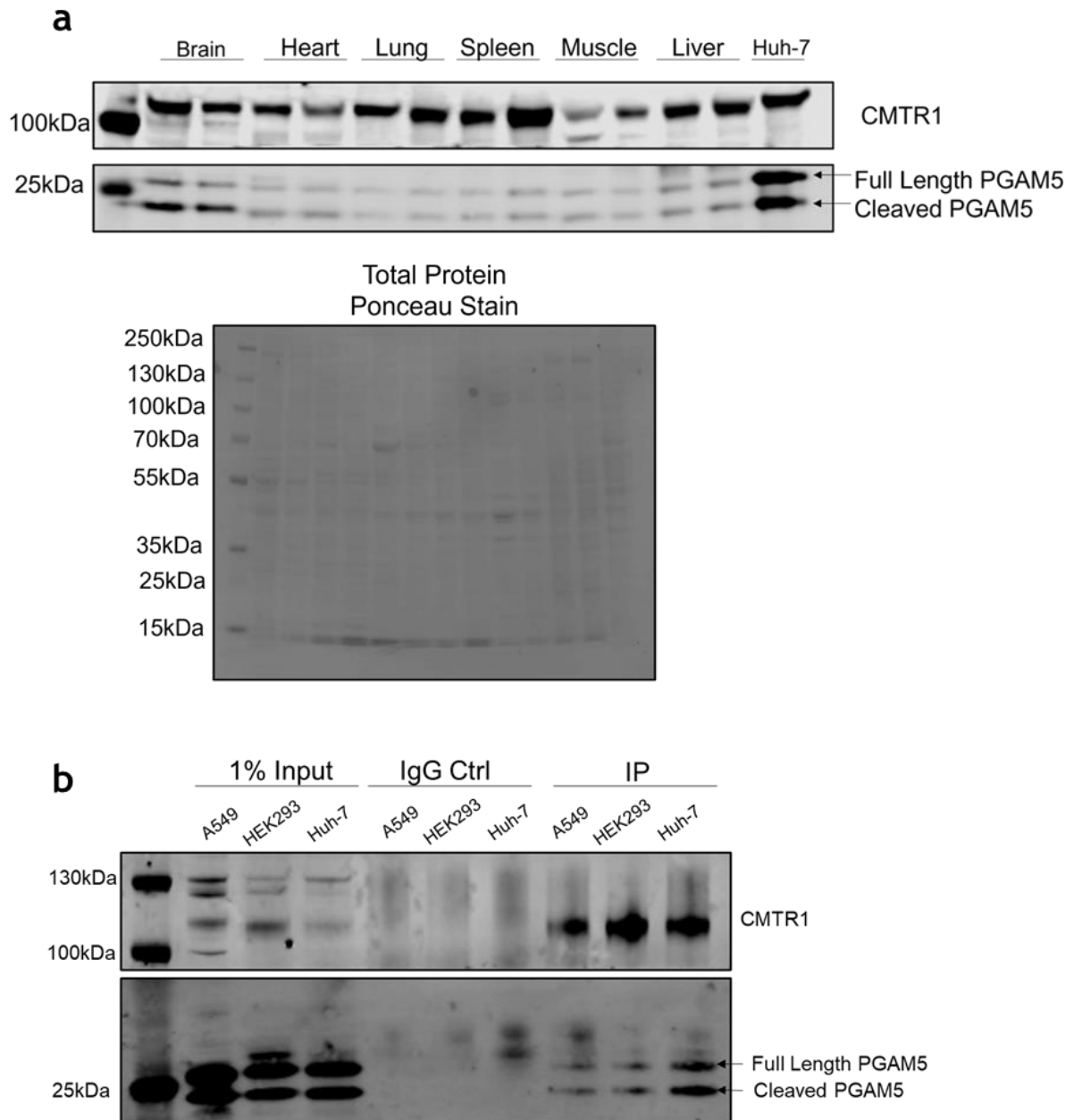


Figure 4.6-PGAM5 and CMTR1 are ubiquitously expressed amongst organs and cell lines, however the extent of PGAM5-CMTR1 interaction varies.

10 μ g of organ and Huh-7 lysate was loaded for western blot, with anti-sheep IgG CMTR1 and anti-rabbit IgG PGAM5 being used to detect these proteins. Total protein staining with ponceau was carried out to determine if loading was equal (a). N=2. 0.5 mg of A549, HEK293 and Huh-7 cell lysate, was used for CMTR1 IP/WB alongside 1 μ g of sheep IgG anti-CMTR1. Western blotting was carried out to detect CMTR1 and PGAM5. Post IP-input samples of 5 μ g were loaded alongside the IP, with $\frac{1}{4}$ of the IP being loaded per sample. An isotype and species matched non-specific antibody was used as an IgG control to confirm specificity of the interaction (b). N=3. Molecular weight is indicated on the left side of the panel. PGAM5 (PGAM family member 5 serine/threonine protein phosphatase), CMTR1 (cap methyltransferase 1), IP/WB (Immunoprecipitation/Western blot)

Expression of translocase of outer mitochondrial membrane 20 (TOM20), a marker of mitochondrial mass (Whitaker-Menezes *et al.*, 2011), was not markedly increased even after 4 hrs of FCCP treatment at a 10 μ M concentration. This indicates that mitochondrial homeostasis was for the most part maintained, even under stress conditions induced by FCCP treatment. To further establish that FCCP treatment induced loss of mitochondrial potential and hence PGAM5 cleavage, flow cytometry was undertaken on Huh-7 cells treated with 10 μ M FCCP for 4 hrs and stained with MitoSpy Red CMXRos and MitoSpy Green FM dyes. The MitoSpy Red CMXRos dye binds to mitochondria dependent on potential and hence a decrease in fluorescence intensity indicates a loss of potential. Binding of MitoSpy Green FM dye occurs independently of changes in mitochondrial potential, with fluorescence intensity acting as an indicator of mitochondrial mass (MitoSpy kit manual, Biologend). Huh-7 cells treated with FCCP displayed a significant loss in mitochondrial potential as determined by MitoSpy Red signal, compared to the vehicle control, whilst mitochondrial mass was significantly increased upon FCCP treatment when compared to the control. Together, these data serve as an indication that treatment with 10 μ M FCCP over 4 hrs induced loss of mitochondrial potential and PGAM5 cleavage yet was well tolerated in Huh-7 cell lines. For this reason, subsequent experiments conducted using FCCP were carried out in the aforementioned conditions.

4.2.7 PGAM5 and CMTR1 both localise to the nucleus in Huh-7 cells, treatment with FCCP does not substantially alter co-localisation

To determine whether CMTR1 and PGAM5 co-localise in Huh-7 cell lines, immunofluorescence staining of these proteins followed by visualisation via confocal microscopy was undertaken (Figure 4.8). As cleavage of PGAM5 has been demonstrated to promote localisation outside mitochondria (Baba *et al.*, 2021 Bernkopf *et al.*, 2018), Huh-7 cells were treated with FCCP prior to immunostaining. CMTR1 staining in Huh-7 cells displayed a strong nuclear pattern, with weak cytoplasmic staining in both control and FCCP treated cells. No change in localisation was noted in CMTR1 upon exposure to FCCP.

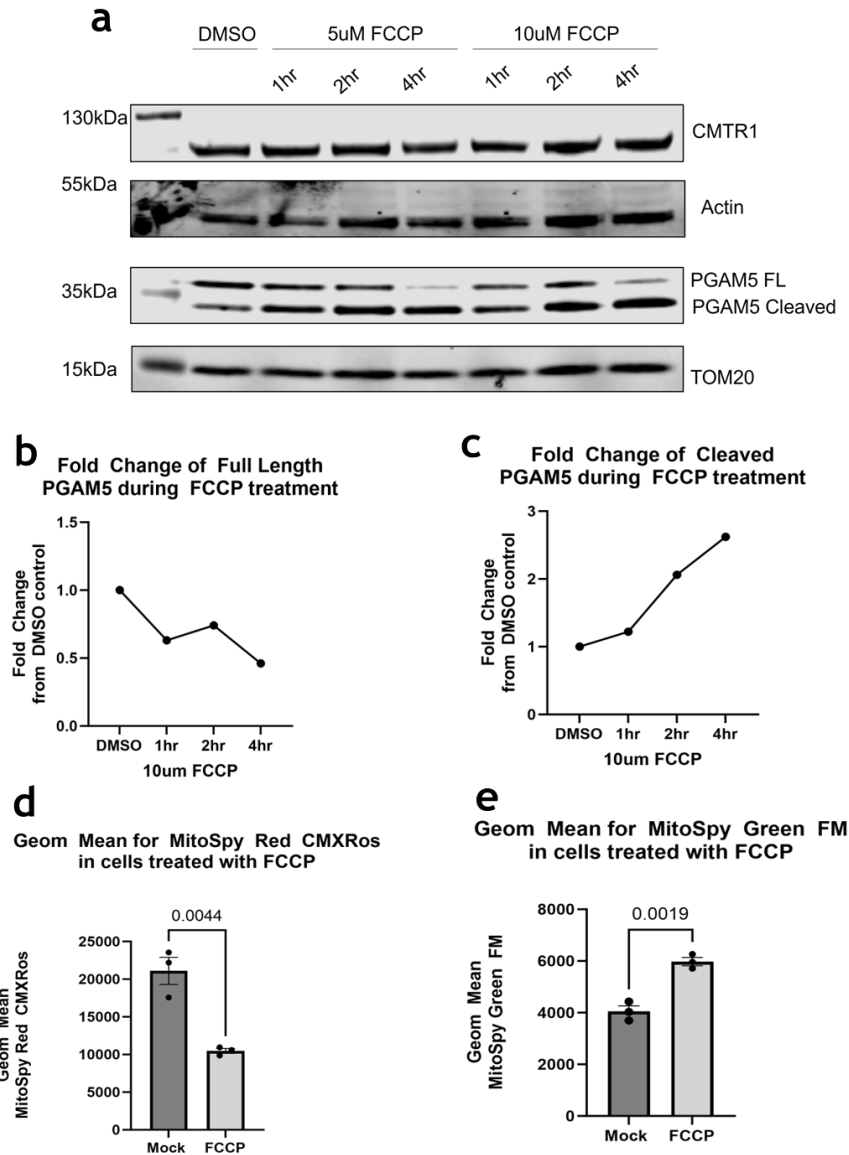


Figure 4.7-Determining if FCCP treatment in Huh-7 cell lines induced PGAM5 cleavage.

Huh-7 cells were treated with 5 or 10 μM of FCCP over the course of 4 hrs and harvested for protein at the indicated time. Western blotting was then performed to determine the extent of protein expression for CMTR1, PGAM5 (Full length and cleaved), and TOM20. Actin was used as a loading control (a). Molecular weight is indicated on the left side of the panel. The signal for full length and cleaved PGAM5 was quantified using Image Studio™ lite and normalised to the expression of actin. The fold change in the signal of full length or cleaved PGAM5 was calculated relative to the DMSO only treated control and plotted over time N=1 (b, c). Huh-7 cells treated with 10 μM of FCCP for 4 hrs were stained with MitoSpy Red CMXRos and MitoSpy Green FM for 30 mins prior to analysis by flow cytometry. The geometric mean of the fluorescent signal provided by the CMXRos and FM dye for each sample for mock vs FCCP treated cells is shown (d, e). Bars show the mean value, with error bars depicting the SEM, each point represents an individual replicate. Students t-test was performed to determine significance. N=3. FCCP (Carbonyl cyanide-p-

trifluoromethoxyphenylhydrazone), CMTR1 (Cap Methyltransferase 1), PGAM5 (PGAM family member 5 mitochondrial serine/threonine protein phosphatase), TOM20 (Translocase of outer mitochondrial membrane 20), SEM (Standard error mean). Gating strategy for flow cytometry experiments can be found in the appendices.

CMTR1 also appeared to be excluded from features within the nucleus that may correspond to the nucleolar compartment. However, this is difficult to ascertain in the absence of a marker.

PGAM5 displayed a similar pattern of localisation to CMTR1, demonstrating both nuclear and cytoplasmic staining in control and FCCP treated cells. Furthermore, cytoplasmic staining corresponded to a specific organelle structure as opposed to diffuse staining. The identity of this organelle however is difficult to confirm in the absence of an appropriate marker such as TOM20. The extent of PGAM5 localisation in the nuclear compartment of vehicle treated Huh-7 cell lines was unexpected, given the majority of PGAM5 would be expected to localise to the mitochondria in healthy cells. Upon FCCP treatment, nuclear immunostaining of PGAM5 in Huh-7 cells remained unchanged. In terms of cytoplasmic immunostaining in response to FCCP treatment, distinct puncta of PGAM5 could be noted outside the nucleus, suggesting localisation within granular structures. Confirming the identity of these granules would require further experimentation, however these may correspond to P-bodies or stress granules.

Given that PGAM5 was not expected to strongly localise to nuclear compartments, particularly in the absence of FCCP treatment, immunostaining was conducted on A549 cell lines to indicate whether this phenomenon was cell line specific. Whilst immunostaining of PGAM5 in A549 cells indicated localisation in the nucleus of control and FCCP treated cells, cytoplasmic immunostaining was more prominent compared to Huh-7 cell lines and was consistent with the expected pattern of staining for a mitochondrial protein. Again however, it cannot be concretely confirmed if PGAM5 immunostaining in the cytoplasm corresponds to the mitochondrial compartment in A549 cells without a marker.

To quantify the degree of colocalization between CMTR1 and PGAM5, colocalization analysis was undertaken (Figure 4.9). This was performed by selecting individual cells as regions of interest from multiple fields of view and

experimental replicates, followed by utilisation of the BIOP JACoP plugin in ImageJ. From this analysis, both the Pearson’s correlation coefficient and Manders colocalization coefficient were calculated. Manders colocalization coefficient generates both M1 and M2 values for the selected region of interest (ROI). In this case the M1 value described the contribution of the red channel (used in this experiment to visualise CMTR1 staining) to the pixels of interest within the image, whilst M2 describes the contribution of the green channel (used in this experiment to visualise PGAM5 staining) to the pixels of interest within the image. Pearson’s coefficient was calculated to be over 0.8 in both control and FCCP treated Huh-7 cells. The average M1 and M2 values for the mock control were over 0.75 and over 0.8 for FCCP treated cells (table 4.4). This suggests that overall, a high level of mutual co-localisation occurs between PGAM5 and CMTR1 in both untreated and FCCP treated cells.

Despite these findings, it is important to state that co-occurrence of signal does not necessarily indicate protein interaction. However, taken together with Co-IP data, these findings indicate that interaction of CMTR1 and PGAM5 is likely to be genuine.

	Mock	FCCP
Pearson’s correlation coefficient (average)	0.87	0.88
M1 (average)	0.78	0.85
M2 (average)	0.91	0.88

Table 4.4- Average Pearson’s correlation coefficient and Mander’s M1/M2 values for mock and FCCP treated Huh-7 cells

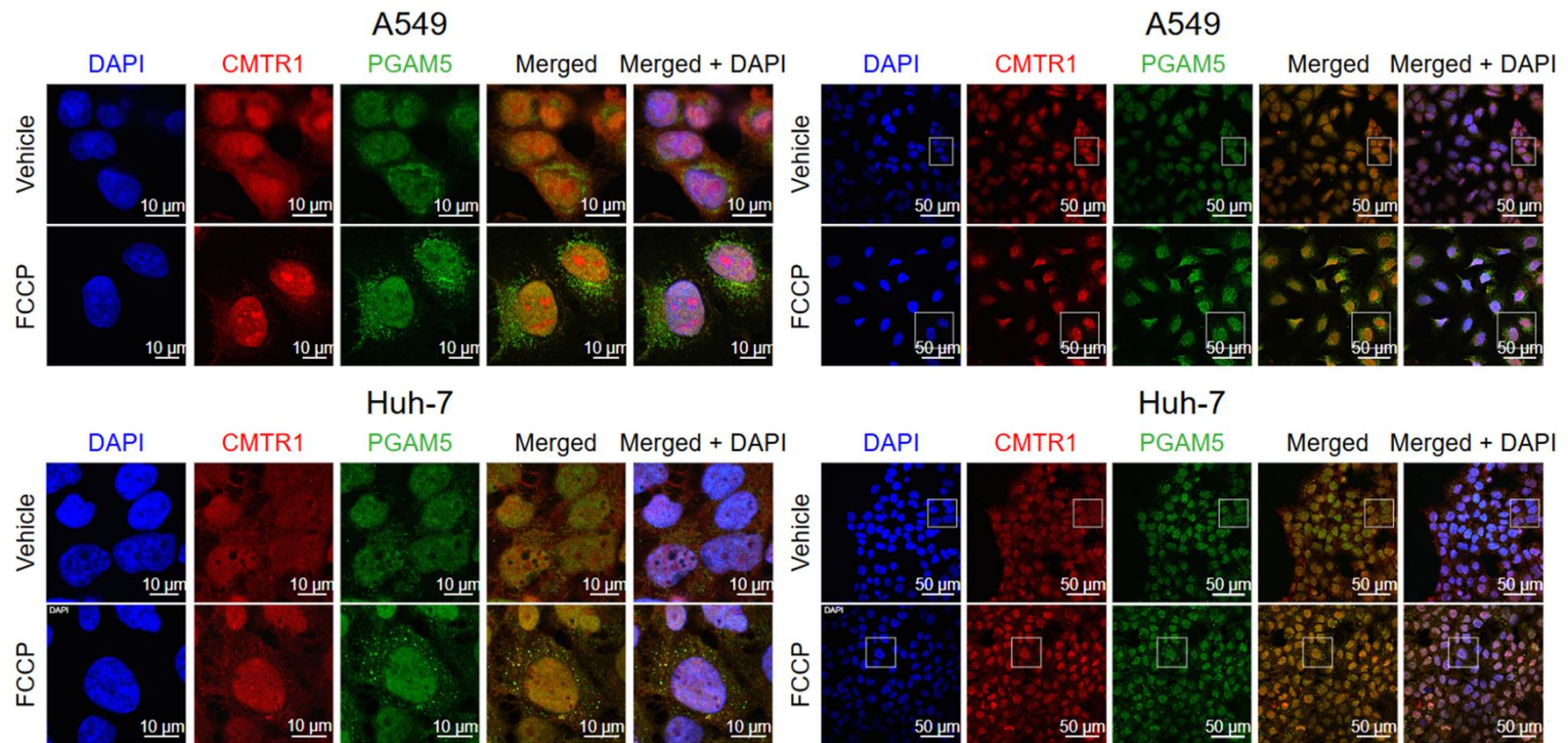


Figure 4.8- PGAM5 and CMTR1 Immunostaining in Huh-7 cells.

Huh-7 (a) (n=3) and A549 (n=1) (b) cell lines were stained with antibodies targeting CMTR1 (Anti-sheep IgG antibody) and PGAM5 (Anti-rabbit IgG antibody) as indicated. DAPI was used as a nuclear marker. Cells were treated with 10 μ M FCCP for 4 hrs prior to fixation. A secondary only control was generated by treating Huh-7 and A549 cells with anti-sheep Alexa 594 and anti-rabbit Alexa 488 secondary antibody. Imaging was performed on the Nikon A1R and analysed with Omero. Scale bars represent a 10 or 50 μ m distance. Images taken on 60x objective. CMTR1 (Cap Methyltransferase 1), PGAM5 (PGAM family member 5 mitochondrial serine/threonine protein phosphatase), DAPI (4',6-diamidino-2-phenylindol), FCCP (Carbonyl cyanide-p-trifluoromethoxyphenylhydrazine).

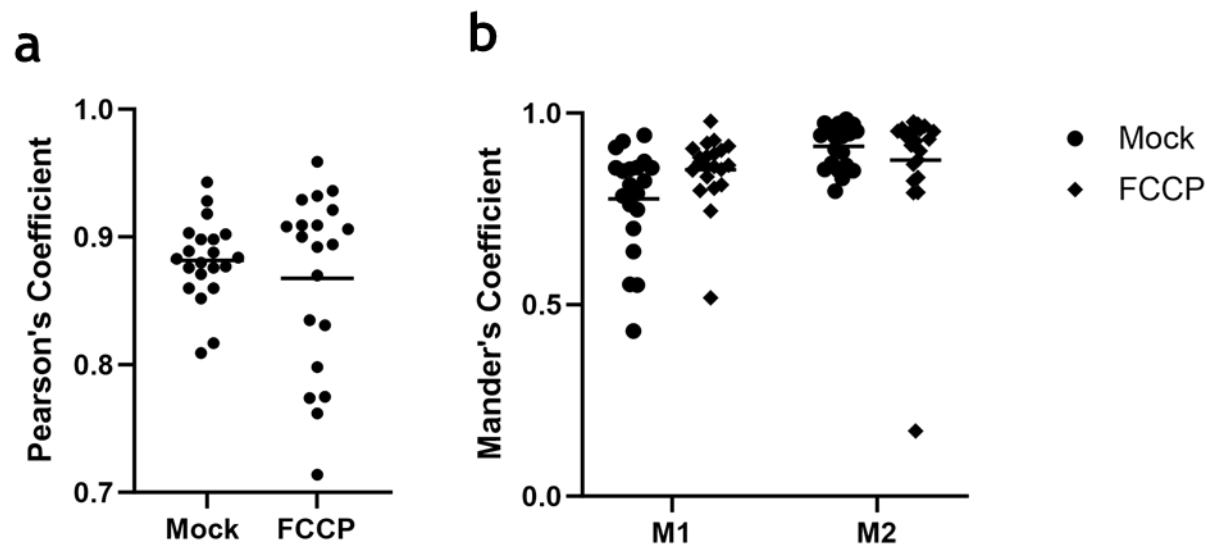


Figure 4.9- Results of Co-localisation assay for CMTR1 and PGAM5 signal in mock and FCCP treated Huh-7 cell lines.

Huh-7 cell lines were stained with antibodies targeting CMTR1 (Anti-sheep IgG antibody) and PGAM5 (Anti-rabbit IgG antibody). Cells were treated with 10 μ M FCCP for 4 hrs prior to fixation. Imaging was performed on the Nikon A1R and analysed with Omero. Regions of interest were selected from multiple replicates across different fields of view (n=21) for co-localisation analysis using the BIOP JACoP plugin in ImageJ software. Li's automatic thresholding was used to differentiate background and foreground. Pearson's (a) and Mander's (b) correlation coefficients were calculated. Bar shows the mean value, each point represents an individual replicate. CMTR1 (Cap Methyltransferase 1), PGAM5 (PGAM family member 5 mitochondrial serine/threonine protein phosphatase), FCCP (Carbonyl cyanide-p-trifluoromethoxyphenylhydrazine), JACOP (Just Another Colocalization Plugin).

4.3- Discussion

Given that preliminary data has suggested a putative role for CMTR1 in liver cancer, characterisation of the CMTR1 interactome in WT and *Ctnnb1*^{ex3/WT}; R26^{-LSL-Myc} murine liver was undertaken to identify differential CMTR1 interacting proteins which may hold relevance to oncogenesis. By conducting mass spectrometry analysis of CMTR1 complexes purified from WT and *Ctnnb1*^{ex3/WT}; R26^{-LSL-Myc} mouse liver, novel CMTR1 interactors could be determined. Validation of two of these potential binding partners, ASS1 and PGAM5 was subsequently undertaken. Both ASS1 and PGAM5 were demonstrated to interact with CMTR1 via CMTR1 Co-IP in liver organ extract. However, this was not the case when Co-IP was attempted in Huh-7 extract, with only PGAM5 being successfully purified. Interaction between PGAM5 and CMTR1 occurs in other cell lines but the extent of this interaction varies. Finally, CMTR1 and PGAM5 were found to co-localise in Huh-7 cells, with PGAM5 being present in both nuclear and cytoplasmic compartments. The implications of these findings are discussed below.

4.3.1 Characteristics of CMTR1 binding partners and differences from previous interactome studies

Within the dataset of potential CMTR1 binding partners, there were several proteins besides ASS1 and PGAM5 which would be of interest to conduct further validation and analysis, owing to their roles in HCC. Although time constraints prevented this from being achieved. One example of these proteins is aldehyde dehydrogenase 2 (ALDH2), a binding partner unique to the WT liver interactome. Low expression of ALDH2 has been noted in tumour tissue compared to healthy controls and predicts poor prognosis in HCC patients. The mechanism of which is thought to be rooted in regulation of AMP-activated protein kinase signalling (Hou *et al.*, 2017).

GO analysis performed on CMTR1 interactors revealed enrichment for terms relating to metabolism, particularly amino acid metabolism. Previous findings have shown that mutations in CMTR1 which prevent inhibition by DHX15 led to increased translation of genes relating to metabolism (Inesta-Vaquera *et al.*, 2018). Whilst this demonstrated a role for CMTR1 in regulating metabolic processes via promotion of translation, it has not yet been shown that CMTR1 is able to exert

this regulatory effect via protein interaction. For this reason, further investigation into the biological consequence of CMTR1s interaction with metabolic proteins would be of interest.

Given that CMTR1 is a cap methyltransferase and binds to RNAPII, it may be expected that binding proteins identified in the liver would primarily be implicated in regulation of the mRNA lifecycle and capping. A previous CMTR1 interactome study conducted in the HEK293 cell line, identified 137 putative CMTR1 interacting proteins. The majority of which were classified into functional categories for mRNA processing, spliceosomal complexes, translation initiation and ribosomal subunits (Simabuco *et al.*, 2019). Amongst proteins indicated to bind to CMTR1 via mass spectrometry analysis, few have been extensively validated. The most well characterised interacting proteins of CMTR1 include RNAPII (Haline-Vaz *et al.*, 2008) and DHX15 (Inesta-Vaquera *et al.*, 2018), the latter of which negatively regulates CMTR1 methyltransferase activity. Additionally, one study analysing the interactome of another capping enzyme CAPAM, demonstrated interaction between this protein and CMTR1. The authors of this study postulate that this interaction serves to facilitate CAPAM activity and promote N6 methylation of the first transcribed adenosine nucleotide (Covelo-Molares *et al.*, 2021). Taken together, these data suggest that CMTR1 interacting partners are likely to be involved in RNA processing and further augment or regulate the function of CMTR1 in this regard. Despite this being the case, the data presented here demonstrates that the CMTR1 interactome in liver mainly consists of proteins with functions relating to amino acid metabolism and protein folding. This suggests specialisation of CMTR1 interaction and function in hepatocytes compared to tissue of other origin.

An additional contrast between the findings presented here and those of previous CMTR1 interactome studies is the localisation of proteins identified as binding partners of CMTR1. Most proteins in the HEK293 dataset were found to localise in either the nucleus (54%) or cytoplasm (33%), with only 1% being mitochondrial (Simabuco *et al.*, 2019). Whilst in the liver interactome dataset 28 and 25% of proteins were found to localise to the mitochondria in WT and *Ctnnb1*^{ex3/WT}; R26-LSL-*Myc* liver, respectively. The high amount of mitochondrial protein interactors

identified was surprising, given that CMTR1 is characterised as a nuclear protein. However, data from other labs (Lee *et al.*, 2020) and findings presented here have demonstrated cytoplasmic immunostaining of CMTR1 occurs in neurones and liver cancer cells. This being a means by which CMTR1 could be interacting with proteins which lack nuclear localisation.

4.3.2 Validating interactors

Co-IP of both ASS1 and PGAM5 from CMTR1 was successful in liver extract. However, this finding could not be replicated in Huh-7 cell lines, this may be attributed to downregulation of ASS1, which is intrinsic to HCC cell lines (Kim *et al.*, 2021). This being the case, investigation into the biological relevance of ASS1-CMTR1 interactions would require alternative models, where ASS1 expression is maintained. To undertake further validation and eliminate concerns of off-target antibody binding, exogenous expression of tagged CMTR1 in liver cell lines followed by co-IP of ASS1 and PGAM5, would be beneficial. Although this would still be problematic to undertake in Huh-7 cell lines owing to low ASS1 expression. It may also be of benefit to determine if interactions are maintained using recombinant protein assay, to further validate binding between ASS1 and PGAM5 with CMTR1. The exact site of binding between CMTR1 and these proteins may also be determined by using recombinant protein fragments.

Western blotting on organ lysate showed that expression of CMTR1 was consistent amongst different tissue types. Expression of PGAM5 meanwhile was highest in Huh-7 cell lines and markedly increased compared to WT liver extract. This lends further credence to the idea that PGAM5 is upregulated in HCC (Cheng *et al.*, 2018). Extract from brain also demonstrated high levels of PGAM5 protein expression, particularly cleaved PGAM5. This is of note as in most cell lines, excess PGAM5 cleavage is associated with loss of mitochondrial potential in response to stress (Sekine *et al.*, 2012). Furthermore, in most other organs, the ratio of PGAM5 Δ 24 and full length PGAM5 were equivalent. It may be that the extent of PGAM5 cleavage in the brain can be attributed to physiological changes occurring during organ extraction, particularly given the relevance of PGAM5 cleavage in neuroprotective responses to brain injury (Liang *et al.*, 2023).

When PGAM5 was Co-IP'd with CMTR1 in HEK293 and A549 cells, the extent of the resultant PGAM5 signal was weaker in these cell lines compared to Huh-7 lines, despite equivalent retrieval of CMTR1. This implies interaction between CMTR1 and PGAM5 may occur to a greater extent in HCC models specifically compared to models of other cancers. Despite this being the case, increases in PGAM5 gene expression have been found to correlate with mortality in non-small cell lung carcinoma patients (Ng Kee Kwong *et al.*, 2018). Whilst in gastric cancer PGAM5 expression is also found to be upregulated, permitting for activation of the PI3K/AKT pathway to sustain increases in proliferation (Meng *et al.*, 2023). These works from the literature demonstrate relevance for PGAM5 in cancer beyond HCC and emphasise the importance of further determining the biological consequences of CMTR1-PGAM5 interaction.

CMTR1-PGAM5 interaction occurred to a greater extent in *Ctnnb1*^{ex3/WT}; R26^{-LSL-Myc} liver compared to WT liver according to both IP/MS and IP/WB data. The underlying mechanisms behind this require further investigation. It may be speculated that post translational modifications or stabilisation of the complex by other proteins occur to achieve this.

4.3.3 Localisation of CMTR1-PGAM5 interactions

As previously inferred in the text, binding of mitochondrial proteins (PGAM5 included) to CMTR1 was unexpected, based on current understanding of CMTR1 localisation. This being the case, concerns arose over the validity of these findings, as these could be attributed to artefacts of lysis. Despite this, it may be theorised that cytoplasmic CMTR1 is capable of interacting with mitochondrial proteins localised on the outer mitochondrial membrane (OMM). Furthermore, it may be the case that mitochondrial proteins identified as CMTR1 binders are capable of translocating to the cytoplasm and/or nucleus and are thus interacting with CMTR1 at these sites.

In terms of PGAM5 specifically, localisation of this protein even within the mitochondria is highly debated. PGAM5 has been demonstrated to interact with several cytoplasmic proteins including, nuclear factor erythroid 2-related factor 2 (NFE2L2) (O'Mealey *et al.*, 2017) and KEAP1 (Zeb *et al.*, 2021), suggesting OMM localisation. However, sucrose density gradient centrifugation found that PGAM5

localised within inner mitochondrial membrane fractions (Sekine *et al.*, 2012). To explain these contradictory findings, it has been proposed that PGAM5 shuttles between the two mitochondrial membranes, accounting for interactions with cytoplasmic proteins in the absence of cleavage (Sugo *et al.*, 2018). This information provides rationale for the occurrence of CMTR1-PGAM5 interactions within the cytoplasmic fraction of cells.

PGAM5 Δ 24 has been demonstrated to translocate to the cytosol upon treatment with FCCP, permitting for interactions between PGAM5 and Axin to occur which facilitate β -catenin dependent transcription as a mechanism of inducing mitochondrial biogenesis (Bernkopf *et al.*, 2018). Experiments conducted on HeLa cells have shown that induction of mitophagy via FCCP resulted in translocation of PGAM5 to the nucleus, enabling dephosphorylation of nuclear serine/arginine rich proteins (Baba *et al.*, 2021). Furthermore, a degree of nuclear localisation for PGAM5 has been noted in the absence of mitochondrial stressors when expression of either cleaved or full length tagged PGAM5 was induced in U2OS cells (Bernkopf *et al.*, 2018). Based on the above literature it was theorised that the interaction between CMTR1 and PGAM5 may solely occur upon cleavage of the latter, as this permits greater motility of PGAM5 within cellular compartments, particularly the nucleus. It is for this reason immunostaining for PGAM5 and CMTR1 was conducted following FCCP treatment. Surprisingly, it was found that even at rest; a substantial proportion of PGAM5 could be found in the nucleus and colocalised with CMTR1. The degree of this colocalization was not substantially different amongst untreated and FCCP treated cells. This suggests that the bulk of CMTR1-PGAM5 interactions occur in the nuclear compartment of Huh-7 cells and may not be dependent on loss of mitochondrial potential.

It should be noted however that co-localisation does not automatically indicate protein-protein interactions are occurring. Rather, it is an indication that proteins may be capable of interacting based on mutual presence in the same cellular compartments. To more definitively prove that CMTR1-PGAM5 interactions are occurring in the nucleus, conduction of super-resolution microscopy or automated fluorescence lifetime imaging may be of use. Additionally, given that the extent of PGAM5 nuclear staining (particularly in the absence of cleavage) was considerably

higher than has been previously reported (Bernkopf *et al.*, 2018, Baba *et al.*, 2021), it would be pertinent to use an additional PGAM5 antibody to validate staining. It may be the case that a relatively high degree of PGAM5 cleavage occurs in Huh-7 cell lines without loss of mitochondrial potential, facilitating a greater degree of localisation to the nucleus at rest. Experiments comparing ratios of full length and PGAM5 Δ 24 amongst a greater number of cell lines by western blot would help ascertain if this was the case. Additionally, purification of PGAM5 by CMTR1 Co-IP after subcellular fractionation may shed further insight into where CMTR1-PGAM5 interactions occur.

To enrich understanding of the biological ramifications of CMTR1-PGAM5 interactions, follow up experiments will be required. From current understanding of the structure and function of these two proteins it is tempting to suggest that PGAM5 may exert phosphatase activity towards CMTR1 to regulate mRNA capping (Takeda *et al.*, 2009, Wilkins *et al.*, 2014). Alternatively, given that PGAM5 has been implicated to facilitate the IFN response and regulate immunogenic forms of cell death it may be the case that CMTR1 and PGAM5 work in tandem to influence innate immune outcomes (Yu *et al.*, 2020, Wang *et al.*, 2012). Further review of this topic can be found in the main discussion chapter (chapter 6).

Chapter 5: Determining the role of CMTR1
phosphorylation in the innate immune response and
Influenza A viral infection

5.1 Introduction

The most established function of the Cap-1 structure (m⁷G(5')ppp(5')Nm), is as a means by which the innate immune system can differentiate self and non-self RNA species, particularly in response to RNA virus infection. Pattern recognition receptors (PRRs) including retinoic acid-inducible gene I (RIG-I, gene symbol: *DDX58*) and melanoma differentiation-associated protein 5 (MDA5, gene symbol: *IFIH1*) have been demonstrated to recognise and respond to RNA lacking 2'-O-ribose methylation (Schuberth-Wagner *et al.*, 2015, Devarkar *et al.*, 2016, Züst *et al.*, 2011). RNA viruses have developed various mechanisms to ensure viral transcript capping, however, nascent genomic viral RNA and replicative intermediates are uncapped and hence prone to detection by PRRs (Decroly *et al.*, 2012, Rehwinkel *et al.*, 2010).

Activation of PRRs permit conformational changes to occur, for subsequent multimerization and association with mitochondrial antiviral signalling protein (MAVS). This permits for binding of various TNF receptor associated factor (TRAF) family members to the MAVS signalosome. The functional consequence of interaction between TRAF proteins and MAVS is activation of TANK binding Kinase 1 (TBK1) and IKK complexes. The TBK1 complex subsequently phosphorylates interferon regulatory factors 3 and 7 (IRF3/7), which translocate to the nucleus and induce transcription of type I IFN. Concurrently, IκB kinase (IKK) phosphorylates IκB, targeting the latter for ubiquitination and subsequent degradation. This permits NF-κB to promote transcription of proinflammatory cytokines, further augmenting the anti-viral response (Rehwinkel and Gack, 2020).

Dysregulation of RNA sensing pathways and IFN production has profound implications in both viral infection and inflammatory disease (Rice *et al.*, 2014, Najm *et al.*, 2024, Jang *et al.*, 2015), indicating that CMTR1 activity is likely to hold relevance to these also. In one study examining asthma patients receiving inhaled corticosteroids, single nucleotide polymorphisms in CMTR1 were associated with increased risk of hospitalization (Dahlin *et al.*, 2015). Infection of Huh-7 cells with Zika and Dengue virus upon CMTR1 knock down resulted in higher expression of viral RNA when compared to controls. In the same study it was also found that depletion of CMTR1 resulted in decreased protein levels of specific interferon

stimulated genes (ISGs), including ISG15, MX1 and IFITM1 (Williams *et al.*, 2020). These decreases in protein expression were found to be mediated by translational inhibition via IFIT1, an ISG product which sequesters RNA lacking 2'-O-ribose methylation (Habjan *et al.*, 2013 Abbas *et al.*, 2017). It can hence be assumed that CMTR1, an ISG in its own right (Haline-Vaz *et al.*, 2008), ensures 2'-O-ribose methylation of fellow ISG transcripts. This likely sustains ISG translation and promotes anti-viral responses, particularly when host transcripts lacking Cap-1 structures are prone to repression by IFIT proteins (Habjan *et al.*, 2013 Abbas *et al.*, 2017) and other immune factors (Schuberth-Wagner *et al.*, 2015, Devarkar *et al.*, 2016, Züst *et al.*, 2011).

Recent data from the Cowling lab has identified 15 sites of phosphorylation at the N-terminus of CMTR1 which promote formation of the Cap-1 structure. Mutation of these 15 phosphorylation sites to alanine negatively impacts CMTR1-dependent gene expression (Lukoszek *et al.*, 2024). To further understanding of role for CMTR1 phosphorylation in innate immunity, ISG expression and outcomes of Influenza A virus (IAV) infection were investigated in MEF cell lines expressing WT and phosphodeficient (15A) CMTR1.

5.2 Results

5.2.1 Pharmacological inhibition of CK2, a kinase responsible for CMTR1 phosphorylation results in decreased levels of ISG mRNA transcripts

Work carried out by Dr Francisco Inesta-Vaquera; a previous member of the Cowling lab, identified that phosphorylation of CMTR1 is catalysed by the enzymatic activity of casein kinase 2 (CK2) (Lukoszek *et al.*, 2024). CK2 is a pleiotropic kinase with a plethora of associated roles, including those concerning immunity and oncogenesis (Sestero *et al.*, 2012, Seldin and Leder, 1995). As previously published data has shown a requirement for CMTR1 expression in sustaining protein expression of select ISGs (Williams *et al.*, 2020), the role of P-CMTR1 in this context was investigated. WT MEF cell lines were pre-treated with a pharmacological inhibitor of CK2, termed Quinalizarin (QZ), prior to addition of 400 U/ml (units per millilitre) recombinant universal type I IFN. Following treatment, RNA extraction and quantitative reverse transcription polymerase chain reaction (RT-qPCR) analysis were undertaken using primers against various murine ISG transcripts including *Ifit1*, *Ifit3*, *Ifih1*, *Dhx58* and *Isg15*. It was found that upon inhibition of CK2 via QZ (and by proxy reductions in CMTR1 phosphorylation), MEFs demonstrated decreased transcript expression of *Ifit1*, *Ifit3*, *Ifih1*, and *Isg15*, compared to cells treated with IFN alone (Figure 5.1). Expression of *Dhx58* was not significantly altered upon QZ pre-treatment, however, there was a general trend of decreased expression.

It should be stated that whilst these findings implicate P-CMTR1 in regulation of ISG expression upon induction of IFN, these do so indirectly as CMTR1 phosphorylation was not assessed. Furthermore, owing to CK2's numerous roles within immunity (Sestero *et al.*, 2012, Liang *et al.*, 2006) it cannot be discounted that alterations in ISG expression upon QZ addition may result from disruption of other biological processes.

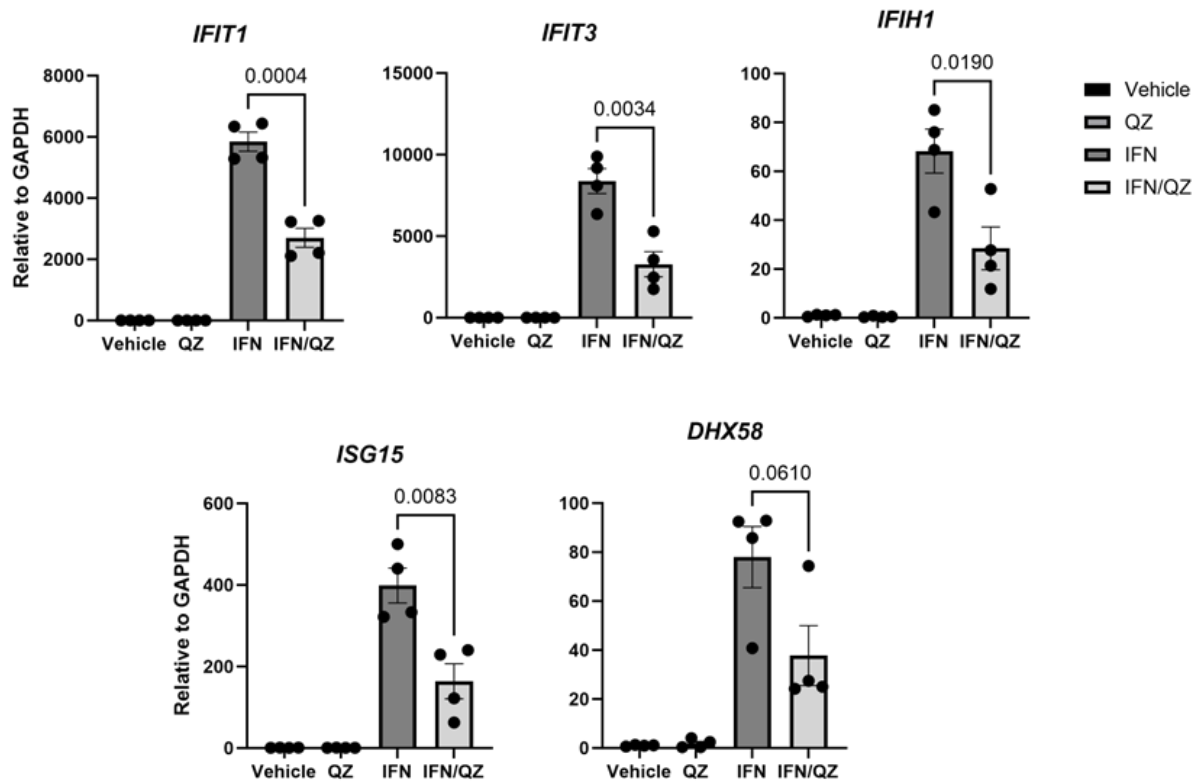


Figure 5.1-Pharmacological inhibition of CK2, a kinase responsible for CMTR1 phosphorylation results in decreased levels of mRNA transcripts for various ISGs.

WT MEF cells were pre-treated with 10 μ M of CK2 inhibitor QZ for 0.5-3 hrs, followed by treatment with 400 U ml IFN for 4 hours, prior to cell lysis, RNA extraction, then RT-qPCR analysis. RT-qPCR analysis was performed using primers specific to various interferon stimulated genes (ISGs) (*Ifit1*, *Ifit3*, *Ifih1*, *Isg15*, and *Dhx58*). Students t-tests were performed to determine if differences in transcript level between cells treated with IFN/QZ and IFN alone were significant. GAPDH was used as a normalisation gene. N=4, MEFs were harvested on different days at 4 different passages. Bars show the mean value, with error bars depicting the SEM, each point represents an individual replicate. Data processing performed by Prof Victoria Cowling. Figure adapted from Lukoszek *et al.*, 2024. CK2 (Casein Kinase 2), CMTR1 (Cap Methyltransferase 1), ISG (Interferon stimulated gene), MEF (Mouse embryonic fibroblast), QZ (Quinalizarin), IFN (Interferon), RT-qPCR (Quantitative reverse transcription polymerase chain reaction), GAPDH (Glyceraldehyde-3-phosphate dehydrogenase), SEM (Standard error mean)

5.2.2 Deletion of endogenous CMTR1 complemented by expression of a phosphodeficient CMTR1 mutant results in delayed expression of IFIT3 and ISG15 in MEF cell lines

Knock-down of CMTR1 by siRNA has been previously demonstrated to abrogate protein expression of select ISGs in response to IFN (Williams *et al.*, 2020). To determine the functionality of P-CMTR1 in this context, MEF cells expressing exogenous 15A-CMTR1 were treated with IFN, followed by analysis of ISG protein expression. These MEF cell lines were generated by extraction of E12.5 embryos from pregnant mice with a transgenic *Cmtr1* allele floxed at exon 3, then transduced with constructs expressing WT-CMTR1 tagged with haemagglutinin at the N-terminus of the protein (HA-WT CMTR1), HA-15A CMTR1 (a phosphodeficient mutant of CMTR1) and an empty vector control (EV). Endogenous CMTR1 expression was disrupted by transfection of a construct expressing cre recombinase to facilitate deletion of *Cmtr1* exon 3, resulting in a null allele. This resulted in the generation of MEF cell lines expressing exogenous HA-WT CMTR1 or HA-15A CMTR1 in the absence of endogenous CMTR1 (Figure 5.2).

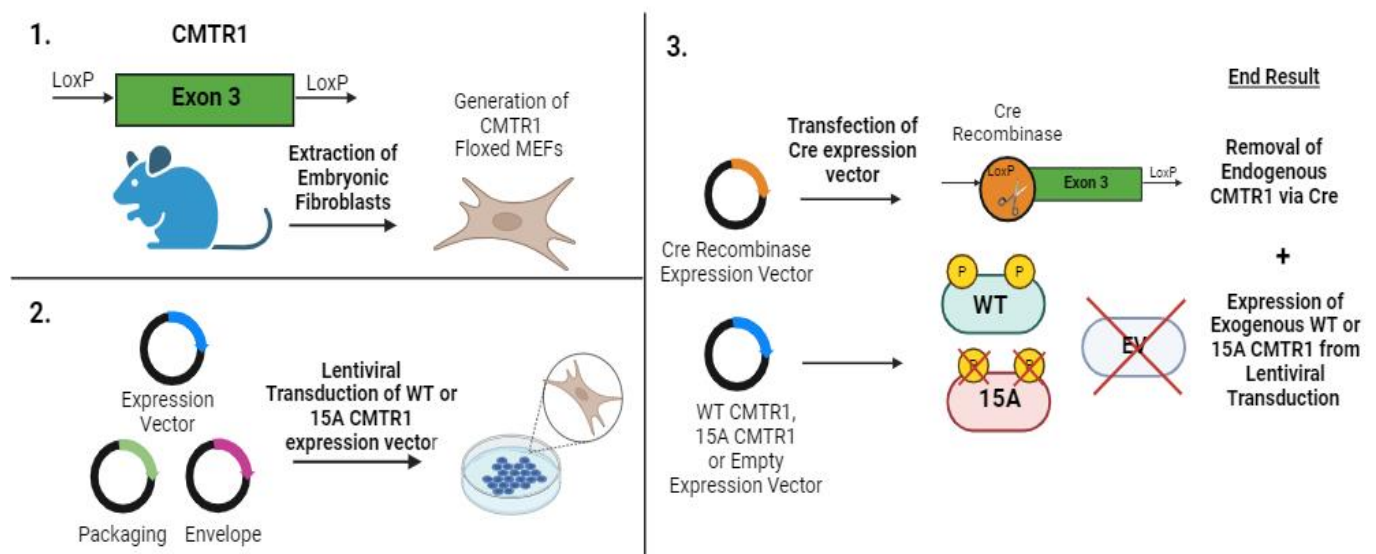


Figure 5.2-Generation of MEF cell lines expressing HA-15A-CMTR1, a phosphodeficient mutant of CMTR1.

MEFs were extracted from pregnant female mice floxed at exon 3 of *Cmtr1*, who had been crossed with male mice of the same genetic background and subsequently immortalised by serial passage (*Cmtr1*^{fl/fl} MEFs) (1). MEFs were transduced under a lentiviral based system with constructs expressing HA-WT CMTR1, a phosphodeficient mutant where 15 individual phospho-sites were

mutated to alanine, termed HA-15A CMTR1, and an empty vector control (2). To eliminate potential interference of endogenous CMTR1 in this model, MEF cells were transfected with a custom vector expressing cre-eGFP fusion protein under the control of a EF1 α promoter. This permitted for deletion of endogenous CMTR1(3). Figure made in BioRender. Adapted from Lukoszek *et al.*, 2024. MEF (Mouse embryonic fibroblast), CMTR1 (Cap Methyltransferase), HA-WT CMTR1 (Haemagglutinin tagged wild type CMTR1), HA-15A CMTR1 (Haemagglutinin tagged phosphodeficient CMTR1), EV (Empty vector), eGFP (Enhanced green fluorescent protein), EF1 α (Elongation factor 1-alpha)

This experiment followed up similar work carried out by Dr Radoslaw Lukoszek in the Cowling lab, where transcript levels of ISGs including *Ifit1*, *Ifit3*, *Ifih1*, *Isg15*, and *Dhx58* were analysed by RT-qPCR in this system upon treatment with recombinant IFN. The data obtained from Dr Lukoszek's experiments showed that expression of all transcripts measured, with the exception of *Dhx58*, were significantly downregulated in HA-15A CMTR1 MEFs compared to the HA-WT CMTR1 control (Lukoszek *et al.*, 2024). To determine if reduced transcript levels resulted in downstream reductions in ISG protein expression; IFIT3 and ISG15 protein expression was measured by western blot on MEF cell lines, post-treatment with IFN over the course of 4, 8 and 24 hrs (Figure 5.3 a).

Treatment of MEFs with IFN induced expression of ISGs in all genotypes 4,8 and 24 hrs post-treatment when compared to the untreated (0 hr) genotype matched controls (Figure 5.3 a). Western blotting showed that induction of IFIT3 protein expression was significantly lower 4 hrs after IFN treatment in EV cell lines, compared to cell lines expressing HA-WT CMTR1. This defect was only partially corrected in the phosphodeficient mutant, where the extent of IFIT3 induction remained significantly lower compared to HA-WT CMTR1 MEFs at the 4hr time point. Induction of ISG15 protein expression was significantly higher in HA-WT CMTR1 MEFs 4 hrs post-IFN treatment, when compared to MEFs expressing HA-15A CMTR1 and an EV. Equivalent expression of ISG15 was noted between genotypes 8 and 24 hrs after IFN treatment (Figure 5.3 b, c). These data corroborate findings of reduced ISG transcript levels upon abrogation of CMTR1 phosphorylation at early time points and demonstrate that loss of P-CMTR1 impacts both mRNA and protein levels of IFIT3 and ISG15 4 hrs post treatment with IFN.

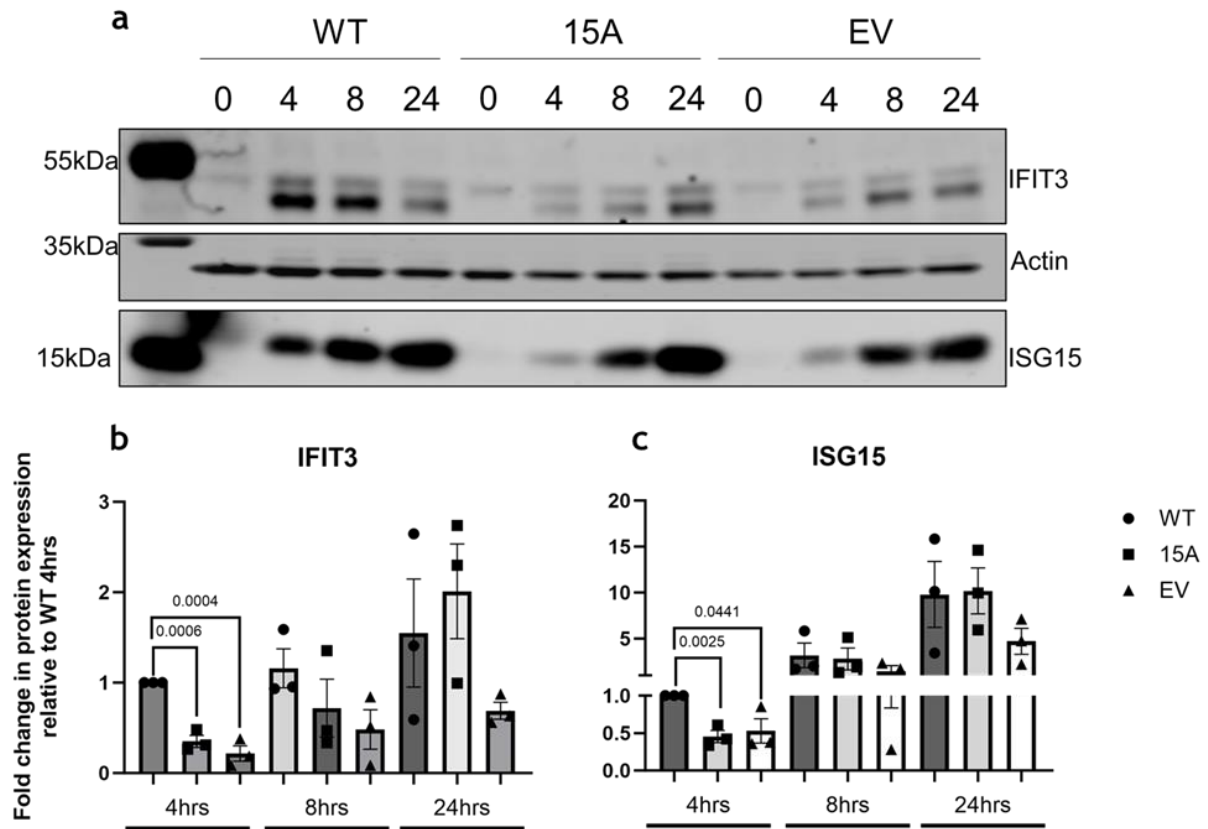


Figure 5.3-Deletion of endogenous CMTR1 complemented by expression of a phosphodeficient CMTR1 mutant results in delayed protein expression of IFIT3 and ISG15 in MEF cell lines.

Cmtr1^{fl/fl} MEF cells, expressing either HA-WT CMTR1, HA-15A CMTR1 or an empty vector control, and cre were treated with 400 U/ml IFN. These cells were harvested at the indicated time points over 24 hrs for protein prior to western blotting analysis. Western blotting was carried out using 20µg of cell lysate with antibodies targeting IFIT3 and ISG15. Actin was used as a loading control. Molecular weight is indicated on the left side of the panel (a). Quantification of signal for each sample and protein of interest was normalised according to actin, in comparison to the WT signal at the 4hr time point (b, c). Students t-tests were performed to determine significance. Quantification was carried out using Image Studio™ Lite (Li-Cor). N=3, MEFs were harvested on different days at 3 different passages. Bars show the mean value, with error bars depicting the SEM, each point represents an individual replicate. Figure adapted from Lukoszek *et al.*, 2024. CMTR1 (Cap Methyltransferase 1), IFIT3 (Interferon-induced protein with tetratricopeptide repeats 3), ISG15 (IFN stimulated gene 15), MEF (Mouse embryonic fibroblast), HA-WT CMTR1 (Haemagglutinin tagged wild type CMTR1), HA-15A CMTR1 (Haemagglutinin tagged phosphodeficient CMTR1), EV (Empty vector), IFN (Interferon), SEM (Standard error mean)

5.2.3 Stimulation of RNA sensing pathways by HWM poly I:C treatment results in delayed ISG expression when CMTR1 cannot be phosphorylated

Pattern recognition receptors implicated in detecting improperly capped nucleic acid include members of the RLR family, which are involved in sensing and coordinating responses to RNA viruses (Kato *et al.*, 2006). Ligands of RLRs include blunt 5' triphosphate ends and double stranded RNA species (Schlee *et al.*, 2009, Goubau *et al.*, 2014), which mark RNA as non-self. Polyinosinic-polycytidylic acid (Poly I:C) is a dsRNA analogue, which closely mimics viral RNA derivatives and can be sensed by TLR3, RIG-I and MDA5 (Im *et al.*, 2023, Li *et al.*, 2021).

To uncover the impact of P-CMTR1 on the RNA sensing pathway and subsequent IFN responses, treatment of MEFs overexpressing HA-WT CMTR1 (HA-WT) and HA-CMTR1 15A (HA-15A) which still maintained endogenous CMTR1 expression was undertaken with Poly I:C. Cells were transfected with high molecular weight (HWM) Poly I:C using lipofectamine 2000 and harvested for protein 17 and 24 hrs post transfection. This was followed by western blotting to determine expression of IFIT3 and ISG15.

Treatment of cells with HMW Poly I:C induced ISG expression, which did not occur when cells were exposed to lipofectamine 2000 only, as a vehicle control. Expression of IFIT3 was lower at both time points in HA-15A CMTR1 cell lines compared to HA-WT controls. On average ISG15 expression in HA-15A CMTR1 and EV MEFs were lower at 17 and 24 hrs compared to HA-WT MEFs after HWM Poly I:C transfection, but these differences were more subtle compared to those in IFIT3 expression. (Figure 5.4 a).

To quantitate protein expression, resultant western blot signals were once again analysed using Image Studio™ and normalised to the signal of loading control actin. Protein expression of IFIT3 was significantly higher at all time points excluding the 0 hr control in HA-WT MEF compared to HA-15A MEF cell lines and the empty vector control (Figure 5.4 b). In terms of ISG15 expression, no significant difference was found between protein levels in HA-WT and HA-15A MEFs at any time points. The decrease in ISG15 expression in HA-15A CMTR1 MEFs was non-significant but consistent, indicating that more replicates may be beneficial to fully assess the role of P-CMTR1 on ISG15 expression induced by Poly I:C.

Significance was obtained between HA-WT MEFs and the empty vector control for ISG15 expression 17 hrs after stimulation (Figure 5.4 c).

To determine if differences seen in IFIT3 protein expression were a consequence of decreases in ISG transcript levels, RT-qPCR was performed on HA-WT CMTR1 and HA-CMTR1 15A MEF cell lines 8 hrs after poly I:C stimulation, using primers targeting murine *Ifit3* and *Isg15* (Figure 5.5). It was shown that transcript levels of *Ifit3* failed to be induced 8 hrs after Poly I:C treatment when CMTR1 was unable to be phosphorylated, at least to the same extent as HA-WT CMTR1 cell lines. This matches findings regarding protein expression. Differences in *Isg15* transcript levels were once again non-significant between HA-WT and HA-15A CMTR1 MEFs, with significance only being found between HA-WT CMTR1 MEFs and the EV control.

It should be noted that unlike experiments conducted with IFN, transfection of cre recombinase vectors was not performed on cells used for experiments involving Poly I:C treatment. Hence, the cells used in Poly I:C experiments maintain expression of endogenous CMTR1. Overexpression of HA-WT CMTR1 amplifies induction of IFIT3 in response to Poly I:C, when compared to HA-15A CMTR1 or EV MEFs, the latter two of which express ISG proteins to a similar extent. This suggests that CMTR1 expression is a limiting factor for ISG induction and that phosphodeficient CMTR1 has a decreased or limited ability to enhance ISG responses at early time points. It is still possible that interference from endogenous CMTR1 impacted the findings presented here. For this reason, repeating this set of experiments after transduction of cells with cre-recombinase expression vectors may be beneficial.

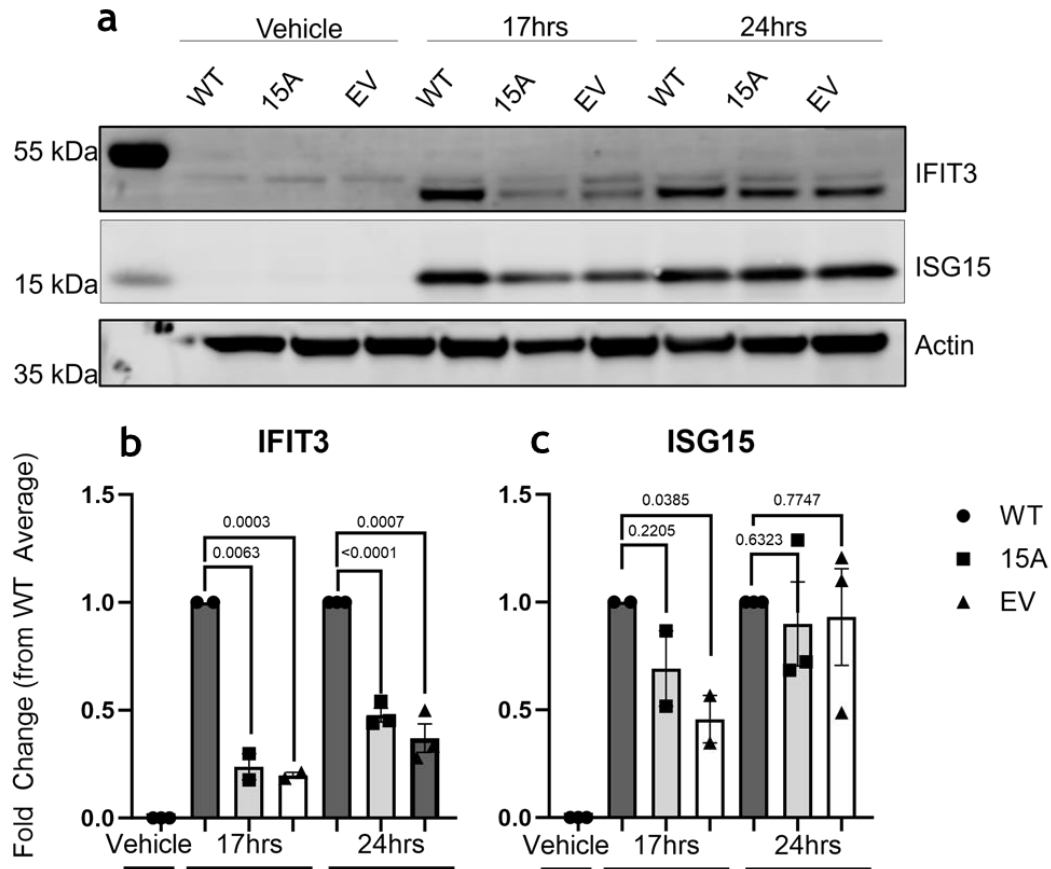


Figure 5.4-Expression of ISG proteins following stimulation with HWM Poly I:C is delayed when CMTR1 cannot be phosphorylated.

MEF cell lines expressing either HA-WT CMTR1, HA-15A CMTR1 or an empty vector control were treated with 5 µg/ml HWM Poly I:C and harvested at the indicated time points over a period of 24 hrs for protein. Western blotting was then performed to determine differences in protein expression amongst genotypes. Western blotting was carried out using 10µg of cell lysate with antibodies targeting IFIT3 and ISG15. Actin was used as a loading control. Molecular weight is indicated on the left side of the panel. Quantification of signal for each sample and protein of interest was normalised according to actin and calculated in comparison to the WT signal at the 17 hr time point (b, c). Students t-tests were performed to determine significance. N=2 for 17 hr time point, N=3 for 24 hr time point. MEFs were harvested on different days at 2 or 3 different passages. Bars show the mean value, with error bars depicting the SEM, each point represents an individual replicate. Quantification was carried out using Image Studio™ Lite (Li-Cor). Figure adapted from Lukoszek *et al.*, 2024. ISG (Interferon stimulated gene), HWM Poly I:C (High molecular weight poly inosinic:polycytidylic acid), CMTR1 (Cap Methyltransferase 1), MEF (Mouse embryonic fibroblast), HA-WT CMTR1 (Haemagglutinin tagged wild type CMTR1), HA-15A CMTR1 (Haemagglutinin tagged phosphodeficient CMTR1), IFIT3 (Interferon-induced protein with tetratricopeptide repeats 3), ISG15 (Interferon stimulated gene 15), SEM (Standard error mean).

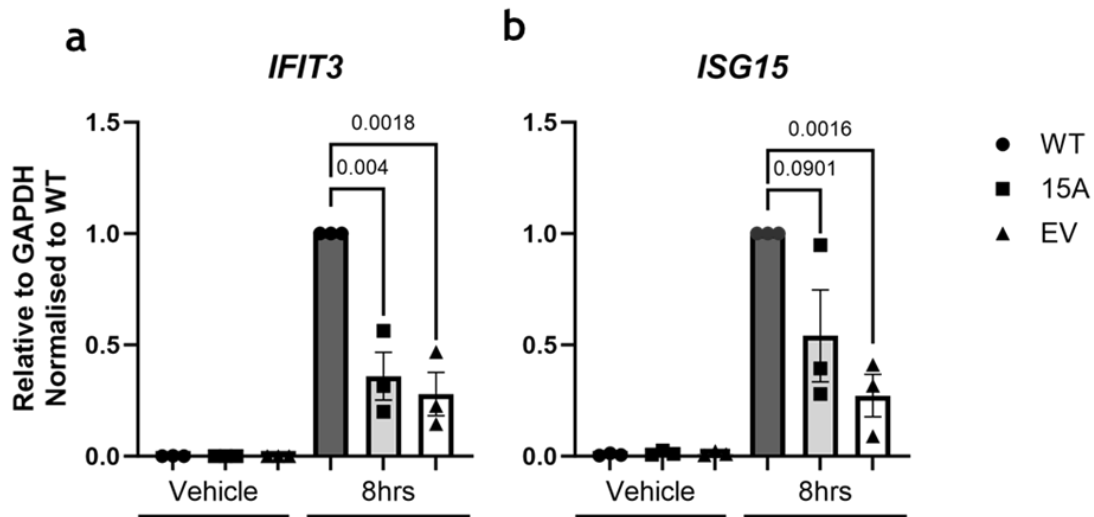


Figure 5.5-Stimulation of RNA sensing pathways with HMW Poly I:C results in decreased expression of IFIT3 transcripts.

MEF cell lines expressing either HA-WT CMTR1, HA-15A CMTR1 or an empty vector control were treated with 5 µg/ml Poly I:C, then harvested 8 hrs post-treatment for RNA. RT-qPCR analysis was performed to determine differences in transcript expression for *Ifit3* (a) and *Isg15* (b), with comparison to the average value for the WT 8 hrs post Poly I:C transfection. GAPDH was used as a normalisation gene. Students t-test was performed to determine significance between genotypes regarding transcript expression. N=3. MEFs were harvested on 3 different days at 3 different passages (biological replicate). Bars show the mean value, with error bars depicting the SEM, each point represents an individual biological replicate, a single one of which is representative of the average value obtained from 3 technical replicates. HWM Poly I:C (High molecular weight polyinosinic:polycytidylic acid), IFIT3 (Interferon-induced protein with tetratricopeptide repeats 3), ISG15 (Interferon stimulated gene 15), MEF (Mouse embryonic fibroblast), HA-WT CMTR1 (Haemagglutinin tagged wild type CMTR1), HA-15A CMTR1 (Haemagglutinin tagged wild type CMTR1), EV (Empty vector), RT-qPCR (Quantitative reverse transcription polymerase chain reaction), GAPDH (Glyceraldehyde-3-phosphate dehydrogenase), SEM (Standard error mean)

5.2.4 CMTR1 phosphorylation is upregulated during the IFN response

Initial characterisation of CMTR1 identified induction of this protein during IFN responses, leading to its classification as an ISG and suggesting a role for CMTR1 in the regulation of anti-viral responses (Haline-Vaz *et al.*, 2008). Given that previous findings in this chapter demonstrated the importance of P-CMTR1 in promoting ISG expression, the status of P-CMTR1 itself was investigated upon IFN treatment in cell lines via Immunoprecipitation/western blot (IP/WB).

CMTR1-IP was undertaken on 0.5 mg of cell extract obtained from IFN treated WT A549 cell lines (Figure 5.6). As CMTR1 is an ISG and hence upregulated in response to IFN, signals for P-CMTR1 would not be comparative between non-IFN treated extract unless the signal for CMTR1 was normalised. This was achieved by loading differing amounts of the IP for non-treated and IFN treated extract, followed by blotting with a total CMTR1 and phospho-specific CMTR1 antibody. When this was undertaken the signal for P-CMTR1 was higher in extract treated with IFN 4 hrs prior to lysis, compared to the non-treated control. This suggests a potential enrichment of CMTR1 phosphorylation upon exposure to IFN and that this may be specifically upregulated as a component of the immune response to IFN. However, as this experiment was only conducted using 2 biological replicates, additional repeats would improve confidence in these findings.

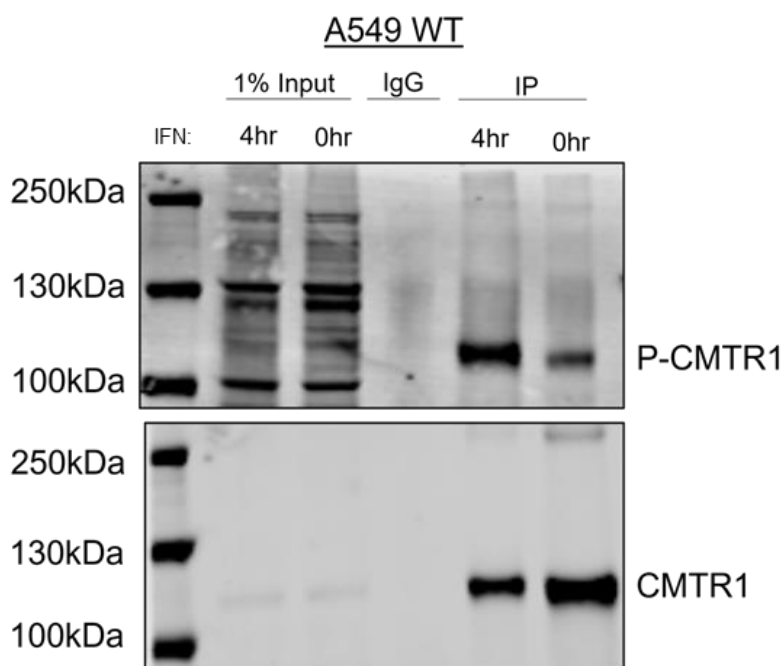


Figure 5.6-CMTR1 phosphorylation is upregulated during the IFN response

0.5 mg of cell lysate from WT-A549 cell lines was used for CMTR1 IP/WB alongside 1 µg of sheep IgG anti-CMTR1. Western blotting was then carried out to detect CMTR1 and P-CMTR1. Post IP-input samples of 5 µg were loaded alongside the IP, with ¼ of the IP being loaded for non-IFN treated cell lines and 1/8 for those treated with IFN for 4 hrs. A species matched non-specific antibody was used as an IgG control to confirm specificity of the interaction. Molecular weight is indicated on the left side of the panel. N=2. CMTR1 (Cap Methyltransferase 1), P-CMTR1 (Phospho-CMTR1), WT (Wild type), IP/WB (Immunoprecipitation/western blot), IFN (Interferon).

5.2.5 P-CMTR1 is a pro-viral factor during IAV infection

The work shown here thus far demonstrates that P-CMTR1 is required for rapid induction of various ISGs upon treatment with IFN and HWM Poly I:C. RNA sensing pathways and IFN responses are crucial components of innate immunity, thus it stands to reason that the phosphorylation status of CMTR1 may impact outcomes of RNA virus infection. To investigate the role of P-CMTR1 in this context, HA-WT and HA-15A CMTR1 MEF cell lines were infected with Influenza A virus (IAV). The strain of IAV used in these experiments were mouse adapted (PR8) and engineered to express mCherry, which was fused to the open reading frame of non-structural protein 1 (NS1). This strain of influenza is referred to as PR8 “ColorFlu” IAV (Fukuyama *et al.*, 2015) (kindly provided by Dr Edward Hutchinson).

Mouse embryonic fibroblast cell lines (MEFs) expressing exogenous CMTR1 and a cre-recombinase construct (which also encodes for eGFP as a marker), were infected with PR8 ColorFlu at a multiplicity of infection (MOI) of 1 for 24 hrs, followed by downstream analysis of NS1-mCherry signal by flow cytometry. The fluorescence intensity of mCherry served as an indirect readout of viral protein production and infection. Surprisingly, the percentage of cells within the total population which were positive for mCherry expression was considerably lower in MEFs expressing HA-15A CMTR1 and the EV control, when compared to MEFs expressing HA-WT CMTR1 (Figure 5.7 a). Statistical analysis showed that these differences were significant (Figure 5.7 b). The geometric mean of fluorescence intensity for mCherry signal was also significantly lower in cells expressing phosphodeficient mutant CMTR1 (Figure 5.7 c, d). These results were somewhat unexpected as these implicate a role for P-CMTR1 as a pro-viral factor, despite previous data showing CMTR1 phosphorylation promotes expression of anti-viral ISGs. This may be attributed to specific host-pathogen interactions required for IAV propagation which will be discussed further on.

In addition to infection assay with IAV, a pilot experiment was carried out where HA-WT and HA-15A CMTR1 MEFs were infected with Sindbis Alpha virus (SINV) expressing a mCherry reporter under the control of the non-structural protein 3 (NSP3) subgenomic promoter (kindly provided by Dr Alfredo Castello).

Protein analysis conducted on these cells after infection at an MOI of 0.1 for 24 hrs, demonstrated that expression of SINV capsid and NSP3 was equivalent amongst genotypes (Figure 5.7e). This again was surprising given previous findings regarding regulation of ISG expression by P-CMTR1. However, alphaviruses including SINV have previously been shown to degrade RNAPII as a strategy of inducing host-transcriptional shut off (Akhrymuk et al., 2012, Akhrymuk et al., 2018). For this reason, RNAPII expression was assessed by western blot and revealed a dramatic loss of signal across all genotypes upon infection when compared to mock treated cells. In conclusion, it may be the case that SINV mediated degradation of RNAPII prevents CMTR1 from carrying out mRNA capping functions and general ISG transcription, both of which are dependent on RNAPII activity. It should be noted that the results of this pilot-experiment were obtained from a single biological replicate and thus firm conclusions cannot be drawn from these data. They are included in this thesis to broaden discussion concerning the role of P-CMTR1 and host pathogen interactions in response to a variety of RNA viruses.

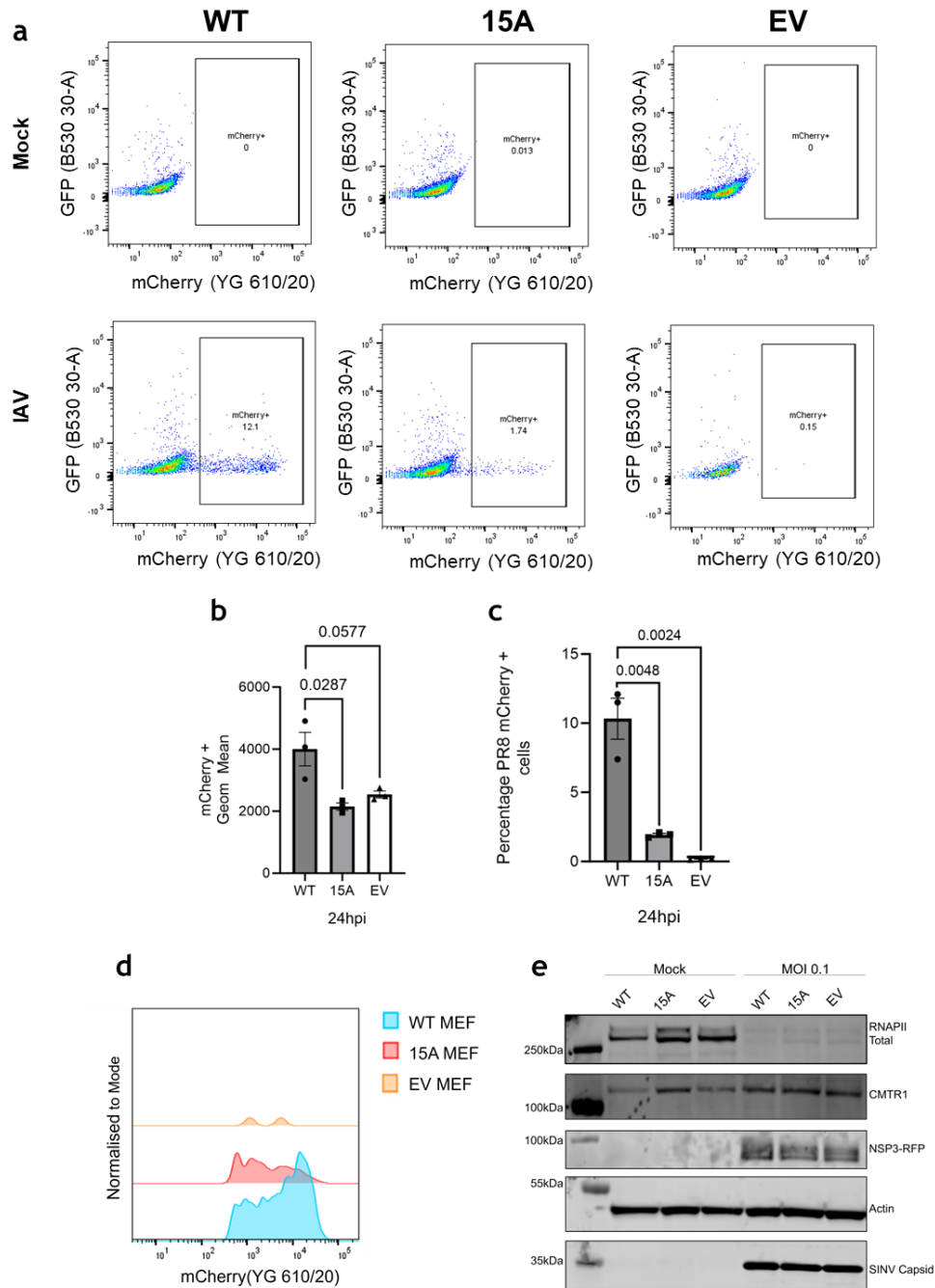


Figure 5.7-The phosphorylation status of CMTR1 impacts IAV infection

CMTR1^{fl/fl} MEFs, expressing either HA-WT CMTR1, HA-15A-CMTR1 or an empty vector control and cre were infected with PR8 ColorFlu expressing mCherry fused to non-structural protein 1, and processed 24 hpi for downstream analysis by flow cytometry. Representative dot plots for each genotype (a), geometric mean for the fluorescent mCherry signal (b), and the percentage of mCherry+ cells within populations of cells analysed (c) are shown. A histogram displaying the fluorescent signal normalised to mode (d) is also depicted. N=3. MEF cell lines expressing either HA-WT CMTR1, HA-15A CMTR1 or an empty vector control were infected with SINV-mCherry at an MOI of 0.1 for 24 hrs, prior to lysis for western blotting. 10 μ g of protein was loaded for western blotting, with antibodies targeting RNAPII, CMTR1, RFP and SINV capsid being used. Actin was used as

a loading control. Molecular weight is indicated on the left side of the panel (e). N=1. Bars show the mean value, with error bars depicting the SEM, each point represents an individual replicate. Figure adapted from Lukoszek *et al.*, 2024. CMTR1 (Cap Methyltransferase 1), IAV (Influenza A virus), MEF (Mouse embryonic fibroblast), HA-WT CMTR1 (Haemagglutinin tagged wild type CMTR1), HA-15A CMTR1 (Haemagglutinin tagged phosphodeficient CMTR1), EV (Empty vector), GFP (Green fluorescent protein), NSP1 (Non-structural protein 1), hpi (Hours post infection), SINV (Sindbis virus), MOI (Multiplicity of infection), RNPII (RNA polymerase II), CMTR1 (Cap Methyltransferase 1), RFP (Red fluorescent protein), SEM (Standard error mean). Gating strategy for flow cytometry experiments can be found in the appendices.

5.3- Discussion

In summary, the findings presented in this chapter have demonstrated that both expression and phosphorylation of CMTR1 by CK2 is required for timely expression of various ISGs, upon stimulation of IFN and RNA sensing pathways in MEF cell lines. Phosphorylation of CMTR1 appears to be enhanced in response to IFN treatment, representing a mechanism by which ISG expression can be further promoted during anti-viral responses. Surprisingly, it was found that P-CMTR1 acted as a pro-viral factor in the context of IAV infection and had little influence on SINV capsid and NSP3 protein production. This may be attributed to the impact of host-pathogen interactions which tend to be unique to specific viruses. Together these data highlight the need to consider the interplay between host and virus when examining CMTR1 function in infection.

5.3.1 CK2 mediated phosphorylation of CMTR1

CK2 was identified as the kinase responsible for phosphorylating CMTR1 on the P-Patch by in-vitro recombinant protein assay (Lukoszek *et al.*, 2024). However, it has not been determined whether CK2 activity is redundant for CMTR1 phosphorylation and if other kinases play a role in regulating P-CMTR1 activity. Given the amino acid sequence of the P-Patch surrounding phosphorylation sites; it is likely that any alternate kinases would be acidophilic in nature, as suggested by Dr Francisco Inesta-Vaquera (Lukoszek *et al.*, 2024). Furthermore, phosphorylation of multiple sites within a single protein is often mediated in a hierarchal fashion, with initial phosphorylation by a single kinase generating additional recognition motifs (Roach, 1991). This suggests that additional kinases may be responsible for phosphorylating CMTR1 in tandem with CK2 and warrants further investigation.

How phosphorylation of CMTR1 is itself regulated remains an open question in this work, particularly in an innate immune context. The cellular response to IFN is highly damaging to the host when dysregulated, with chronic production being associated with various pathologies (Akwa *et al.*, 1998, Baechler *et al.*, 2003). This being the case, it stands to reason that timely regulation of CMTR1 phosphorylation would also be of import in modulating these. CK2 is not directly regulated by IFN, However, pro-inflammatory transcription factor NF- κ B which is often induced concurrently with IFN responses (Seth *et al.*, 2005, Kawai *et al.*, 2005), appears to

enhance *CK2a* promoter activity (Krehan *et al.*, 2000). Alternatively, phosphorylation of CMTR1 may be regulated during innate immune responses by an alternate kinase which is directly induced by IFN, such as protein kinase R (Kuhlen and Samuel, 1997). It can also be speculated that regulation of CMTR1 phosphorylation is dependent on the activity of specific phosphatases. CMTR1-interactome experiments and follow up validation conducted in liver identified the phosphatase PGAM5 as a CMTR1 interactor (chapter 4). Although the biological relevance of this interaction has yet to be uncovered, it may be the case that PGAM5 or other phosphatases dephosphorylate CMTR1 to regulate the phosphorylation status of this protein during the IFN response.

5.3.2 Regulation of ISG expression by CMTR1

The data presented here found that P-CMTR1 promoted expression of ISGs including *Ifit1*, *Ifit3*, *Ifih1*, and *Isg15* on both the protein and transcript level. These contrast interestingly with previous work conducted by Williams *et al.*, who observed marked decreases in protein but not transcript expression of ISG15, MX1, and IFITM1 upon total CMTR1 deletion in Huh-7 (human hepatoma) and THP-1 (human monocyte) cell lines. Additionally, Williams *et al.*, found no marked differences in the expression of IFIT1 and IFIT3 during CMTR1 KD. The authors of this paper uncovered that loss of ISG15, MX1, and IFITM1 protein expression in response to CMTR1 knock down could be attributed to IFIT1 mediated translational inhibition. They further demonstrated that reductions in protein expression of these select ISGs were due to RNA elements in the 5'UTR of transcripts, which predispose these to inhibition by IFIT1 in the absence of the Cap-1 structure (Williams *et al.*, 2020).

It may be the case that discrepancies between the findings of Williams *et al.*, and those shown here are due to differences between experimental models. A weakness of the murine model used in these experiments when trying to extrapolate these findings to human biology and disease is the evolutionary divergence between mouse and human ISGs. For example, despite sharing a common name; human and mouse IFIT1 are not orthologous, sharing only 53% of their amino acid identity and possessing unique molecular functions. Divergence between ISGs amongst species is unsurprising, given the general trend of host

specificity amongst viruses and the need to develop differing strategies to overcome these (Daugherty *et al.*, 2016). The fact that a fibroblast rather than liver or monocyte cell line was used for experiments may also explain differences between the findings presented here and those of similar work. Furthermore, phosphorylation of CMTR1 is not found in primary liver tissue (Chapter 3, Figure 3.4) and would be unlikely to influence ISG expression in cell lines of liver origin if tested. It must be stated however, that P-CMTR1 status has not been analysed in Huh-7 cell lines specifically and may be altered upon induction of IFN.

The data shown here demonstrated that deficits in ISG expression upon loss of CMTR1 phosphorylation occur on both a translational and transcriptional level, which once again contrasts to previous findings (Williams *et al.*, 2020). Despite this, CMTR1 has been noted to regulate gene expression in this manner previously. The exact mechanisms of how CMTR1 achieves transcriptional regulation in this model has not been thoroughly examined; but these may be attributed to promotion of RNAPII binding to TSS via CMTR1, or the protective effect of the Cap-1 structure against exonuclease cleavage (Liang *et al.*, 2022, Picard-Jean *et al.*, 2018). It is likely that in the model presented here, abrogation of ISG transcription consequently leads to downstream reduction in protein translation, with translational inhibition of RNA lacking 2'-O-ribose methylation by IFIT proteins contributing further to this phenomenon.

In contradiction to our findings and those by Williams *et al.*, one study has described upregulation of IFN- β expression upon CMTR1 KO in A549 cells infected with IAV for 16 hours (Li *et al.*, 2020). Preliminary work not shown here demonstrated upregulation of ISG transcript expression after Poly I:C stimulation when measured 24hrs rather than 8hrs post treatment; amongst HA-15A CMTR1 and EV MEFs compared to HA-WT CMTR1 cells, in the absence of cre recombinase. Although this data was not found to be significant due to variation in the extent of IFN induction. It may also be noted that average protein expression of IFIT3 24 hrs after IFN treatment was lower in HA-WT CMTR1 MEFs, compared to HA-15A CMTR1 MEFs, despite the opposite trend occurring at the 8hr time point. This suggests that P-CMTR1 may be involved in both the promotion of ISG expression during early responses to IFN and negative regulation of these same responses at later stages.

For these reasons, discrepancies between findings presented here and those of Li *et al.*, may be attributed to a role for P-CMTR1 in ensuring expression of ISG transcripts that are involved in temporal and negative regulation of the IFN response. To assess if this is the case, interrogation of how expression of genes implicated in negative regulation of IFN pathways are affected by loss of P-CMTR1 would be of use. Alternatively, loss of capping activity might drive detection of self-transcripts, which would propel uncontrolled IFN signalling during later stages of a sustained innate immune response.

One further critique of the model used in the bulk of experiments presented in this chapter, is the use of a transient cre recombinase vector to eliminate endogenous CMTR1 expression. The use of transient over stable integration of cre recombinase, may have resulted in recovery of low levels of endogenous CMTR1 by the time experiments were conducted (Di Blasi *et al.*, 2021), which could have interfered with data interpretation. To overcome this issue, an A549 CRISPR/Cas9 CMTR1 KO cell line has been developed and is awaiting validation prior to stable transfection of WT and 15A-CMTR1 constructs. Once this alternate model has been fully realised, repeating experiments on these cell lines would be of benefit and may also determine if findings in MEFs are applicable to human cell lines.

5.3.3 Potential mechanisms of CMTR1 anti and pro-viral activity

As shown previously, abrogation of either total or phosphorylated CMTR1 inhibits expression of IAV NSP1 protein tagged to a mCherry reporter, as determined by flow cytometry. This contrasts with previous findings highlighting the role of CMTR1 in promoting anti-viral IFN responses (Lukoszek *et al.*, 2024, Williams *et al.*, 2020) and inhibiting infection of Dengue and Zika virus (Williams *et al.*, 2020). It should be noted however that unlike IAV, Dengue and Zika viruses are members of the Flaviviridae family and encode their own capping machinery (Ray *et al.*, 2006, Saeedi and Geiss, 2013).

Data from the literature supports a pro-viral role for CMTR1 in IAV infection specifically, matching with findings presented here. Use of trifluoromethyl-tubercidin (TFMT), an inhibitor of CMTR1 methyltransferase activity was found to reduce IAV replication (Tsukamoto *et al.*, 2023). Deficits in IAV replication upon TFMT treatment was not found to occur due to alterations in IFN and ISG

expression induced by repression of CMTR1. Rather, inhibition of IAV replication occurred concurrently with a reduction in capped viral mRNA (Tsukamoto *et al.*, 2023). Genome-wide CRISPR screens conducted on A549-Cas9 cells also identified CMTR1 as a host dependency factor for IAV replication, with a decrease in capped viral RNA being observed in CMTR1 KO cells (Li *et al.*, 2020).

Many structural studies indicate efficient binding occurs between the influenza polymerase PB2 subunit and the m7G cap in the absence of methylation of the first transcribed nucleotide of CMTR1 (Xie *et al.*, 2016, Guilligay *et al.*, 2008). Despite this, work conducted in cell lines as described above demonstrates a clear dependency on CMTR1 activity for efficient cap snatching by IAV (Tsukamoto *et al.*, 2023, Li *et al.*, 2020), with one biochemical study describing a 14-fold increase in priming activity upon 2'-O-ribose methylation of the first nucleotide (Bouloy *et al.*, 1980). Thus, it is reasonable to conclude that P-CMTR1 may act as a pro-viral factor during IAV infection by ensuring availability of mature Cap-1 structures for snatching. Further evidence for this stems from the observation that there is a noted reduction in RNA structures possessing 2'-O-ribose methylation upon CMTR1 phosphodeficiency (Lukoszek *et al.*, 2024), as determined by cap analysis with minimal analyte processing (CAP-MAP) (Galloway *et al.*, 2020). Whilst initial binding between the Cap-0 structure and the IAV RNA polymerase may occur, it is likely that the Cap-1 structure is necessary to further stabilise this interaction. Alternatively, the Cap-1 structure may also permit conformational changes within the viral RNA polymerase to occur which are essential for efficient priming.

In this work it was found that timely expression of IFIT1 and 3 is dependent on CMTR1 phosphorylation. Although not directly assessed in this work, fellow IFIT family member IFIT2 has been found to promote influenza virus gene expression (Tran *et al.*, 2020). This opens up the possibility that CMTR1 activity may further promote IAV infection by enabling expression of host factors which are repurposed into pro-viral effectors.

The findings here show that upon CMTR1 phosphodeficiency, expression of viral NSP1 protein as measured by reporter fluorescence is significantly reduced. A limitation of determining IAV infectivity by this metric is that this fails to account for which aspect of the viral life cycle is inhibited and if this can be attributed to

deficits in cap snatching activity. Reductions noted in NS1-mCherry fluorescence could be a consequence of deficits in viral protein translation, transcription, or the entry of virus into cells. As this is the case it would be of benefit to further examine mechanisms of P-CMTR1 mediated promotion of NS1 protein expression, drawing particular focus on examination of cap-snatching in this context. This may be achieved by RT-qPCR of IAV hybrid RNA, or pull-down experiments utilising antibody for cap binding proteins followed by RT-qPCR for viral transcripts.

Even though conclusions drawn from IAV infection assays point towards a pro-viral function for P-CMTR1, it is likely that P-CMTR1 possesses anti-viral activity against viruses which are not dependent on host capping machinery. This has been previously demonstrated to be the case in terms of total-CMTR1 expression during Dengue and Zika virus infection (Williams *et al.*, 2020).

Alphaviruses, including SINV are not dependent on cap snatching from host transcripts, nor do they encode their own capping machinery to ensure 2'-O-ribose methylation (Ahola and Kääriäinen 1995, Daughtery *et al.*, 2016), instead they are dependent on efficient induction of transcriptional shutoff via RNAPII degradation to attenuate host immune responses (Akhrymuk *et al.*, 2018). Given that this is the case, it is relatively unsurprising that the data shown indicates that P-CMTR1 has minimal effect on expression of SINV NSP3, as host-transcriptional shut-off would likely prevent CMTR1 from promoting ISG expression and exerting anti-viral activity. Viruses have evolved immune evasion strategies in order to successfully replicate in host cells and prevent clearance, making it unsurprising that both SINV and IAV possesses mechanisms to circumvent CMTR1's anti-viral effect. It should be stated however, that the data presented here regarding P-CMTR1 and SINV infection come from a single replicate that showed no differences in viral capsid and non-structural protein production occurred upon abrogation of P-CMTR1. To determine a role for P-CMTR1 in alphavirus infection, IFN treatment of HA-WT and HA-15A MEF cells prior to inoculation of SINV would be beneficial, as this would permit for induction of ISG expression prior to RNAPII degradation.

Chapter 6: Discussion

6.1 Summary

The two aims of this project centred around characterising CMTR1 in the context of hepatocellular carcinoma (HCC) and uncovering a role for CMTR1 phosphorylation in innate immune responses to viral infection. Dysregulation of two oncogenes *CTNNB1* and *MYC* (*Ctnnb1*^{ex3/WT}; *R26*^{-LSL-MYC}) within the liver is an established murine model of HCC, which mimics common genetic alterations found in human HCC patients (Bisso *et al.*, 2020, Schulze *et al.*, 2015). Preliminary findings from the Sansom lab indicate a tumour suppressive role for CMTR1 in HCC initiation, as deletion of this protein quickened tumorigenesis in *Ctnnb1*^{ex3/WT}; *R26*^{-LSL-MYC} mouse liver. Through further investigation I uncovered that expression of hepatic CMTR1 is altered in mouse liver 10 days after induction of *Ctnnb1*^{ex3/WT}; *R26*^{-LSL-MYC} via cre recombinase, when compared to WT controls (Figure 3.1). CMTR1 also maintains interaction with negative regulator DHX15 in the liver (Figure 3.3) which was initially identified in HeLa and HEK293 cell lines (Inesta-Vaquera *et al.*, 2018) and is minimally phosphorylated regardless of oncogene status (Figure 3.4). By conducting immunoprecipitation/mass spectrometry (IP/MS) two proteins implicated in HCC oncogenesis were identified as novel CMTR1 protein interactors, ASS1 and PGAM5. These proteins were selected for downstream validation and co-immunoprecipitated with CMTR1 in mouse liver extracts (Figure 4.5, 4.6). However, the ASS1 interaction with CMTR1 was not detected in Huh-7 cell extracts, which may be attributed to low expression of ASS1 in these and other HCC cell lines (Figure 4.6). Subsequently, immunostaining was conducted on Huh-7 cell lines to determine the sub-cellular localisation of both CMTR1 and PGAM5. Both proteins displayed a similar distribution within Huh-7 cells and were found to co-localise (Figure 4.8). These data suggest that the interaction between CMTR1 and PGAM5 is genuine.

Previous work conducted in the Cowling lab identified a region of 15 amino acids which were phosphorylated at the N-terminus of CMTR1, which promoted CMTR1 dependent gene expression. I investigated if phosphorylation of CMTR1 at these sites impacted expression of interferon stimulated genes (ISGs). This was achieved through the use of mouse embryonic fibroblasts (MEFs) expressing phosphomutant CMTR1 (where phosphorylated amino acids were replaced by alanine), where it

was uncovered that both transcript and protein expression of various ISGs were significantly decreased when CMTR1 could not be phosphorylated. The biological relevance of this finding was then investigated by infecting CMTR1 phosphodeficient MEFs with Influenza A virus (IAV). In these cells P-CMTR1 was found to play a pro-viral role, with expression of viral protein NS1-mCherry being abrogated upon phosphodeficiency.

Follow up work is needed to determine the functional relevance of heightened CMTR1 expression alongside protein interactions between CMTR1 and ASS1/PGAM5 in cancer. Current knowledge of CMTR1 activity and how this may relate to liver oncogenesis is discussed below. In terms of anti-viral responses impacted by CMTR1 phosphorylation, the data presented here demonstrate that P-CMTR1 is required for normal induction of ISGs on both the transcriptional and translational level in MEFs. Conversely, despite sustaining anti-viral responses, we uncovered that P-CMTR1 acts as a pro-viral host factor in IAV infection. This chapter will subsequently focus on discussion of CMTR1 in innate immunity, the biological relevance this may have in infection of distinct viral species not mentioned before, and the implications for the use of CMTR1 as a therapeutic target.

6.2 CMTR1 mediated immune responses in Hepatocellular Carcinoma

Tumour promoting inflammation was incorporated as a second enabling characteristic of cancer by Hanahan and Weinberg in 2011, via complementation of genome instability. This is particularly prominent in the case of HCC, which frequently occurs subsequent to chronic hepatitis and associated diseased states (Yu *et al.*, 2018). The role of innate immune responses in cancer is multifaceted, whilst inflammation often drives aberrant alteration of growth signalling pathways and genomic instability (Li *et al.*, 2013, Verzella *et al.*, 2020), it is in other contexts able to suppress cancer by promoting apoptosis and immune rejection of tumour cells (Chew *et al.*, 2010, Duewell *et al.*, 2014, Diamond *et al.*, 2011). This dual role for inflammation in oncogenesis reflects the complexity and nuances of the immune system in cancer, which must be considered for further discussion.

Loss of CMTR1 expression has been demonstrated to induce inflammation, due to the triggering of an anti-viral response by recognition of incompletely capped self-RNA (Dohnalkova *et al.*, 2023, Li *et al.*, 2020). However, this observation is not universal amongst all tissue types and cell lines (Williams *et al.*, 2020). Combined with the fact that CMTR1 promotes ISG expression (Williams *et al.*, 2020, Lukoszek *et al.*, 2024), this information suggests that the relationship between CMTR1 and inflammation is nuanced and likely to be dependent on the cellular context and other factors.

NF- κ B is activated downstream of RIG-I like receptors (RLRs) (Lee *et al.*, 2019, Dong *et al.*, 2013), which are responsible for the sensing of improperly capped and viral RNA species (Züst *et al.*, 2011, Schuberth-Wagner *et al.*, 2015). Heightened activation of NF- κ B is noted to occur in almost all chronic diseases of the liver which are associated with enhanced susceptibility to HCC (Mandrekar and Szabo, 2009, Boya *et al.*, 2001, Videla *et al.*, 2009). In hepatocytes NF- κ B activation renders cells resistant to tumour necrosis factor or lipopolysaccharide induced apoptosis (Heinrichsdorff *et al.*, 2008), this heightened extent of survival in response to liver injury is mediated through crosstalk between NF- κ B signalling with JNK and MAPK signalling cascades (Heinrichsdorff *et al.*, 2008). This presents a mechanism by which NF- κ B contributes to HCC initiation, by promoting survival

of damaged hepatocytes (Luedde and Schwabe, 2011, Ringelhan *et al.*, 2018). In the liver, conditional knock out (cKO) of CMTR1 induces hepatic inflammation (Dohnalkova *et al.*, 2023, Samson lab, personal communication), presumably due to the presence of improperly capped self RNA. Given the strong association between hepatitis and HCC (Yu *et al.*, 2018), it may be the case that depletion of CMTR1 drives tumour promoting inflammation in non-transformed cells.

Whilst a pro-tumorigenic role has been highlighted for dysregulated NF- κ B signalling and chronic inflammation in HCC, the IFN response has been demonstrated to exert anti-cancer effects by promoting cell death and tumour antigen presentation (Duewell *et al.*, 2014, Peng *et al.*, 2009). For example, previous work involving treatment of pancreatic cancer cell lines with RLR ligands was shown to result in the induction of type I IFN production. Activation of pathways downstream of RLR ligand stimulation in this model were found to result in increases of inflammatory tumour cell death and promoted tumour antigen presentation to naïve CD8⁺ T-cells, sensitizing tumour cells to Fas-mediated apoptosis (Duewell *et al.*, 2014). In a liver context, it has been demonstrated that delivery of poly I:C via liposome induces apoptosis of HepG2 cells, downstream of RIG-I and MDA5 signalling (Peng *et al.*, 2009). Considering that loss of CMTR1 and the subsequent production of transcripts lacking Cap-1 structures would activate RLR signalling (Züst *et al.*, 2011, Devarkar *et al.*, 2016, Schuberth-Wagner *et al.*, 2015), it is possible that loss of CMTR1 would be disadvantageous in terms of enabling immune evasion during tumour maintenance.

IFN and IRF3 signalling are fundamentally impaired in liver cancer (Hou *et al.*, 2014). Expression of RLR family member RIG-I is significantly lower in HCC compared to matched control tissue and appears to be mediated by deregulation of gene histone methylation. Furthermore, low expression of RIG-I in HCC patients correlates with poor survival, potentially through impaired responses to IFN- α and suppression of STAT1 activation (Hou *et al.*, 2014). In commonly used liver cancer cell lines including HepG2 and Huh-7 cells, induction of IFN- β promoters is either negligible or temporally deregulated upon stimulation of toll like receptor 3 (TLR3) or poly I:C treatment (Khvalevsky *et al.*, 2007). Experiments involving infection of liver cancer cell lines with Hepatitis E virus revealed differential expression of

PRRs, Interferon regulatory factors and ISGs, with Huh-7.5 cells exhibiting specific defects in RIG-I and TLR3 pathways (Devhare *et al.*, 2016). In comparison to healthy primary hepatocytes, human HCC cells express an alternatively spliced isoform of IRF3. This alternate isoform is transcriptionally inactive and confers susceptibility to oncolytic vesicular stomatitis virus (Marozin *et al.*, 2007). Expression of MDA5, like fellow RLR member RIG-I appears to be impaired in Huh-7 cell lines but can be restored upon metabolic reprogramming via knockdown of hexokinase 2 (Perrin-Cocon *et al.*, 2021).

Overall, the exact role that innate immune signalling pathways downstream of RLR activation in HCC is unclear and at times appears contradictory (Luedde *et al.*, 2007, Heinrichsdorff *et al.*, 2008, Kawaguchi *et al.*, 2019). It is likely that external factors and the context in which HCC oncogenesis occurs influences the role components downstream of RNA sensing pathways play in tumour development. It may be the case that in the absence of CMTR1 and efficient capping of endogenous transcripts, PRRs react inappropriately to drive IFN/NF- κ B signalling and induce chronic hepatitis. This acts as a source of inflammation which then drives pro-tumorigenic signalling and inappropriate responses to liver injury, laying the groundwork for development of fibrosis and eventually HCC. It should be stated however, that whilst deletion of CMTR1 is useful for establishing tumour promoting inflammation before cancer initiation, this is unlikely to be the case upon development of fully fledged HCC. Evidence to support this theory is the fact that whilst cKO of CMTR1 in the liver of WT mice results in aberrant inflammation (Dohnalkova *et al.*, 2023, Sansom lab, personal communication), depletion of CMTR1 in Huh-7 cells does not (Williams *et al.*, 2020). This may be attributed to defects in IFN and RLR signalling which are conserved in a considerable number of liver cancer cell lines and primary tumours derived from HCC patients (Hou *et al.*, 2014, Khvalevsky *et al.*, 2007, Devhare *et al.*, 2016, Marozin *et al.*, 2007).

During tumour maintenance, it may be the case that sustaining expression of CMTR1 would be beneficial in evading host responses to improperly capped RNA (should the tumour maintain RNA sensing pathways). Additionally, CMTR1 is responsible for the expression of specific genes which are implicated in the pathogenesis of HCC, such as the cytokine *IL6* and metabolic factor *FASN* (fatty

acid synthase) amongst many (You *et al.*, 2023, Inesta-Vaquera *et al.*, 2018, Vanauberg *et al.*, 2023). Hence, high expression of CMTR1 in established tumours would likely be advantageous to maintain a transcriptional profile which favours aberrant metabolism and growth.

6.3 The potential role of CMTR1 regulated gene expression in Hepatocellular Carcinoma

As alluded to in the discussion section of chapter 3, enhancements in CMTR1 dependent gene expression of metabolic and cell cycle factors are noted to coincide with enhanced proliferation of mammary epithelial tumour cells, upon abrogation of the interaction between CMTR1 and negative regulator DHX15 (Inesta-Vaquera *et al.*, 2018). These findings suggest that CMTR1 may influence cancer cell proliferation through regulation of specific genes. Emerging data from the literature has indicated that CMTR1 specifically regulates ribosome biogenesis, histone production and snoRNA processing (Liang *et al.*, 2022, Lukoszek *et al.*, 2024, Wolter *et al.*, 2023, Preprint) all of which have been previously implicated in the pathogenesis of HCC (Baral *et al.*, 2018, Gaillard *et al.*, 2015).

Depletion of CMTR1 during embryonic stem cell (ESC) differentiation resulted in substantial impairments in histone and ribosomal gene transcription (Liang *et al.*, 2022). This finding was partially replicated upon KO of CMTR1 in HEK293, which also displayed significant defects in ribosomal protein transcription (Wolter *et al.*, 2023, Preprint), suggesting regulation of ribosomal expression by CMTR1 is a common feature amongst cell lines. Dysregulated ribosome biogenesis is believed to play a role in carcinogenesis by promoting metastasis and enhancing translational capacity to sustain uncontrolled proliferation (Hwang and Denicourt, 2024). In a subset of HCC tumours, expression of heat shock factor protein 1 is driven by enhanced ribosome activity and biogenesis (Yang *et al.*, 2024). This alters hepatic metabolism and induces steatosis, in a manner which promotes malignancy (Santagata *et al.*, 2013, Jin *et al.*, 2011).

Depletion of CMTR1 in HEK293 resulted in reduced transcription of snoRNA host genes and mRNA containing 5' terminal oligopyrimidine tract (5'TOP) motifs (Wolter *et al.*, 2023, Preprint). Small nucleolar RNAs (snoRNAs) are responsible for processing rRNAs and small nuclear RNAs (snRNA) (Kiss, 2002), whilst 5'TOP motifs are a common feature of transcripts encoding ribosomal proteins and other translation factors (Yamashita *et al.*, 2008). In HCC, dysregulation of multiple snoRNA species has been noted, with these possessing both oncogenic and tumour suppressor effects (Baral *et al.*, 2018). For example, expression of snoRNA ACA11 is

significantly increased in HCC tumour tissues compared to matched controls and is believed to contribute to metastasis by positively regulating PI3K/AKT signalling. (Wu *et al.*, 2017).

Conversely, Liang *et al.*, observed replication stress, as determined by expression of phosphorylated H2A histone family member X (γ -H2AX), upon CMTR1 depletion in ESC (Liang *et al.*, 2022). Prolonged and sustained replication stress results in genomic instability, heightening the chance of introducing oncogenic lesions into the genome (Gaillard *et al.*, 2015). Increased levels of γ -H2AX, a marker of DNA damage, are found in the majority of HCC tumours and at an even higher rate in pre-neoplastic liver nodules (Matsuda *et al.*, 2013).

In terms of non-inflammatory function, CMTR1 regulated gene expression of ribosomal proteins and snoRNA may promote tumour maintenance by enhancing translational capacity. In turn, CMTR1 appears to protect ESC against DNA damage by regulating histone expression, which may protect liver cells against genomic instability and eventual carcinogenesis, if this finding is found to be applicable to hepatocyte models. The fact that CMTR1 expression was significantly higher in *Ctnnb1*^{ex3/WT}; R26-LSL-MYC liver compared to controls, may indicate that CMTR1 contributes to liver tumorigenicity. However, further work on these models with emphasis on investigating CMTR1 regulated gene expression of ribosomal proteins, histones and snoRNA would be beneficial to determine if this is the case.

6.4 Biological relevance of models used in this work

Hepatocellular carcinoma is a heterogeneous disease, with tumours displaying a variety of genetic lesions, which are in part dependent on underlying aetiology. Alcohol-related HCCs display enrichment for mutations in *CTNNB1*, *TERT* and *CDKN2A*, whilst mutations in *TP53* are strongly associated with cases of HCC with underlying HBV and Aflatoxin aetiologies (Schulze *et al.*, 2015, Gouas *et al.*, 2009). Overexpression of c-Myc is associated with most HCC cases of known aetiologies including alcohol abuse, HBV and HCV but not in cryptogenic HCC patients (Schlaeger *et al.*, 2008). In mouse models used for this work, tumorigenesis was induced through expression of a stable β -catenin mutant and overexpression of c-Myc. Whilst the liver cancer cell line used in this work, Huh-7 cell lines, originate from a 57-year-old male Japanese patient and are negative for HBV X and S-gene integration (Nakabayashi *et al.*, 1982, Hsu *et al.*, 1993). In terms of characterised mutations, Huh-7 cells carry a C228T mutation in the *TERT* gene promoter (Cevik *et al.*, 2015) and a A220G mutation in *TP53* (Hsu *et al.*, 1993). The models used in this thesis may be said to possess genetic aberrations which are representative of HCC cases arising from alcohol abuse, a major contributing factor for HCC in western countries (Liu *et al.*, 2019). On a global scale however, causes relating to HBV and HCV infection contribute to 54% of all HCC related deaths (Akinyemiju *et al.*, 2017). This highlights the need to expand the range of models and cell lines representing HCC within this work, as this will help determine if alterations in CMTR1 expression and interaction are a universal feature of HCC or vary according to underlying aetiology.

6.5 Biological implications of putative CMTR1 protein interactions

Although this work established PGAM5 and ASS1 as interactors of CMTR1, time constraints prevented further examination into the biological relevance of these interactions. This section shall hence focus on the established functions of CMTR1, PGAM5, and ASS1, postulating as to how interaction between these proteins may impact function.

One of the most well characterised functions of PGAM5 is as a Ser/Thr/His phosphatase. Established targets of PGAM5 phosphatase activity include FUN14 domain containing 1 protein (FUNDC1), and nucleoside-diphosphate kinase B (NDPK-B) (Chen *et al.*, 2014, Yu *et al.*, 2020, Nag *et al.*, 2023, Takeda *et al.*, 2009, Panda *et al.*, 2016). Both NDPK-B and FUNDC1 are phosphorylated by CK2, the same kinase which phosphorylates CMTR1 at the N-terminal P-patch (Chen *et al.*, 2014, Biondi *et al.*, 1996, Lukoszek *et al.*, 2024). In the case of FUNDC1, phosphorylation of the Ser-13 residue by CK2 functions to maintain mitochondrial integrity at resting states. Upon exposure to oxidative stress, interaction between PGAM5 and FUNDC1 is enhanced, permitting for PGAM5 to exert phosphatase activity on FUNDC1 to induce mitophagy. This highlights a mechanism by which PGAM5 and CK2 work in tandem to coordinate cellular responses (Chen *et al.*, 2014).

Previous work has also highlighted a role for PGAM5 in the regulation of nuclear factors involved in mRNA processing. Upon cleavage induced by mitochondrial uncoupler FCCP, PGAM5 is able to translocate to the nucleus to dephosphorylate serine/arginine repetitive matrix protein 1 (SRm160) and serine/arginine-rich splicing factor 1 (SRSF1) (Baba *et al.*, 2021). SRm160 functions as a co-activator of pre-mRNA splicing (Blencowe *et al.*, 1998), whilst SRSF1 promotes translation initiation of target mRNAs by suppressing eukaryotic translation initiation factor 4E-binding protein 1 activity, a competitive inhibitor of eIF4E (Maslon *et al.*, 2014). Interestingly, SRSF1 has been identified as a potential CMTR1 interacting protein in a HEK293 interactome study (Simabuco *et al.*, 2018). The significance of PGAM5 dephosphorylation of serine rich arginine proteins is yet to be fully elucidated, the authors of the study postulated that this may occur to coordinate gene expression in a manner which supports mitophagy (Baba *et al.*, 2021). It

therefore stands to reason that PGAM5 may also exert phosphatase activity on CMTR1 as a mechanism of gene regulation.

Targets of protein kinases can be predicted to some degree, as kinases preferentially bind to specific sequence elements surrounding the phosphoacceptor site, termed a consensus sequence. For example, CK2 being an acidophilic kinase requires one or more acidic residue to be present in the C-terminal direction of the phosphoacceptor site, with the consensus sequence for CK2 phosphorylation being S/T-X-X-D/E (X= any amino acid) (Marin *et al.*, 1992). Protein phosphatases are considerably less represented in the human genome than protein kinases, with 518 known protein kinases being encoded compared to roughly 200 protein and lipid phosphatases (Sacco *et al.*, 2012). Protein phosphatases are capable of dephosphorylating sites introduced by a variety of kinases, suggesting that relationships between specific kinases and phosphatase are not necessarily reciprocal. Furthermore, phosphatase consensus sequences tend to be poorly defined (Kennelly and Krebs, 1991). Despite this, biochemical study of PGAM5 substrate specificity have revealed that PGAM5 preferentially targets phosphopeptides containing serine or threonine and is most active against those with additional negative/acidic residues (Wilkins *et al.*, 2014). This is attributed to the positive charge of amino acid residues adjacent to the catalytic pocket of the PGAM phosphatase domain (Takeda *et al.*, 2009). The CMTR1 P-patch contains a multitude of serine/threonine residues which are surrounded by negatively charged amino acids, (Lukoszek *et al.*, 2024), thus it is reasonable to come to the conclusion that CMTR1 is likely to be a target for PGAM5 phosphatase activity.

As is the case for CMTR1, PGAM5 has also been noted to regulate innate immune responses mediated by RLR and IFN signalling. PGAM5 deficient cell lines fail to express genes downstream of IFN- β signalling when stimulated with intracellular Poly I:C or 5'pppdsRNA (MDA5 and RIG-I ligands respectively), independent of phosphatase activity. Mechanistically, PGAM5 multimers physically interact with MAVS to promote TBK1 phosphorylation, inducing IFN production via the TBK1/IRF3 pathway. The biological consequence of PGAM5 deficiency in MEF cells upon VSV infection is inhibited expression of both *IFNB* and *IFIT1* mRNA, resulting in increases in viral load (Yu *et al.*, 2020). CMTR1 and PGAM5 share roles in

coordinating and facilitating immune responses, specifically those implicated to occur downstream of viral RNA sensing and the IFN pathway. Hence, it stands to reason that these proteins may interact in order to regulate anti-viral immune responses. This highlights that examination of if and how abrogation of the CMTR1-PGAM5 interaction impacts innate immunity is worth further investigation.

CMTR1 has been shown to regulate expression of genes implicated in metabolism (Inesta-Vaquera *et al.*, 2018) and mitochondrial respiration (Meisel *et al.*, 2024). One very recent study demonstrated that CMTR1 could influence transcription of paralogous mRNAs encoding mitochondrial proteins which were sequestered in cytoplasmic P-bodies, upon loss of the G-patch domain (Meisel *et al.*, 2024). Interestingly, PGAM5 has also been found to localise in P-bodies (Jain *et al.*, 2016). Immunostaining featured in chapter 4 of this work show that PGAM5 localises to cytoplasmic granules upon FCCP treatment, which could correspond to translocation in P-bodies, although follow-up experiments with an appropriate staining marker would be required to demonstrate this. It is of note that CMTR1 does not share this feature in the presence or absence of FCCP in Huh-7 cell lines, when immunostaining is undertaken.

The metabolic enzyme ASS1 was selected for further validation as a CMTR1 interacting protein alongside PGAM5 and could be purified with CMTR1 when co-immunoprecipitation was performed in WT and *Cttnb1*^{ex3/WT}; R26-LSL-MYC liver lysate. The RNA-enzyme-metabolite (REM) hypothesis, states that metabolic enzymes such as ASS1 possess moonlight functions as RNA binding proteins, facilitating alterations in gene expression in response to metabolic stimuli (Hentze and Preiss 2010). Current knowledge of how ASS1 influences gene expression is relatively limited but this protein has been shown to interact with both RNA and chromatin (Lim *et al.*, 2024, Castello *et al.*, 2012). Upon DNA damage, levels of P53 are upregulated, which in turn elevates expression of ASS1. Upon entry into the nucleus ASS1 binds to chromatin and succinates SWI/SNF Related, Matrix Associated, Actin Dependent Regulator of Chromatin Subfamily C Member 1 (SMARCC1), reducing the accessibility of chromatin for cell cycle gene transcription (Lim *et al.*, 2024). Multiple metabolic enzymes were found to interact with CMTR1 when IP/MS was performed on both WT and *Cttnb1*^{ex3/WT}; R26-

-LSL-Myc mouse liver extract. Given current knowledge and the REM hypothesis, it may be the case that interaction between CMTR1 and these enzymes acts as a means by which metabolism is further interlinked with gene expression.

6.6 The role of CMTR1 in viral infection and implications for treatment

Current literature has demonstrated that CMTR1 plays contrary roles in viral infection. Total CMTR1 acts as an anti-viral factor in Dengue, Vesicular stomatitis Virus, and Zika virus infection (Williams *et al.*, 2020) but promotes infection with IAV and IBV (Tsukamoto *et al.*, 2023, Li *et al.*, 2020, Lukoszek *et al.*, 2024) and has a negligible impact on the propagation of Sindbis virus and cap snatching bunyaviruses (Tsukamoto *et al.*, 2023). Through conducting work presented in this thesis, we demonstrated that abrogation of P-CMTR1 negatively impacts expression of IAV proteins when tagged to an mCherry promoter. This indicates that the phosphorylation status of CMTR1 also acts a pro-viral factor in IAV infection.

These contradictions in regard to the role of CMTR1 during infection may in part be explained by the variety of host-pathogen interactions employed by individual viral species to ensure immune invasion and viral RNA capping, as previously touched on in chapter 5. This section will expand upon how CMTR1 and P-CMTR1 is likely to impact infection of viral species which have not been mentioned previously and what the implications are for the use of CMTR1 or P-CMTR1 as a therapeutic target.

Multiple researchers have identified that IAV, an Orthomyxovirus, is dependent on CMTR1 activity for efficient infection in both human and murine models. Genetic aberration or pharmacological inhibition of CMTR1 results in reduced readouts of infectivity (Tsukamoto *et al.*, 2023, Li *et al.*, 2020, Lukoszek *et al.*, 2024). In this work we identified that phosphorylation of CMTR1, a post-translational modification which enables capping activity, is also essential for this function (Lukoszek *et al.*, 2024). These observations have been attributed to the role of CMTR1 in ensuring availability of Cap-1 structures in host mRNAs from which IAV can cap-snatch (Tsukamoto *et al.*, 2023, Li *et al.*, 2020). This is complemented by the observation that expression of phosphodeficient CMTR1 substantially decreases

the formation of cap structures with 2'-O-ribose methylation on the first nucleotide (Lukoszek *et al.*, 2024).

Curiously, Tsukamoto *et al.*, found that inhibition of CMTR1 failed to impact outcomes of viral infection in cells inoculated with other Orthomyxoviruses (excluding IAV/IBV) and Bunyaviruses, which also display cap-snatching activity (Decroly *et al.*, 2012, Weber *et al.*, 1996, Garcin *et al.*, 1995). Examples of which include Thogoto virus (THOV) and Hazara virus (Tsukamoto *et al.*, 2020).

THOV is a genus within the Orthomyxoviridae family, THOV is transmitted by tick and preferentially infects livestock. However, rare cases of human infection have been reported (Fuchs *et al.*, 2022). This genus possesses a six-segmented negative sense-RNA genome which encodes for an RNA-dependent polymerase which is structurally similar to the IAV RNA polymerase (Clerx *et al.*, 1983, Portela *et al.*, 1992). The IAV polymerase cleaves host mRNA 10-13 nucleotides downstream of the cap-structure to generate extraneous sequences (Reich *et al.*, 2014), which are absent at the 5' cap of THOV RNAs (Weber *et al.*, 1996). It was previously theorised that THOV does not employ a classical cap-stealing mechanism and instead utilises the PA subunit to exert endonuclease activity only 1 or 2 nucleotides downstream of cellular mRNA caps, with these being sufficient to prime THOV transcription (Weber *et al.*, 1996). However, recent publication of THOV polymerase Cryo-EM structures cast great doubt on this theory. There is a high level of divergence between key residues in the IAV and THOV endonuclease and putative cap-snatching domains, suggesting cap-snatching is non-functional in the THOV polymerase (Xue *et al.*, 2024). This complements biochemical studies which demonstrated the THOV polymerase PA domain lacks endonuclease and divalent cation binding activity (Guilligay *et al.*, 2014). How THOV mechanistically obtains Cap-1 structures remains elusive, but it is theorised this may be via use of free capped dinucleotides generated from RNA degradation or decapping machinery (Xue *et al.*, 2024, Guilligay *et al.*, 2014).

Bunyaviridae viruses possess cap snatching machinery but differ from Orthomyxoviridae, as they replicate in the cytoplasm as opposed to the nucleus (Olschewski *et al.*, 2020). Cap snatching in Bunyaviruses is mediated by the viral L protein which possesses endonuclease activity. However, a definitive cap binding

domain in L proteins is yet to be fully characterised (Olschewski *et al.*, 2020). Deletion of CMTR1 in A549 cell lines resulted in no significant alteration in the outcomes when infection was carried out with Hazara virus, a member of the Bunyaviridae order, suggesting that this virus is not dependent on CMTR1 to provide host caps for snatching (Tsukamoto *et al.*, 2023). Interestingly, Bunyaviruses appear to display some preference for cap-snatching from RNA containing premature stop codons, which localise to P-bodies and stress granules (Mir *et al.*, 2008). Genome-wide RNAi screens have also identified that decapping enzyme DCP2 restricted Bunyavirus infection by limiting the accessibility of an mRNA pool from which this virus could perform cap-snatching (Hopkins *et al.*, 2013).

The preference of IAV for targeting particular RNA transcripts for snatching is highly debated, with some studies indicating that IAV preferentially snatches from small non-coding RNAs and others stating that IAV snatches from a broader range of transcripts, dependent on availability (Sikora *et al.*, 2017, Gu *et al.*, 2015). Gu *et al.*, described high representation of U1 and U2 snRNAs after conducting viral CapSeq on IAV infected A549 cell lines, whilst Tsukamoto *et al.*, identified defects in IAV mRNA snatched specifically from U2 snRNAs upon CMTR1 KO in A549's. Aberration of CMTR1 activity has been demonstrated to alter splicing of specific transcripts through an unknown mechanism. Additionally, some snoRNA host genes which guide modifications of snRNA, appear to be dependent on CMTR1 for expression (Dohnalkova *et al.*, 2023, Wolter *et al.*, 2023- Preprint). Taken together this information suggests that IAV may depend on CMTR1 as a host factor to ensure maintenance of splicing machinery and availability of fully capped U1 and U2 snRNA to snatch from, through both direct CMTR1 capping activity and indirectly via CMTR1-dependent gene expression. This may explain why Bunyavirus infectivity which is dependent on snatching from transcripts targeted for storage in P-bodies is impacted to a far lesser degree by CMTR1 KO.

However, the question remains as to why this is the case, when transcripts sequestered in P-bodies would also be expected to lack Cap-1 structures after CMTR1 KO has been established. Redundancy between CMTR1 and CMTR2 for methylation of the 2'O-ribose of the first nucleotide has been identified in fly

models (Hausmann *et al.*, 2022), it has yet to be established however, if this finding is applicable to mammals. Alternatively, it could be the case that viral cap snatching of mRNA which lacks the Cap-1 structure but is methylated at the second transcribed nucleotide is sufficient for immune evasion, as CMTR2 activity further reduces the ability of RIG-I to interact with RNA (Despic and Jaffrey, 2023). The PB2 subunit of the IAV polymerase is believed to require CMTR1 mediated methylation for efficient cap snatching (Tsukamoto *et al.*, 2023, Bouloy *et al.*, 1980) but it is not clear if this is the case for Bunyaviruses (Olschewski *et al.*, 2020). It is possible that unlike IAV, Bunyaviruses are capable of cap snatching from RNAs which possess cap structures lacking 2'O-ribose methylation of the first nucleotide, with this being sufficient to ensure translation of viral proteins. Immune evasion factors encoded by the virus may then prevent identification of improperly capped viral structures by PRRs and downstream responses to enable replication (Alff *et al.*, 2006, Taylor *et al.*, 2009)

Pharmacological agents which inhibit CMTR1 methyltransferase activity have shown promise as an anti-influenza drug in human A549 cell lines and mouse models (Tsukamoto *et al.*, 2023). Treatment of IAV infected mice with trifluoromethyl-tubercidin (TFMT), a compound which competes with S-Adenosyl methionine for CMTR1 binding, inhibited viral replication without inducing weight loss or cytotoxicity (Tsukamoto *et al.*, 2023). Whilst this data is promising, further study in the clinic will be required to determine if this treatment is suitable for human patients. The work featured in this thesis has demonstrated that total and phosphorylated CMTR1 is required for sufficient and timely expression of ISGs including IFIT proteins. Influenza viruses suppress and manipulate host immune factors including IFIT family members to promote propagation (Tran *et al.*, 2020), but these are in turn crucial for efficient clearance of other viral species (Raychoudhuri *et al.*, 2011, Pichlmair *et al.*, 2011). This indicates that prolonged treatment of patients with CMTR1 inhibitors may increase the risk of secondary viral infection.

Given the role for CMTR1 in promoting IFN responses highlighted in this thesis and other works (Williams *et al.*, 2020), it may be hypothesised that modulation of CMTR1 may also influence diseased states where dysregulation of IFN signalling is

implicated. Elevated levels of type I IFN have been associated in the pathogenesis of autoimmune disease including rheumatoid arthritis and systemic sclerosis (Ünlü *et al.*, 2022, Wu and Assassi, 2013, Lübbers *et al.*, 2013). This presents yet another avenue for the therapeutic use of CMTR1 or CK2 inhibitors.

In conclusion, the above information highlights that CMTR1 influences outcomes of viral infection. The status of CMTR1 as a pro or anti-viral factor is dependent on specific host-pathogen interactions which vary amongst viral species. Viruses which are directly dependent on CMTR1 to conduct cap-snatching activities (e.g. IAV) (Tsukamoto *et al.*, 2023) are likely to utilise CMTR1 as a pro-viral factor, indicating that inhibition of CMTR1 may be therapeutic in this context. Although stringent clinical testing will be required to determine efficacy alongside the risk of off-target effects in human patients. The use of CMTR1 inhibitors may also offer therapeutic benefit in diseased states driven by pathogenic IFN signalling, such as rheumatoid arthritis and systemic sclerosis (Ünlü *et al.*, 2022, Wu and Assassi, 2013, Lübbers *et al.*, 2013). Conversely, CMTR1/P-CMTR1 is likely to exert inhibitory activities towards viruses which are not dependent on its cap methyltransferase activity to undertake cap-snatching, providing that host cells are able to effectively generate IFN responses against these viruses. This hypothesis is tied to the fact that CMTR1 expression and phosphorylation promotes induction of a variety of ISGs downstream of RLR/IFN signalling (Lukoszek *et al.*, 2024) and restricts replication of Dengue and ZIKA viruses (Williams *et al.*, 2020). CMTR1 appears to have a negligible impact on outcomes of viral infection with Bunyaviruses and several Orthomyxoviridae family members (excluding Influenza) (Tsukamoto *et al.*, 2023), likely due to the fact that these viruses are not dependent on CMTR1 activity for their propagation (Xue *et al.*, 2024) and can effectively evade IFN responses (Alff *et al.*, 2006, Taylor *et al.*, 2009). Further work will be required to characterise the impact of CMTR1/P-CMTR1 on individual viruses, as findings cannot be extrapolated amongst species without enriching current understanding of underlying viral biology and host interactions.

6.7 Future work

In this thesis, protein expression of CMTR1 and RNMT capping enzymes were identified to be upregulated in *Ctnnb1^{ex3/WT}; R26-LSL-MYC* liver extract, compared to controls. The functional consequences of this observation, however, require further examination. Genes which may play proto-oncogenic functions have been previously identified as CMTR1-regulated (Inesta-Vaquera *et al.*, 2018), hence, it would be of use to determine if these are differentially expressed in HCC via RT-qPCR or western blotting. Furthermore, given that CMTR1 is implicated in translation, ribosome biogenesis and splicing (Dohnalkova *et al.*, 2023, Liang *et al.*, 2022, Wolter *et al.*, 2023, Preprint), examination of how these are altered by CMTR1 upregulation in HCC is of interest. This may be achieved by RNA-sequencing to characterise the HCC transcriptome and polysome profiling.

The murine models used in this thesis reflect initiation of tumorigenesis, as liver was extracted from mice 10 days after induction of β -catenin and c-Myc dysregulation. To enhance understanding of how CMTR1 may influence maintenance of HCC once established, measuring growth or colony formation in liver cancer cell lines where CMTR1 is depleted or overexpressed would be beneficial.

In previous sections of this discussion, the potential role of CMTR1 in immunity and how this may impact HCC has been alluded to. However, I have yet to fully investigate if this link exists in the models used in this work. To achieve this, characterisation of immune responses in cell lines derived from mouse models of liver hyperplasia upon CMTR1 knockdown or overexpression may be of use. The data shown here demonstrated a role for P-CMTR1 in promoting innate immune responses. Phosphorylation of CMTR1 was found to be minimal in murine liver but this was not examined in established human tumour cell lines. To further determine a role of P-CMTR1 in HCC, inducing CK2 overexpression or use of phosphomimetic CMTR1 mutants in HCC cell lines may be conducted, followed by characterisation of the transcriptome.

Proteins ASS-1 and PGAM5 were identified as binding partners of CMTR1 in the liver. However, time constraints prevented investigation into the functional implications of these interactions. As PGAM5 exerts phosphatase activity (Takeda

et al., 2009), it would be of interest to identify if PGAM5 is capable of dephosphorylating CMTR1, which may be achieved via treatment of cell extract with recombinant PGAM5 followed by determination of CMTR1 phosphorylation. By using truncated protein fragments, exact binding regions of CMTR1 and ASS1/PGAM5 may also be identified. This will permit for the generation of models where these interactions are disrupted and allow for determination as to whether this impacts capping, immunity, gene expression, metabolism or mitochondrial dynamics. Once this has been conducted any potential findings may be applied to liver cancer models to determine if these interactions influence tumorigenesis.

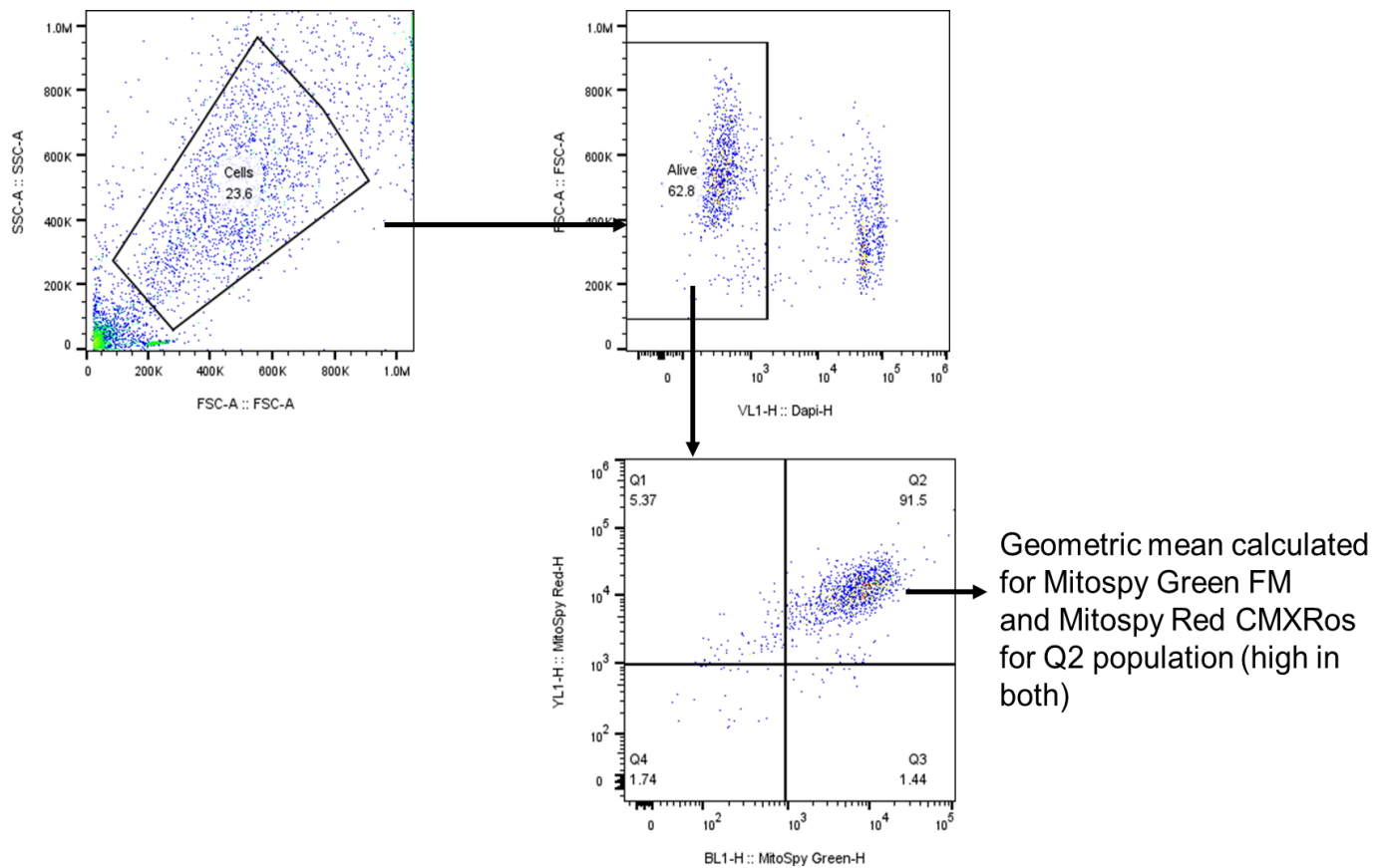
In this thesis, we identified that P-CMTR1 functions as a pro-viral factor in IAV infection. Given differential mechanisms of capping and immune evasion between RNA viruses, further investigation into how P-CMTR1 influences outcomes of infection of other viral species is warranted. In contrast with findings by Williams *et al.*, work presented here indicates that P-CMTR1 influences ISG expression at the mRNA level, thus impacting protein expression (Williams *et al.*, 2020, Lukoszek *et al.*, 2024). As CMTR1 has been previously demonstrated to recruit RNAPII to transcription start sites (Liang *et al.*, 2022), this may be investigated as a potential mechanism by which this occurs. Chromatin immunoprecipitation experiments will aid in determining the extent of CMTR1 and RNAPII retention at ISG promoter sites.

6.8 Conclusions

In this thesis, I undertook characterisation of CMTR1 in both WT and *Ctnnb1*^{ex3/WT}; R26-^{LSL-Myc} murine liver, which will continue to provide a stepping stone for further determination into a role for this protein in cancer. Specific interactions between CMTR1 and proteins PGAM5 and ASS1 have been established, the former of which is found to occur to a greater extent in l *Ctnnb1*^{ex3/WT}; R26-^{LSL-MYC} liver extract and cancer cell lines. This interaction is hence likely to be of relevance in hepatocellular carcinoma, but the exact functional consequences require further examination.

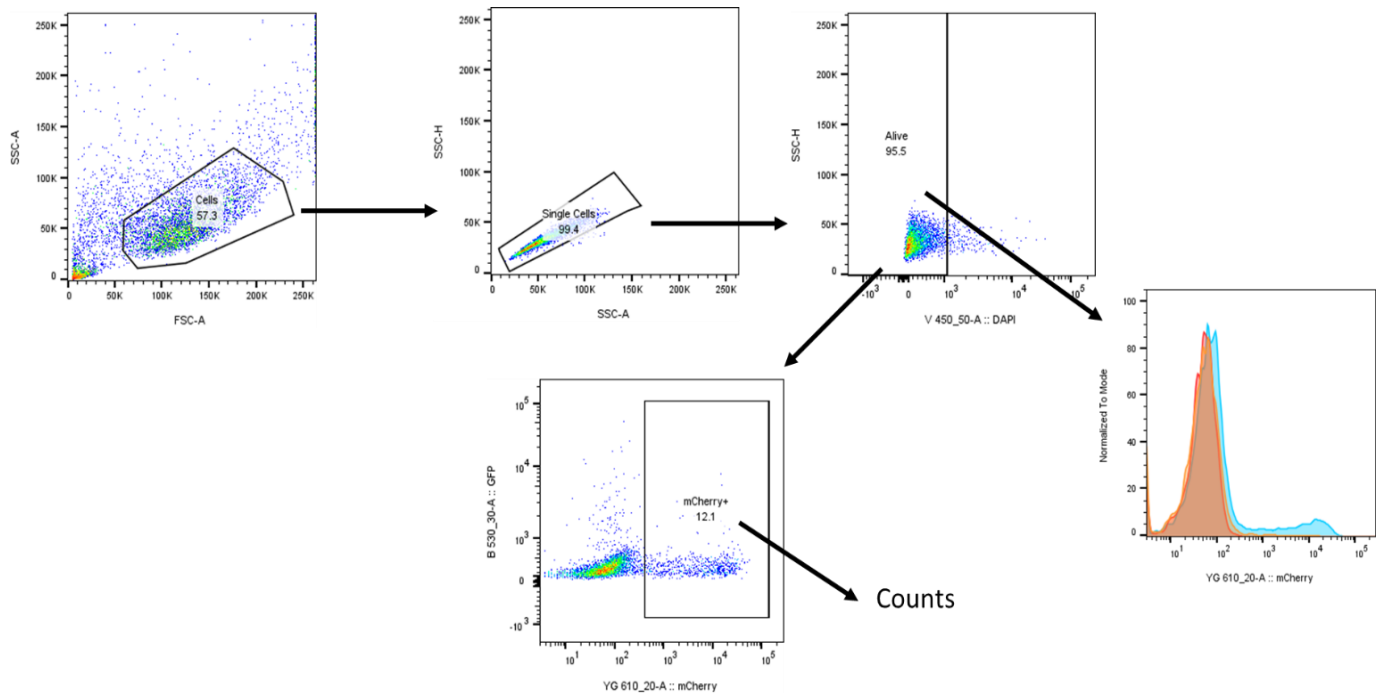
In this work we have established that phosphorylation of CMTR1 is required to maintain and ensure timely expression of various interferon stimulated genes in response to treatment with IFN and poly I:C, the mechanisms of which are yet to be elucidated. Infection of phosphodeficient mouse embryonic fibroblasts with Influenza A virus results in reduced readouts of viral protein production compared to WT controls, indicating that despite promoting innate immune responses P-CMTR1 possesses differential roles in viral infection. This has substantial implications for the use of therapeutic agents which target CMTR1 and highlights the need to consider specific host-pathogen interactions when determining a role for CMTR1 in viral infection.

Chapter 7: Appendices



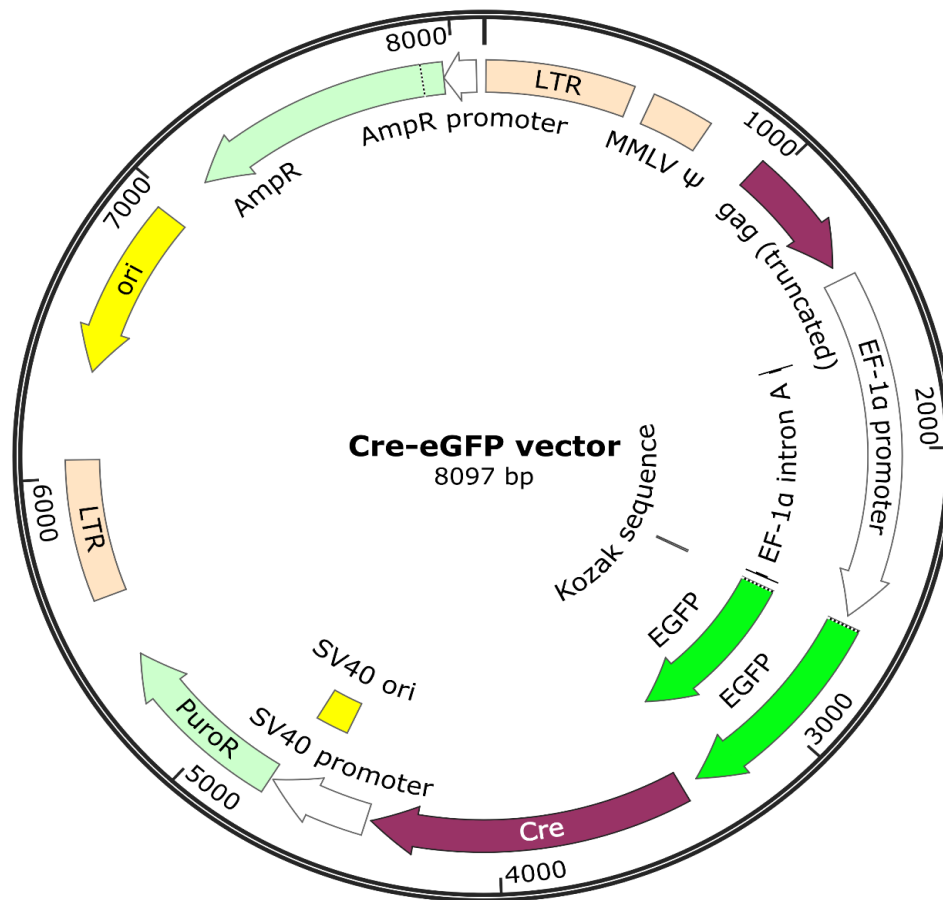
Supplementary Figure 1- Gating Strategy for flow cytometry experiments depicted in Figure 4.7

Gating strategy for flow cytometry analysis of mitochondrial potential and mass in Huh-7 cell lines post treatment with 10 μ M FCCP for 4 hrs. Numbers indicate percentage of cells within each gate. FCCP (Non-structural protein 1), FSC (forward scatter), SSC (side scatter).



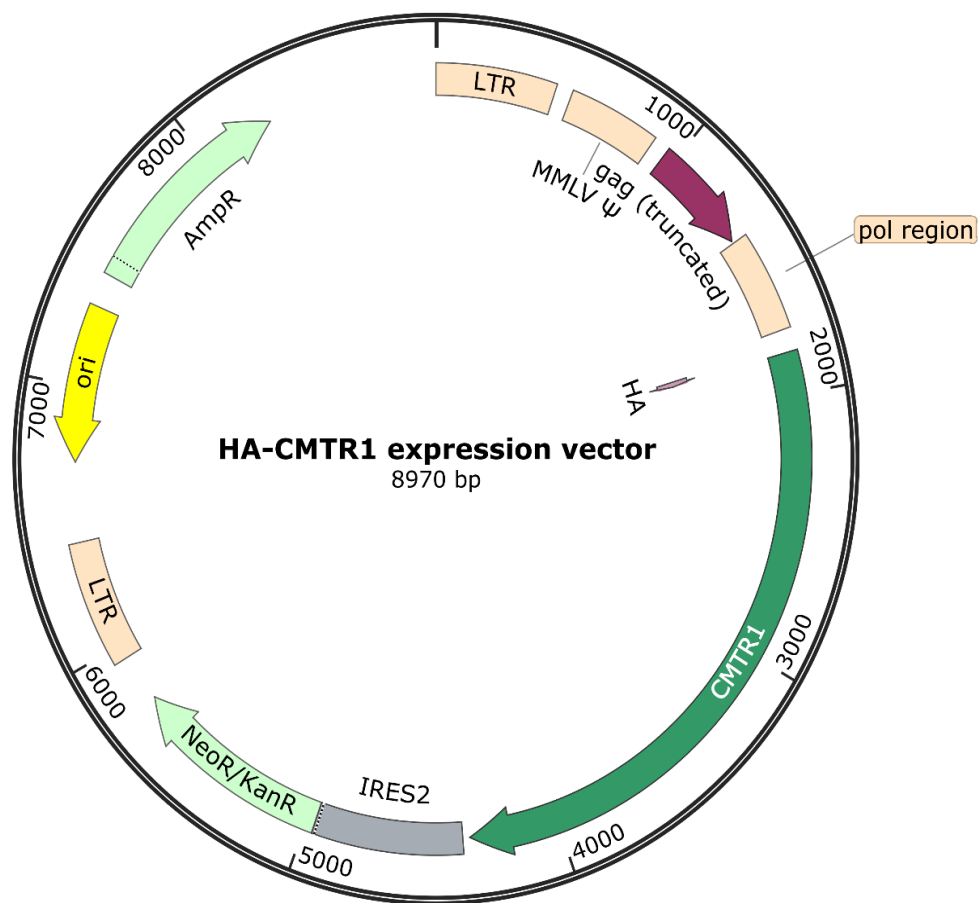
Supplementary Figure 2- Gating Strategy for flow cytometry experiments depicted in Figure 5.7

Gating strategy for flow cytometry analysis of NS1-mCherry protein production in MEFs expressing either HA-WT-CMTR1, HA-15A CMTR1, or an empty vector control following infection with PR8 IAV mCherry Colorflu. Numbers indicate percentage of cells within each gate. NS1 (Non-structural protein 1), MEF (Mouse embryonic fibroblast), CMTR1 (Cap Methyltransferase 1), IAV (Influenza A Virus), SSC (Side scatter), FSC (Forward scatter), DAPI (4',6-diamidino-2-phenylindole), GFP (Green fluorescent protein).



Supplementary Figure 3- cre-eGFP vector map

An expression vector encoding both cre and eGFP was generated by using Sal I restriction enzyme for digestion of both a pBABE-puro vector backbone and a PCR cloned expression cassette containing EF1- α promoter, eGFP, and Cre sequences originating from a pBS598 EF1alpha-EGFPcre plasmid. This expression cassette was then inserted into the pBABE-puro vector to generate the final product as depicted above. Cloning was performed by Dr Radoslaw Lukoszek. eGFP (enhanced green fluorescent protein), EF1- α (Elongation factor 1- α).



Supplementary Figure 4- HA-CMTR1 expression vector map

An expression vector encoding either a HA-WT CMTR1 or phosphodeficient mutant version of CMTR1 (HA-15A CMTR1) was generated via digestion of pBMN-I-GFP vector with Not I restriction enzyme. This was followed by ligation of either a construct encoding HA-WT CMTR1, or a construct generated by *in vitro* mutagenesis encoding for HA-15A CMTR1, where the following substitutions were performed: S26A, S28A, T30A, S31A, S46A, S49A, S51A, S53A, S55A, T57A, S63A, S64A, S66A, S75A, S89A. *In vitro* mutagenesis and cloning was performed by DSTT. HA-WT CMTR1 (Haemagglutinin tagged wild type CMTR1), HA-15A CMTR1 (Haemagglutinin tagged phosphodeficient CMTR1), DSTT (Division of signal transduction therapy, University of Dundee).

The following paper, copied below, contains the data adapted to generate figures 1.4, 5.1, 5.3, 5.4 and 5.7. All data presented in this thesis which can also be found in this paper is my own work. Exception to this is data found in figure 5.1, whilst the author of this thesis carried out the experimental procedure Prof Victoria Cowling carried out data processing, as mentioned in the figure legend. Figure 5.2 depicts generation of the MEF model, extraction of mouse embryonic fibroblasts and lentiviral transduction was performed by Dr Radoslaw Lukoszek, transfection of MEFs with a cre eGFP vector and creation of the figure was carried out by the author of this work. This is explicitly mentioned in Chapter 2: Materials and Methods under heading 2.1. Some data found in the paper which was generated by other authors is alluded to in text only within this thesis and explicit attribution is given.

The paper “ CK2 phosphorylation of CMTR1 promotes RNA cap formation and influenza virus infection” was published in open access journal Cell Reports under a Creative Commons Attribution (CC BY 4.0) license and thus can be shared and adapted freely as long as attribution is given.

CK2 phosphorylation of CMTR1 promotes RNA cap formation and influenza virus infection

Radoslaw Lukoszek^{1,6} · Francisco Inesta-Vaquera^{1,2,6} · Natasha J.M. Brett^{1,3,4,6} · Shang Liang³ · Lydia A. Hepburn³ · David J. Hughes⁵ · Chiara Pirillo³ · Edward W. Roberts^{3,4} · Victoria H. Cowling^{1,3,4,7}

1 School of Life Sciences, University of Dundee, Dundee DD1 5EH, UK

2 Department of Biochemistry and Molecular Biology and Genetics, School of Sciences, Universidad de Extremadura, Avenida de Elvas, s/n, 06006 Badajoz, Spain

3 Cancer Research UK Scotland Institute, Gartcube Estate, Switchback Road, Glasgow G61 1BD, UK

4 School of Cancer Sciences, University of Glasgow, Gartcube Estate, Switchback Road, Glasgow G61 1QH, UK

5 School of Biology, University of St Andrews, Biomedical Sciences Research Complex, St Andrews KY16 9ST, UK

6 These authors contributed equally

7 Lead contact

Summary

The RNA cap methyltransferase CMTR1 methylates the first transcribed nucleotide of RNA polymerase II transcripts, impacting gene expression mechanisms, including during innate immune responses. Using mass spectrometry, we identify a multiply phosphorylated region of CMTR1 (phospho-patch [P-Patch]), which is a substrate for the kinase CK2 (casein kinase II). CMTR1 phosphorylation alters intramolecular interactions, increases recruitment to RNA polymerase II, and promotes RNA cap methylation. P-Patch phosphorylation occurs during the G1 phase of the cell cycle, recruiting CMTR1 to RNA polymerase II during a period of rapid transcription and RNA cap formation. CMTR1 phosphorylation is required for the expression of specific RNAs, including ribosomal protein gene transcripts, and promotes cell proliferation. CMTR1 phosphorylation is also required for interferon-stimulated gene expression. The cap-snatching virus, influenza A, utilizes host CMTR1

phosphorylation to produce the caps required for virus production and infection. We present an RNA cap methylation control mechanism whereby CK2 controls CMTR1, enhancing co-transcriptional capping.

Introduction

CMTR1 (cap methyltransferase 1) is an RNA cap methyltransferase that has influential roles in gene expression and innate immune responses.^{1,2} During pre-mRNA maturation, CMTR1 methylates the first transcribed nucleotide ribose at the O-2 position, creating the RNA cap modification N1 2'-O-Me, which alters the affinity of the RNA cap for interacting proteins.^{3,4,5,6} An absence of cap N1 2'-O-Me contributes to mRNA being detected as “non-self”; these immature caps interact with proteins that target RNA for decapping and degradation.^{2,5,7} Once the RNA cap has N1 2'-O-Me, interactions with proteins of the RNA degradation pathway decrease, and interactions with proteins involved in RNA processing and translation factors alter, associated with the increased expression of specific genes.^{2,8} CMTR1 was first investigated as an interferon-stimulated gene (ISG95)^{9,10,11,12,13}; the interferon-induced translation of select ISGs was found to be dependent on this RNA cap methyltransferase.¹³ CMTR1 is also upregulated during embryonic stem cell differentiation and is critical for the proliferation of differentiating cells in a mechanism linked to the expression of histone and ribosomal protein gene transcripts.^{14,15} Across diverse species, specific genes are responsive to CMTR1 levels, with regulation observed at the level of RNA and translation.^{1,8,14,16,17,18,19,20,21,22}

The methyltransferase domain is centrally positioned in CMTR1, flanked by domains that influence the interactions and activity of the enzyme. A nuclear localization signal and the G-Patch (glycine-rich) domain are N-terminal to the methyltransferase domain with the non-catalytic guanylyltransferase-like (GT-like) and WW domains residing at the C terminus^{3,4} (Figure 1). CMTR1 methylates RNA caps during transcription when the CMTR1 WW domain interacts with the RNA polymerase II (RNA Pol II) large subunit C-terminal domain (CTD) phosphorylated on serine-5 (S5P)^{14,18,23} and the CMTR1 GT-like domain interacts with RNA Pol II RPB7.²⁴ These interactions recruit CMTR1 to RNA Pol II at the initiation of

transcription after guanosine cap addition.^{14,24} Interaction with RNA may also aid the recruitment of CMTR1 to RNA Pol II.²⁰ Repression of CMTR1 results in a loss of RNA Pol II binding to the transcription start site and repression of transcription, indicating a role for this enzyme and the RNA cap modification, N1 2'-O-Me, in transcription and/or co-transcriptional RNA stability.^{14,15} The genes with the highest CMTR1 and RNA Pol II binding are the most responsive to the repression of CMTR1. The CMTR1 G-Patch domain also binds directly to the DHX15 helicase (DEAH-box helicase 15) through the OB-fold (oligonucleotide/oligosaccharide-binding), an interaction that modulates CMTR1 and DHX15 activities and prevents interaction with RNA Pol II.^{18,19,22}

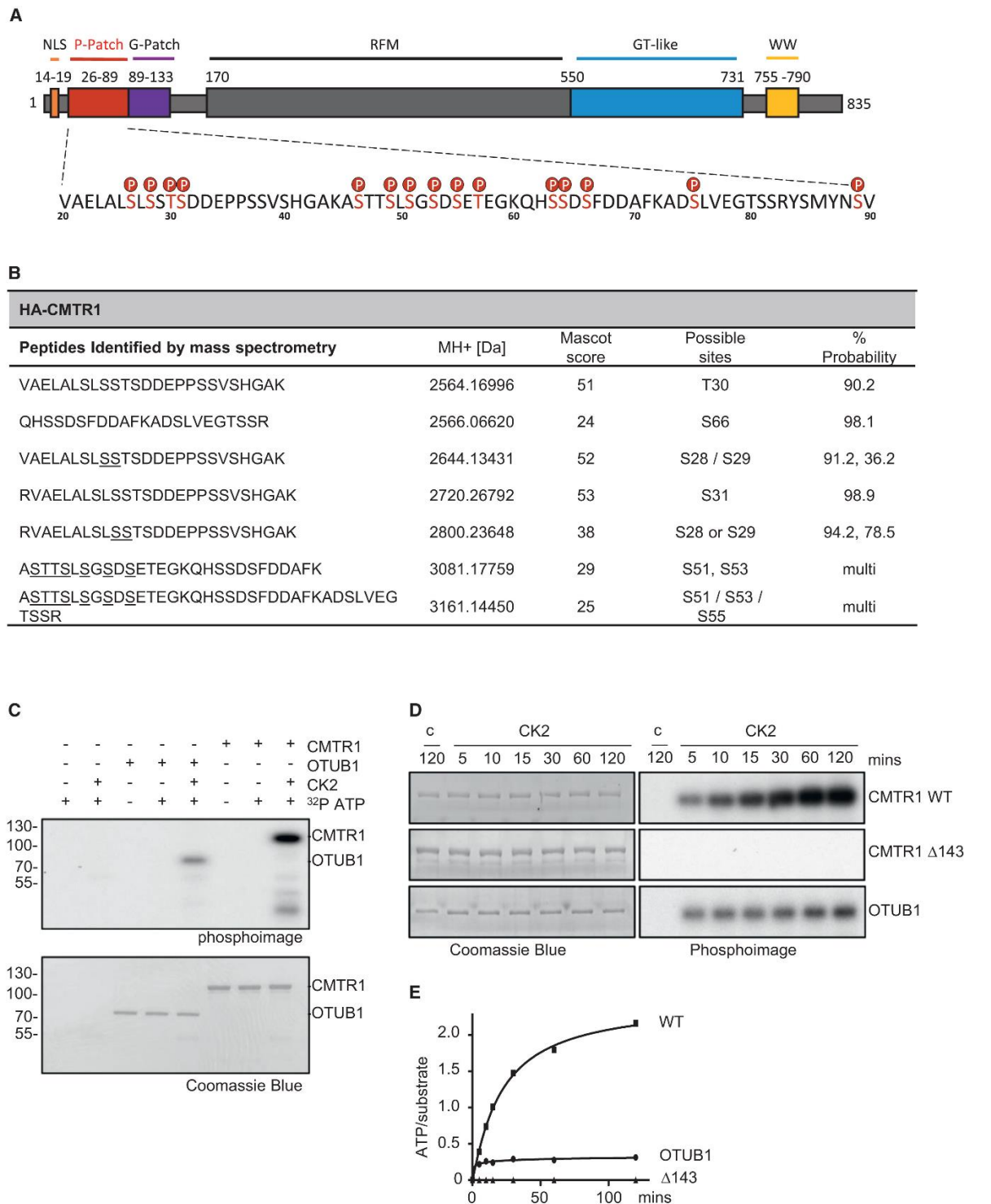


Figure 1 CMTR1 contains a highly phosphorylated P-Patch at the N terminus

(A) Diagram of human CMTR1. Domains and positions indicated. P-Patch is amino acids 26-89 (red). High-confidence phosphorylation sites are labeled “P.”

(B) HA-CMTR1 was expressed in HeLa cells and immunoprecipitated via the HA tag. Phospho-peptides were identified by mass spectrometry, and the mass was reported. High-confidence phosphorylation sites are stated in “possible sites” with the percentage of

probability given. For peptides with several potential sites, the most likely are stated and all are underlined.

(C) *In vitro* phosphorylation of recombinant CMTR1 and OTUB1 by CK2. Reaction constituents indicated. Phospho-analysis of proteins (top). Coomassie blue staining of proteins (bottom).

(D) *In vitro* phosphorylation of recombinant CMTR1, CMTR1 Δ 143, and OTUB1 over a time course, as above. “c” indicates a reaction without CK2.

(E) Quantitation of moles of ATP incorporated into moles of substrates in (D).

Here, we demonstrate that CMTR1 function is controlled by the kinase CK2 (casein kinase II). CK2 phosphorylates CMTR1 on multiple residues in the N-terminal phospho-patch (P-Patch), which alters intramolecular interactions and promotes recruitment to the RNA Pol II CTD. CMTR1 P-Patch phosphorylation is required for mature cap formation, specific gene expression, and cell proliferation. The expression of ribosomal protein genes and select ISGs is particularly dependent on CMTR1 phosphorylation. The cap-snatching virus, influenza A virus (IAV), requires host cell CMTR1 phosphorylation for viral infection.

Results

CK2 phosphorylates CMTR1 on multiple amino acids in the N-terminal P-Patch. To identify signaling pathways that influence RNA cap formation, we analyzed phosphorylated residues of the cap methyltransferase CMTR1. Human hemagglutinin (HA)-CMTR1 was expressed in HeLa cells, immunoprecipitated, and analyzed by LC-MS (liquid chromatography-mass spectrometry) (Figures 1A, 1B, and S1A). A cluster of phosphorylated amino acids was identified in an N-terminal region, which we named the P-Patch (amino acids S26-S89; Figures 1A, 1B, and S1B). The phosphorylated amino acids identified with the highest confidence were S28, T30, S31, and S66 (Figures 1A and 1B). The *CMTR1* cDNA was mutated to encode alanine in substitution of phosphorylated amino acids, and, as previously, this CMTR1 protein was expressed in cells and analyzed by LC-MS, resulting in the identification of additional phosphorylation sites (Figures 1A and S2). This process was repeated until 15 phosphorylated amino acids were identified: S26, S28, T30, S31, S46, S49, S51, S53, S55, T57, S63, S64, S66, S75, and S89 (Figures 1A, S1,

and S2). HA-CMTR1 15A cDNA was generated to encode CMTR1 with all detected phosphorylated amino acids mutated to alanine. No phosphorylation was detected in HA-CMTR1 15A, despite 91% protein being analyzed by LC-MS, including the entire P-Patch (Figures S1B and S2).

We investigated the kinases that phosphorylate the CMTR1 P-Patch based on consensus motifs. CK2, a pleiotropic kinase that phosphorylates serines and threonines upstream of acidic residues, was a candidate P-Patch kinase.^{25,26,27,28} Recombinant CMTR1 was phosphorylated by recombinant CK2 *in vitro* (Figure 1C). OTUB1, an established CK2 substrate, was included as a positive control.²⁹ CMTR1 Δ 1-143 (lacking the nuclear localization sequence [NLS], P-Patch, and G-Patch) was not phosphorylated in this assay, consistent with the CK2 phosphorylation sites being restricted to the N terminus of CMTR1 (Figures 1D and 1E). More than 2 mol of phosphate was incorporated into each mole of CMTR1, indicating that CMTR1 proteins were multiply phosphorylated (Figure 1E). To characterize CMTR1 phosphorylation, polyclonal antibodies were raised against a CMTR1 peptide phosphorylated on S28, T30, and S31. In a dot blot, the anti-pCMTR1 (phospho-CMTR1) antibody had enhanced affinity for recombinant CMTR1 when phosphorylated by CK2 (Figure 2A). When HA-CMTR1 was immunoprecipitated from cell extracts, the pCMTR1 antibody bound with higher affinity to the wild-type (WT) protein compared to the 15A mutant, consistent with WT CMTR1 phosphorylation (Figure 2B). Transfection of HeLa cells with a CK2 expression vector resulted in increased endogenous pCMTR1, and transfection with kinase-dead CK2 (CK2-KD) resulted in reduced pCMTR1, consistent with CK2 phosphorylation of CMTR1 in cells (Figure 2C).

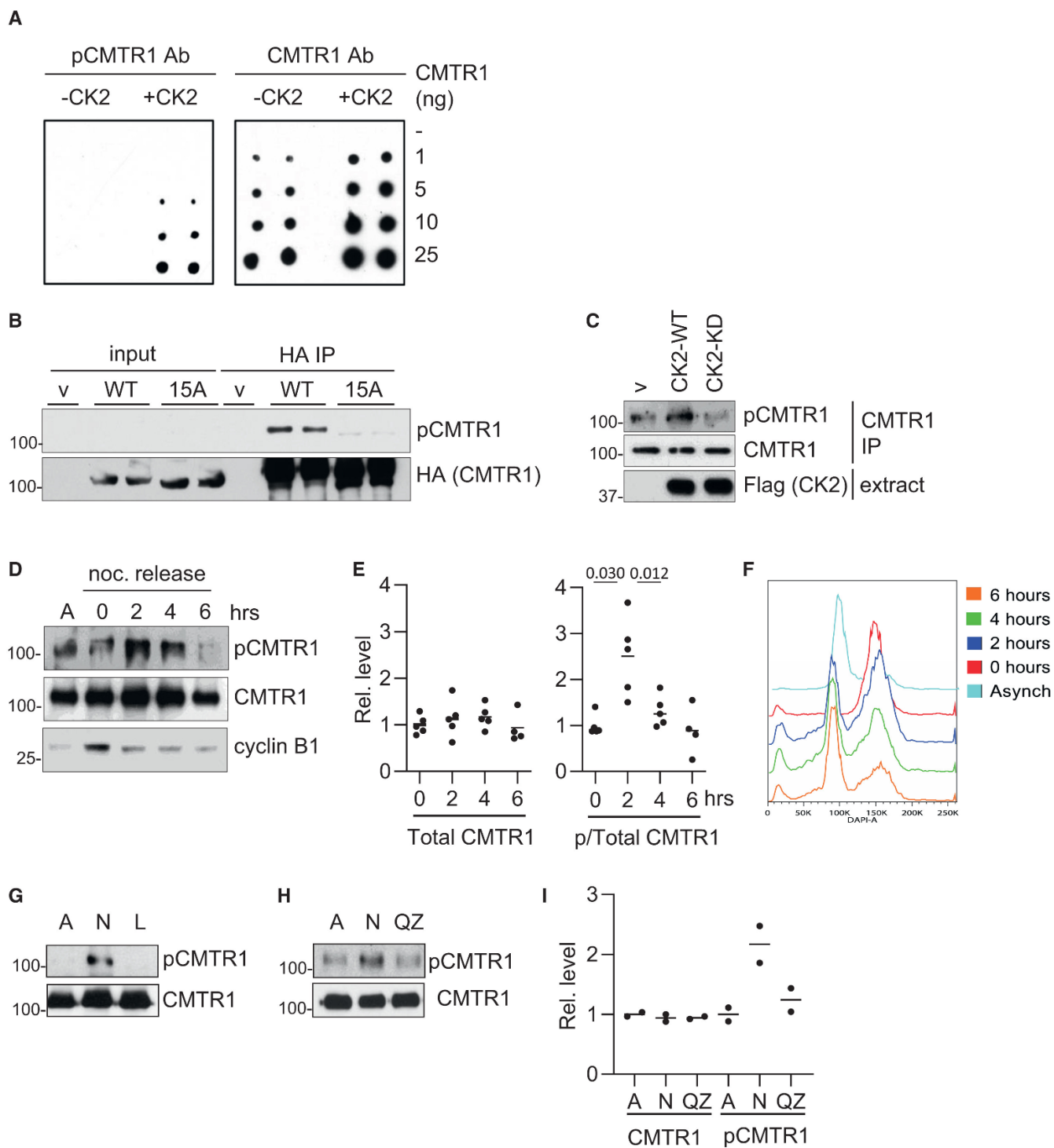


Figure 2 CMTR1 is phosphorylated by CK2 during G1 phase

(A) Recombinant CMTR1 was in vitro phosphorylated with CK2 and a titration was blotted onto PVDF (ng indicated). Blots were probed with pCMTR1 antibody or (pan) CMTR1 antibody. (B) HA-CMTR1 WT, HA-CMTR1 15A, or empty vector (v) were transiently expressed in HeLa cells. HA-CMTR1 proteins were immunoprecipitated via the HA tag and

analyzed by western blot. (C) FLAG-CK2 WT, D156A (kinase dead [KD]), or empty vector (v) were transiently expressed in HeLa cells. Endogenous CMTR1 was immunoprecipitated and analyzed by western blot. (D) HeLa cells were arrested in G2/M phase using nocodazole and released into the cell cycle by replacement with fresh medium. CMTR1 was immunoprecipitated over a time course of nocodazole release or from asynchronous cells (A) and analyzed by western blot for phospho-CMTR1 and total CMTR1 (representative shown). Cyclin B expression was analyzed. (E) pCMTR1/CMTR1 and total CMTR1 were quantitated. Dots indicate data for 4 or 5 independent experiments. Line indicates the average. Student's t test was performed, and p values are stated. (F) Cell cycle progression in (D) was analyzed by flow cytometry using DAPI DNA stain. The proportion of cells in each stage of the cell cycle is indicated. (G) Cells released from nocodazole block for 2 h were untreated (N), treated with lambda phosphatase (L), or asynchronous (A). (H) As in (G) except cells were treated with quinalizarin (QZ). (I) Detection of pCMTR1/CMTR1 and total CMTR1 was quantitated for 2 independent experiments. Dots indicate data, and line indicates the average.

CMTR1 is phosphorylated predominantly during G1 phase

The guanosine cap is methylated by RNMT predominantly during G1 phase of the cell cycle.³⁰ We used nocodazole-based cell synchronization, which releases cells from a late G2/M arrest into G1 phase to determine that CMTR1 phosphorylation increases during G1 phase of the cell cycle (Figures 2D-2F). CMTR1 phosphorylation (ratio of pCMTR1 to CMTR1) peaked at 2 h following the release from nocodazole block, whereas total CMTR1 levels were not altered. Once the phase of the cell cycle when CMTR1 is phosphorylated was determined, we could further verify the pCMTR1 antibody as phosphate specific. CMTR1 was immunoprecipitated from cells 2 h after nocodazole release, and immunoprecipitates were treated with lambda phosphatase, resulting in reduced pCMTR1 levels (Figure 2G). To verify that CK2 was a kinase responsible for CMTR1 phosphorylation during the cell cycle, cells were treated with quinalizarin, a CK2 inhibitor, which reduced detection of pCMTR1 (Figures 2H and 2I).³¹

CMTR1 phosphorylation increases interaction with RNA Pol II

We investigated the impact of P-Patch phosphorylation on CMTR1 function. *In vitro*, CK2 phosphorylation of recombinant CMTR1 did not significantly impact methyltransferase activity (Figure S3A). Similarly, using lambda phosphatase to reduce the phosphorylation of HA-CMTR1 immunoprecipitated from cells did not impact methyltransferase activity (Figures 2G and S3B). CMTR1 function can be influenced by interaction with the helicase DHX15.^{18,19} An equivalent quantity of DHX15 was found in HA-CMTR1 WT and 15A complexes immunoprecipitated from HeLa cells, indicating that phosphorylation of CMTR1 does not influence this interaction (Figure S3C). As a control, the CMTR1 G-Patch 3L/A mutant had reduced interaction with DHX15¹⁸ (Figure S3C). The CMTR1 P-Patch is adjacent to the NLS (Figure 1A).^{18,32} To investigate whether CMTR1 phosphorylation impacts the cellular localization of the protein, GFP-CMTR1 WT and 15A were transfected into HeLa cells (Figure S4). As observed previously, GFP-CMTR1 WT has a predominantly diffuse nuclear localization, and GFP-CMTR1 15A has an equivalent nuclear localization.¹⁸ As controls, GFP-CMTR1 25-831 and GFP-CMTR1 4/K/E, mutants with a deleted or mutated NLS, were predominantly cytoplasmic.¹⁸

CMTR1 is recruited to nascent RNA caps by an interaction of the WW domain with the RNA Pol II CTD phosphorylated on S5^{14,18} and by an interaction of the GT-like domain with RNA Pol II PBP7.²⁴ To investigate whether the interaction of the RNA Pol II CTD with CMTR1 is influenced by phosphorylation, HA-CMTR1 WT, 15A, and vector control were expressed in MEFs (mouse embryonic fibroblasts) and HeLa cells (Figures 3A and 3B, respectively). HA-CMTR1 WT was immunoprecipitated from cell extracts in a complex with RNA Pol II S5P and S2P of the CTD (Figures 3A and 3B). The phospho-defective CMTR1 15A mutant had significantly reduced interaction with the CTD, consistent with CMTR1 phosphorylation promoting or permitting this interaction. To validate the role of CK2 in the CMTR1-RNA Pol II interaction, CK2 WT and KD were transiently expressed in HeLa cells (Figure 3C). Expression of CK2 WT, but not CK2 KD, resulted in increased CMTR1 phosphorylation and increased interaction with RNA Pol II (Figure 3C).

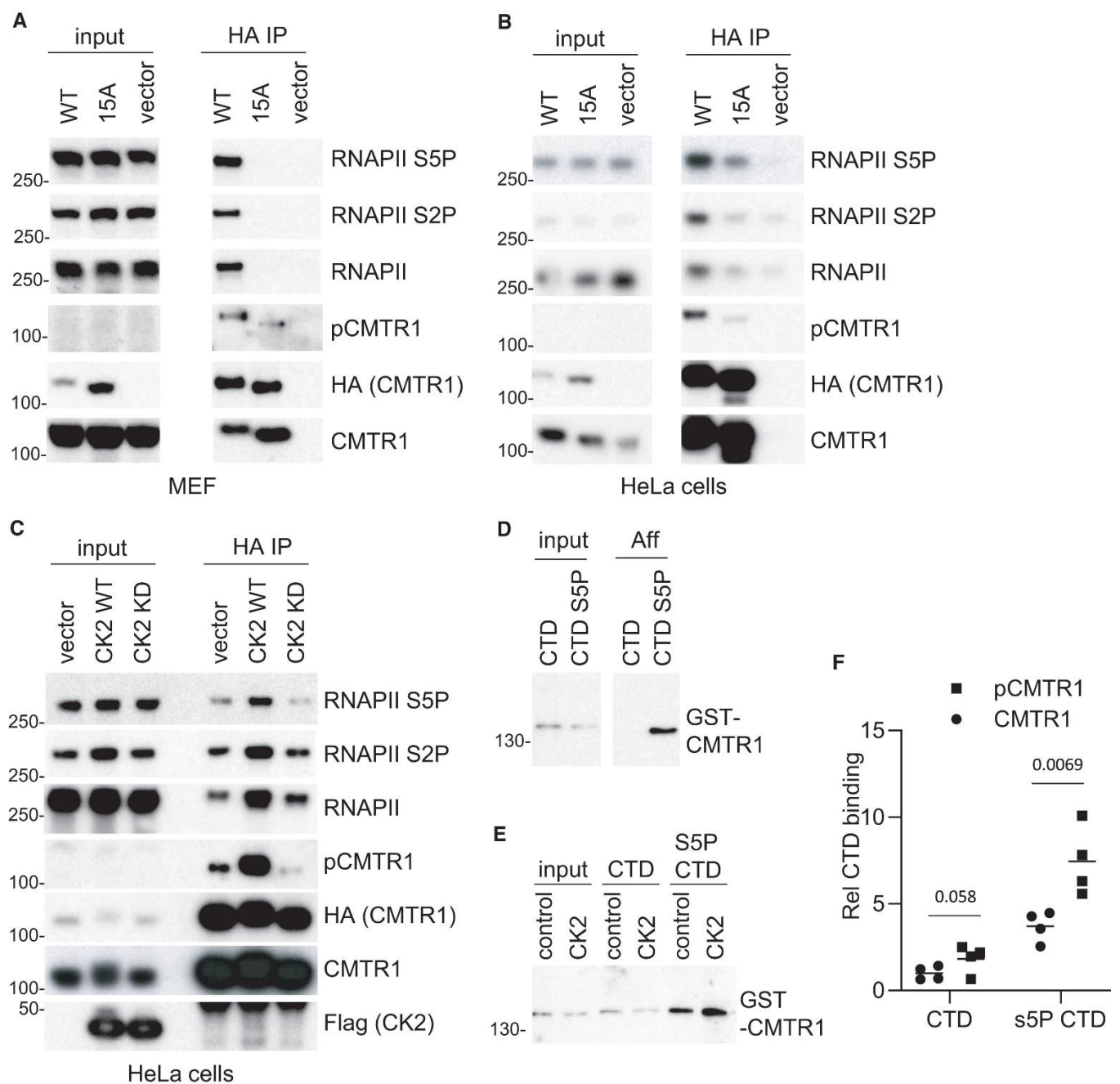


Figure 3 CK2 phosphorylation of CMTR1 increased interaction with RNA Pol II

(A and B) HA-CMTR1 WT, 15A, or vector control. Dots indicate data were transiently expressed in (A) MEFs or (B) HeLa cells. HA-CMTR1 WT or 15A was immunoprecipitated from cell extracts via the HA tag. Western blots were performed on input material and immunoprecipitates (IPs). (C) HA-CMTR1 was transiently co-expressed in HeLa cells with CK2 WT, CK2 KD, or vector control. Western blots were performed on input material and HA-CMTR1 IPs for the antigens indicated. (D) Recombinant GST-CMTR1 was incubated with

biotinylated CTD peptide, unphosphorylated (CTD), or phosphorylated on serine-5 (CTD S5P). CMTR1 was detected by western blot in inputs and streptavidin pull-downs (Aff). (E) As in (D) except GST-CMTR1 was *in vitro* phosphorylated by incubation with CK2 prior to CTD and CTD-S5P pull-downs. (F) GST-CMTR1 binding to CTD was quantitated for 4 independent experiments. Dots indicate data, and line indicates the average. Student's *t* test was performed, and *p* values are stated.

To investigate whether CK2 phosphorylation of CMTR1 directly influences the interaction with the RNA Pol II CTD, an *in vitro* binding assay was performed. As observed previously, recombinant CMTR1 interacted directly with the CTD peptide, with enhanced binding to the S5P CTD peptide (Figure 3D).¹⁸ Phosphorylation of recombinant CMTR1 with CK2 increased its interaction with the RNA Pol II CTD (Figures 3E and 3F).

Intramolecular interactions of CMTR1 are controlled by P-Patch phosphorylation

CMTR1 recruitment to the RNA Pol II CTD requires the CMTR1 WW domain.¹⁸ Here, we observe that phosphorylation of the CMTR1 P-Patch influences the RNA Pol II-CMTR1 interaction (Figure 3). Since phosphorylation of the CMTR1 N-terminal P-Patch influences an interaction of the C-terminal WW domain with RNA Pol II, this indicates a phosphorylation-induced change in conformation or an intramolecular interaction of CMTR1. To investigate the interactions between the different domains of CMTR1 a series of HA-CMTR1 N-terminal deletions and GFP-CMTR1 C-terminal deletions were made and co-expressed in HEK293 cells (Figure 4A). In co-immunoprecipitation experiments, GFP-CMTR1 Δ WW (GFP- Δ WW) interacted with HA-CMTR1-WW (lane 9, Figure 4B) or HA-CMTR1-GT-WW (lane 9, Figure 4C). This revealed an interaction between the CMTR1 WW domain and another part of CMTR1. The more extensive deletion mutant GFP-CMTR1 1-143 (GFP-1-143) failed to interact with HA-CMTR1-WW (lane 8, Figure 4B) or HA-CMTR1-GT-WW (lane 8, Figure 4C), indicating that the CMTR1 RFM-GT-like (Rossmann-fold methyltransferase-guanylyltransferase-like) domain is required for the interaction with the CMTR1 WW domain. These CMTR1 domain interactions are likely to reflect intramolecular interactions rather than *trans* interactions of two CMTR1 proteins since GFP-CMTR1 WT does not bind to any CMTR1 deletion mutant or another CMTR1 WT (Figures 4B and 4C, lane 10; data not shown). Consistent with this, in

the AlphaFold2 prediction of the CMTR1 structure, the WW, GT-like, and RFM domains have multiple interactions^{33,34} (Figure 4D).

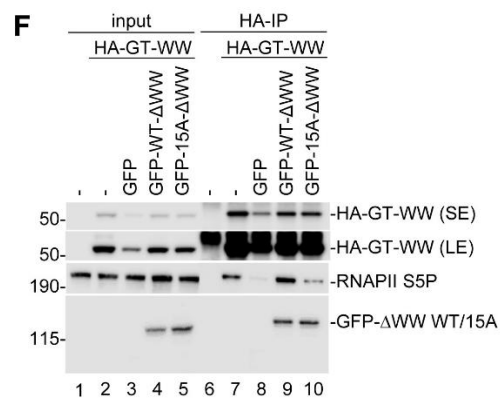
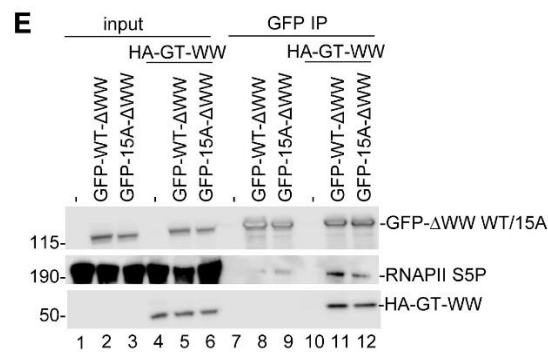
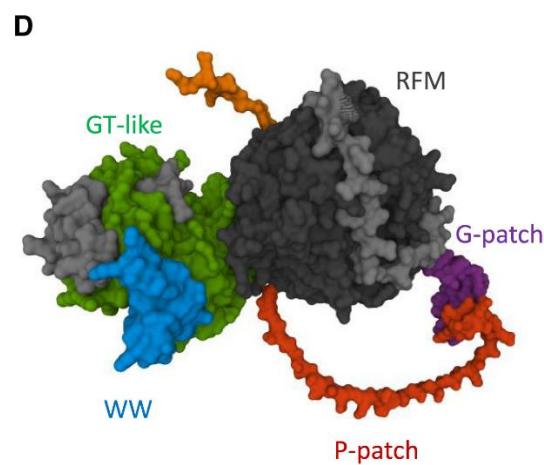
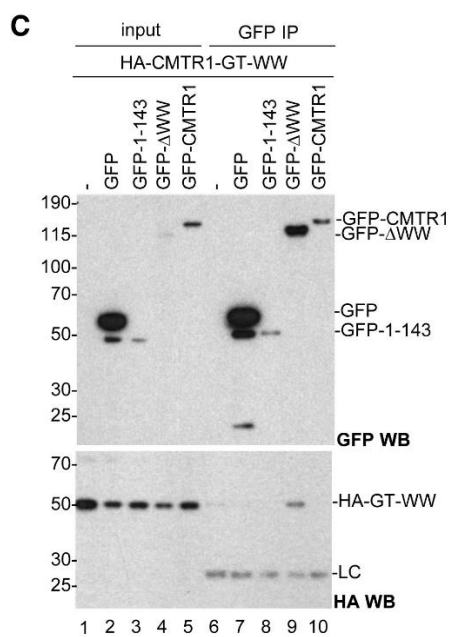
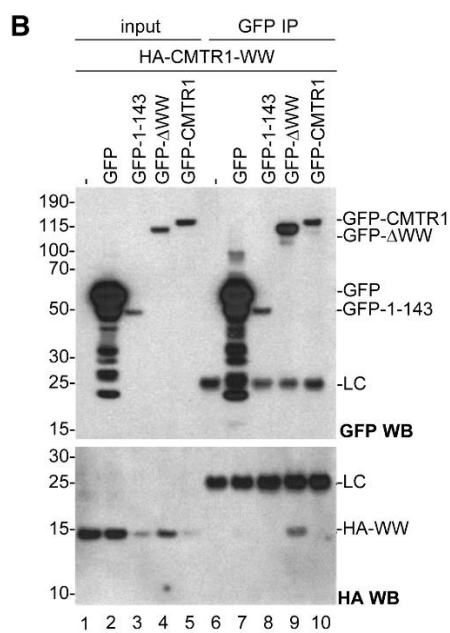
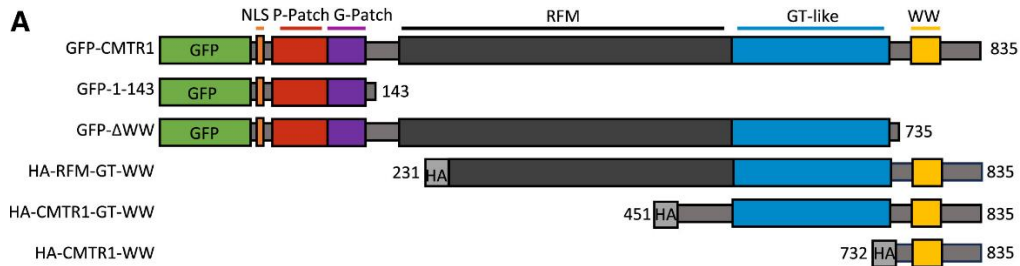


Figure 4 Intramolecular interactions of CMTR1

(A) Diagram of CMTR1 mutants used. (B) HA-CMTR1-WW was transiently co-expressed with the GFP-CMTR1 WT and mutants indicated above blots in HeLa cells. GFP-CMTR1 proteins were immunoprecipitated using GFP nanobodies and western blots performed to detect HA-WW (anti-HA antibody) and GFP-tagged protein (anti-GFP antibodies). (C) As in (B) except HA-CMTR1-GT-WW was co-expressed with GFP-tagged CMTR1 mutants. (D) The predicted structure of CMTR1 by AlphaFold2. The domains of interest are indicated. (E and F) HA-CMTR1-GT-WW was expressed with GFP-CMTR1 WT, 15A, or GFP alone. (E) GFP-CMTR1 proteins immunoprecipitated with nanobodies. (F) HA-GT-WW was immunoprecipitated using anti-HA antibodies. RNA Pol II S5P and other antigens were detected by western blot.

The impact of CMTR1 intramolecular interactions on recruitment to RNA Pol II was investigated (Figures 4E and 4F). As published previously,¹⁸ GFP-CMTR1 Δ WW (WT or 15A) does not interact significantly with RNA Pol II (lanes 8 and 9, Figure 4E). When HA-CMTR1-GT-WW (HA-GT-WW) is expressed with GFP-CMTR1 Δ WW (GFP-WT- Δ WW), they form a complex, permitting GFP-CMTR1 Δ WW to bind to RNA Pol II (Figure 4E, lane 11). GFP-CMTR1 Δ WW with 15A mutations (GFP-15A- Δ WW) also interacts with HA-GT-WW, but this complex has reduced RNA Pol II binding (Figure 4E, lane 12). These data are consistent with the CMTR1 P-Patch interacting with the CMTR1 CTD and this interaction promoting binding to RNA Pol II in a phospho-dependent manner. In the AlphaFold2-predicted structure, the P-Patch is a disordered region, which may contact the rest of CMTR1 at multiple points, enhancing the intramolecular interaction (Figure 4D).

Evidence supporting that the phosphorylated P-Patch promotes CMTR1-RNA Pol II interactions comes from experiments in which HA-CMTR1-GT-WW (HA-GT-WW) was expressed in cells and immunoprecipitated with RNA Pol II CTD S5P (Figure 4F, lane 7), consistent with the RNA Pol II CTD-CMTR1 WW domain interaction.¹⁸ Although GFP-CMTR1 Δ WW (GFP-WT- Δ WW) has a weak affinity for RNA Pol II, expression of it increases the interaction of HA-CMTR1-GT-WW and RNA Pol II (Figure 4D, compare lanes 8 and 9). GFP-CMTR1 Δ WW 15A (GFP-15A- Δ WW) also interacts with HA-CMTR1-GT-WW (HA-GT-WW) but does not increase the interaction with RNA Pol II

(Figure 4F, compare lanes 8 and 10). Thus, P-Patch phosphorylation (even on a distinct peptide) positively influences the interaction of the RNA Pol II CTD and CMTR1.

CMTR1 phosphorylation increases RNA cap formation and cell proliferation

To investigate the impact of CMTR1 phosphorylation in cells, we utilized MEFs in which the *Cmtr1* gene is floxed in exon 3, resulting in gene deletion upon expression of Cre recombinase (Figure S5). In these cells, HA-CMTR1 WT and 15A were expressed following retroviral infection (at a level lower than endogenous CMTR1), and subsequently, the endogenous *Cmtr1* gene was deleted (Figure S5C). Using this method, we avoided cell adaptation to long-term *Cmtr1* gene deletion, which we observed previously (CMTR1 15A expression increases relative to WT over time in *Cmtr1*^{-/-} cells; data not shown). The impact of CMTR1 15A on RNA cap formation was analyzed by CAP-MAP (cap analysis protocol with minimal analyte processing) MS.³⁵ Consistent with CMTR1 being required for N1 2'-O-Me (O-2 methylation of the first transcribed nucleotide ribose), *Cmtr1* deletion resulted in a reduction in the N1 O-2-Me-containing mature RNA caps ^{m7}Gppp^{m6}A_m, ^{m7}GpppA_m, and ^{m7}GpppG_m and an increase in the incomplete caps ^{m7}Gppp^{m6}A, ^{m7}GpppA, and ^{m7}GpppG in comparison to cells expressing CMTR1 WT (Figure 5A). Expression of CMTR1 15A only partially rescued the abundance of mature caps, consistent with CMTR1 phosphorylation promoting cellular RNA cap O-2 methylation.

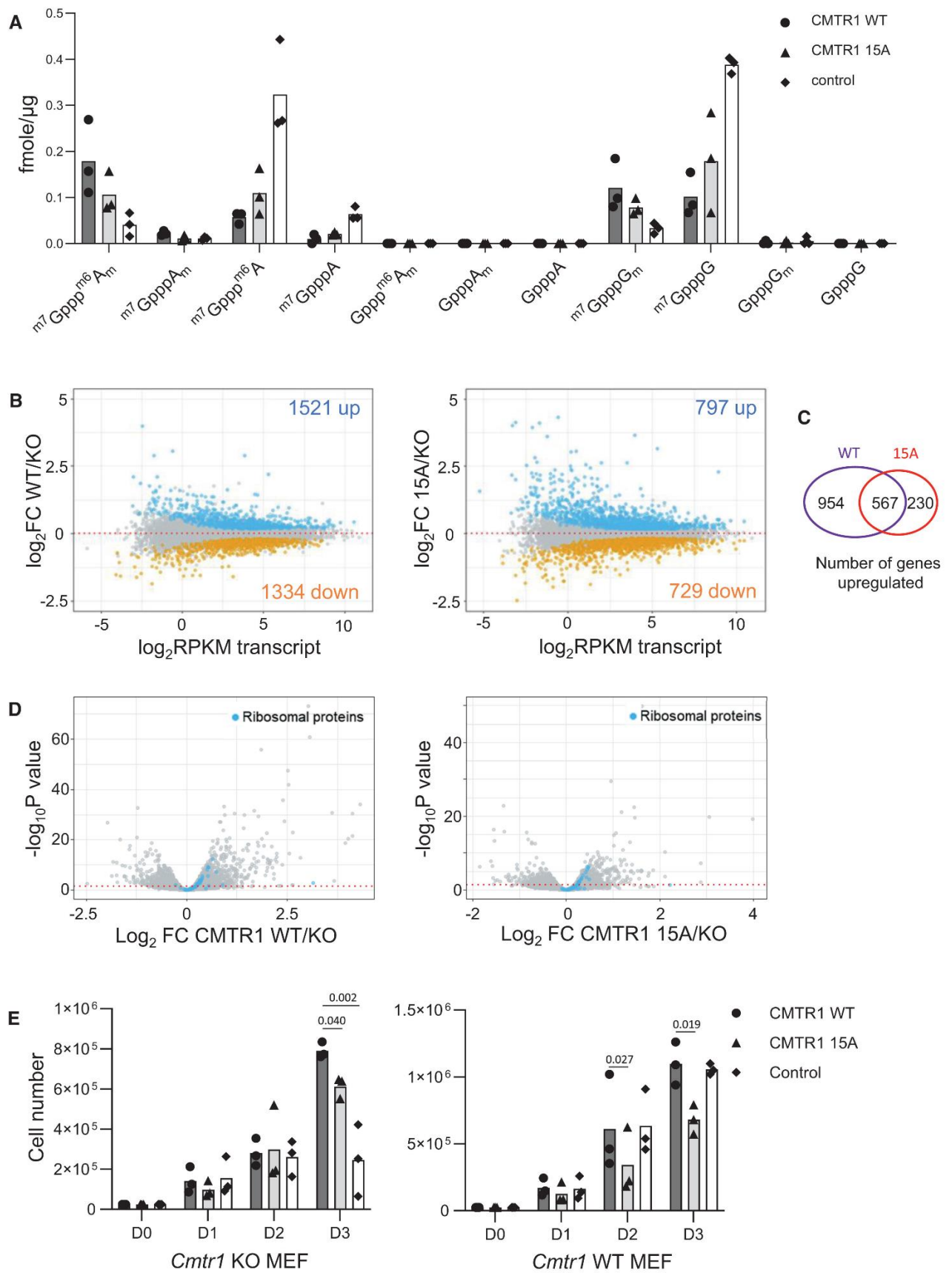


Figure 5 CMTR1 phosphorylation is required for RNA cap methylation and gene expression

MEF lines were created to express HA-CMTR1 WT, 15A, and vector control. Cre recombinase was expressed to delete the *Cmtr1* gene.

(A) Relative abundance of cap structures in *Cmtr1* knockout (KO) MEFs expressing HA-CMTR1 WT, 15A, or vector control. Data presented are from three independent experiments, and bar indicates the average. (B) MA plots of transcript levels (\log_2 RPKM [reads per kilobase per million mapped reads]) and \log_2 fold change of CMTR1 WT vs. KO (left) and CMTR1 15A vs. KO (right). Genes significantly down-/up-regulated (EdgeR exactTest, false discovery rate [FDR]-adjusted $p < 0.05$) are highlighted. (C) Venn diagram of numbers of genes increased by expression of CMTR1 WT and 15A, defined as those gene transcripts significantly up-regulated relative to *Cmtr1* KO. (D) Volcano plots indicating the relationship between \log_2 FC and $-\log_{10}$ FDR-adjusted p value for CMTR1 WT vs. KO (left) and CMTR1 15A vs. KO (right). Ribosomal protein genes (79 genes) are highlighted. (E) MEF lines with and without Cre-directed *Cmtr1* deletion. MEFs were plated and counted each day. Data shown are for 3 experiments, and bar indicates the average. Student's t test was performed, and p values are stated.

Phospho-defective mutation 15A reduces CMTR1-dependent gene expression

CMTR1 and its product N1 2'-*O*-Me have roles in gene expression, with the target genes determined by the cell lineage.^{8,13,14,17,18,20,21} RNA sequencing analysis was carried out on log-phase MEFs expressing HA-CMTR1 WT, 15A, or vector control, in which the endogenous *Cmtr1* gene was deleted (Figure S5). In previous studies, CMTR1 repression had been demonstrated to impact RNA levels.^{14,15} In RNA sequencing analysis, 12,516 RNAs (transcripts mapping to single genes) were detected that had more than one count per million reads in more than 3 samples (Table S1). Expression of HA-CMTR1 WT resulted in significantly increased levels of 1,521 RNAs and significantly decreased levels of 1,334 RNAs (Figures 5B and 5C). Expression of HA-CMTR1 15A also resulted in altered RNA levels but to a lesser extent than HA-CMTR1 WT, consistent with CMTR1 phosphorylation being required for RNA Pol II binding and RNA capping. 797 RNAs were significantly increased in response to the expression of HA-CMTR1 15A, and 729 RNAs were significantly reduced (Figures 5B and 5C). 567 of the same RNAs were increased in HA-CMTR1 WT- and 15A-expressing cells; RNAs upregulated in response to CMTR1 15A were largely a subset of those upregulated in response to the WT protein (Figure 5C).

Furthermore, HA-CMTR1 WT expression resulted in higher increases in RNA levels compared to CMTR1 15A. Of the top 100 RNAs increased in response to CMTR1 WT, the average LFC (log fold change) was 1.96, whereas for the top 100 RNAs that increased in response to CMTR1 15A, the average LFC was 1.53 (Table S1).

Gene Ontology term analysis revealed that genes upregulated by both WT and 15A included genes involved in RNA translation, consistent with previous studies (Figure S6).^{14,15} One of the most CMTR1-dependent gene families in embryonic stem cells is the ribosomal protein genes, correlating with high RNA Pol II-gene binding.¹⁴ Ribosomal protein gene transcripts were also induced in response to CMTR1 WT and 15A, indicating the conservation of their CMTR1 dependency across cell types (Figure 5D; Table S1). CMTR1 WT induced ribosomal protein gene transcripts more than the 15A mutant, consistent with increased RNA Pol II binding.¹⁴ Consistent with reduced gene expression, deletion of the *Cmtr1* gene in MEFs resulted in reduced cell proliferation (Figure 5E). Expression of CMTR1 WT rescued this defect more than 15A (Figure 5E, left). In cells expressing endogenous CMTR1, expression of CMTR1 15A acted as a dominant negative, reducing cell proliferation (Figure 5E, right).

CMTR1 phosphorylation is required for the interferon response

CMTR1 has previously been demonstrated to be required for the expression of ISGs.¹³ Here, we observed that the ISGs IFIT1, IFIT3, IFIH1, ISG15, and DHX58 are upregulated in response to interferon addition in CMTR1 WT-expressing *Cmtr1*^{-/-} MEFs (Figure 6A). Interferon-induced expression of IFIT1, IFIT3, IFIH1, and ISG15 was significantly reduced in MEFs expressing CMTR1 15A (Figure 6A). Consistent with these observations, interferon-induced expression of IFIT3 and ISG15 proteins was delayed in *Cmtr1*^{-/-} MEFs compared to those expressing HA-CMTR1 WT (Figure 6B). This was most apparent at the 4 h time point. Expression of HA-CMTR1 15A did not rescue this defect. PolyI:C (polyinosinic:polycytidylic acid) mimics RNA species generated during viral replication and is sensed by TLR3, MDA5, and RIG-I, resulting in interferon expression and other impacts.³⁶ Transfection of MEFs with polyI:C resulted in IFIT1

and IFIT3 expression in cells expressing CMTR1 WT, and this was attenuated in cells expressing CMTR1 15A (Figure 6C). Since the induction of the ISGs is dependent on an intact P-Patch, this implies that CK2 phosphorylation of CMTR1 is important in the interferon response. We used the highly selective CK2 competitive inhibitor quinalizarin to further investigate the role of CK2 in the interferon response.³¹ Pretreatment of MEFs with quinalizarin reduced the interferon-dependent induction of ISGs (Figure 6D) (we note that many proteins involved in the response to interferon are phosphorylated by CK2, and therefore quinalizarin is likely to have impacts beyond CMTR1 phosphorylation²⁶).

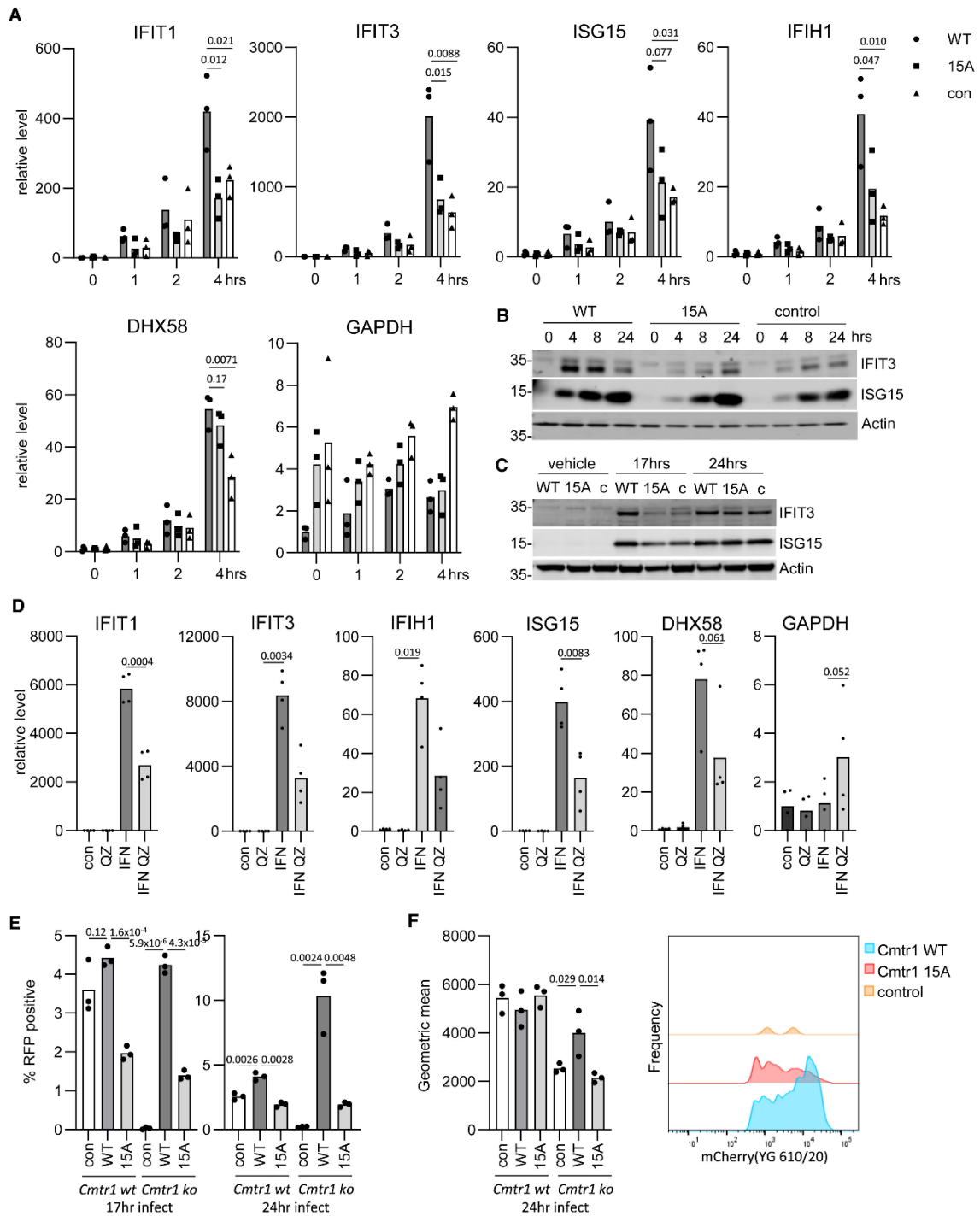


Figure 6 Induction of interferon-stimulated genes is dependent on CMTR1 P-Patch phosphorylation

(A) *Cmtr1* KO MEF lines expressing HA-CMTR1 WT, 15A, and vector control were incubated in 400 U/mL interferon for 1, 2, and 4 h. RNA was harvested and RNAs detected by PCR. Data are from 3 independent experiments, and bar indicates the average. Student's t test was performed, and p values are indicated.

(B and C) MEFs were (B) incubated with 400 U/mL interferons for 0, 4, 8, and 24 h and (C) transfected with 5 µg/mL polyI:C for 17 and 24 h. IFIT3 and ISG15 proteins were analyzed by western blot. Actin was used as a loading control.

(D) WT MEFs were incubated with 10 µM QZ for 0.5-3 h and 400 U/mL interferon for a subsequent 4 h. RT-PCR was performed as above. Data are from 4 independent experiments. Student's t test was performed, and p values are indicated. (E) *Cmtr1* WT and KO MEF lines expressing HA-CMTR1 WT, 15A, and vector control (con) were incubated with PR8 ColorFlu expressing a mCherry reporter gene. Cells producing virus were detected by fluorescence-activated cell sorting at 17 and 24 h post-infection. Data are from 3 independent wells. Student's t test was performed, and p values are indicated. (F) For mCherry-positive cells, the geometric mean of red fluorescence was reported. A sample histogram is presented for *Cmtr1*^{-/-} MEFs expressing HA-CMTR1 WT, 15A, and vector control, normalized to the mode.

CMTR1 phosphorylation is required for influenza infection

IAV is a negative-sense, single-stranded RNA virus that is dependent on the removal of host cell RNA caps via endonucleases for ligation to viral transcripts, a process known as cap snatching.³⁷ Influenza virus infection of A549 cells is dependent on CMTR1.³⁸ We investigated whether the defect in RNA cap production in cells expressing CMTR1 15A impacts influenza infection. A mouse-adapted PR8 IAV strain expressing a fluorescent mCherry reporter fused to the open reading frame of the viral NS1 gene was used to infect MEFs, with infected cells detected by mCherry protein expression at 17 and 24 h post-infection (Figure 6E).³⁹ Deletion of *Cmtr1* resulted in a significant reduction in the number of infected cells, and this could be rescued by the expression of CMTR1 WT. The expression of CMTR1 15A could partially rescue the defect, but the number of infected cells was significantly lower than that in cells expressing CMTR1 WT. CMTR1 phosphorylation could also be linked to viral protein detection (Figure 6F). Of the cells positive for viral infection, the geometric mean fluorescence intensity for NS1 expression was significantly higher in cells expressing CMTR1 WT in a *Cmtr1*^{-/-} background compared to CMTR1 15A. Therefore, although CMTR1 phosphorylation is required for the interferon response, which can suppress aspects of viral infection, in the context of IAV infection, CMTR1 phosphorylation acts as a pro-viral factor. This can

be potentially attributed to the dependence of IAV on cap-snatching mechanisms for efficient expression of viral mRNAs alongside its ability to suppress the interferon response.⁴⁰ In addition, members of the interferon-stimulated IFIT family are pro-viral factors that promote the translation of IAV mRNA^{41,42}; therefore, the CMTR1 phosphorylation-dependent expression of IFIT mRNAs may also contribute to efficient infection.

Discussion

RNA Pol II transcripts are methylated at the O-2 position of first transcribed nucleotide ribose (N1 2'-O-Me), a modification that is part of the RNA cap.^{2,5} Here, we report that CMTR1, the N1 2'-O-Me cap methyltransferase, is regulated by CK2-dependent phosphorylation on an N-terminal domain, which we named the P-Patch. Multiple serines and threonines in the P-Patch (CMTR1 amino acids 28-89) are substrates for CK2, although this domain may be phosphorylated by other kinases too. CMTR1 is recruited to the hypomethylated RNA cap by interactions with the RNA Pol II complex at the initiation of transcription.^{14,18,24} When the P-Patch is phosphorylated, the affinity of CMTR1 for the RNA Pol II CTD increases. Consistent with enhanced recruitment to RNA Pol II, we report that phosphorylation of CMTR1 is required for cap ribose-O-2 methylation and the expression of a subsets of RNAs, including ribosomal protein gene transcripts and ISGs. Phosphorylation of CMTR1 is also required for production of influenza virus, which cap snatches, taking the RNA cap from host cell transcripts for the priming of viral transcription and evasion of host immunity.⁴³ CK2 is a potent kinase that directs cellular functions.^{25,26,27,28} CK2 can phosphorylate specific amino acids on substrates or deposit patches of phosphorylation, with impacts on protein expression, substrate interactions, localization, and activity.^{44,45,46} CK2 or CK2-dependent phosphorylation is deregulated in many cancers, neurological conditions, and immune disorders. Inhibiting CK2 has biological impacts in specific disease areas, and as a result, CK2-targeting strategies are being investigated.^{27,28,45,46} Here, we demonstrate that CK2-dependent phosphorylation of CMTR1 is required for efficient cell proliferation, the interferon response, and influenza virus production.

CMTR1 is phosphorylated during G1 phase of the cell cycle and promotes cell proliferation. Phosphorylation of another RNA cap methyltransferase, the cap guanosine N-7 methyltransferase (RNMT, RNA guanine-7 methyltransferase), also promotes cell proliferation.³⁰ RNMT is phosphorylated by CDK1-cyclin B during late G2/M phase through to G1 phase, a modification that increases catalytic activity.³⁰ Being present during G1 phase, RNMT phosphorylation and CMTR1 phosphorylation enhance RNA cap formation when most transcripts are being synthesized. CK2 is not a cell cycle-regulated kinase, but it does interact with many proteins involved in chromatin dynamics and transcription including RNA Pol II.⁴⁷ CMTR1 may be phosphorylated by proximal CK2 when it is recruited to the transcribing RNA Pol II during G1 phase. Of note, CK2 also modulates the action of signaling and mechanistic proteins involved in transcription and translation.^{27,47}

CMTR1 makes at least 2 contacts with the RNA Pol II complex: the CMTR1 C-terminal WW domain interacts with the RNA Pol II CTD and the adjacent CMTR1 GT-like domain interacts with the RBP7 subunit.^{18,24} How does phosphorylation of the P-Patch at the N terminus of CMTR1 impact the interaction of the C-terminal WW domain with the RNA Pol II CTD? We confirmed that the WW domain is required for interaction with RNA Pol II. Additionally, we report that other regions of CMTR1 can interact with the WW domain and indirectly promote interaction with the polymerase. This stimulatory impact of CMTR1 is dependent on P-Patch phosphorylation; mutation of the P-Patch phospho-sites nullifies the stimulatory impact on the WW domain-RNA Pol II interaction. Structural information about the P-Patch is not available; based on AlphaFold predictions, it is likely to be disordered. We speculate that the phosphorylated P-Patch may interact with a positively charged patch in the WW domain (or proximal region), resulting in intramolecular alterations that support the CMTR1 and RNA Pol II CTD interaction.

The gene specificity of CMTR1 in altering RNA levels is important to understand because it dictates its biological impact. CMTR1 has direct and indirect roles in transcription and RNA stability, both of which will impact RNA levels.^{14,15} Current information about the factors dictating gene specificity is limited: high levels of RNA Pol II and CMTR1 gene binding correlate loosely with a response of genes to

CMTR1 inhibition, but other factors are indicated, and differential affinity for 5' RNA sequences may also have a role.^{14,15,20} Which RNAs are CMTR1 dependent varies with cell lineage.^{1,8,14,16,17,18,19,20,21} In MEFs, expression of the phospho-defective CMTR1 15A mutant regulates the expression of a similar set of RNAs as the WT protein but simply regulates them less effectively. Approximately half as many RNAs are upregulated to threshold levels by CMTR1 15A, compared to WT, in log-phase conditions. As in embryonic stem cells, major CMTR1 targets include the ribosomal protein gene transcripts. Ribosomal protein genes have some of the highest levels of RNA Pol II and CMTR1 bound to the transcription start site.^{14,15}

CMTR1 phosphorylation also has a role in the interferon response; it is an ISG (interferon-stimulated gene), which facilitates the expression of other ISGs.¹³ Here, we demonstrate that ISG expression is dependent on CMTR1 phosphorylation. In liver hepatoma cells and human monocyte cell lines, CMTR1 has little impact on ISG RNA levels but does impact on protein levels,¹³ whereas we report that in MEFs, CMTR1 impacts the RNA levels of ISGs. The cap interacts with multiple complexes involved in RNA processing and degradation; which processes are most dependent on ribose O-2 methylation will depend on the cellular context, including the levels of the different cap-binding proteins. In addition, CMTR1 can have impacts on transcription, either by the RNA cap protecting transcripts from degradation or by a more direct impact on transcription.¹⁵ Although CMTR1 is an ISG itself, in MEFs, the IFN-induced increase in CMTR1 protein occurs after 12-24 h and therefore will only contribute to the interferon response at these later time points.

The impact of CMTR1 phosphorylation on the interferon response is likely to protect cells from a range of infections. However, in the context of influenza infection, inhibition of CMTR1 phosphorylation reduced the expression of the viral protein NS1 and the number of infected cells. Influenza viruses acquire RNA caps for their transcripts by removing them from cellular transcripts (cap snatching) and are therefore dependent on host capped mRNA abundance for efficient transcription and subsequent translation of viral mRNAs.^{38,48,49} Other viruses that do not require cellular caps may be inhibited by CMTR1-dependent regulation of

the interferon response. Unusually, influenza viruses also require IFIT family members, known ISGs, for efficient infection.^{41,42} Therefore, CMTR1 phosphorylation-dependent expression of IFIT genes and the requirement for CMTR1 phosphorylation-dependent cellular caps may both contribute to efficient IAV infection.

In conclusion, we present a mechanism, CK2-dependent CMTR1 phosphorylation, that enhances mRNA capping during critical transcriptional bursts, such as cell cycle progression or immune defense.

Limitations of the study

Here, we demonstrate that the pleiotropic kinase CK2 phosphorylates the RNA cap methyltransferase CMTR1, resulting in a conformational change that promotes interaction with RNA Pol II and RNA cap methylation. Our data demonstrate that CK2 is the predominant CMTR1 kinase in HeLa cells; however, it is possible that other kinases phosphorylate the P-Patch. Indeed, proteins that are phosphorylated at multiple sites are often substrates for multiple kinases, with the kinases acting independently or in a hierarchical manner. Initial phosphorylation can often generate recognition motifs for subsequent kinases to be recruited and act on the same region. The amino acid sequence of the CMTR1 P-Patch may be a substrate for alternative acidophilic kinases, including CK1, GSK3b, Plk, or Fam20C.

Acknowledgments

We would like to thank Gopal Sapkota, University of Dundee; Rick Randall, University of St Andrews; Ed Hutchinson and Alfredo Castello, University of Glasgow; and the Cowling lab for advice, reagents, and technical assistance. We would like to thank the MRC Protein Phosphorylation and Ubiquitination Unit, Division of Signal Transduction Therapies, and University of Dundee TAGC for technical assistance. We thank the Core Services and Advanced Technologies at the Cancer Research UK Scotland Institute (A31287), with particular thanks to the Beatson Advanced Imaging Resource. The manuscript was critically reviewed by Catherine Winchester (CRUK Scotland Institute). This work was supported by Cancer Research UK core grant number A17196/A31287 to the CRUK Scotland

Institute and CTRQR-2021\100006 to the CRUK Scotland Centre. Research was funded by European Research Council Award 769080 TCAPS, Medical Research Council Senior Fellowship MR/K024213/1, a Lister Research Prize Fellowship, a Wellcome Trust PhD studentship 097462/Z/11/Z, Royal Society Wolfson Research Merit Award WRM\R1\180008, Wellcome Trust Investigator Award 219416/A/19/Z, and Wellcome Trust GRE Centre Award 097945/Z/11/Z.

Author contributions

Conceptualization, F.I.V. and V.H.C.; data curation, all authors; analysis, all authors; investigation, all authors; writing, all authors; supervision, V.H.C.

Declaration of interests

The authors declare no competing interests.

References

1.

Dohnalkova, M. · Krasnykov, K. · Mendel, M. ...

Essential roles of RNA cap-proximal ribose methylation in mammalian embryonic development and fertility

Cell Rep. 2023; 42, 112786

2.

Inesta-Vaquera, F. · Cowling, V.H.

Regulation and function of CMTR1-dependent mRNA cap methylation

Wiley Interdiscip. Rev. RNA. 2017; 8, e1450

3.

Belanger, F. · Stepinski, J. · Darzynkiewicz, E. ...

Characterization of hMTr1, a human Cap1 2'-O-ribose methyltransferase

J. Biol. Chem. 2010; 285:33037-33044

4.

Smietanski, M. · Werner, M. · Purta, E. ...

Structural analysis of human 2'-O-ribose methyltransferases involved in mRNA cap structure formation

Nat. Commun. 2014; 5:3004

5.

Pelletier, J. · Schmeing, T.M. · Sonenberg, N.

The multifaceted eukaryotic cap structure

Wiley Interdiscip. Rev. RNA. 2021; **12**, e1636

6.

Kruse, S. · Zhong, S. · Bodi, Z. ...

A novel synthesis and detection method for cap-associated adenosine modifications in mouse mRNA

Sci. Rep. 2011; **1**:126

7.

Grudzien-Nogalska, E. · Kiledjian, M.

New insights into decapping enzymes and selective mRNA decay

Wiley Interdiscip. Rev. RNA. 2017; **8**

8.

Sikorski, P.J. · Warminski, M. · Kubacka, D. ...

The identity and methylation status of the first transcribed nucleotide in eukaryotic mRNA 5' cap modulates protein expression in living cells

Nucleic Acids Res. 2020; **48**:1607-1626

9.

Su, A.I. · Pezacki, J.P. · Wodicka, L. ...

Genomic analysis of the host response to hepatitis C virus infection

Proc. Natl. Acad. Sci. USA. 2002; **99**:15669-15674

10.

Geiss, G.K. · Carter, V.S. · He, Y. ...

Gene expression profiling of the cellular transcriptional network regulated by alpha/beta interferon and its partial attenuation by the hepatitis C virus nonstructural 5A protein

J. Virol. 2003; **77**:6367-6375

11.

Guerra, S. · López-Fernández, L.A. · Pascual-Montano, A. ...

Cellular gene expression survey of vaccinia virus infection of human HeLa cells

J. Virol. 2003; **77**:6493-6506

12.

Kato, A. · Homma, T. · Batchelor, J. ...

Interferon-alpha/beta receptor-mediated selective induction of a gene cluster by CpG oligodeoxynucleotide 2006

BMC Immunol. 2003; 4:8

13.

Williams, G.D. · Gokhale, N.S. · Snider, D.L. ...

The mRNA Cap 2'-O-Methyltransferase CMTR1 Regulates the Expression of Certain Interferon-Stimulated Genes

mSphere. 2020; 5:e00202

14.

Liang, S. · Silva, J.C. · Suska, O. ...

CMTR1 is recruited to transcription start sites and promotes ribosomal protein and histone gene expression in embryonic stem cells

Nucleic Acids Res. 2022; 50:2905-2922

15.

Liang, S. · Almohammed, R. · Cowling, V.H.

The RNA cap methyltransferases RNMT and CMTR1 co-ordinate gene expression during neural differentiation

Biochem. Soc. Trans. 2023; 51:1131-1141

16.

Kuge, H. · Brownlee, G.G. · Gershon, P.D. ...

Cap ribose methylation of c-mos mRNA stimulates translation and oocyte maturation in *Xenopus laevis*

Nucleic Acids Res. 1998; 26:3208-3214

17.

Lee, Y.L. · Kung, F.C. · Lin, C.H. ...

CMTR1-Catalyzed 2'-O-Ribose Methylation Controls Neuronal Development by Regulating Camk2 alpha Expression Independent of RIG-I Signaling

Cell Rep. 2020; 33, 108269

18.

Inesta-Vaquera, F. · Chaugule, V.K. · Galloway, A. ...

DHX15 regulates CMTR1-dependent gene expression and cell proliferation

Life Sci. Alliance. 2018; 1, e201800092

19.

Toczydlowska-Socha, D. · Zielinska, M.M. · Kurkowska, M. ...

Human RNA cap1 methyltransferase CMTr1 cooperates with RNA helicase DHX15 to modify RNAs with highly structured 5' termini

Philos. Trans. R. Soc. Lond. B Biol. Sci. 2018; 373, 20180161

20.

Hausmann, I.U. · Wu, Y. · Nallasivan, M.P. ...

CMTr cap-adjacent 2'-O-ribose mRNA methyltransferases are required for reward learning and mRNA localization to synapses

Nat. Commun. 2022; 13:1209

21.

You, A.B. · Yang, H. · Lai, C.P. ...

CMTR1 promotes colorectal cancer cell growth and immune evasion by transcriptionally regulating STAT3

Cell Death Dis. 2023; 14:245

22.

Meisel, J.D. · Wiesenthal, P.P. · Mootha, V.K. ...

CMTR-1 RNA methyltransferase mutations activate widespread expression of a dopaminergic neuron-specific mitochondrial complex I gene

Curr. Biol. 2024;

23.

Haline-Vaz, T. · Silva, T.C.L. · Zanchin, N.I.T.

The human interferon-regulated ISG95 protein interacts with RNA polymerase II and shows methyltransferase activity

Biochem. Biophys. Res. Commun. 2008; 372:719-724

24.

Garg, G. · Dienemann, C. · Farnung, L. ...

Structural insights into human co-transcriptional capping

Mol. Cell. 2023; 83:2464-2477.e5

25.

St-Denis, N. · Gabriel, M. · Turowec, J.P. ...

Systematic investigation of hierarchical phosphorylation by protein kinase CK2

J. Proteomics. 2015; **118**:49-62

26.

Hong, H. · Benveniste, E.N.

The Immune Regulatory Role of Protein Kinase CK2 and Its Implications for Treatment of Cancer

Biomedicines. 2021; **9**, 1932

27.

Roffey, S.E. · Litchfield, D.W.

CK2 Regulation: Perspectives in 2021

Biomedicines. 2021; **9**, 1361

28.

Firna, M.B. · Brieger, A.

CK2 and the Hallmarks of Cancer

Biomedicines. 2022; **10**, 1987

29.

Herhaus, L. · Perez-Oliva, A.B. · Cozza, G. ...

Casein kinase 2 (CK2) phosphorylates the deubiquitylase OTUB1 at Ser16 to trigger its nuclear localization

Sci. Signal. 2015; **8**, ra35

30.

Aregger, M. · Kaskar, A. · Varshney, D. ...

CDK1-Cyclin B1 Activates RNMT, Coordinating mRNA Cap Methylation with G1 Phase Transcription

Mol. Cell. 2016; **61**:734-746

31.

Cozza, G. · Mazzorana, M. · Papinutto, E. ...

Quinalizarin as a potent, selective and cell-permeable inhibitor of protein kinase CK2

Biochem. J. 2009; **421**:387-395

32.

Werner, M. · Purta, E. · Kaminska, K.H. ...

2'-O-ribose methylation of cap2 in human: function and evolution in a horizontally mobile family

Nucleic Acids Res. 2011; **39**:4756-4768

33.

Jumper, J. · Evans, R. · Pritzel, A. ...

Highly accurate protein structure prediction with AlphaFold

Nature. 2021; **596**:583-589

34.

Varadi, M. · Anyango, S. · Deshpande, M. ...

AlphaFold Protein Structure Database: massively expanding the structural coverage of protein-sequence space with high-accuracy models

Nucleic Acids Res. 2022; **50**:D439-D444

35.

Galloway, A. · Atrih, A. · Grzela, R. ...

CAP-MAP: cap analysis protocol with minimal analyte processing, a rapid and sensitive approach to analysing mRNA cap structures

Open Biol. 2020; **10**, 190306

36.

Gitlin, L. · Barchet, W. · Gilfillan, S. ...

Essential role of mda-5 in type I IFN responses to polyriboinosinic:polyribocytidylic acid and encephalomyocarditis picornavirus

Proc. Natl. Acad. Sci. USA. 2006; **103**:8459-8464

37.

Plotch, S.J. · Bouloy, M. · Ulmanen, I. ...

A unique cap(m7GpppXm)-dependent influenza virion endonuclease cleaves capped RNAs to generate the primers that initiate viral RNA transcription

Cell. 1981; **23**:847-858

38.

Tsukamoto, Y. · Hiono, T. · Yamada, S. ...

Inhibition of cellular RNA methyltransferase abrogates influenza virus capping and replication

Science. 2023; **379**:586-591

39.

Fukuyama, S. · Katsura, H. · Zhao, D. ...

Multi-spectral fluorescent reporter influenza viruses (Color-flu) as powerful tools for in vivo studies

Nat. Commun. 2015; 6:6600

40.

Randall, R.E. · Goodbourn, S.

Interferons and viruses: an interplay between induction, signalling, antiviral responses and virus countermeasures

J. Gen. Virol. 2008; 89:1-47

41.

Tran, V. · Ledwith, M.P. · Thamamongood, T. ...

Influenza virus repurposes the antiviral protein IFIT2 to promote translation of viral mRNAs

Nat. Microbiol. 2020; 5:1490-1503

42.

King, C.R. · Liu, Y. · Amato, K.A. ...

Pathogen-driven CRISPR screens identify TREX1 as a regulator of DNA self-sensing during influenza virus infection

Cell Host Microbe. 2023; 31:1552-1567.e8

43.

Furuichi, Y.

Discovery of m(7)G-cap in eukaryotic mRNAs

Proc. Jpn. Acad. 2015; 91:394-409

44.

Meggio, F. · Pinna, L.A.

One-thousand-and-one substrates of protein kinase CK2?

FASEB J. 2003; 17:349-368

45.

Borgo, C. · Ruzzene, M.

Protein kinase CK2 inhibition as a pharmacological strategy

Adv. Protein Chem. Struct. Biol. 2021; 124:23-46

46.

Salvi, M. · Borgo, C. · Pinna, L.A. ...

Targeting CK2 in cancer: a valuable strategy or a waste of time?

Cell Death Discov. 2021; 7:325

47.

Borgo, C. · D'Amore, C. · Sarno, S. ...

Protein kinase CK2: a potential therapeutic target for diverse human diseases

Signal Transduct. Target. Ther. 2021; 6:183

48.

Li, B. · Clohisey, S.M. · Chia, B.S. ...

Genome-wide CRISPR screen identifies host dependency factors for influenza A virus infection

Nat. Commun. 2020; 11:164

49.

Bowie, A.G. · Unterholzner, L.

Viral evasion and subversion of pattern-recognition receptor signalling

Nat. Rev. Immunol. 2008; 8:911-922

Chapter 8: References

Abbas, Y.M., Laudenbach, B.T., Martínez-Montero, S., Cencic, R., Habjan, M., Pichlmair, A., Damha, M.J., Pelletier, J., Nagar, B., 2017. Structure of human IFIT1 with capped RNA reveals adaptable mRNA binding and mechanisms for sensing N1 and N2 ribose 2'-O methylations. *Proceedings of the National Academy of Sciences* 114, E2106-E2115.

Adjibade, P., Mazroui, R., 2014. Control of mRNA turnover: Implication of cytoplasmic RNA granules. *Seminars in Cell & Developmental Biology, mRNA stability and degradation & Timing of mammalian embryogenesis & Positioning of the Mitotic Spindle* 34, 15-23. <https://doi.org/10.1016/j.semcdb.2014.05.013>

Ahn, S.H., Kim, M., Buratowski, S., 2004. Phosphorylation of Serine 2 within the RNA Polymerase II C-Terminal Domain Couples Transcription and 3' End Processing. *Molecular Cell* 13, 67-76.

Ahola, T., Kääriäinen, L., 1995. Reaction in alphavirus mRNA capping: formation of a covalent complex of nonstructural protein nsP1 with 7-methyl-GMP. *Proc Natl Acad Sci U S A* 92, 507-511.

Akhrymuk, I., Frolov, I., Frolova, E.I., 2018. Sindbis Virus Infection Causes Cell Death by nsP2-Induced Transcriptional Shutoff or by nsP3-Dependent Translational Shutoff. *Journal of Virology* 92, 10.1128/jvi.01388-18.

Akhrymuk, I., Kulemzin, S.V., Frolova, E.I., 2012. Evasion of the Innate Immune Response: the Old World Alphavirus nsP2 Protein Induces Rapid Degradation of Rpb1, a Catalytic Subunit of RNA Polymerase II. *J Virol* 86, 7180-7191.

Akichika, S., Hirano, S., Shichino, Y., Suzuki, Takeo, Nishimasu, H., Ishitani, R., Sugita, A., Hirose, Y., Iwasaki, S., Nureki, O., Suzuki, Tsutomu, 2019. Cap-specific terminal N 6-methylation of RNA by an RNA polymerase II-associated methyltransferase. *Science* 363,

Akinyemiju, T., Abera, S., Ahmed, M., Alam, N., Alemayohu, M.A., Allen, C., Al-Raddadi, R., Alvis-Guzman, N., Amoako, Y., Artaman, A., Ayele, T.A., Barac, A., Bensenor, I., Berhane, A., Bhutta, Z., Castillo-Rivas, J., Chitheer, A., Choi, J.-Y., Cowie, B., Dandona, L., Dandona, R., Dey, S., Dicker, D., Phuc, H., Ekwueme., 2017. The Burden of Primary Liver Cancer and Underlying Etiologies From 1990 to 2015 at the Global, Regional, and National Level. *JAMA Oncol* 3, 1683-1691.

Akwa, Y., Hassett, D.E., Eloranta, M.L., Sandberg, K., Masliah, E., Powell, H., Whitton, J.L., Bloom, F.E., Campbell, I.L., 1998. Transgenic expression of IFN-alpha in the central nervous system of mice protects against lethal neurotropic viral infection but induces inflammation and neurodegeneration. *J Immunol* 161, 5016-5026.

Albano, E., Clot, P., Morimoto, M., Tomasi, A., Ingelman-Sundberg, M., French, S.W., 1996. Role of cytochrome P450E1-dependent formation of hydroxyethyl free radical in the development of liver damage in rats intragastrically fed with ethanol. *Hepatology* 23, 155-163.

Alexopoulou, L., Holt, A.C., Medzhitov, R., Flavell, R.A., 2001. Recognition of double-stranded RNA and activation of NF- κ B by Toll-like receptor 3. *Nature* 413, 732-738.

Alff, P.J., Gavrilovskaya, I.N., Gorbunova, E., Endriss, K., Chong, Y., Geimonen, E., Sen, N., Reich, N.C., Mackow, E.R., 2006. The Pathogenic NY-1 Hantavirus G1 Cytoplasmic Tail Inhibits RIG-I- and TBK-1-Directed Interferon Responses. *Journal of Virology* 80, 9676-9686.

Alliegro, M.C., 2000. Effects of Dithiothreitol on Protein Activity Unrelated to Thiol-Disulfide Exchange: For Consideration in the Analysis of Protein Function with Cleland's Reagent. *Analytical Biochemistry* 282, 102-106.

Ally, A., Balasundaram, M., Carlsen, R., Chuah, E., Clarke, A., Dhalla, N., Holt, R.A., Jones, S.J.M., Lee, D., Ma, Y., Marra, M.A., Mayo, M., Moore, R.A., Mungall,

A.J., Schein, J.E., Sipahimalani, P., Tam, A., Thiessen, N., Cheung, D., Wong, T., Brooks, D., Robertson, A.G., Bowlby, R., Mungall, K., Sadeghi, S., Xi, L., Covington, K., Shinbrot, E., Wheeler, D.A., Gibbs, R.A., Donehower, L.A., Wang, L., Bowen, J., Gastier-Foster, J.M., Gerken, M., Hessel, C., Leraas, K.M., 2017. Comprehensive and Integrative Genomic Characterization of Hepatocellular Carcinoma. *Cell* 169, 1327-1341.

Alva-Medina, J., Dent, M.A.R., Aranda-Anzaldo, A., 2010. Aged and post-mitotic cells share a very stable higher-order structure in the cell nucleus in vivo. *Biogerontology* 11, 703-716.

Anantharaman, V., Koonin, E.V., Aravind, L., 2002. Comparative genomics and evolution of proteins involved in RNA metabolism. *Nucleic Acids Res* 30, 1427-1464.

Aoki, M., Hecht, A., Kruse, U., Kemler, R., Vogt, P.K., 1999. Nuclear endpoint of Wnt signaling: neoplastic transformation induced by transactivating lymphoid-enhancing factor 1. *Proc Natl Acad Sci U S A* 96, 139-144.

Aravind, L., Koonin, E.V., 1999. G-patch: a new conserved domain in eukaryotic RNA-processing proteins and type D retroviral polyproteins. *Trends in Biochemical Sciences* 24, 342-344.

Aregger, M., Cowling, V.H., 2013. Human cap methyltransferase (RNMT) N-terminal non-catalytic domain mediates recruitment to transcription initiation sites. *Biochem J* 455, 67-73.

Aregger, M., Kaskar, A., Varshney, D., Fernandez-Sanchez, M.E., Inesta-Vaquera, F.A., Weidlich, S., Cowling, V.H., 2016. CDK1-Cyclin B1 Activates RNMT, Coordinating mRNA Cap Methylation with G1 Phase Transcription. *Molecular Cell* 61, 734-746.

Asao, H., Fu, X.-Y., 2000. Interferon- γ Has Dual Potentials in Inhibiting or Promoting Cell Proliferation*. *Journal of Biological Chemistry* 275, 867-874.

Baba, T., Tanimura, S., Yamaguchi, A., Horikawa, K., Yokozeki, M., Hachiya, S., Iemura, S.-I., Natsume, T., Matsuda, N., Takeda, K., 2021. Cleaved PGAM5 dephosphorylates nuclear serine/arginine-rich proteins during mitophagy. *Biochim Biophys Acta Mol Cell Res* 1868, 119045.

Badis, G., Saveanu, C., Fromont-Racine, M., Jacquier, A., 2004. Targeted mRNA Degradation by Deadenylation-Independent Decapping. *Molecular Cell* 15, 5-15.

Baechler, E.C., Batliwalla, F.M., Karypis, G., Gaffney, P.M., Ortmann, W.A., Espe, K.J., Shark, K.B., Grande, W.J., Hughes, K.M., Kapur, V., Gregersen, P.K., Behrens, T.W., 2003. Interferon-inducible gene expression signature in peripheral blood cells of patients with severe lupus. *Proc Natl Acad Sci U S A* 100, 2610-2615.

Bage, M.G., Almohammed, R., Cowling, V.H., Pislakov, A.V., 2021. A novel RNA pol II CTD interaction site on the mRNA capping enzyme is essential for its allosteric activation. *Nucleic Acids Res* 49, 3109-3126.

Bailey, S.M., Cunningham, C.C., 1998. Acute and chronic ethanol increases reactive oxygen species generation and decreases viability in fresh, isolated rat hepatocytes. *Hepatology* 28, 1318-1326.

Barak, A.J., Beckenhauer, H.C., Tuma, D.J., 1990. Methionine metabolism in the Buffalo rat following ethanol feeding. *Journal of the American College of Nutrition* 9, 97-100.

Baral, D., Wu, L., Katwal, G., Yan, X., Wang, Y., Ye, Q., 2018. Clinical significance and biological roles of small nucleolar RNAs in hepatocellular carcinoma. *Biomed Rep* 8, 319-324.

Beaudet, A.L., O'Brien, W.E., Bock, H.G., Freytag, S.O., Su, T.S., 1986. The human argininosuccinate synthetase locus and citrullinemia. *Adv Hum Genet* 15, 161-196, 291-292.

Becker, S.A., Lee, T.-H., Butel, J.S., Slagle, B.L., 1998. Hepatitis B Virus X Protein Interferes with Cellular DNA Repair. *Journal of Virology* 72, 266-272.

Beelman, C.A., Stevens, A., Caponigro, G., LaGrandeur, T.E., Hatfield, L., Fortner, D.M., Parker, R., 1996. An essential component of the decapping enzyme required for normal rates of mRNA turnover. *Nature* 382, 642-646.

Beer, S., Zetterberg, A., Ihrle, R.A., McTaggart, R.A., Yang, Q., Bradon, N., Arvanitis, C., Attardi, L.D., Feng, S., Ruebner, B., Cardiff, R.D., Felsher, D.W., 2004. Developmental Context Determines Latency of MYC-Induced Tumorigenesis. *PLOS Biology* 2, e332.

Beinke, S., Ley, S.C., 2004. Functions of NF- κ B1 and NF- κ B2 in immune cell biology. *Biochemical Journal* 382, 393-409.

Bélanger, F., Stepinski, J., Darzynkiewicz, E., Pelletier, J., 2010. Characterization of hMTr1, a Human Cap1 2'-O-Ribose Methyltransferase. *J Biol Chem* 285, 33037-33044.

Belsom, A., Rappsilber, J., 2021. Anatomy of a crosslinker. *Current Opinion in Chemical Biology, Omics* 60, 39-46.

Benarroch, D., Egloff, M.-P., Mulard, L., Guerreiro, C., Romette, J.-L., Canard, B., 2004. A Structural Basis for the Inhibition of the NS5 Dengue Virus mRNA 2'-O-Methyltransferase Domain by Ribavirin 5'-Triphosphate *. *Journal of Biological Chemistry* 279, 35638-35643.

Bernkopf, D.B., Jalal, K., Brückner, M., Knaup, K.X., Gentzel, M., Schambony, A., Behrens, J., 2018. Pgam5 released from damaged mitochondria induces mitochondrial biogenesis via Wnt signaling. *J Cell Biol* 217, 1383-1394.

Biondi, R.M., Engel, M., Sauane, M., Welter, C., Issinger, O.-G., Jiménez de Asúa, L., Passeron, S., 1996. Inhibition of nucleoside diphosphate kinase activity by in

vitro phosphorylation by protein kinase CK2 Differential phosphorylation of NDP kinases in HeLa cells in culture. *FEBS Letters* 399, 183-187.

Bisso, A., Filipuzzi, M., Gamarra Figueroa, G.P., Brumana, G., Biagioni, F., Doni, M., Ceccotti, G., Tanaskovic, N., Morelli, M.J., Pendino, V., Chiacchiera, F., Pasini, D., Olivero, D., Campaner, S., Sabò, A., Amati, B., 2020. Cooperation Between MYC and β -Catenin in Liver Tumorigenesis Requires Yap/Taz. *Hepatology* 72, 1430. [h](#)

Blencowe, B.J., Issner, R., Nickerson, J.A., Sharp, P.A., 1998. A coactivator of pre-mRNA splicing. *Genes Dev.* 12, 996-1009.

Bohnsack, K.E., Ficner, R., Bohnsack, M.T., Jonas, S., 2021. Regulation of DEAD-box RNA helicases by G-patch proteins. *Biological Chemistry* 402, 561-579.

Bollati, M., Milani, M., Mastrangelo, E., Ricagno, S., Tedeschi, G., Nonnis, S., Decroly, E., Selisko, B., De Lamballerie, X., Coutard, B., Canard, B., Bolognesi, M., 2009. Recognition of RNA Cap in the Wesselsbron Virus NS5 Methyltransferase Domain: Implications for RNA-Capping Mechanisms in Flavivirus. *Journal of Molecular Biology* 385, 140-152.

Bork, P., Sudol, M., 1994. The WW domain: a signalling site in dystrophin? *Trends Biochem Sci* 19, 531-533.

Bouloy, M., Plotch, S.J., Krug, R.M., 1980. Both the 7-methyl and the 2'-O-methyl groups in the cap of mRNA strongly influence its ability to act as primer for influenza virus RNA transcription. *Proc Natl Acad Sci U S A* 77, 3952-3956.

Boya, P., Larrea, E., Sola, I., Majano, P.L., Jiménez, C., Civeira, M.P., Prieto, J., 2001. Nuclear factor-kappa B in the liver of patients with chronic hepatitis C: decreased RelA expression is associated with enhanced fibrosis progression. *Hepatology* 34, 1041-1048.

Brawerman, G., 1981. The Role of the Poly(A) Sequence in Mammalian Messenger RN. *Critical Reviews in Biochemistry* 10, 1-38.

Brito Querido, J., Díaz-López, I., Ramakrishnan, V., 2024a. The molecular basis of translation initiation and its regulation in eukaryotes. *Nat Rev Mol Cell Biol* 25, 168-186.

Brito Querido, J., Sokabe, M., Díaz-López, I., Gordiyenko, Y., Fraser, C.S., Ramakrishnan, V., 2024b. The structure of a human translation initiation complex reveals two independent roles for the helicase eIF4A. *Nat Struct Mol Biol* 31, 455-464.

Bujnicki, J.M., 1999. Comparison of protein structures reveals monophyletic origin of the AdoMet-dependent methyltransferase family and mechanistic convergence rather than recent differentiation of N4-cytosine and N6-adenine DNA methylation. *In Silico Biol* 1, 175-182.

Buratowski, S., 2009. Progression through the RNA Polymerase II CTD Cycle. *Molecular Cell* 36, 541-546.

Byszewska, M., Śmietański, M., Purta, E., Bujnicki, J.M., 2015. RNA methyltransferases involved in 5' cap biosynthesis. *RNA Biol* 11, 1597-1607.

Campeanu, I.J., Jiang, Y., Afisllari, H., Dzinic, S., Polin, L., Yang, Z.-Q., 2024. Multi-omics analysis reveals CMTR1 upregulation in cancer and roles in ribosomal protein gene expression and tumor growth.

Cantoni, G.L., Chiang, P.K., 1980. The Role of S-Adenosylhomocysteine and S-Adenosylhomocysteine Hydrolase in the Control of Biological Methylations, in: Cavallini, D., Gaull, G.E., Zappia, V. (Eds.), *Natural Sulfur Compounds: Novel Biochemical and Structural Aspects*. Springer US, Boston, MA, pp. 67-80.

Castello, A., Fischer, B., Eichelbaum, K., Horos, R., Beckmann, B.M., Strein, C., Davey, N.E., Humphreys, D.T., Preiss, T., Steinmetz, L.M., Krijgsveld, J., Hentze,

M.W., 2012. Insights into RNA Biology from an Atlas of Mammalian mRNA-Binding Proteins. *Cell* 149, 1393-1406.

Cevik, D., Yildiz, G., Ozturk, M., 2015. Common telomerase reverse transcriptase promoter mutations in hepatocellular carcinomas from different geographical locations. *World J Gastroenterol* 21, 311-317.

Chaikuad, A., Filippakopoulos, P., Marcisin, S.R., Picaud, S., Schröder, M., Sekine, S., Ichijo, H., Engen, J.R., Takeda, K., Knapp, S., 2017. Structures of PGAM5 Provide Insight into Active Site Plasticity and Multimeric Assembly. *Structure* 25, 1089-1099.e3.

Chang, L.-C., Fan, C.-W., Tseng, W.-K., Chein, H.-P., Hsieh, T.-Y., Chen, J.-R., Hwang, C.-C., Hua, C.-C., 2017. The ratio of thioredoxin/Keap1 protein level is a predictor of distant metastasis in colorectal cancer. *Biomarkers in Medicine* 11, 1103-1111.

Chang, M.H., Chen, C.J., Lai, M.S., Hsu, H.M., Wu, T.C., Kong, M.S., Liang, D.C., Shau, W.Y., Chen, D.S., 1997. Universal hepatitis B vaccination in Taiwan and the incidence of hepatocellular carcinoma in children. Taiwan Childhood Hepatoma Study Group. *N Engl J Med* 336, 1855-1859.

Chen, G., Han, Z., Feng, D., Chen, Y., Chen, L., Wu, H., Huang, L., Zhou, C., Cai, X., Fu, C., Duan, L., Wang, X., Liu, L., Liu, X., Shen, Y., Zhu, Y., Chen, Q., 2014. A Regulatory Signaling Loop Comprising the PGAM5 Phosphatase and CK2 Controls Receptor-Mediated Mitophagy. *Molecular Cell* 54, 362-377.

Chen, H.I., Sudol, M., 1995. The WW domain of Yes-associated protein binds a proline-rich ligand that differs from the consensus established for Src homology 3-binding modules. *Proc Natl Acad Sci U S A* 92, 7819-7823.

Cheng, A.-L., Kang, Y.-K., Chen, Z., Tsao, C.-J., Qin, S., Kim, J.S., Luo, R., Feng, J., Ye, S., Yang, T.-S., Xu, J., Sun, Y., Liang, H., Liu, J., Wang, J., Tak, W.Y., Pan, H., Burock, K., Zou, J., Voliotis, D., Guan, Z., 2009. Efficacy and safety of

sorafenib in patients in the Asia-Pacific region with advanced hepatocellular carcinoma: a phase III randomised, double-blind, placebo-controlled trial. *Lancet Oncol* 10, 25-34.

Cheng, B., Price, D.H., 2007. Properties of RNA polymerase II elongation complexes before and after the P-TEFb-mediated transition into productive elongation. *J Biol Chem* 282, 21901-21912.

Chen, C.-Y.A., Shyu, A.-B., 2011. Mechanisms of deadenylation-dependent decay. *WIREs RNA* 2, 167-183.

Cheng, H., Dufu, K., Lee, C.-S., Hsu, J.L., Dias, A., Reed, R., 2006. Human mRNA Export Machinery Recruited to the 5' End of mRNA. *Cell* 127, 1389-1400.

Cheng, J., Qian, D., Ding, X., Song, T., Cai, M., Dan Xie, Wang, Y., Zhao, J., Liu, Z., Wu, Z., Pang, Q., Zhu, L., Wang, P., Hao, X., Yuan, Z., 2018. High PGAM5 expression induces chemoresistance by enhancing Bcl-xL-mediated anti-apoptotic signaling and predicts poor prognosis in hepatocellular carcinoma patients. *Cell Death Dis* 9, 1-16.

Chew, V., Tow, C., Teo, M., Wong, H.L., Chan, J., Gehring, A., Loh, M., Bolze, A., Quek, R., Lee, V.K.M., Lee, K.H., Abastado, J.-P., Toh, H.C., Nardin, A., 2010. Inflammatory tumour microenvironment is associated with superior survival in hepatocellular carcinoma patients. *Journal of Hepatology* 52, 370-379.

Chiu, Y.L., Coronel, E., Ho, C.K., Shuman, S., Rana, T.M., 2001. HIV-1 Tat protein interacts with mammalian capping enzyme and stimulates capping of TAR RNA. *J Biol Chem* 276, 12959-12966.

Cho, E.-J., Kobor, M.S., Kim, M., Greenblatt, J., Buratowski, S., 2001. Opposing effects of Ctk1 kinase and Fcp1 phosphatase at Ser 2 of the RNA polymerase II C-terminal domain. *Genes Dev.* 15, 3319-3329.

Cho, E.-J., Takagi, T., Moore, C.R., Buratowski, S., 1997. mRNA capping enzyme is recruited to the transcription complex by phosphorylation of the RNA polymerase II carboxy-terminal domain. *Genes Dev* 11, 3319-3326.

Cho, H., Han, S., Choe, J., Park, S.G., Choi, S.S., Kim, Y.K., 2013. SMG5-PNRC2 is functionally dominant compared with SMG5-SMG7 in mammalian nonsense-mediated mRNA decay. *Nucleic Acids Research* 41, 1319-1328.

Clark, K., Peggie, M., Plater, L., Sorcek, R.J., Young, E.R.R., Madwed, J.B., Hough, J., McIver, E.G., Cohen, P., 2011. Novel cross-talk within the IKK family controls innate immunity. *Biochemical Journal* 434, 93-104.

Clerx, J.P., Fuller, F., Bishop, D.H., 1983. Tick-borne viruses structurally similar to Orthomyxoviruses. *Virology* 127, 205-219.

Cole, M.D., Cowling, V.H., 2009. Specific regulation of mRNA cap methylation by the c-Myc and E2F1 transcription factors. *Oncogene* 28, 1169-1175.

Correa, P., 1995. Helicobacter pylori and gastric carcinogenesis. *Am J Surg Pathol* 19 Suppl 1, S37-43.

Cougot, N., Babajko, S., Séraphin, B., 2004. Cytoplasmic foci are sites of mRNA decay in human cells. *J Cell Biol* 165, 31-40.

Coussens, L.M., Werb, Z., 2002. Inflammation and cancer. *Nature* 420, 860-867.

Covelo-Molares, H., Obrdlik, A., Poštulková, I., Dohnálková, M., Gregorová, P., Ganji, R., Potěšil, D., Gawriyski, L., Varjosalo, M., Vaňáčková, Š., 2021. The comprehensive interactomes of human adenosine RNA methyltransferases and demethylases reveal distinct functional and regulatory features. *Nucleic Acids Research* 49, 10895-10910.

Cowling, V.H., 2010. Enhanced mRNA cap methylation increases Cyclin D1 expression and promotes cell transformation. *Oncogene* 29, 930-936.

Cowling, V.H., Cole, M.D., 2007. The Myc Transactivation Domain Promotes Global Phosphorylation of the RNA Polymerase II Carboxy-Terminal Domain Independently of Direct DNA Binding. *Mol Cell Biol* 27, 2059-2073.

Cox, J., Mann, M., 2008. MaxQuant enables high peptide identification rates, individualized p.p.b.-range mass accuracies and proteome-wide protein quantification. *Nat Biotechnol* 26, 1367-1372.

Cox, J., Neuhauser, N., Michalski, A., Scheltema, R.A., Olsen, J.V., Mann, M., 2011. Andromeda: A Peptide Search Engine Integrated into the MaxQuant Environment. *J. Proteome Res.* 10, 1794-1805.

Cui, S., Eisenächer, K., Kirchhofer, A., Brzózka, K., Lammens, A., Lammens, K., Fujita, T., Conzelmann, K.-K., Krug, A., Hopfner, K.-P., 2008. The C-Terminal Regulatory Domain Is the RNA 5'-Triphosphate Sensor of RIG-I. *Molecular Cell* 29, 169-179.

Culjkovic, B., Topisirovic, I., Skrabanek, L., Ruiz-Gutierrez, M., Borden, K.L.B., 2005. eIF4E promotes nuclear export of cyclin D1 mRNAs via an element in the 3'UTR. *J Cell Biol* 169, 245-256.

Culjkovic-Kraljacic, B., Skrabanek, L., Revuelta, M.V., Gasiorek, J., Cowling, V.H., Cerchietti, L., Borden, K.L.B., 2020. The eukaryotic translation initiation factor eIF4E elevates steady-state m7G capping of coding and noncoding transcripts. *Proceedings of the National Academy of Sciences* 117, 26773-26783.

Dadonaite, B., Gilbertson, B., Knight, M.L., Trifkovic, S., Rockman, S., Laederach, A., Brown, L.E., Fodor, E., Bauer, D.L.V., 2019. The structure of the influenza A virus genome. *Nat Microbiol* 4, 1781-1789.

Daffis, S., Szretter, K.J., Schriewer, J., Li, J., Youn, S., Errett, J., Lin, T.-Y., Schneller, S., Zust, R., Dong, H., Thiel, V., Sen, G.C., Fensterl, V., Klimstra, W.B., Pierson, T.C., Buller, R.M., Gale Jr, M., Shi, P.-Y., Diamond, M.S., 2010. 2'-O methylation of the viral mRNA cap evades host restriction by IFIT family members. *Nature* 468, 452-456.

Dahlin, A., Denny, J., Roden, D.M., Brilliant, M.H., Ingram, C., Kitchner, T.E., Linneman, J.G., Shaffer, C.M., Weeke, P., Xu, H., Kubo, M., Tamari, M., Clemmer, G.L., Ziniti, J., McGeachie, M.J., Tantisira, K.G., Weiss, S.T., Wu, A.C., 2015. CMTR1 is associated with increased asthma exacerbations in patients taking inhaled corticosteroids. *Immunity, Inflammation and Disease* 3, 350-359.

Daksis, J.I., Lu, R.Y., Facchini, L.M., Marhin, W.W., Penn, L.J., 1994. Myc induces cyclin D1 expression in the absence of de novo protein synthesis and links mitogen-stimulated signal transduction to the cell cycle. *Oncogene* 9, 3635-3645.

Daneholt, B., 2001. Assembly and transport of a premessenger RNP particle. *Proceedings of the National Academy of Sciences* 98, 7012-7017.

Daugherty, M.D., Schaller, A.M., Geballe, A.P., Malik, H.S., 2016. Evolution-guided functional analyses reveal diverse antiviral specificities encoded by IFIT1 genes in mammals. *eLife* 5, e14228.

D'Cunha, J., Knight, E., Haas, A.L., Truitt, R.L., Borden, E.C., 1996. Immunoregulatory properties of ISG15, an interferon-induced cytokine. *Proc Natl Acad Sci U S A* 93, 211-215.

De la Peña, M., Kyrieleis, O.J.P., Cusack, S., 2007. Structural insights into the mechanism and evolution of the vaccinia virus mRNA cap N7 methyl-transferase. *EMBO J* 26, 4913-4925.

De Martel, C., Maucort-Boulch, D., Plummer, M., Franceschi, S., 2015. World-wide relative contribution of hepatitis B and C viruses in hepatocellular carcinoma. *Hepatology* 62, 1190-1200.

De Veer, M.J., Holko, M., Frevel, M., Walker, E., Der, S., Paranjape, J.M., Silverman, R.H., Williams, B.R., 2001. Functional classification of interferon-stimulated genes identified using microarrays. *J Leukoc Biol* 69, 912-920.

Deane, N.G., Parker, M.A., Aramandla, R., Diehl, L., Lee, W.-J., Washington, M.K., Nanney, L.B., Shyr, Y., Beauchamp, R.D., 2001. Hepatocellular Carcinoma Results from Chronic Cyclin D1 Overexpression in Transgenic Mice¹. *Cancer Research* 61, 5389-5395.

Decroly, E., Canard, B., 2017. Biochemical principles and inhibitors to interfere with viral capping pathways. *Curr Opin Virol* 24, 87-96.

Decroly, E., Ferron, F., Lescar, J., Canard, B., 2012. Conventional and unconventional mechanisms for capping viral mRNA. *Nat Rev Microbiol* 10, 51-65.

Despic, V., Jaffrey, S.R., 2023. mRNA ageing shapes the Cap2 methylome in mammalian mRNA. *Nature* 614, 358-366.

Devarkar, S.C., Wang, C., Miller, M.T., Ramanathan, A., Jiang, F., Khan, A.G., Patel, S.S., Marcotrigiano, J., 2016. Structural basis for m7G recognition and 2'-O-methyl discrimination in capped RNAs by the innate immune receptor RIG-I. *Proc Natl Acad Sci U S A* 113, 596-601.

Devhare, P.B., Desai, S., Lole, K.S., 2016. Innate immune responses in human hepatocyte-derived cell lines alter genotype 1 hepatitis E virus replication efficiencies. *Sci Rep* 6, 26827.

Dhanasekaran, R., Deutzmann, A., Mahauad-Fernandez, W.D., Hansen, A.S., Gouw, A.M., Felsher, D.W., 2022. The MYC oncogene – the grand orchestrator of cancer growth and immune evasion. *Nat Rev Clin Oncol* 19, 23-36.

Di Blasi, R., Marbiah, M.M., Siciliano, V., Polizzi, K., Ceroni, F., 2021. A call for caution in analysing mammalian co-transfection experiments and implications of resource competition in data misinterpretation. *Nat Commun* 12, 2545.

Diamond, M.S., Kinder, M., Matsushita, H., Mashayekhi, M., Dunn, G.P., Archambault, J.M., Lee, H., Arthur, C.D., White, J.M., Kalinke, U., Murphy, K.M., Schreiber, R.D., 2011. Type I interferon is selectively required by dendritic cells for immune rejection of tumors. *Journal of Experimental Medicine* 208, 1989-2003.

Diao, J., Garces, R., Richardson, C.D., 2001. X protein of hepatitis B virus modulates cytokine and growth factor related signal transduction pathways during the course of viral infections and hepatocarcinogenesis. *Cytokine & Growth Factor Reviews* 12, 189-205.

Diebold, S.S., Kaisho, T., Hemmi, H., Akira, S., Reis e Sousa, C., 2004. Innate Antiviral Responses by Means of TLR7-Mediated Recognition of Single-Stranded RNA. *Science* 303, 1529-1531.

Dohnalkova, M., Krasnykov, K., Mendel, M., Li, L., Panasenko, O., Fleury-Olela, F., Vågbø, C.B., Homolka, D., Pillai, R.S., 2023. Essential roles of RNA cap-proximal ribose methylation in mammalian embryonic development and fertility. *Cell Reports* 42, 112786.

Dong, X.-Y., Liu, W.-J., Zhao, M.-Q., Wang, J.-Y., Pei, J.-J., Luo, Y.-W., Ju, C.-M., Chen, J.-D., 2013. Classical swine fever virus triggers RIG-I and MDA5-dependent signaling pathway to IRF-3 and NF- κ B activation to promote secretion of interferon and inflammatory cytokines in porcine alveolar macrophages. *Virology* 453, 279-286.

Drummond, D.R., Armstrong, J., Colman, A., 1985. The effect of capping and polyadenylation on the stability, movement and translation of synthetic messenger RNAs in *Xenopus* oocytes. *Nucleic Acids Res* 13, 7375-7394.

Du, X., Shao, Y., Gao, H., Zhang, X., Zhang, H., Ban, Y., Qin, H., Tai, Y., 2018. CMTR1-ALK: an ALK fusion in a patient with no response to ALK inhibitor crizotinib. *Cancer Biol Ther* 19, 962-966.

Du, Y., Duan, T., Feng, Y., Liu, Q., Lin, M., Cui, J., Wang, R.-F., 2018. LRRC25 inhibits type I IFN signaling by targeting ISG15-associated RIG-I for autophagic degradation. *EMBO J* 37, 351-366.

Duewell, P., Steger, A., Lohr, H., Bourhis, H., Hoelz, H., Kirchleitner, S.V., Stieg, M.R., Grassmann, S., Kobold, S., Siveke, J.T., Endres, S., Schnurr, M., 2014. RIG-I-like helicases induce immunogenic cell death of pancreatic cancer cells and sensitize tumors toward killing by CD8⁺ T cells. *Cell Death Differ* 21, 1825-1837.

Eberle, A.B., Lykke-Andersen, S., Mühlemann, O., Jensen, T.H., 2009. SMG6 promotes endonucleolytic cleavage of nonsense mRNA in human cells. *Nat Struct Mol Biol* 16, 49-55.

Egloff, M., Benarroch, D., Selisko, B., Romette, J., Canard, B., 2002. An RNA cap (nucleoside-2'-O-)-methyltransferase in the flavivirus RNA polymerase NS5: crystal structure and functional characterization. *The EMBO Journal* 21, 2757-2768.

Ekbom Anders, Helmick Charles, Zack Matthew, Adami Hans-Olov, 1990. Ulcerative Colitis and Colorectal Cancer. *New England Journal of Medicine* 323, 1228-1233.

Enomoto, H., Tao, L., Eguchi, R., Sato, A., Honda, M., Kaneko, S., Iwata, Y., Nishikawa, H., Imanishi, H., Iijima, H., Tsujimura, T., Nishiguchi, S., 2017. The in vivo antitumor effects of type I-interferon against hepatocellular carcinoma: the suppression of tumor cell growth and angiogenesis. *Sci Rep* 7, 12189.

Fan, H., Sakuraba, K., Komuro, A., Kato, S., Harada, F., Hirose, Y., 2003. PCIF1, a novel human WW domain-containing protein, interacts with the phosphorylated RNA polymerase II. *Biochemical and Biophysical Research Communications* 301, 378-385.

Fan, J.-B., Arimoto, K., Motamedchaboki, K., Yan, M., Wolf, D.A., Zhang, D.-E., 2015. Identification and characterization of a novel ISG15-ubiquitin mixed chain and its role in regulating protein homeostasis. *Sci Rep* 5, 12704.

Fang, R., Jiang, Q., Zhou, X., Wang, C., Guan, Y., Tao, J., Xi, J., Feng, J.-M., Jiang, Z., 2017. MAVS activates TBK1 and IKK ϵ through TRAFs in NEMO dependent and independent manner. *PLoS Pathog* 13, e1006720.

Feng, Q., Hato, S.V., Langereis, M.A., Zoll, J., Virgen-Slane, R., Peisley, A., Hur, S., Semler, B.L., van Rij, R.P., van Kuppeveld, F.J.M., 2012. MDA5 detects the double-stranded RNA replicative form in picornavirus-infected cells. *Cell Rep* 2, 1187-1196.

Fernandez-Sanchez, M.E., Gonatopoulos-Pournatzis, T., Preston, G., Lawlor, M.A., Cowling, V.H., 2009. S-Adenosyl Homocysteine Hydrolase Is Required for Myc-Induced mRNA Cap Methylation, Protein Synthesis, and Cell Proliferation. *Molecular and Cellular Biology* 29, 6182-6191.

Fitzgerald, K.A., McWhirter, S.M., Faia, K.L., Rowe, D.C., Latz, E., Golenbock, D.T., Coyle, A.J., Liao, S.-M., Maniatis, T., 2003. IKK ϵ and TBK1 are essential components of the IRF3 signaling pathway. *Nat Immunol* 4, 491-496.

Flaherty, S.M., Fortes, P., Izaurralde, E., Mattaj, I.W., Gilmartin, G.M., 1997. Participation of the nuclear cap binding complex in pre-mRNA 3' processing. *Proc Natl Acad Sci U S A* 94, 11893-11898.

Fleith, R.C., Mears, H.V., Leong, X.Y., Sanford, T.J., Emmott, E., Graham, S.C., Mansur, D.S., Sweeney, T.R., 2018. IFIT3 and IFIT2/3 promote IFIT1-mediated translation inhibition by enhancing binding to non-self RNA. *Nucleic Acids Research* 46, 5269-5285.

Foster, G.R., Rodrigues, O., Ghouze, F., Schulte-Frohlinde, E., Testa, D., Liao, M.J., Stark, G.R., Leadbeater, L., Thomas, H.C., 1996. Different Relative Activities

of Human Cell-Derived Interferon- α Subtypes: IFN- α 8 Has Very High Antiviral Potency. *Journal of Interferon & Cytokine Research* 16, 1027-1033.

Fothergill-Gilmore, L.A., Watson, H.C., 1989. The phosphoglycerate mutases. *Adv Enzymol Relat Areas Mol Biol* 62, 227-313.

Fox, L.E., Locke, M.C., Lenschow, D.J., 2020. Context Is Key: Delineating the Unique Functions of IFN α and IFN β in Disease. *Front. Immunol.* 11.

Fu, X.Y., Kessler, D.S., Veals, S.A., Levy, D.E., Darnell, J.E., 1990. ISGF3, the transcriptional activator induced by interferon alpha, consists of multiple interacting polypeptide chains. *Proc Natl Acad Sci U S A* 87, 8555-8559.

Fuchs, J., Lamkiewicz, K., Kolesnikova, L., Hölzer, M., Marz, M., Kochs, G., 2022. Comparative Study of Ten Thogotovirus Isolates and Their Distinct In Vivo Characteristics. *Journal of Virology* 96, e01556-21.

Fukumoto, K., Ito, K., Saer, B., Taylor, G., Ye, S., Yamano, M., Toriba, Y., Hayes, A., Okamura, H., Fustin, J.-M., 2022. Excess S-adenosylmethionine inhibits methylation via catabolism to adenine. *Commun Biol* 5, 313.

Fukushi, S., Katayama, K., Kurihara, C., Ishiyama, N., Hoshino, F.B., Ando, T., Oya, A., 1994. Complete 5' Noncoding Region Is Necessary for the Efficient Internal Initiation of Hepatitis C Virus RNA. *Biochemical and Biophysical Research Communications* 199, 425-432.

Fukuyama, S., Katsura, H., Zhao, D., Ozawa, M., Ando, T., Shoemaker, J.E., Ishikawa, I., Yamada, S., Neumann, G., Watanabe, S., Kitano, H., Kawaoka, Y., 2015. Multi-spectral fluorescent reporter influenza viruses (Color-flu) as powerful tools for in vivo studies. *Nat Commun* 6, 6600.

Furuichi, Y., Morgan, M., Shatkin, A.J., Jelinek, W., Salditt-Georgieff, M., Darnell, J.E., 1975. Methylated, blocked 5 termini in HeLa cell mRNA. *Proceedings of the National Academy of Sciences* 72, 1904-1908.

Gaillard, H., García-Muse, T., Aguilera, A., 2015. Replication stress and cancer. *Nat Rev Cancer* 15, 276-289.

Galloway, A., Atrih, A., Grzela, R., Darzynkiewicz, E., Ferguson, M.A.J., Cowling, V.H., 2020. CAP-MAP: cap analysis protocol with minimal analyte processing, a rapid and sensitive approach to analysing mRNA cap structures. *Open Biology* 10, 190306.

Galloway, A., Kaskar, A., Ditsova, D., Atrih, A., Yoshikawa, H., Gomez-Moreira, C., Suska, O., Warminski, M., Grzela, R., Lamond, A.I., Darzynkiewicz, E., Jemielity, J., Cowling, V.H., 2021. Upregulation of RNA cap methyltransferase RNMT drives ribosome biogenesis during T cell activation. *Nucleic Acids Res* 49, 6722-6738.

Gao, B., Bataller, R., 2011. Alcoholic Liver Disease: Pathogenesis and New Therapeutic Targets. *Gastroenterology* 141, 1572-1585.

Gao, C., Wang, Y., Broaddus, R., Sun, L., Xue, F., Zhang, W., 2017. Exon 3 mutations of CTNNB1 drive tumorigenesis: a review. *Oncotarget* 9, 5492-5508. <https://doi.org/10.18632/oncotarget.23695>

Gao, M., Fritz, D.T., Ford, L.P., Wilusz, J., 2000. Interaction between a Poly(A)-Specific Ribonuclease and the 5' Cap Influences mRNA Deadenylation Rates In Vitro. *Molecular Cell* 5, 479-488.

Garcin, D., Lezzi, M., Dobbs, M., Elliott, R.M., Schmaljohn, C., Kang, C.Y., Kolakofsky, D., 1995. The 5' ends of Hantaan virus (Bunyaviridae) RNAs suggest a prime-and-realign mechanism for the initiation of RNA synthesis. *Journal of Virology* 69, 5754-5762.

Garg, G., Dienemann, C., Farnung, L., Schwarz, J., Linden, A., Urlaub, H., Cramer, P., 2023. Structural insights into human co-transcriptional capping. *Molecular Cell* 83, 2464-2477.e5.

Gavva, N.R., Gavva, R., Ermekova, K., Sudol, M., Shen, C.-K.J., 1997. Interaction of WW Domains with Hematopoietic Transcription Factor p45/NF-E2 and RNA Polymerase II *. *Journal of Biological Chemistry* 272, 24105-24108.

Gekas, C., D'Altri, T., Aligué, R., González, J., Espinosa, L., Bigas, A., 2016. B-Catenin is required for T-cell leukemia initiation and MYC transcription downstream of Notch1. *Leukemia* 30, 2002-2010.

Geng, J., Chrabaszczewska, M., Kurpiejewski, K., Stankiewicz-Drogon, A., Jankowska-Anyszka, M., Darzynkiewicz, E., Grzela, R., 2024. Cap-related modifications of RNA regulate binding to IFIT proteins. *RNA* rna.080011.124.

Ghose, C., Raushel, F.M., 1985. Determination of the mechanism of the argininosuccinate synthetase reaction by static and dynamic quench experiments. *Biochemistry* 24, 5894-5898.

Gibson, S.A., Yang, W., Yan, Z., Liu, Y., Rowse, A.L., Weinmann, A.S., Qin, H., Benveniste, E.N., 2017. Protein Kinase CK2 Controls the Fate between Th17 Cell and Regulatory T Cell Differentiation. *The Journal of Immunology* 198, 4244-4254.

Gillian-Daniel, D.L., Gray, N.K., Aström, J., Barkoff, A., Wickens, M., 1998. Modifications of the 5' cap of mRNAs during *Xenopus* oocyte maturation: independence from changes in poly(A) length and impact on translation. *Mol Cell Biol* 18, 6152-6163.

Gonatopoulos-Pournatzis, T., Dunn, S., Bounds, R., Cowling, V.H., 2011. RAM/Fam103a1 Is Required for mRNA Cap Methylation. *Molecular Cell* 44, 585.

Goto, M., Omi, R., Miyahara, I., Sugahara, M., Hirotsu, K., 2003. Structures of Argininosuccinate Synthetase in Enzyme-ATP Substrates and Enzyme-AMP Product Forms. *Journal of Biological Chemistry* 278, 22964-22971.

Gouas, D., Shi, H., Hainaut, P., 2009. The aflatoxin-induced TP53 mutation at codon 249 (R249S): Biomarker of exposure, early detection and target for therapy. *Cancer Letters, Hepatocellular - A Worldwide Translational Approach* 286, 29-37.

Goubau, D., Schlee, M., Deddouche, S., Pruijssers, A.J., Zillinger, T., Goldeck, M., Schuberth, C., Van der Veen, A.G., Fujimura, T., Rehwinkel, J., Iskarpatyoti, J.A., Barchet, W., Ludwig, J., Dermody, T.S., Hartmann, G., Reis e Sousa, C., 2014. Antiviral immunity via RIG-I-mediated recognition of RNA bearing 5'-diphosphates. *Nature* 514, 372-375.

Grochowski, M., Lipińska-Zubrycka, L., Townsend, S., Golisz-Mocydlarz, A., Zakrzewska-Płaczek, M., Brzyżek, G., Jurković, B., Świeżewski, S., Ralser, M., Małecki, M., 2024. Uridylation regulates mRNA decay directionality in fission yeast. *Nat Commun* 15, 8359.

Groelly, F.J., Fawkes, M., Dagg, R.A., Blackford, A.N., Tarsounas, M., 2023. Targeting DNA damage response pathways in cancer. *Nat Rev Cancer* 23, 78-94.

Grosso, A.R., Leite, A.P., Carvalho, S., Matos, M.R., Martins, F.B., Vítor, A.C., Desterro, J.M., Carmo-Fonseca, M., de Almeida, S.F., n.d. Pervasive transcription read-through promotes aberrant expression of oncogenes and RNA chimeras in renal carcinoma. *eLife* 4, e09214.

Grudzien-Nogalska, E., Kiledjian, M., 2017. New insights into decapping enzymes and selective mRNA decay. *Wiley Interdiscip Rev RNA* 8.

Gu, W., Gallagher, G.R., Dai, W., Liu, P., Li, R., Trombly, M.I., Gammon, D.B., Mello, C.C., Wang, J.P., Finberg, R.W., 2015. Influenza A virus preferentially snatches noncoding RNA caps. *RNA* 21, 2067-2075.

Guerra, S., López-Fernández, L.A., Pascual-Montano, A., Muñoz, M., Harshman, K., Esteban, M., 2003. Cellular gene expression survey of vaccinia virus infection of human HeLa cells. *Journal of Virology* 77, 6493-6506.

Guilligay, D., Tarendeau, F., Resa-Infante, P., Coloma, R., Crepin, T., Sehr, P., Lewis, J., Ruigrok, R.W.H., Ortin, J., Hart, D.J., Cusack, S., 2008. The structural basis for cap binding by influenza virus polymerase subunit PB2. *Nat Struct Mol Biol* 15, 500-506.

Guilligay, D., Kadlec, J., Crépin, T., Lunardi, T., Bouvier, D., Kochs, G., Ruigrok, R.W.H., Cusack, S., 2014. Comparative Structural and Functional Analysis of Orthomyxovirus Polymerase Cap-Snatching Domains. *PLOS ONE* 9, e84973.

Haberle, V., Stark, A., 2018. Eukaryotic core promoters and the functional basis of transcription initiation. *Nat Rev Mol Cell Biol* 19, 621-637.

Habjan, M., Hubel, P., Lacerda, L., Benda, C., Holze, C., Eberl, C.H., Mann, A., Kindler, E., Gil-Cruz, C., Ziebuhr, J., Thiel, V., Pichlmair, A., 2013. Sequestration by IFIT1 Impairs Translation of 2'O-unmethylated Capped RNA. *PLOS Pathogens* 9, e1003663.

Haline-Vaz, T., Lima Silva, T.C., Zanchin, N.I.T., 2008. The human interferon-regulated ISG95 protein interacts with RNA polymerase II and shows methyltransferase activity. *Biochemical and Biophysical Research Communications* 372, 719-724.

Halpern, K.B., Shenhav, R., Matcovitch-Natan, O., Toth, B., Lemze, D., Golan, M., Massasa, E.E., Baydatch, S., Landen, S., Moor, A.E., Brandis, A., Giladi, A., Avihail, A.S., David, E., Amit, I., Itzkovitz, S., 2017. Single-cell spatial reconstruction reveals global division of labour in the mammalian liver. *Nature* 542, 352-356.

Hampsey, M., 1998. Molecular genetics of the RNA polymerase II general transcriptional machinery. *Microbiol Mol Biol Rev* 62, 465-503.

Hanahan, D., Weinberg, R.A., 2011. Hallmarks of Cancer: The Next Generation. *Cell* 144, 646-674.

Harada, N., Miyoshi, H., Murai, N., Oshima, H., Tamai, Y., Oshima, M., Taketo, M.M., 2002. Lack of tumorigenesis in the mouse liver after adenovirus-mediated expression of a dominant stable mutant of β -catenin. *Cancer Research* 62, 1971-1977.

Hart, R.P., McDevitt, M.A., Nevins, J.R., 1985. Poly(A) site cleavage in a HeLa nuclear extract is dependent on downstream sequences. *Cell* 43, 677-683.

Hausmann, I.U., Wu, Y., Nallasivan, M.P., Archer, N., Bodi, Z., Hebenstreit, D., Waddell, S., Fray, R., Soller, M., 2022. CMT_r cap-adjacent 2'-O-ribose mRNA methyltransferases are required for reward learning and mRNA localization to synapses. *Nat Commun* 13, 1209.

He, F., Jacobson, A., 2015. Control of mRNA decapping by positive and negative regulatory elements in the Dcp2 C-terminal domain. *RNA* 21, 1633-1647.

He, S., Tang, S., 2020. WNT/ β -catenin signaling in the development of liver cancers. *Biomedicine & Pharmacotherapy* 132, 110851.

He, T.C., Sparks, A.B., Rago, C., Hermeking, H., Zawel, L., da Costa, L.T., Morin, P.J., Vogelstein, B., Kinzler, K.W., 1998. Identification of c-MYC as a target of the APC pathway. *Science* 281, 1509-1512.

He, Y., Andersen, G.R., Nielsen, K.H., 2010. Structural basis for the function of DEAH helicases. *EMBO Rep* 11, 180-186.

Heinrichsdorff, J., Luedde, T., Perdiguero, E., Nebreda, A.R., Pasparakis, M., 2008. p38 alpha MAPK inhibits JNK activation and collaborates with I κ B kinase 2 to prevent endotoxin-induced liver failure. *EMBO Rep* 9, 1048-1054.

Hentze, M.W., Preiss, T., 2010. The REM phase of gene regulation. *Trends in Biochemical Sciences* 35, 423-426.

Hinnebusch, A.G., Lorsch, J.R., 2012. The Mechanism of Eukaryotic Translation Initiation: New Insights and Challenges. *Cold Spring Harb Perspect Biol* 4, a011544.

Hirose, Y., Iwamoto, Y., Sakuraba, K., Yunokuchi, I., Harada, F., Ohkuma, Y., 2008. Human phosphorylated CTD-interacting protein, PCIF1, negatively modulates gene expression by RNA polymerase II. *Biochemical and Biophysical Research Communications* 369, 449-455.

Hirose, Y., Manley, J.L., 1998. RNA polymerase II is an essential mRNA polyadenylation factor. *Nature* 395, 93-96.

Hirsch, R.C., Lavine, J.E., Chang, L.J., Varmus, H.E., Ganem, D., 1990. Polymerase gene products of hepatitis B viruses are required for genomic RNA packaging as well as for reverse transcription. *Nature* 344, 552-555.

Hiscott, J., Pitha, P., Genin, P., Nguyen, H., Heylbroeck, C., Mamane, Y., Algarte, M., Lin, R., 1999. Triggering the interferon response: the role of IRF-3 transcription factor. *J Interferon Cytokine Res* 19, 1-13.

Ho, C.K., Shuman, S., 1999. Distinct Roles for CTD Ser-2 and Ser-5 Phosphorylation in the Recruitment and Allosteric Activation of Mammalian mRNA Capping Enzyme. *Molecular Cell* 3, 405-411.

Ho, C.K., Sriskanda, V., McCracken, S., Bentley, D., Schwer, B., Shuman, S., 1998. The Guanylyltransferase Domain of Mammalian mRNA Capping Enzyme Binds to the Phosphorylated Carboxyl-terminal Domain of RNA Polymerase II *. *Journal of Biological Chemistry* 273, 9577-9585.

Hodel, A.E., Gershon, P.D., Quijcho, F.A., 1998. Structural Basis for Sequence-Nonspecific Recognition of 5'-Capped mRNA by a Cap-Modifying Enzyme. *Molecular Cell* 1, 443-447.

Hoffmeyer, K., Raggioli, A., Rudloff, S., Anton, R., Hierholzer, A., Del Valle, I., Hein, K., Vogt, R., Kemler, R., 2012. Wnt/B-Catenin Signaling Regulates Telomerase in Stem Cells and Cancer Cells. *Science* 336, 1549-1554.

Honda, K., Yanai, H., Negishi, H., Asagiri, M., Sato, M., Mizutani, T., Shimada, N., Ohba, Y., Takaoka, A., Yoshida, N., Taniguchi, T., 2005. IRF-7 is the master regulator of type-I interferon-dependent immune responses. *Nature* 434, 772-777.

Honke, N., Shaabani, N., Zhang, D.-E., Hardt, C., Lang, K.S., 2016. Multiple functions of USP18. *Cell Death Dis* 7, e2444-e2444.

Hopkins, K.C., McLane, L.M., Maqbool, T., Panda, D., Gordesky-Gold, B., Cherry, S., 2013. A genome-wide RNAi screen reveals that mRNA decapping restricts bunyaviral replication by limiting the pools of Dcp2-accessible targets for cap-snatching. *Genes Dev.* 27, 1511-1525.

Hopkins, K.C., Tartell, M.A., Herrmann, C., Hackett, B.A., Taschuk, F., Panda, D., Menghani, S.V., Sabin, L.R., Cherry, S., 2015. Virus-induced translational arrest through 4EBP1/2-dependent decay of 5'-TOP mRNAs restricts viral infection. *Proc Natl Acad Sci U S A* 112, E2920-E2929.

Hou, F., Sun, L., Zheng, H., Skaug, B., Jiang, Q.-X., Chen, Z.J., 2011. MAVS forms functional prion-like aggregates to activate and propagate antiviral innate immune response. *Cell* 146, 448-461.

Hou, G., Chen, L., Liu, G., Li, L., Yang, Y., Yan, H.-X., Zhang, H.-L., Tang, J., Yang, Y.C., Lin, X., Chen, X., Luo, G. Juan, Zhu, Y., Tang, S., Zhang, J., Liu, H., Gu, Q., Zhao, L.-H., Li, Y., Liu, L., Zhou, W., Wang, H., 2017. Aldehyde dehydrogenase-2 (ALDH2) opposes hepatocellular carcinoma progression by regulating AMP-activated protein kinase signaling in mice. *Hepatology* 65, 1628.

Hou, J., Zhou, Y., Zheng, Y., Fan, J., Zhou, W., Ng, I.O.L., Sun, H., Qin, L., Qiu, S., Lee, J.M.F., Lo, C.-M., Man, K., Yang, Yuan, Yang, Yun, Yang, Yingyun, Zhang,

Q., Zhu, X., Li, N., Wang, Zhengxin, Ding, G., Zhuang, S.-M., Zheng, L., Luo, X., Xie, Y., Liang, A., Wang, Zhugang, Zhang, M., Xia, Q., Liang, T., Yu, Y., Cao, X., 2014. Hepatic RIG-I Predicts Survival and Interferon- α Therapeutic Response in Hepatocellular Carcinoma. *Cancer Cell* 25, 49-63.

Hsu, C.-S., Chao, Y.-C., Lin, H.H., Chen, D.-S., Kao, J.-H., 2015. Systematic Review: Impact of Interferon-based Therapy on HCV-related Hepatocellular Carcinoma. *Sci Rep* 5, 9954. H

Hsu, I.C., Tokiwa, T., Bennett, W., Metcalf, R.A., Welsh, J.A., Sun, T., Harris, C.C., 1993. p53 gene mutation and integrated hepatitis B viral DNA sequences in human liver cancer cell lines. *Carcinogenesis* 14, 987-992.

Huang, A., Yang, X.-R., Chung, W.-Y., Dennison, A.R., Zhou, J., 2020. Targeted therapy for hepatocellular carcinoma. *Sig Transduct Target Ther* 5, 1-13.

Huang, D.Q., Mathurin, P., Cortez-Pinto, H., Loomba, R., 2023. Global epidemiology of alcohol-associated cirrhosis and HCC: trends, projections and risk factors. *Nat Rev Gastroenterol Hepatol* 20, 37-49.

Huang, F.W., Hodis, E., Xu, M.J., Kryukov, G.V., Chin, L., Garraway, L.A., 2013. Highly Recurrent TERT Promoter Mutations in Human Melanoma. *Science* 339, 957-959.

Hubstenberger, A., Courel, M., Bénard, M., Souquere, S., Ernoult-Lange, M., Chouaib, R., Yi, Z., Morlot, J.-B., Munier, A., Fradet, M., Daunesse, M., Bertrand, E., Pierron, G., Mozziconacci, J., Kress, M., Weil, D., 2017. P-Body Purification Reveals the Condensation of Repressed mRNA Regulons. *Molecular Cell* 68, 144-157

Hui, D.J., Bhasker, C.R., Merrick, W.C., Sen, G.C., 2003. Viral Stress-inducible Protein p56 Inhibits Translation by Blocking the Interaction of eIF3 with the Ternary Complex eIF2·GTP·Met-tRNAⁱ·. *Journal of Biological Chemistry* 278, 39477-39482.

Huntzinger, E., Kashima, I., Fauser, M., Saulière, J., Izaurralde, E., 2008. SMG6 is the catalytic endonuclease that cleaves mRNAs containing nonsense codons in metazoan. *RNA* 14, 2609-2617.

Huse, K., Böhme, H.-J., Scholz, G.H., 2002. Purification of antibodies by affinity chromatography. *Journal of Biochemical and Biophysical Methods* 51, 217-231.

Hwang, J., Sato, H., Tang, Y., Matsuda, D., Maquat, L.E., 2010. UPF1 Association With the Cap-binding Protein, CBP80, Promotes Nonsense-mediated mRNA Decay at Two Distinct Steps. *Mol Cell* 39, 396-409.

Hwang, S.-P., Denicourt, C., 2024. The impact of ribosome biogenesis in cancer: from proliferation to metastasis. *NAR Cancer* 6, zcae017.

Im, J.H., Duic, I., Yoshimura, S.H., Onomoto, K., Yoneyama, M., Kato, H., Fujita, T., 2023. Mechanisms of length-dependent recognition of viral double-stranded RNA by RIG-I. *Sci Rep* 13, 6318.

Imbalzano, A.N., Kwon, H., Green, M.R., Kingston, R.E., 1994. Facilitated binding of TATA-binding protein to nucleosomal DNA. *Nature* 370, 481-485.

Inesta-Vaquera, F., Chaugule, V.K., Galloway, A., Chandler, L., Rojas-Fernandez, A., Weidlich, S., Peggie, M., Cowling, V.H., 2018. DHX15 regulates CMTR1-dependent gene expression and cell proliferation. *Life Sci Alliance* 1, e201800092.

Ingelfinger, D., Arndt-Jovin, D.J., Lührmann, R., Achsel, T., 2002. The human LSm1-7 proteins colocalize with the mRNA-degrading enzymes Dcp1/2 and Xrn1 in distinct cytoplasmic foci. *RNA* 8, 1489-1501.

Iordanov, M.S., Wong, J., Bell, J.C., Magun, B.E., 2001. Activation of NF- κ B by Double-Stranded RNA (dsRNA) in the Absence of Protein Kinase R and RNase L Demonstrates the Existence of Two Separate dsRNA-Triggered Antiviral Programs. *Mol Cell Biol* 21, 61-72.

Ishikawa, T., 2008. Secondary prevention of recurrence by interferon therapy after ablation therapy for hepatocellular carcinoma in chronic hepatitis C patients. *World J Gastroenterol* 14, 6140-6144.

Ito, S., Koso, H., Sakamoto, K., Watanabe, S., 2017. RNA helicase DHX15 acts as a tumour suppressor in glioma. *Br J Cancer* 117, 1349-1359.

Izaurrealde E, Lewis J, Gamberi C, Jarmolowski A, McGuigan C, Mattaj Iw, 1995. A cap-binding protein complex mediating U snRNA export. *Nature* 376.

Izaurrealde, E., Lewis, J., McGuigan, C., Jankowska, M., Darzynkiewicz, E., Mattaj, I.W., 1994. A nuclear cap binding protein complex involved in pre-mRNA splicing. *Cell* 78, 657-668.

Jain, S., Wheeler, J.R., Walters, R.W., Agrawal, A., Barsic, A., Parker, R., 2016. ATPase modulated stress granules contain a diverse proteome and substructure. *Cell* 164, 487-498.

Jang, M.-A., Kim, E.K., Now, H., Nguyen, N.T.H., Kim, W.-J., Yoo, J.-Y., Lee, J., Jeong, Y.-M., Kim, C.-H., Kim, O.-H., Sohn, S., Nam, S.-H., Hong, Y., Lee, Y.S., Chang, S.-A., Jang, S.Y., Kim, J.-W., Lee, M.-S., Lim, S.Y., Sung, K.-S., Park, K.-T., Kim, B.J., Lee, J.-H., Kim, D.-K., Kee, C., Ki, C.-S., 2015. Mutations in DDX58, which Encodes RIG-I, Cause Atypical Singleton-Merten Syndrome. *The American Journal of Human Genetics* 96, 266-274.

Jensen, P., Patel, B., Smith, S., Sabnis, R., Koboord, B., 2021. Improved Immunoprecipitation to Mass Spectrometry Method for the Enrichment of Low-Abundant Protein Targets, in: Posch, A. (Ed.), *Proteomic Profiling: Methods and Protocols*. Springer US, New York, NY, pp. 229-246.

Jiang, F., Ramanathan, A., Miller, M.T., Tang, G.-Q., Gale, M., Patel, S.S., Marcotrigiano, J., 2011. Structural basis of RNA recognition and activation by innate immune receptor RIG-I. *Nature* 479, 423-427.

Jiang, X., Kinch, L.N., Brautigam, C.A., Chen, X., Du, F., Grishin, N.V., Chen, Z.J., 2012. Ubiquitin-induced oligomerization of the RNA sensors RIG-I and MDA5 activates antiviral innate immune response. *Immunity* 36, 959-973.

Jin, X., Moskophidis, D., Mivechi, N.F., 2011. Heat Shock Transcription Factor 1 Is a Key Determinant of HCC Development by Regulating Hepatic Steatosis and Metabolic Syndrome. *Cell Metabolism* 14, 91-103.

Jinek, M., Coyle, S.M., Doudna, J.A., 2011. Coupled 5' nucleotide recognition and processivity in Xrn1-mediated mRNA decay. *Mol Cell* 41, 600-608.

Johnson, D.E., O'Keefe, R.A., Grandis, J.R., 2018. Targeting the IL-6/JAK/STAT3 signalling axis in cancer. *Nat Rev Clin Oncol* 15, 234-248.

Kalkhof, S., Sinz, A., 2008. Chances and pitfalls of chemical cross-linking with amine-reactive N-hydroxysuccinimide esters. *Anal Bioanal Chem* 392, 305-312.

Kalra, N., Kumar, V., 2006. The X protein of hepatitis B virus binds to the F box protein Skp2 and inhibits the ubiquitination and proteasomal degradation of c-Myc. *FEBS Lett* 580, 431-436.

Kang, D., Gopalkrishnan, R.V., Wu, Q., Jankowsky, E., Pyle, A.M., Fisher, P.B., 2002. mda-5: An interferon-inducible putative RNA helicase with double-stranded RNA-dependent ATPase activity and melanoma growth-suppressive properties. *Proc Natl Acad Sci U S A* 99, 637-642.

Kanwal, F., Kramer, J., Asch, S.M., Chayanupatkul, M., Cao, Y., El-Serag, H.B., 2017. Risk of Hepatocellular Cancer in HCV Patients Treated With Direct-Acting Antiviral Agents. *Gastroenterology* 153, 996-1005.e1.

Karin, M., 1999. How NF- κ B is activated: the role of the I κ B kinase (IKK) complex. *Oncogene* 18, 6867-6874.

Karlberg, T., Collins, R., Van Den Berg, S., Flores, A., Hammarström, M., Högbom, M., Holmberg Schiavone, L., Uppenberg, J., 2008. Structure of human argininosuccinate synthetase. *Acta Crystallographica Section D* 64, 279-286.

Kashima, I., Yamashita, A., Izumi, N., Kataoka, N., Morishita, R., Hoshino, S., Ohno, M., Dreyfuss, G., Ohno, S., 2006. Binding of a novel SMG-1-Upf1-eRF1-eRF3 complex (SURF) to the exon junction complex triggers Upf1 phosphorylation and nonsense-mediated mRNA decay. *Genes Dev* 20, 355-367.

Kato, H., Takeuchi, O., Mikamo-Satoh, E., Hirai, R., Kawai, T., Matsushita, K., Hiiragi, A., Dermody, T.S., Fujita, T., Akira, S., 2008. Length-dependent recognition of double-stranded ribonucleic acids by retinoic acid-inducible gene-I and melanoma differentiation-associated gene 5. *Journal of Experimental Medicine* 205, 1601-1610.

Kato, H., Takeuchi, O., Sato, S., Yoneyama, M., Yamamoto, M., Matsui, K., Uematsu, S., Jung, A., Kawai, T., Ishii, K.J., Yamaguchi, O., Otsu, K., Tsujimura, T., Koh, C.-S., Reis e Sousa, C., Matsuura, Y., Fujita, T., Akira, S., 2006. Differential roles of MDA5 and RIG-I helicases in the recognition of RNA viruses. *Nature* 441, 101-105.

Kato, T., Delhase, M., Hoffmann, A., Karin, M., 2003. CK2 Is a C-Terminal I κ B Kinase Responsible for NF- κ B Activation during the UV Response. *Mol Cell* 12, 829-839.

Kawaguchi, S., Sakuraba, H., Haga, T., Matsumiya, T., Seya, K., Endo, T., Sawada, N., Iino, C., Kikuchi, H., Hiraga, H., Fukuda, S., Imaizumi, T., 2019. Melanoma Differentiation-Associated Gene 5 Positively Modulates TNF- α -Induced CXCL10 Expression in Cultured HuH-7 and HLE Cells. *Inflammation* 42, 2095-2104.

Kawai, T., Takahashi, K., Sato, S., Coban, C., Kumar, H., Kato, H., Ishii, K.J., Takeuchi, O., Akira, S., 2005. IPS-1, an adaptor triggering RIG-I- and Mda5-mediated type I interferon induction. *Nat Immunol* 6, 981-988.

Keasler, V.V., Hodgson, A.J., Madden, C.R., Slagle, B.L., 2007. Enhancement of hepatitis B virus replication by the regulatory X protein in vitro and in vivo. *J Virol* 81, 2656-2662.

Kennelly, P.J., Krebs, E.G., 1991. Consensus sequences as substrate specificity determinants for protein kinases and protein phosphatases. *J Biol Chem* 266, 15555-15558.

Keshet, R., Lee, J.S., Adler, L., Iraqi, M., Ariav, Y., Lim, L.Q.J., Lerner, S., Rabinovich, S., Oren, R., Katzir, R., Weiss Tishler, H., Stettner, N., Goldman, O., Landesman, H., Galai, S., Kuperman, Y., Kuznetsov, Y., Brandis, A., Mehlman, T., Malitsky, S., Itkin, M., Koehler, S.E., Zhao, Y., Talsania, K., Shen, T., Peled, N., Ulitsky, I., Porgador, A., Ruppin, E., Erez, A., 2020. Targeting purine synthesis in ASS1-expressing tumors enhances the response to immune checkpoint inhibitors. *Nat Cancer* 1, 894-908.

Kessler, D.S., Levy, D.E., Darnell, J.E., 1988. Two interferon-induced nuclear factors bind a single promoter element in interferon-stimulated genes. *Proc Natl Acad Sci U S A* 85, 8521-8525. <https://doi.org/10.1073/pnas.85.22.8521>

Khvalevsky, E., Rivkin, L., Rachmilewitz, J., Galun, E., Giladi, H., 2007. TLR3 signaling in a hepatoma cell line is skewed towards apoptosis. *Journal of Cellular Biochemistry* 100, 1301-1312.

Kim, H.-J., Jeong, S.-H., Heo, J.-H., Jeong, S.-J., Kim, S.-T., Youn, H.-D., Han, J.-W., Lee, H.-W., Cho, E.-J., 2004. mRNA capping enzyme activity is coupled to an early transcription elongation. *Mol Cell Biol* 24, 6184-6193.

Kim, J.L., Nikolov, D.B., Burley, S.K., 1993. Co-crystal structure of TBP recognizing the minor groove of a TATA element. *Nature* 365, 520-527.

Kim, S., Lee, M., Song, Y., Lee, S.-Y., Choi, I., Park, I.-S., Kim, Jiho, Kim, Jin-sun, Kim, K. mo, Seo, H.R., 2021. Argininosuccinate synthase 1 suppresses tumor progression through activation of PERK/eIF2 α /ATF4/CHOP axis in hepatocellular carcinoma. *Journal of Experimental & Clinical Cancer Research* 40, 127.

Kiss, T., 2002. Small Nucleolar RNAs: An Abundant Group of Noncoding RNAs with Diverse Cellular Functions. *Cell* 109, 145-148.

Köhler, A., Hurt, E., 2007. Exporting RNA from the nucleus to the cytoplasm. *Nat Rev Mol Cell Biol* 8, 761-773.

Komarnitsky, P., Cho, E.-J., Buratowski, S., 2000. Different phosphorylated forms of RNA polymerase II and associated mRNA processing factors during transcription. *Genes Dev.* 14, 2452-2460.

Komuro, A., Horvath, C.M., 2006. RNA- and Virus-Independent Inhibition of Antiviral Signaling by RNA Helicase LGP2. *Journal of Virology* 80, 12332-12342.

Kon, M., Kiffin, R., Koga, H., Chapochnik, J., Macian, F., Varticovski, L., Cuervo, A.M., 2011. Chaperone-Mediated Autophagy Is Required for Tumor Growth. *Science Translational Medicine* 3, 109ra117-109ra117.

Kowalinski, E., Lunardi, T., McCarthy, A.A., Louber, J., Brunel, J., Grigorov, B., Gerlier, D., Cusack, S., 2011. Structural basis for the activation of innate immune pattern-recognition receptor RIG-I by viral RNA. *Cell* 147, 423-435.

Krafcikova, P., Silhan, J., Nencka, R., Boura, E., 2020. Structural analysis of the SARS-CoV-2 methyltransferase complex involved in RNA cap creation bound to sinefungin. *Nat Commun* 11, 3717.

Krehan, A., Ansuini, H., Böcher, O., Grein, S., Wirkner, U., Pyerin, W., 2000. Transcription Factors Ets1, NF- κ B, and Sp1 Are Major Determinants of the Promoter

Activity of the Human Protein Kinase CK2 α Gene *. Journal of Biological Chemistry 275, 18327-18336.

Kruse, S., Zhong, S., Bodi, Z., Button, J., Alcocer, M.J.C., Hayes, C.J., Fray, R., 2011. A novel synthesis and detection method for cap-associated adenosine modifications in mouse mRNA. Sci Rep 1, 126.

Kubo, S., Nishiguchi, S., Hirohashi, K., Tanaka, H., Shuto, T., Yamazaki, O., Shiomi, S., Tamori, A., Oka, H., Igawa, S., Kuroki, T., Kinoshita, H., 2001. Effects of long-term postoperative interferon-alpha therapy on intrahepatic recurrence after resection of hepatitis C virus-related hepatocellular carcinoma. A randomized, controlled trial. Ann Intern Med 134, 963-967.

Kudo, M., Finn, R.S., Ikeda, M., Sung, M.W., Baron, A.D., Okusaka, T., Kobayashi, M., Kumada, H., Kaneko, S., Pracht, M., Meyer, T., Nagao, S., Saito, K., Mody, K., Ramji, Z., Dubrovsky, L., Llovet, J.M., 2023. A Phase 1b Study of Lenvatinib plus Pembrolizumab in Patients with Unresectable Hepatocellular Carcinoma: Extended Analysis of Study 116. Liver Cancer 1-7.

Kuge, H., Brownlee, G.G., Gershon, P.D., Richter, J.D., 1998. Cap ribose methylation of c- mos mRNA stimulates translation and oocyte maturation in *Xenopus laevis*. Nucleic Acids Research 26, 3208-3214.

Kuhen, K.L., Samuel, C.E., 1997. Isolation of the Interferon-Inducible RNA-Dependent Protein Kinase *Pkr* Promoter and Identification of a Novel DNA Element within the 5'-Flanking Region of Human and Mouse *Pkr* Genes. Virology 227, 119-130.

Kumar, P., Hellen, C.U.T., Pestova, T.V., 2016. Toward the mechanism of eIF4F-mediated ribosomal attachment to mammalian capped mRNAs. Genes Dev 30, 1573-1588.

Lai, C., Struckhoff, J.J., Schneider, J., Martinez-Sobrido, L., Wolff, T., García-Sastre, A., Zhang, D.-E., Lenschow, D.J., 2009. Mice lacking the ISG15 E1 enzyme

UbE1L demonstrate increased susceptibility to both mouse-adapted and non-mouse-adapted influenza B virus infection. *J Virol* 83, 1147-1151.

LaPointe, A.T., Moreno-Contreras, J., Sokoloski, K.J., 2018. Increasing the Capping Efficiency of the Sindbis Virus nsP1 Protein Negatively Affects Viral Infection. *mBio* 9, e02342-18.

Lau, N.-C., Kolkman, A., van Schaik, F.M.A., Mulder, K.W., Pijnappel, W.W.M.P., Heck, A.J.R., Timmers, H.Th.M., 2009. Human Ccr4-Not complexes contain variable deadenylase subunits. *Biochemical Journal* 422, 443-453.

Lavoie, T.B., Kalie, E., Crisafulli-Cabatu, S., Abramovich, R., DiGioia, G., Moolchan, K., Pestka, S., Schreiber, G., 2011. Binding and activity of all human alpha interferon subtypes. *Cytokine* 56, 282-289.

Lee, J., Lee, Y., Xu, L., White, R., Sullenger, B.A., 2017. Differential Induction of Immunogenic Cell Death and Interferon Expression in Cancer Cells by Structured ssRNAs. *Mol Ther* 25, 1295-1305.

Lee, Y.-L., Kung, F.-C., Lin, C.-H., Huang, Y.-S., 2020. CMTR1-Catalyzed 2'-O-Ribose Methylation Controls Neuronal Development by Regulating *Camk2a* Expression Independent of RIG-I Signaling. *Cell Reports* 33, 108269.

Leenaars, M., Hendriksen, C.F.M., 2005. Critical Steps in the Production of Polyclonal and Monoclonal Antibodies: Evaluation and Recommendations. *ILAR Journal* 46, 269-279.

Le Hir, H., Gatfield, D., Izaurralde, E., Moore, M.J., 2001. The exon-exon junction complex provides a binding platform for factors involved in mRNA export and nonsense-mediated mRNA decay. *EMBO J* 20, 4987-4997.

Lenhausen, A.M., Wilkinson, A.S., Lewis, E.M., Dailey, K.M., Scott, A.J., Khan, S., Wilkinson, J.C., 2016. Apoptosis Inducing Factor Binding Protein PGAM5 Triggers

Mitophagic Cell Death That Is Inhibited by the Ubiquitin Ligase Activity of X-Linked Inhibitor of Apoptosis. *Biochemistry* 55, 3285-3302.

Lenschow, D.J., Lai, C., Frias-Staheli, N., Giannakopoulos, N.V., Lutz, A., Wolff, T., Osiak, A., Levine, B., Schmidt, R.E., García-Sastre, A., Leib, D.A., Pekosz, A., Knobeloch, K.-P., Horak, I., Virgin, H.W., 2007. IFN-stimulated gene 15 functions as a critical antiviral molecule against influenza, herpes, and Sindbis viruses. *Proceedings of the National Academy of Sciences* 104, 1371-1376.

Lepage, C., Capocaccia, R., Hackl, M., Lemmens, V., Molina, E., Pierannunzio, D., Sant, M., Trama, A., Faivre, J., EUROCORE-5 Working Group:, 2015. Survival in patients with primary liver cancer, gallbladder and extrahepatic biliary tract cancer and pancreatic cancer in Europe 1999-2007: Results of EUROCORE-5. *Eur J Cancer* 51, 2169-2178.

Leviyang, S., 2021. Interferon stimulated binding of ISRE is cell type specific and is predicted by homeostatic chromatin state. *Cytokine X* 3, 100056.

Levy, D.E., Kessler, D.S., Pine, R., Darnell, J.E., 1989. Cytoplasmic activation of ISGF3, the positive regulator of interferon-alpha-stimulated transcription, reconstituted in vitro. *Genes Dev* 3, 1362-1371.

Li, B., Clohisey, S.M., Chia, B.S., Wang, B., Cui, A., Eisenhaure, T., Schweitzer, L.D., Hoover, P., Parkinson, N.J., Nachshon, A., Smith, N., Regan, T., Farr, D., Gutmann, M.U., Bukhari, S.I., Law, A., Sangesland, M., Gat-Viks, I., Digard, P., Vasudevan, S., Lingwood, D., Dockrell, D.H., Doench, J.G., Baillie, J.K., Hacohen, N., 2020. Genome-wide CRISPR screen identifies host dependency factors for influenza A virus infection. *Nat Commun* 11, 164.

Li, S., Yang, J., Zhu, Y., Wang, H., Ji, X., Luo, J., Shao, Q., Xu, Y., Liu, X., Zheng, W., Meurens, F., Chen, N., Zhu, J., 2021. Analysis of Porcine RIG-I Like Receptors Revealed the Positive Regulation of RIG-I and MDA5 by LGP2. *Front Immunol* 12, 609543.

Li, X., Fang, P., Mai, J., Choi, E.T., Wang, H., Yang, X., 2013. Targeting mitochondrial reactive oxygen species as novel therapy for inflammatory diseases and cancers. *Journal of Hematology & Oncology* 6, 19.

Liang, M.D., Zhang, Y., McDevit, D., Marecki, S., Nikolajczyk, B.S., 2006. The interleukin-1beta gene is transcribed from a poised promoter architecture in monocytes. *J Biol Chem* 281, 9227-9237.

Liang, M.-Z., Lu, T.-H., Chen, L., 2023. Timely expression of PGAM5 and its cleavage control mitochondrial homeostasis during neurite re-growth after traumatic brain injury. *Cell & Bioscience* 13, 96.

Liang, S., Silva, J.C., Suska, O., Lukoszek, R., Almohammed, R., Cowling, V.H., 2022. CMTR1 is recruited to transcription start sites and promotes ribosomal protein and histone gene expression in embryonic stem cells. *Nucleic Acids Research* 50, 2905-2922.

Lim, L.Q.J., Adler, L., Hajaj, E., Soria, L.R., Perry, R.B.-T., Darzi, N., Brody, R., Furth, N., Lichtenstein, M., Bab-Dinitz, E., Porat, Z., Melman, T., Brandis, A., Aylon, Y., Ben-Dor, S., Orr, I., Pri-Or, A., Seger, R., Shaul, Y., Ruppin, E., Oren, M., Perez, M., Meier, J., Brunetti-Pierri, N., Shema, E., Ulitsky, I., Erez, A., Malitsky, S., Itkin, M., 2024a. ASS1 metabolically contributes to the nuclear and cytosolic p53-mediated DNA damage response. *Nat Metab* 1-16.

Lim, L.Q.J., Adler, L., Hajaj, E., Soria, L.R., Perry, R.B.-T., Darzi, N., Brody, R., Furth, N., Lichtenstein, M., Bab-Dinitz, E., Porat, Z., Melman, T., Brandis, A., Malitsky, S., Itkin, M., Aylon, Y., Ben-Dor, S., Orr, I., Pri-Or, A., Seger, R., Shaul, Y., Ruppin, E., Oren, M., Perez, M., Meier, J., Brunetti-Pierri, N., Shema, E., Ulitsky, I., Erez, A., 2024b. ASS1 metabolically contributes to the nuclear and cytosolic p53-mediated DNA damage response. *Nat Metab* 1-16.

Lin, C.-P., Liu, C.-R., Lee, C.-N., Chan, T.-S., Liu, H.E., 2010. Targeting c-Myc as a novel approach for hepatocellular carcinoma. *World J Hepatol* 2, 16-20.

Liu, L., Cao, Y., Chen, C., Zhang, X., McNabola, A., Wilkie, D., Wilhelm, S., Lynch, M., Carter, C., 2006. Sorafenib blocks the RAF/MEK/ERK pathway, inhibits tumor angiogenesis, and induces tumor cell apoptosis in hepatocellular carcinoma model PLC/PRF/5. *Cancer Res* 66, 11851-11858.

Liu, Q., Liu, L., Zhao, Y., Zhang, J., Wang, D., Chen, J., He, Y., Wu, J., Zhang, Z., Liu, Z., 2011. Hypoxia induces genomic DNA demethylation through the activation of HIF-1 α and transcriptional upregulation of MAT2A in hepatoma cells. *Mol Cancer Ther* 10, 1113-1123.

Liu, S.-Y., Aliyari, R., Chikere, K., Li, G., Marsden, M.D., Smith, J.K., Pernet, O., Guo, H., Nusbaum, R., Zack, J.A., Freiberg, A.N., Su, L., Lee, B., Cheng, G., 2013. Interferon-Inducible Cholesterol-25-Hydroxylase Broadly Inhibits Viral Entry by Production of 25-Hydroxycholesterol. *Immunity* 38, 92-105.

Liu, S., Chen, J., Cai, X., Wu, J., Chen, X., Wu, Y.-T., Sun, L., Chen, Z.J., 2013. MAVS recruits multiple ubiquitin E3 ligases to activate antiviral signaling cascades. *eLife* 2, e00785.

Liu, Y., Wu, F., 2010. Global Burden of Aflatoxin-Induced Hepatocellular Carcinoma: A Risk Assessment. *Environ Health Perspect* 118, 818-824.

Liu, Z., Jiang, Y., Yuan, H., Fang, Q., Cai, N., Suo, C., Jin, L., Zhang, T., Chen, X., 2019. The trends in incidence of primary liver cancer caused by specific etiologies: Results from the Global Burden of Disease Study 2016 and implications for liver cancer prevention. *Journal of Hepatology* 70, 674-683.

Llovet, J.M., Kelley, R.K., Villanueva, A., Singal, A.G., Pikarsky, E., Roayaie, S., Lencioni, R., Koike, K., Zucman-Rossi, J., Finn, R.S., 2021. Hepatocellular carcinoma. *Nat Rev Dis Primers* 7, 1-28.

Llovet, J.M., Ricci, S., Mazzaferro, V., Hilgard, P., Gane, E., Blanc, J.-F., de Oliveira, A.C., Santoro, A., Raoul, J.-L., Forner, A., Schwartz, M., Porta, C., Zeuzem, S., Bolondi, L., Greten, T.F., Galle, P.R., Seitz, J.-F., Borbath, I., Häussinger, D., Giannaris, T., Shan, M., Moscovici, M., Voliotis, D., Bruix, J., SHARP Investigators Study Group, 2008. Sorafenib in advanced hepatocellular carcinoma. *N Engl J Med* 359, 378-390.

Lo, S.-C., Hannink, M., 2006. PGAM5, a Bcl-XL-interacting Protein, Is a Novel Substrate for the Redox-regulated Keap1-dependent Ubiquitin Ligase Complex *. *Journal of Biological Chemistry* 281, 37893-37903.

Loeb, K.R., Haas, A.L., 1992. The interferon-inducible 15-kDa ubiquitin homolog conjugates to intracellular proteins. *J Biol Chem* 267, 7806-7813.

Loeffen, J., Elpeleg, O., Smeitink, J., Smeets, R., Stöckler-Ipsiroglu, S., Mandel, H., Sengers, R., Trijbels, F., van den Heuvel, L., 2001. Mutations in the complex I NDUFS2 gene of patients with cardiomyopathy and encephalomyopathy. *Ann Neurol* 49, 195-201.

Loh, B., Jonas, S., Izaurralde, E., 2013. The SMG5-SMG7 heterodimer directly recruits the CCR4-NOT deadenylase complex to mRNAs containing nonsense codons via interaction with POP2. *Genes Dev* 27, 2125-2138.

Loizou, J.I., El-Khamisy, S.F., Zlatanou, A., Moore, D.J., Chan, D.W., Qin, J., Sarno, S., Meggio, F., Pinna, L.A., Caldecott, K.W., 2004. The protein kinase CK2 facilitates repair of chromosomal DNA single-strand breaks. *Cell* 117, 17-28.

Louber, J., Kowalinski, E., Bloyet, L.-M., Brunel, J., Cusack, S., Gerlier, D., 2014. RIG-I Self-Oligomerization Is Either Dispensable or Very Transient for Signal Transduction. *PLOS ONE* 9, e108770.

Lu, P.J., Zhou, X.Z., Shen, M., Lu, K.P., 1999. Function of WW domains as phosphoserine- or phosphothreonine-binding modules. *Science* 283, 1325-1328.

Lu, S.C., Mato, J.M., 2012. S-adenosylmethionine in Liver Health, Injury, and Cancer. *Physiological Reviews*.

Lu, W., Sun, J., Yoon, J.S., Zhang, Y., Zheng, L., Murphy, E., Mattson, M.P., Lenardo, M.J., 2016. Mitochondrial Protein PGAM5 Regulates Mitophagic Protection against Cell Necroptosis. *PLoS One* 11, e0147792.

Lübbbers, J., Brink, M., van de Stadt, L.A., Vosslamber, S., Wesseling, J.G., van Schaardenburg, D., Rantapää-Dahlqvist, S., Verweij, C.L., 2013. The type I IFN signature as a biomarker of preclinical rheumatoid arthritis. *Ann Rheum Dis* 72, 776-780.

Luedde, T., Beraza, N., Kotsikoris, V., Loo, G. van, Nenci, A., Vos, R.D., Roskams, T., Trautwein, C., Pasparakis, M., 2007. Deletion of NEMO/IKK γ in Liver Parenchymal Cells Causes Steatohepatitis and Hepatocellular Carcinoma. *Cancer Cell* 11, 119-132.

Luedde, T., Schwabe, R.F., 2011. NF- κ B in the liver—linking injury, fibrosis and hepatocellular carcinoma. *Nat Rev Gastroenterol Hepatol* 8, 108-118.

Lukoszek, R., Inesta-Vaquera, F., Brett, N.J.M., Liang, S., Hepburn, L.A., Hughes, D.J., Pirillo, C., Roberts, E.W., Cowling, V.H., 2024. CK2 phosphorylation of CMTR1 promotes RNA cap formation and influenza virus infection. *Cell Reports* 43.

Lund, M.K., Guthrie, C., 2005. The DEAD-box protein Dbp5p is required to dissociate Mex67p from exported mRNPs at the nuclear rim. *Mol Cell* 20, 645-651.

Luo, D., Ding, S.C., Vela, A., Kohlway, A., Lindenbach, B.D., Pyle, A.M., 2011. Structural Insights into RNA Recognition by RIG-I. *Cell* 147, 409-422.

Luo, Y., Na, Z., Slavoff, S.A., 2018. P-Bodies: Composition, Properties, and Functions. *Biochemistry* 57, 2424-2431.

Macias, M.J., Hyvönen, M., Baraldi, E., Schultz, J., Sudol, M., Saraste, M., Oschkinat, H., 1996. Structure of the WW domain of a kinase-associated protein complexed with a proline-rich peptide. *Nature* 382, 646-649.

Maeda, S., Wada, H., Naito, Y., Nagano, H., Simmons, S., Kagawa, Y., Naito, A., Kikuta, J., Ishii, T., Tomimaru, Y., Hama, N., Kawamoto, K., Kobayashi, S., Eguchi, H., Umeshita, K., Ishii, H., Doki, Y., Mori, M., Ishii, M., 2014. Interferon- α Acts on the S/G2/M Phases to Induce Apoptosis in the G1 Phase of an IFNAR2-expressing Hepatocellular Carcinoma Cell Line. *J Biol Chem* 289, 23786-23795.

Mandal, S.S., Chu, C., Wada, T., Handa, H., Shatkin, A.J., Reinberg, D., 2004. Functional interactions of RNA-capping enzyme with factors that positively and negatively regulate promoter escape by RNA polymerase II. *Proceedings of the National Academy of Sciences* 101, 7572-7577.

Mandrekar, P., Szabo, G., 2009. Signalling pathways in alcohol-induced liver inflammation. *J Hepatol* 50, 1258-1266.

Mann, B., Gelos, M., Siedow, A., Hanski, M.L., Gratchev, A., Ilyas, M., Bodmer, W.F., Moyer, M.P., Riecken, E.O., Buhr, H.J., Hanski, C., 1999. Target genes of beta-catenin-T cell-factor/lymphoid-enhancer-factor signaling in human colorectal carcinomas. *Proc Natl Acad Sci U S A* 96, 1603-1608.

Mann, M., Jensen, O.N., 2003. Proteomic analysis of post-translational modifications. *Nat Biotechnol* 21, 255-261.

Mao, Y., Shi, D., Li, G., Jiang, P., 2022. Citrulline depletion by ASS1 is required for proinflammatory macrophage activation and immune responses. *Molecular Cell* 82, 527-541.e7.

Marin, O., Meggio, F., Draetta, G., Pinna, L.A., 1992. The consensus sequences for cdc2 kinase and for casein kinase-2 are mutually incompatible A study with peptides derived from the β -subunit of casein kinase-2. *FEBS Letters* 301, 111-114.

Marozin, S., Altomonte, J., Stadler, F., Thasler, W.E., Schmid, R.M., Ebert, O., 2008. Inhibition of the IFN- β Response in Hepatocellular Carcinoma by Alternative Spliced Isoform of IFN Regulatory Factor-3. *Molecular Therapy* 16, 1789-1797.

Marshall, N.F., Peng, J., Xie, Z., Price, D.H., 1996. Control of RNA Polymerase II Elongation Potential by a Novel Carboxyl-terminal Domain Kinase*. *Journal of Biological Chemistry* 271, 27176-27183.

Martínez-Alonso, M., Hengrung, N., Fodor, E., 2016. RNA-Free and Ribonucleoprotein-Associated Influenza Virus Polymerases Directly Bind the Serine-5-Phosphorylated Carboxyl-Terminal Domain of Host RNA Polymerase II. *Journal of Virology* 90, 6014-6021.

Maslon, M.M., Heras, S.R., Bellora, N., Eyra, E., Cáceres, J.F., 2014. The translational landscape of the splicing factor SRSF1 and its role in mitosis. *eLife* 3, e02028.

Matsuda, Y., Wakai, T., Kubota, M., Osawa, M., Takamura, M., Yamagiwa, S., Aoyagi, Y., Sanpei, A., Fujimaki, S., 2013. DNA Damage Sensor γ -H2AX Is Increased in Preneoplastic Lesions of Hepatocellular Carcinoma. *ScientificWorldJournal* 2013, 597095.

Matsumoto, S., Häberle, J., Kido, J., Mitsubuchi, H., Endo, F., Nakamura, K., 2019. Urea cycle disorders—update. *J Hum Genet* 64, 833-847.

Mauer, J., Luo, X., Blanjoie, A., Jiao, X., Grozhik, A.V., Patil, D.P., Linder, B., Pickering, B.F., Vasseur, J.-J., Chen, Q., Gross, S.S., Elemento, O., Debart, F., Kiledjian, M., Jaffrey, S.R., 2017. Reversible methylation of m6Am in the 5' cap controls mRNA stability. *Nature* 541, 371-375.

McCracken, S., Fong, N., Rosonina, E., Yankulov, K., Brothers, G., Siderovski, D., Hessel, A., Foster, S., Program, A.E., Shuman, S., Bentley, D.L., 1997. 5'-Capping enzymes are targeted to pre-mRNA by binding to the phosphorylated carboxy-terminal domain of RNA polymerase II. *Genes Dev.* 11, 3306-3318.

McNab, F., Mayer-Barber, K., Sher, A., Wack, A., O'Garra, A., 2015. Type I interferons in infectious disease. *Nat Rev Immunol* 15, 87-103.

Meisel, J.D., Wiesenthal, P.P., Mootha, V.K., Ruvkun, G., 2024. CMTR-1 RNA methyltransferase mutations activate widespread expression of a dopaminergic neuron-specific mitochondrial complex I gene. *Current Biology* 34, 2728-2738.e6.

Meng, L., Hu, P., Xu, A., 2023. PGAM5 promotes tumorigenesis of gastric cancer cells through PI3K/AKT pathway. *Pathol Res Pract* 244, 154405.

Menssen, A., Hermeking, H., 2002b. Characterization of the c-MYC-regulated transcriptome by SAGE: identification and analysis of c-MYC target genes. *Proc Natl Acad Sci U S A* 99, 6274-6279.

Mercer, T.R., Dinger, M.E., Bracken, C.P., Kolle, G., Szubert, J.M., Korbie, D.J., Askarian-Amiri, M.E., Gardiner, B.B., Goodall, G.J., Grimmond, S.M., Mattick, J.S., 2010. Regulated post-transcriptional RNA cleavage diversifies the eukaryotic transcriptome. *Genome Res* 20, 1639-1650.

Mercurio, F., Zhu, H., Murray, B.W., Shevchenko, A., Bennett, B.L., Li, J., Young, D.B., Barbosa, M., Mann, M., Manning, A., Rao, A., 1997. IKK-1 and IKK-2: cytokine-activated I κ B kinases essential for NF- κ B activation. *Science* 278, 860-866.

Merrick, W.C., Pavitt, G.D., 2018. Protein Synthesis Initiation in Eukaryotic Cells. *Cold Spring Harb Perspect Biol* 10, a033092.

Mi, S., Stollar, V., 1991. Expression of Sindbis virus nsP1 and methyltransferase activity in *Escherichia coli*. *Virology* 184, 423-427.

Miller, S., Yasuda, M., Coats, J.K., Jones, Y., Martone, M.E., Mayford, M., 2002. Disruption of Dendritic Translation of CaMKII α Impairs Stabilization of Synaptic Plasticity and Memory Consolidation. *Neuron* 36, 507-519.

Mir, M.A., Duran, W.A., Hjelle, B.L., Ye, C., Panganiban, A.T., 2008. Storage of cellular 5' mRNA caps in P bodies for viral cap-snatching. *Proceedings of the National Academy of Sciences* 105, 19294-19299.

Miyashita, M., Oshiumi, H., Matsumoto, M., Seya, T., 2011. DDX60, a DEXD/H Box Helicase, Is a Novel Antiviral Factor Promoting RIG-I-Like Receptor-Mediated Signaling. *Molecular and Cellular Biology* 31, 3802-3819.

Molina-Sánchez, P., de Galarreta, M.R., Yao, M.A., Lindblad, K.E., Bresnahan, E., Bitterman, E., Martin, T.C., Rubenstein, T., Nie, K., Golas, J., Choudhary, S., Bárcena-Varela, M., Elmas, A., Miguela, V., Ding, Y., Kan, Z., Grinspan, L.T., morCooperation between distinct cancer driver genes underlies inter-tumor heterogeneity in hepatocellular carcinoma. *Gastroenterology* 159, 2203-2220.e14.

Moraga, I., Harari, D., Schreiber, G., Uzé, G., Pellegrini, S., 2009. Receptor Density Is Key to the Alpha2/Beta Interferon Differential Activities. *Molecular and Cellular Biology* 29, 4778-4787.

Mosallanejad, K., Sekine, Y., Ishikura-Kinoshita, S., Kumagai, K., Nagano, T., Matsuzawa, A., Takeda, K., Naguro, I., Ichijo, H., 2014. The DEAH-Box RNA Helicase DHX15 Activates NF- κ B and MAPK Signaling Downstream of MAVS During Antiviral Responses. *Science Signaling* 7, ra40-ra40.

Moteki, S., Price, D., 2002. Functional coupling of capping and transcription of mRNA. *Mol Cell* 10, 599-609.

Muhlrad, D., Decker, C.J., Parker, R., 1994. Deadenylation of the unstable mRNA encoded by the yeast MFA2 gene leads to decapping followed by 5'-->3' digestion of the transcript. *Genes Dev* 8, 855-866.

Mukherjee, C., Patil, D.P., Kennedy, B.A., Bakthavachalu, B., Bundschuh, R., Schoenberg, D.R., 2012. Identification of cytoplasmic capping targets reveals a role for cap homeostasis in translation and mRNA stability. *Cell Rep* 2, 674-684.

Müller, M., May, S., Hall, H., Kendall, T.J., McGarry, L., Blukacz, L., Nuciforo, S., Jamieson, T., Phinichkusolchit, N., Dhayade, S., Leslie, J., Sprangers, J., Malviya, G., Mrowinska, A., Johnson, E., McCain, M., Halpin, J., Kiourtis, C., Georgakopoulou, A., Nixon, C., Clark, W., Shaw, R., Hedley, A., Drake, T.M., Tan, E.H., Neilson, M., Murphy, D.J., Lewis, D., Reeves, H.L., Mann, D.A., Blyth, K., Heim, M.H., Carlin, L.M., Sansom, O.J., Miller, C., Bird, T.G., 2022. Human-correlated genetic HCC models identify combination therapy for precision medicine.

Murali, A., Li, X., Ranjith-Kumar, C.T., Bhardwaj, K., Holzenburg, A., Li, P., Kao, C.C., 2008. Structure and Function of LGP2, a DEX(D/H) Helicase That Regulates the Innate Immunity Response. *J Biol Chem* 283, 15825-15833.

Muthukrishnan, S., Both, G.W., Furuichi, Y., Shatkin, A.J., 1975. 5'-Terminal 7-methylguanosine in eukaryotic mRNA is required for translation. *Nature* 255, 33-37.

Muthusamy, G., Liu, C.-C., Johnston, A.N., 2023. Deletion of PGAM5 Downregulates FABP1 and Attenuates Long-Chain Fatty Acid Uptake in Hepatocellular Carcinoma. *Cancers* 15, 4796.

Nag, S., Szederkenyi, K., Gorbenko, O., Tyrrell, H., Yip, C.M., McQuibban, G.A., 2023. PGAM5 is an MFN2 phosphatase that plays an essential role in the regulation of mitochondrial dynamics. *Cell Rep* 42, 112895.

Nagahama, M., Hara, Y., Seki, A., Yamazoe, T., Kawate, Y., Shinohara, T., Hatsuzawa, K., Tani, K., Tagaya, M., 2004. NVL2 Is a Nucleolar AAA-ATPase that Interacts with Ribosomal Protein L5 through Its Nucleolar Localization Sequence. *Mol Biol Cell* 15, 5712-5723.

Najm, R., Yavuz, L., Jain, R., El Naofal, M., Ramaswamy, S., Abuhammour, W., Loney, T., Nowotny, N., Alsheikh-Ali, A., Abou Tayoun, A., Kandasamy, R.K., n.d. IFIH1 loss of function predisposes to inflammatory and SARS-CoV-2-related infectious diseases. *Scandinavian Journal of Immunology* n/a, e13373.

Nakabayashi, H., Taketa, K., Miyano, K., Yamane, T., Sato, J., 1982. Growth of human hepatoma cells lines with differentiated functions in chemically defined medium. *Cancer research*.

Narita, T., Yung, T.M.C., Yamamoto, J., Tsuboi, Y., Tanabe, H., Tanaka, K., Yamaguchi, Y., Handa, H., 2007. NELF Interacts with CBC and Participates in 3' End Processing of Replication-Dependent Histone mRNAs. *Molecular Cell* 26, 349-365.

Nault, J.C., Mallet, M., Pilati, C., Calderaro, J., Bioulac-Sage, P., Laurent, C., Laurent, A., Cherqui, D., Balabaud, C., Zucman-Rossi, J., 2013. High frequency of telomerase reverse-transcriptase promoter somatic mutations in hepatocellular carcinoma and preneoplastic lesions. *Nat Commun* 4, 2218.

Nault, J.-C., Zucman-Rossi, J., 2016. TERT promoter mutations in primary liver tumors. *Clin Res Hepatol Gastroenterol* 40, 9-14.

Ng Kee Kwong, F., Nicholson, A.G., Pavlidis, S., Adcock, I.M., Chung, K.F., 2018. PGAM5 expression and macrophage signatures in non-small cell lung cancer associated with chronic obstructive pulmonary disease (COPD). *BMC Cancer* 18, 1238.

Nickless, A., Bailis, J.M., You, Z., 2017. Control of gene expression through the nonsense-mediated RNA decay pathway. *Cell & Bioscience* 7, 26.

Nishida, N., Fukuda, Y., Komeda, T., Kita, R., Sando, T., Furukawa, M., Amenomori, M., Shibagaki, I., Nakao, K., Ikenaga, M., 1994. Amplification and overexpression of the cyclin D1 gene in aggressive human hepatocellular carcinoma. *Cancer Res* 54, 3107-3110.

Nojima, T., Hirose, T., Kimura, H., Hagiwara, M., 2007. The Interaction between Cap-binding Complex and RNA Export Factor Is Required for Intronless mRNA Export *. *Journal of Biological Chemistry* 282, 15645-15651.

Obaya, A.J., Kotenko, I., Cole, M.D., Sedivy, J.M., 2002. The Proto-oncogene *c-myc* Acts through the Cyclin-dependent Kinase (Cdk) Inhibitor p27Kip1 to Facilitate the Activation of Cdk4/6 and Early G1Phase Progression*. *Journal of Biological Chemistry* 277, 31263-31269.

Oelgeschläger, T., 2002. Regulation of RNA polymerase II activity by CTD phosphorylation and cell cycle control. *Journal of Cellular Physiology* 190, 160-169.

Okada-Katsuhata, Y., Yamashita, A., Kutsuzawa, K., Izumi, N., Hirahara, F., Ohno, S., 2012. N- and C-terminal Upf1 phosphorylations create binding platforms for SMG-6 and SMG-5:SMG-7 during NMD. *Nucleic Acids Res* 40, 1251-1266.

Okumura, A., Pitha, P.M., Harty, R.N., 2008. ISG15 inhibits Ebola VP40 VLP budding in an L-domain-dependent manner by blocking Nedd4 ligase activity. *Proceedings of the National Academy of Sciences* 105, 3974-3979.

Olschewski, S., Cusack, S., Rosenthal, M., 2020. The Cap-Snatching Mechanism of Bunyaviruses. *Trends in Microbiology* 28, 293-303.

O'Mealey, G.B., Plafker, K.S., Berry, W.L., Janknecht, R., Chan, J.Y., Plafker, S.M., 2017. A PGAM5-KEAP1-Nrf2 complex is required for stress-induced mitochondrial retrograde trafficking. *Journal of Cell Science* 130, 3467-3480.

Otsuka, Y., Kedersha, N.L., Schoenberg, D.R., 2009. Identification of a Cytoplasmic Complex That Adds a Cap onto 5'-Monophosphate RNA. *Mol Cell Biol* 29, 2155-2167.

Ozgur, S., Buchwald, G., Falk, S., Chakrabarti, S., Prabu, J.R., Conti, E., 2015. The conformational plasticity of eukaryotic RNA-dependent ATPases. *The FEBS Journal* 282, 850-863.

Pabis, M., Neufeld, N., Steiner, M.C., Bojic, T., Shav-Tal, Y., Neugebauer, K.M., 2013. The nuclear cap-binding complex interacts with the U4/U6·U5 tri-snRNP and promotes spliceosome assembly in mammalian cells. *RNA* 19, 1054.

Panda, S., Srivastava, S., Li, Z., Vaeth, M., Fuhs, S.R., Hunter, T., Skolnik, E.Y., 2016. Identification of PGAM5 as a Mammalian Protein Histidine Phosphatase that Plays a Central Role to Negatively Regulate CD4(+) T Cells. *Mol Cell* 63, 457-469.

Park, H.-R., Tomida, A., Sato, S., Tsukumo, Y., Yun, J., Yamori, T., Hayakawa, Y., Tsuruo, T., Shin-ya, K., 2004. Effect on Tumor Cells of Blocking Survival Response to Glucose Deprivation. *JNCI: Journal of the National Cancer Institute* 96, 1300-1310.

Parker, T.W., Neufeld, K.L., 2020. APC controls Wnt-induced β -catenin destruction complex recruitment in human colonocytes. *Sci Rep* 10, 2957.

Peisley, A., Wu, B., Yao, H., Walz, T., Hur, S., 2013. RIG-I Forms Signaling-Competent Filaments in an ATP-Dependent, Ubiquitin-Independent Manner. *Molecular Cell* 51, 573-583.

Peng, S., Geng, J., Sun, R., Tian, Z., Wei, H., 2009. Polyinosinic-polycytidylic acid liposome induces human hepatoma cells apoptosis which correlates to the up-regulation of RIG-I like receptors. *Cancer Science* 100, 529-536.

Perrin-Cocon, L., Vidalain, P.-O., Jacquemin, C., Aublin-Gex, A., Olmstead, K., Panthu, B., Rautureau, G.J.P., André, P., Nyczka, P., Hütt, M.-T., Amoedo, N., Rossignol, R., Filipp, F.V., Lotteau, V., Diaz, O., 2021. A hexokinase isoenzyme switch in human liver cancer cells promotes lipogenesis and enhances innate immunity. *Commun Biol* 4, 1-15.

Perveen, S., Yazdi, A.K., Hajian, T., Li, F., Vedadi, M., 2024. Kinetic characterization of human mRNA guanine-N7 methyltransferase. *Sci Rep* 14, 4509.

Picard-Jean, F., Brand, C., Tremblay-Létourneau, M., Allaire, A., Beaudoin, M.C., Boudreault, S., Duval, C., Rainville-Sirois, J., Robert, F., Pelletier, J., Geiss, B.J., Bisailon, M., 2018. 2'-O-methylation of the mRNA cap protects RNAs from decapping and degradation by DXO. *PLoS One* 13, e0193804.

Piccirillo, C., Khanna, R., Kiledjian, M., 2003. Functional characterization of the mammalian mRNA decapping enzyme hDcp2. *RNA* 9, 1138-1147.

Pichlmair, A., Lassnig, C., Eberle, C.-A., Góna, M.W., Baumann, C.L., Burkard, T.R., Bürckstümmer, T., Stefanovic, A., Krieger, S., Bennett, K.L., Rüllicke, T., Weber, F., Colinge, J., Müller, M., Superti-Furga, G., 2011. IFIT1 is an antiviral protein that recognizes 5'-triphosphate RNA. *Nat Immunol* 12, 624-630.

Piehler, J., Thomas, C., Garcia, K.C., Schreiber, G., 2012. Structural and dynamic determinants of type I interferon receptor assembly and their functional interpretation. *Immunological Reviews* 250, 317-334.

Pine, R., 1992. Constitutive expression of an ISGF2/IRF1 transgene leads to interferon-independent activation of interferon-inducible genes and resistance to virus infection. *J Virol* 66, 4470-4478.

Pinna, L.A., Meggio, F., 1997. Protein kinase CK2 ("casein kinase-2") and its implication in cell division and proliferation. *Prog Cell Cycle Res* 3, 77-97.

Platanias, L.C., 2005. Mechanisms of type-I- and type-II-interferon-mediated signalling. *Nat Rev Immunol* 5, 375-386.

Portela, A., Jones, L.D., Nuttall, P., 1992. Identification of viral structural polypeptides of Thogoto virus (a tick-borne orthomyxo-like virus) and functions associated with the glycoprotein. *Journal of General Virology* 73, 2823-2830.

Posternak, V., Ung, M.H., Cheng, C., Cole, M.D., 2017. MYC Mediates mRNA Cap Methylation of Canonical Wnt/ β -Catenin Signaling Transcripts By Recruiting CDK7 and RNA Methyltransferase. *Mol Cancer Res* 15, 213-224.

Provost, E., Yamamoto, Y., Lizardi, I., Stern, J., D'Aquila, T.G., Gaynor, R.B., Rimm, D.L., 2003. Functional Correlates of Mutations in β -Catenin Exon 3 Phosphorylation Sites *. *Journal of Biological Chemistry* 278, 31781-31789.

Pujol, C., Bratic-Hench, I., Sumakovic, M., Hench, J., Mourier, A., Baumann, L., Pavlenko, V., Trifunovic, A., 2013. Succinate Dehydrogenase Upregulation Destabilize Complex I and Limits the Lifespan of gas-1 Mutant. *PLoS One* 8, e59493.

Ramanathan, A., Robb, G.B., Chan, S.-H., 2016. mRNA capping: biological functions and applications. *Nucleic Acids Res* 44, 7511-7526.

Rasmussen, E.B., Lis, J.T., 1993. In vivo transcriptional pausing and cap formation on three *Drosophila* heat shock genes. *Proceedings of the National Academy of Sciences* 90, 7923-7927.

Ray, D., Shah, A., Tilgner, M., Guo, Y., Zhao, Y., Dong, H., Deas, T.S., Zhou, Y., Li, H., Shi, P.-Y., 2006. West Nile Virus 5'-Cap Structure Is Formed by Sequential Guanine N-7 and Ribose 2'-O Methylations by Nonstructural Protein 5. *Journal of Virology* 80, 8362-8370.

Raychoudhuri, A., Shrivastava, S., Steele, R., Kim, H., Ray, R., Ray, R.B., 2011. ISG56 and IFITM1 Proteins Inhibit Hepatitis C Virus Replication. *Journal of Virology* 85, 12881-12889.

Rehwinkel, J., Gack, M.U., 2020. RIG-I-like receptors: their regulation and roles in RNA sensing. *Nat Rev Immunol* 20, 537-551.

Rehwinkel, J., Tan, C.P., Goubau, D., Schulz, O., Pichlmair, A., Bier, K., Robb, N., Vreede, F., Barclay, W., Fodor, E., Sousa, C.R. e, 2010. RIG-I Detects Viral Genomic RNA during Negative-Strand RNA Virus Infection. *Cell* 140, 397-408.

Reich, S., Guilligay, D., Pflug, A., Malet, H., Berger, I., Crépin, T., Hart, D., Lunardi, T., Nanao, M., Ruigrok, R.W.H., Cusack, S., 2014. Structural insight into cap-snatching and RNA synthesis by influenza polymerase. *Nature* 516, 361-366.

Reinisch, K.M., Nibert, M.L., Harrison, S.C., 2000. Structure of the reovirus core at 3.6 Å resolution. *Nature* 404, 960-967.

Rice, G.I., del Toro Duany, Y., Jenkinson, E.M., Forte, G.M., Anderson, B.H., Ariaudo, G., Bader-Meunier, B., Baildam, E.M., Battini, R., Beresford, M.W., Casarano, M., Chouchane, M., Cimaz, R., Collins, A.E., Cordeiro, N.J., Dale, R.C., Davidson, J.E., De Waele, L., Desguerre, I., Faivre, L., Fazzi, E., Isidor, B., Lagae, L., Latchman, A.R., Lebon, P., Li, C., Livingston, J.H., Lourenço, C.M., Mancardi, M.M., Masurel-Paulet, A., McInnes, I.B., Menezes, M.P., Mignot, C., O'Sullivan, J., Orcesi, S., Picco, P.P., Riva, E., Robinson, R.A., Rodriguez, D., Salvatici, E., Scott, C., Szybowska, M., Tolmie, J.L., Vanderver, A., Vanhulle, C., Vieira, J.P., Webb, K., Whitney, R.N., Williams, S.G., Wolfe, L.A., Zuberi, S.M., Hur, S., Crow, Y.J., 2014. Gain-of-function mutations in IFIH1 cause a spectrum of human disease phenotypes associated with upregulated type I interferon signaling. *Nat Genet* 46, 503-509.

Ringelhan, M., Pfister, D., O'Connor, T., Pikarsky, E., Heikenwalder, M., 2018. The immunology of hepatocellular carcinoma. *Nat Immunol* 19, 222-232.

Roach, P.J., 1991. Multisite and hierarchal protein phosphorylation. *Journal of Biological Chemistry* 266, 14139-14142.

Rodriguez, K.R., Bruns, A.M., Horvath, C.M., 2014. MDA5 and LGP2: Accomplices and Antagonists of Antiviral Signal Transduction. *J Virol* 88, 8194-8200.

Ross, J.S., Ali, S.M., Fasan, O., Block, J., Pal, S., Elvin, J.A., Schrock, A.B., Suh, J., Nozad, S., Kim, S., Jeong Lee, H., Sheehan, C.E., Jones, D.M., Vergilio, J.-A., Ramkissoon, S., Severson, E., Daniel, S., Fabrizio, D., Frampton, G., Miller, V.A., Stephens, P.J., Gay, L.M., 2017. ALK Fusions in a Wide Variety of Tumor Types Respond to Anti-ALK Targeted Therapy. *Oncologist* 22, 1444-1450.

Rothenfusser, S., Goutagny, N., DiPerna, G., Gong, M., Monks, B.G., Schoenemeyer, A., Yamamoto, M., Akira, S., Fitzgerald, K.A., 2005. The RNA helicase Lgp2 inhibits TLR-independent sensing of viral replication by retinoic acid-inducible gene-I. *J Immunol* 175, 5260-5268.

Rubach, J.K., Wasik, B.R., Rupp, J.C., Kuhn, R.J., Hardy, R.W., Smith, J.L., 2009. Characterization of purified Sindbis virus nsP4 RNA-dependent RNA polymerase activity in vitro. *Virology* 384, 201-208.

Rumgay, H., Arnold, M., Ferlay, J., Lesi, O., Cabasag, C.J., Vignat, J., Laversanne, M., McGlynn, K.A., Soerjomataram, I., 2022. Global burden of primary liver cancer in 2020 and predictions to 2040. *Journal of Hepatology* 77, 1598-1606.

Runge, S., Sparrer, K.M.J., Lässig, C., Hembach, K., Baum, A., García-Sastre, A., Söding, J., Conzelmann, K.-K., Hopfner, K.-P., 2014. In Vivo Ligands of MDA5 and RIG-I in Measles Virus-Infected Cells. *PLoS Pathog* 10, e1004081.

Sacco, F., Perfetto, L., Castagnoli, L., Cesareni, G., 2012. The human phosphatase interactome: An intricate family portrait. *FEBS Lett* 586, 2732-2739.

Saeedi, B.J., Geiss, B.J., 2013. Regulation of Flavivirus RNA Synthesis and Capping. *Wiley Interdiscip Rev RNA* 4, 723-735.

Sager, R., 1997. Expression genetics in cancer: Shifting the focus from DNA to RNA. *Proc Natl Acad Sci U S A* 94, 952-955.

Saguez, C., Schmid, M., Olesen, J.R., Ghazy, M.A.E.-H., Qu, X., Poulsen, M.B., Nasser, T., Moore, C., Jensen, T.H., 2008. Nuclear mRNA Surveillance in THO/sub2 Mutants Is Triggered by Inefficient Polyadenylation. *Molecular Cell* 31, 91-103.

Saito, T., Hirai, R., Loo, Y.-M., Owen, D., Johnson, C.L., Sinha, S.C., Akira, S., Fujita, T., Gale, M., 2007. Regulation of innate antiviral defenses through a shared repressor domain in RIG-I and LGP2. *Proc Natl Acad Sci U S A* 104, 582-587.

Santagata, S., Mendillo, M.L., Tang, Y., Subramanian, A., Perley, C.C., Roche, S.P., Wong, B., Narayan, R., Kwon, H., Koeva, M., Amon, A., Golub, T.R., Porco, J.A., Whitesell, L., Lindquist, S., 2013. Tight coordination of protein translation and HSF1 activation supports the anabolic malignant state. *Science* 341, 1238303.

Satoh, T., Kato, H., Kumagai, Y., Yoneyama, M., Sato, S., Matsushita, K., Tsujimura, T., Fujita, T., Akira, S., Takeuchi, O., 2010. LGP2 is a positive regulator of RIG-I- and MDA5-mediated antiviral responses. *Proceedings of the National Academy of Sciences* 107, 1512-1517.

Schaeffer, L., Roy, R., Humbert, S., Moncollin, V., Vermeulen, W., Hoeijmakers, J.H.J., Chambon, P., Egly, J.-M., 1993. DNA Repair Helicase: a Component of BTF2 (TFIIH) Basic Transcription Factor. *Science* 260, 58-63.

Schaub, F.X., Dhankani, V., Berger, A.C., Trivedi, M., Richardson, A.B., Shaw, R., Zhao, W., Zhang, X., Ventura, A., Liu, Y., Ayer, D.E., Hurlin, P.J., Cherniack, A.D., 2018. Pan-cancer Alterations of the MYC Oncogene and Its Proximal Network across the Cancer Genome Atlas. *cells* 6, 282-300.e2.

Scheffler, I.E., 2015. Mitochondrial disease associated with complex I (NADH-CoQ oxidoreductase) deficiency. *Journal of Inherited Metabolic Disease* 38, 405-415.

Schindler, C., Levy, D.E., Decker, T., 2007. JAK-STAT Signaling: From Interferons to Cytokines. *Journal of Biological Chemistry* 282, 20059-20063.

Schlaeger, C., Longerich, T., Schiller, C., Bewerunge, P., Mehrabi, A., Toedt, G., Kleeff, J., Ehemann, V., Eils, R., Lichter, P., Schirmacher, P., Radlwimmer, B., 2008. Etiology-dependent molecular mechanisms in human hepatocarcinogenesis. *Hepatology* 47, 511-520.

Schlee, M., Roth, A., Hornung, V., Hagmann, C.A., Wimmenauer, V., Barchet, W., Coch, C., Janke, M., Mihailovic, A., Wardle, G., Juranek, S., Kato, H., Kawai, T., Poeck, H., Fitzgerald, K.A., Takeuchi, O., Akira, S., Tuschl, T., Latz, E., Ludwig, J., Hartmann, G., 2009. Recognition of 5' triphosphate by RIG-I helicase requires short blunt double-stranded RNA as contained in panhandle of negative-strand virus. *Immunity* 31, 25-34.

Schneider, W.M., Chevillotte, M.D., Rice, C.M., 2014. Interferon-Stimulated Genes: A Complex Web of Host Defenses. *Annu Rev Immunol* 32, 513-545.

Schnierle, B.S., Gershon, P.D., Moss, B., 1992. Cap-specific mRNA (nucleoside-O^{2'}-)-methyltransferase and poly(A) polymerase stimulatory activities of vaccinia virus are mediated by a single protein. *Proc Natl Acad Sci U S A* 89, 2897-2901.

Schoggins, J.W., Rice, C.M., 2011. Interferon-stimulated genes and their antiviral effector functions. *Curr Opin Virol* 1, 519-525.

Schoggins, J.W., Wilson, S.J., Panis, M., Murphy, M.Y., Jones, C.T., Bieniasz, P., Rice, C.M., 2011. A diverse range of gene products are effectors of the type I interferon antiviral response. *Nature* 472, 481-485.

Schuberth-Wagner, C., Ludwig, J., Bruder, A.K., Herzner, A.-M., Zillinger, T., Goldeck, M., Schmidt, T., Schmid-Burgk, J.L., Kerber, R., Wolter, S., Stümpel, J.-P., Roth, A., Bartok, E., Drosten, C., Coch, C., Hornung, V., Barchet, W., Kümmerer, B.M., Hartmann, G., Schlee, M., 2015. A Conserved Histidine in the

RNA Sensor RIG-I Controls Immune Tolerance to N1-2'O-Methylated Self RNA. *Immunity* 43, 41-51.

Schul, W., Groenhout, B., Koberna, K., Takagaki, Y., Jenny, A., Manders, E.M., Raska, I., van Driel, R., de Jong, L., 1996. The RNA 3' cleavage factors CstF 64 kDa and CPSF 100 kDa are concentrated in nuclear domains closely associated with coiled bodies and newly synthesized RNA. *EMBO J* 15, 2883-2892.

Schulze, K., Imbeaud, S., Letouzé, E., Alexandrov, L.B., Calderaro, J., Rebouissou, S., Couchy, G., Meiller, C., Shinde, J., Soysouvanh, F., Calatayud, A.-L., Pinyol, R., Pelletier, L., Balabaud, C., Laurent, A., Blanc, J.-F., Mazzaferro, V., Calvo, F., Villanueva, A., Nault, J.-C., Bioulac-Sage, P., Stratton, M.R., Llovet, J.M., Zucman-Rossi, J., 2015. Exome sequencing of hepatocellular carcinomas identifies new mutational signatures and potential therapeutic targets. *Nat Genet* 47, 505-511.

Sekine, S., Kanamaru, Y., Koike, M., Nishihara, A., Okada, M., Kinoshita, H., Kamiyama, M., Maruyama, J., Uchiyama, Y., Ishihara, N., Takeda, K., Ichijo, H., 2012. Rhomboid Protease PARL Mediates the Mitochondrial Membrane Potential Loss-induced Cleavage of PGAM5*. *Journal of Biological Chemistry* 287, 34635-34645.

Seldin, D.C., Leder, P., 1995. Casein Kinase II α Transgene-Induced Murine Lymphoma: Relation to Theileriosis in Cattle. *Science* 267, 894-897.

Semlow, D.R., Blanco, M.R., Walter, N.G., Staley, J.P., 2016. Spliceosomal DEAH-Box ATPases Remodel Pre-mRNA to Activate Alternative Splice Sites. *Cell* 164, 985-998.

Sestero, C.M., McGuire, D.J., De Sarno, P., Brantley, E.C., Soldevila, G., Axtell, R.C., Raman, C., 2012. CD5-dependent CK2 activation pathway regulates threshold for T cell energy. *J Immunol* 189, 2918-2930.

Seth, R.B., Sun, L., Ea, C.-K., Chen, Z.J., 2005. Identification and Characterization of MAVS, a Mitochondrial Antiviral Signaling Protein that Activates NF- κ B and IRF3. *Cell* 122, 669-682.

Shatkin, A.J., 1976. Capping of eucaryotic mRNAs. *Cell* 9, 645-653.

Shay, J.W., Wright, W.E., 2019. Telomeres and telomerase: three decades of progress. *Nat Rev Genet* 20, 299-309.

Shemesh, M., Lochte, S., Piehler, J., Schreiber, G., 2021. IFNAR1 and IFNAR2 play distinct roles in initiating type I interferon-induced JAK-STAT signaling and activating STATs. *Science Signaling* 14, eabe4627.

Sheth, U., Parker, R., 2003. Decapping and decay of messenger RNA occur in cytoplasmic processing bodies. *Science* 300, 805-808.

Shi, H.-X., Yang, K., Liu, X., Liu, X.-Y., Wei, B., Shan, Y.-F., Zhu, L.-H., Wang, C., 2010. Positive regulation of interferon regulatory factor 3 activation by Herc5 via ISG15 modification. *Mol Cell Biol* 30, 2424-2436.

Shopland, L.S., Hirayoshi, K., Fernandes, M., Lis, J.T., 1995. HSF access to heat shock elements in vivo depends critically on promoter architecture defined by GAGA factor, TFIID, and RNA polymerase II binding sites. *Genes Dev* 9, 2756-2769.

Shtutman, M., Zhurinsky, J., Simcha, I., Albanese, C., D'Amico, M., Pestell, R., Ben-Ze'ev, A., 1999. The cyclin D1 gene is a target of the β -catenin/LEF-1 pathway. *Proc Natl Acad Sci U S A* 96, 5522-5527.

Shuman, S., 1995. Capping Enzyme in Eukaryotic mRNA Synthesis¹, in: Cohn, W.E., Moldave, K. (Eds.), *Progress in Nucleic Acid Research and Molecular Biology*. Academic Press, pp. 101-129.

- Sigal, S.H., Gupta, S., Gebhard, D.F., Holst, P., Neufeld, D., Reid, L.M., 1995. Evidence for a terminal differentiation process in the rat liver. *Differentiation* 59, 35-42.
- Sikora, D., Rocheleau, L., Brown, E.G., Pelchat, M., 2017. Influenza A virus cap-snatches host RNAs based on their abundance early after infection. *Virology* 509, 167-177.
- Sikorski, P.J., Warminski, M., Kubacka, D., Ratajczak, T., Nowis, D., Kowalska, J., Jemielity, J., 2020. The identity and methylation status of the first transcribed nucleotide in eukaryotic mRNA 5' cap modulates protein expression in living cells. *Nucleic Acids Res* 48, 1607-1626.
- Silverman, E.J., Maeda, A., Wei, J., Smith, P., Beggs, J.D., Lin, R.-J., 2004. Interaction between a G-Patch Protein and a Spliceosomal DEXD/H-Box ATPase That Is Critical for Splicing. *Mol Cell Biol* 24, 10101-10110.
- Simabuco, F.M., Pavan, I.C.B., Pestana, N.F., Carvalho, P.C., Basei, F.L., Campos Granato, D., Paes Leme, A.F., Zanchin, N.I.T., 2019. Interactome analysis of the human Cap-specific mRNA (nucleoside-2'-O-)-methyltransferase 1 (hMTTr1) protein. *Journal of Cellular Biochemistry* 120, 5597-5611.
- Singal, A.G., Kanwal, F., Llovet, J.M., 2023. Global trends in hepatocellular carcinoma epidemiology: implications for screening, prevention and therapy. *Nat Rev Clin Oncol* 20, 864-884.
- Singer, Z.S., Ambrose, P.M., Danino, T., Rice, C.M., 2021. Quantitative measurements of early alphaviral replication dynamics in single cells reveals the basis for superinfection exclusion. *Cell Systems* 12, 210-219.e3.
<https://doi.org/10.1016/j.cels.2020.12.005>
- Smietanski, M., Werner, M., Purta, E., Kaminska, K.H., Stepinski, J., Darzynkiewicz, E., Nowotny, M., Bujnicki, J.M., 2014. Structural analysis of human

2'-O-ribose methyltransferases involved in mRNA cap structure formation. *Nat Commun* 5, 3004.

Sousa, M.M., Steen, K.W., Hagen, L., Slupphaug, G., 2011. Antibody cross-linking and target elution protocols used for immunoprecipitation significantly modulate signal-to noise ratio in downstream 2D-PAGE analysis. *Proteome Science* 9, 45.

Spangler, L., Wang, X., Conaway, J.W., Conaway, R.C., Dvir, A., 2001. TFIIF action in transcription initiation and promoter escape requires distinct regions of downstream promoter DNA. *Proceedings of the National Academy of Sciences* 98, 5544-5549.

Stamos, J.L., Weis, W.I., 2013. The B-Catenin Destruction Complex. *Cold Spring Harb Perspect Biol* 5, a007898.

Standart, N., Weil, D., 2018. P-Bodies: Cytosolic Droplets for Coordinated mRNA Storage. *Trends in Genetics* 34, 612-626.
<https://doi.org/10.1016/j.tig.2018.05.005>

Stoecklin, G., Mayo, T., Anderson, P., 2006. ARE-mRNA degradation requires the 5'-3' decay pathway. *EMBO Rep* 7, 72-77.

Su, A.I., Pezacki, J.P., Wodicka, L., Brideau, A.D., Supekova, L., Thimme, R., Wieland, S., Bukh, J., Purcell, R.H., Schultz, P.G., Chisari, F.V., 2002. Genomic analysis of the host response to hepatitis C virus infection. *Proceedings of the National Academy of Sciences* 99, 15669-15674.

Sugo, M., Kimura, H., Arasaki, K., Amemiya, T., Hirota, N., Dohmae, N., Imai, Y., Inoshita, T., Shiba-Fukushima, K., Hattori, N., Cheng, J., Fujimoto, T., Wakana, Y., Inoue, H., Tagaya, M., 2018. Syntaxin 17 regulates the localization and function of PGAM5 in mitochondrial division and mitophagy. *The EMBO Journal* 37, e98899.

Sun, Q., Huang, M., Wei, Y., 2021. Diversity of the reaction mechanisms of SAM-dependent enzymes. *Acta Pharm Sin B* 11, 632-650.

Tahara, S.M., Morgan, M.A., Shatkin, A.J., 1981. Two forms of purified m7G-cap binding protein with different effects on capped mRNA translation in extracts of uninfected and poliovirus-infected HeLa cells. *Journal of Biological Chemistry* 256, 7691-7694.

Takeda, K., Komuro, Y., Hayakawa, T., Oguchi, H., Ishida, Y., Murakami, S., Noguchi, T., Kinoshita, H., Sekine, Y., Iemura, S., Natsume, T., Ichijo, H., 2009. Mitochondrial phosphoglycerate mutase 5 uses alternate catalytic activity as a protein serine/threonine phosphatase to activate ASK1. *Proc Natl Acad Sci U S A* 106, 12301-12305.

Takeuchi, K., Choi, Y.L., Togashi, Y., Soda, M., Hatano, S., Inamura, K., Takada, S., Ueno, T., Yamashita, Y., Satoh, Y., Okumura, S., Nakagawa, K., Ishikawa, Y., Mano, H., 2009. KIF5B-ALK, a Novel Fusion Oncokinase Identified by an Immunohistochemistry-based Diagnostic System for ALK-positive Lung Cancer. *Clinical Cancer Research* 15, 3143-3149.

Tao, X., Zuo, Q., Ruan, H., Wang, H., Jin, H., Cheng, Z., Lv, Y., Qin, W., Wang, C., 2019. Argininosuccinate synthase 1 suppresses cancer cell invasion by inhibiting STAT3 pathway in hepatocellular carcinoma. *ABBS* 51, 263-276.

Tarasenko, T.N., Gomez-Rodriguez, J., McGuire, P.J., 2015. Impaired T cell function in argininosuccinate synthetase deficiency. *J Leukoc Biol* 97, 273-278.

Taylor, S.L., Krempel, R.L., Schmaljohn, C.S., 2009. Inhibition of TNF- α -induced Activation of NF- κ B by Hantavirus Nucleocapsid Proteins. *Annals of the New York Academy of Sciences* 1171, E86-E93.

Teixeira, D., Sheth, U., Valencia-Sanchez, M.A., Brengues, M., Parker, R., 2005. Processing bodies require RNA for assembly and contain nontranslating mRNAs. *RNA* 11, 371-382.

Tenen, D.G., Chai, L., Tan, J.L., 2020. Metabolic alterations and vulnerabilities in hepatocellular carcinoma. *Gastroenterol Rep (Oxf)* 9, 1-13.

Teng, Y.-W., Mehedint, M.G., Garrow, T.A., Zeisel, S.H., 2011. Deletion of Betaine-Homocysteine S-Methyltransferase in Mice Perturbs Choline and 1-Carbon Metabolism, Resulting in Fatty Liver and Hepatocellular Carcinomas. *J Biol Chem* 286, 36258-36267.

Teixeira, D., Sheth, U., Valencia-Sanchez, M.A., Brengues, M., Parker, R., 2005. Processing bodies require RNA for assembly and contain nontranslating mRNAs. *RNA* 11, 371-382.

Tharun, S., He, W., Mayes, A.E., Lennertz, P., Beggs, J.D., Parker, R., 2000. Yeast Sm-like proteins function in mRNA decapping and decay. *Nature* 404, 515-518.

Toczydlowska-Socha, D., Zielinska, M.M., Kurkowska, M., Astha, null, Almeida, C.F., Stefaniak, F., Purta, E., Bujnicki, J.M., 2018. Human RNA cap1 methyltransferase CMTr1 cooperates with RNA helicase DHX15 to modify RNAs with highly structured 5' termini. *Philosophical Transactions of the Royal Society B: Biological Sciences* 373, 20180161.

Totoki, Y., Tatsuno, K., Covington, K.R., Ueda, H., Creighton, C.J., Kato, M., Tsuji, S., Donehower, L.A., Slagle, B.L., Nakamura, H., Yamamoto, S., Shinbrot, E., Hama, N., Lehmkuhl, M., Hosoda, F., Arai, Y., Walker, K., Dahdouli, M., Gotoh, K., Nagae, G., Gingras, M.-C., Muzny, D.M., Ojima, H., Shimada, K., Midorikawa, Y., Goss, J.A., Cotton, R., Hayashi, A., Shibahara, J., Ishikawa, S., Guiteau, J., Tanaka, M., Urushidate, T., Ohashi, S., Okada, N., Doddapaneni, H., Wang, M., Zhu, Y., Dinh, H., Okusaka, T., Kokudo, N., Kosuge, T., Takayama, T., Fukayama, M., Gibbs, R.A., Wheeler, D.A., Aburatani, H., Shibata, T., 2014. Trans-ancestry mutational landscape of hepatocellular carcinoma genomes. *Nat Genet* 46, 1267-1273.

Tran, E.J., Zhou, Y., Corbett, A.H., Wentz, S.R., 2007. The DEAD-Box Protein Dbp5 Controls mRNA Export by Triggering Specific RNA:Protein Remodeling Events. *Molecular Cell* 28, 850-859.

Tran, V., Ledwith, M.P., Thamamongood, T., Higgins, C.A., Tripathi, S., Chang, M.W., Benner, C., Garcia-Sastre, A., Schwemmle, M., Boon, A.C.M., Diamond, M.S., Mehle, A., 2020. Influenza virus repurposes the antiviral protein IFIT2 to promote translation of viral mRNAs. *Nat Microbiol* 5, 1490-1503.

Triantafylou, K., Vakakis, E., Kar, S., Richer, E., Evans, G.L., Triantafylou, M., 2012. Visualisation of direct interaction of MDA5 and the dsRNA replicative intermediate form of positive strand RNA viruses. *Journal of Cell Science* 125, 4761-4769.

Tripathy, A., Thakurela, S., Sahu, M.K., Uthanasingh, K., Behera, M., Ajay, A.K., Kumari, R., 2018. The molecular connection of histopathological heterogeneity in hepatocellular carcinoma: A role of Wnt and Hedgehog signaling pathways. *PLOS ONE* 13, e0208194.

Tsukamoto, Y., Hiono, T., Yamada, S., Matsuno, K., Faist, A., Claff, T., Hou, J., Namasivayam, V., vom Hemdt, A., Sugimoto, S., Ng, J.Y., Christensen, M.H., Tesfamariam, Y.M., Wolter, S., Juranek, S., Zillinger, T., Bauer, S., Hirokawa, T., Schmidt, F.I., Kochs, G., Shimojima, M., Huang, Y.-S., Pichlmair, A., Kümmerer, B.M., Sakoda, Y., Schlee, M., Brunotte, L., Müller, C.E., Igarashi, M., Kato, H., 2023. Inhibition of cellular RNA methyltransferase abrogates influenza virus capping and replication. *Science* 379, 586-591.

Tyanova, S., Temu, T., Sinitcyn, P., Carlson, A., Hein, M.Y., Geiger, T., Mann, M., Cox, J., 2016. The Perseus computational platform for comprehensive analysis of (prote)omics data. *Nat Methods* 13, 731-740.

Uchida, N., Hoshino, S., Katada, T., 2004. Identification of a Human Cytoplasmic Poly(A) Nuclease Complex Stimulated by Poly(A)-binding Protein*. *Journal of Biological Chemistry* 279, 1383-1391.

Ünlü, B., Türsen, Ü., Rajabi, Z., Jabalameli, N., Rajabi, F., 2022. The Immunogenetics of Systemic Sclerosis, in: Rezaei, N., Rajabi, F. (Eds.), *The Immunogenetics of Dermatologic Diseases*. Springer International Publishing, Cham, pp. 259-298.

Unterholzner, L., Izaurralde, E., 2004. SMG7 Acts as a Molecular Link between mRNA Surveillance and mRNA Decay. *Molecular Cell* 16, 587-596.

Urushibara, T., Furuichi, Y., Nishimura, C., Miura, K., 1975. A modified structure at the 5'-terminus of mRNA of vaccinia virus. *FEBS Letters* 49, 385-389.

Vaca, C.E., Fang, J.-L., Schweda, E.K.H., 1995. Studies of the reaction of acetaldehyde with deoxynucleosides. *Chemico-Biological Interactions* 98, 51-67.

Valean, S., Acalovschi, M., Dumitrascu, D.L., Ciobanu, L., Nagy, G., Chira, R., 2019. Hepatocellular carcinoma in patients with autoimmune hepatitis - a systematic review of the literature published between 1989-2016. *Med Pharm Rep* 92, 99-105.

Vanauberg, D., Schulz, C., Lefebvre, T., 2023. Involvement of the pro-oncogenic enzyme fatty acid synthase in the hallmarks of cancer: a promising target in anti-cancer therapies. *Oncogenesis* 12, 1-10.

Van Dijk, E., Cougot, N., Meyer, S., Babajko, S., Wahle, E., Séraphin, B., 2002. Human Dcp2: a catalytically active mRNA decapping enzyme located in specific cytoplasmic structures. *EMBO J* 21, 6915-6924.

Van Riggelen, J., Yetil, A., Felsher, D.W., 2010. MYC as a regulator of ribosome biogenesis and protein synthesis. *Nat Rev Cancer* 10, 301-309.

Varshney, D., Petit, A.-P., Bueren-Calabuig, J.A., Jansen, C., Fletcher, D.A., Peggie, M., Weidlich, S., Scullion, P., Pisljakov, A.V., Cowling, V.H., 2016. Molecular basis of RNA guanine-7 methyltransferase (RNMT) activation by RAM. *Nucleic Acids Research* 44, 10423-10436.

Vasiljeva, L., Merits, A., Auvinen, P., Kääriäinen, L., 2000. Identification of a novel function of the alphavirus capping apparatus. RNA 5'-triphosphatase activity of Nsp2. *J Biol Chem* 275, 17281-17287. H

Venook, A.P., Papandreou, C., Furuse, J., de Guevara, L.L., 2010. The incidence and epidemiology of hepatocellular carcinoma: a global and regional perspective. *Oncologist* 15 Suppl 4, 5-13.

Verdecia, M.A., Bowman, M.E., Lu, K.P., Hunter, T., Noel, J.P., 2000. Structural basis for phosphoserine-proline recognition by group IV WW domains. *Nat Struct Biol* 7, 639-643.

Verhelst, J., Parthoens, E., Schepens, B., Fiers, W., Saelens, X., 2012. Interferon-Inducible Protein Mx1 Inhibits Influenza Virus by Interfering with Functional Viral Ribonucleoprotein Complex Assembly. *J Virol* 86, 13445-13455.

Verma, M., Charles, R.C.M., Chakrapani, B., Coumar, M.S., Govindaraju, G., Rajavelu, A., Chavali, S., Dhayalan, A., 2017. PRMT7 Interacts with ASS1 and Citrullinemia Mutations Disrupt the Interaction. *Journal of Molecular Biology* 429, 2278-2289.

Verzella, D., Pescatore, A., Capece, D., Vecchiotti, D., Ursini, M.V., Franzoso, G., Alesse, E., Zazzeroni, F., 2020. Life, death, and autophagy in cancer: NF- κ B turns up everywhere. *Cell Death Dis* 11, 1-14.

Videla, L.A., Tapia, G., Rodrigo, R., Pettinelli, P., Haim, D., Santibañez, C., Araya, A.V., Smok, G., Csendes, A., Gutierrez, L., Rojas, J., Castillo, J., Korn, O.,

Maluenda, F., Díaz, J.C., Rencoret, G., Poniachik, J., 2009. Liver NF-kappaB and AP-1 DNA binding in obese patients. *Obesity* (Silver Spring)

Villanueva, A., 2019. Hepatocellular Carcinoma. *New England Journal of Medicine* 380, 1450-1462.

Villar, V.H., Allega, M.F., Deshmukh, R., Ackermann, T., Nakasone, M.A., Vande Voorde, J., Drake, T.M., Oetjen, J., Bloom, A., Nixon, C., Müller, M., May, S., Tan, E.H., Vereecke, L., Jans, M., Blancke, G., Murphy, D.J., Huang, D.T., Lewis, D.Y., Bird, T.G., Sansom, O.J., Blyth, K., Sumpton, D., Tardito, S., 2023. Hepatic glutamine synthetase controls N5-methylglutamine in homeostasis and cancer. *Nat Chem Biol* 19, 292-300.

Wang, D.J., Ratnam, N.M., Byrd, J.C., Guttridge, D.C., 2014. NF- κ B Functions in Tumor Initiation by Suppressing the Surveillance of Both Innate and Adaptive Immune Cells. *Cell Rep* 9, 90-103.

Wang, J., Alvin Chew, B.L., Lai, Y., Dong, H., Xu, L., Balamkundu, S., Cai, W.M., Cui, L., Liu, C.F., Fu, X.-Y., Lin, Z., Shi, P.-Y., Lu, T.K., Luo, D., Jaffrey, S.R., Dedon, P.C., 2019. Quantifying the RNA cap epitranscriptome reveals novel caps in cellular and viral RNA. *Nucleic Acids Res* 47, e130.

Wang, M., Liu, Y., Cheng, Y., Wei, Y., Wei, X., 2019. Immune checkpoint blockade and its combination therapy with small-molecule inhibitors for cancer treatment. *Biochimica et Biophysica Acta (BBA) - Reviews on Cancer* 1871, 199-224.

Wang, T., Ma, F., Qian, H., 2021. Defueling the cancer: ATP synthase as an emerging target in cancer therapy. *Mol Ther Oncolytics* 23, 82-95.

Wang, Y., Liu, J., Huang, B., Xu, Y.-M., Li, J., Huang, L.-F., Lin, J., Zhang, J., Min, Q.-H., Yang, W.-M., Wang, X.-Z., 2015. Mechanism of alternative splicing and its regulation. *Biomedical Reports* 3, 152-158.

Wang, Z., Jiang, H., Chen, S., Du, F., Wang, X., 2012. The Mitochondrial Phosphatase PGAM5 Functions at the Convergence Point of Multiple Necrotic Death Pathways. *Cell* 148, 228-243.

Weber, F., Haller, O., Kochs, G., 1996. Nucleoprotein viral RNA and mRNA of Thogoto virus: a novel "cap-stealing" mechanism in tick-borne orthomyxoviruses? *J Virol* 70, 8361-8367.

Wei, C.M., Gershowitz, A., Moss, B., 1975. Methylated nucleotides block 5' terminus of HeLa cell messenger RNA. *Cell* 4, 379-386.

Werner, M., Purta, E., Kaminska, K.H., Cymerman, I.A., Campbell, D.A., Mitra, B., Zamudio, J.R., Sturm, N.R., Jaworski, J., Bujnicki, J.M., 2011. 2'-O-ribose methylation of cap2 in human: function and evolution in a horizontally mobile family. *Nucleic Acids Res* 39, 4756-4768.

Whitaker-Menezes, D., Martinez-Outschoorn, U.E., Flomenberg, N., Birbe, R., Witkiewicz, A.K., Howell, A., Pavlides, S., Tsigos, A., Ertel, A., Pestell, R.G., Broda, P., Minetti, C., Lisanti, M.P., Sotgia, F., 2011. Hyperactivation of oxidative mitochondrial metabolism in epithelial cancer cells in situ: Visualizing the therapeutic effects of metformin in tumor tissue. *Cell Cycle* 10, 4047-4064.

Wilkins, J.M., McConnell, C., Tipton, P.A., Hannink, M., 2014. A Conserved Motif Mediates both Multimer Formation and Allosteric Activation of Phosphoglycerate Mutase 5 *. *Journal of Biological Chemistry* 289, 25137-25148.

Wilkinson, M.E., Charenton, C., Nagai, K., 2020. RNA Splicing by the Spliceosome. *Annu. Rev. Biochem.* 89, 359-388.

Williams, G.D., Gokhale, N.S., Snider, D.L., Horner, S.M., 2020. The mRNA Cap 2'-O-Methyltransferase CMTR1 Regulates the Expression of Certain Interferon-Stimulated Genes. *mSphere* 5, e00202-20.

Wolter, S., Hennig, T., Wallerath, C., Schlee-Guimaraes, T.M., Kirchhoff, A., Urban, C., Piras, A., Stukalov, A., Juranek, S., Engelke, M., Boehm, V., Gehring, N.H., Hartmann, G., Pichlmair, A., Friedel, C.C., Dölken, L., Schlee, M., 2023. mRNA N1-2'O-methylation by CMTR1 affects NVL2 mRNA splicing (PrePrint).

Wong, R.J., Gish, R., Frederick, T., Bzowej, N., Frenette, C., 2011. Development of Hepatocellular Carcinoma in Autoimmune Hepatitis Patients: A Case Series. *Dig Dis Sci* 56, 578-585.

Wu, B., Peisley, A., Richards, C., Yao, H., Zeng, X., Lin, C., Chu, F., Walz, T., Hur, S., 2013. Structural basis for dsRNA recognition, filament formation, and antiviral signal activation by MDA5. *Cell* 152, 276-289.

Wu, J., Sun, L., Chen, X., Du, F., Shi, H., Chen, C., Chen, Z.J., 2013. Cyclic GMP-AMP Is an Endogenous Second Messenger in Innate Immune Signaling by Cytosolic DNA. *Science* 339, 826-830.

Wu, L., Zheng, J., Chen, P., Liu, Q., Yuan, Y., 2017. Small nucleolar RNA ACA11 promotes proliferation, migration and invasion in hepatocellular carcinoma by targeting the PI3K/AKT signaling pathway. *Biomed Pharmacother* 90, 705-712.

Wu, M., Assassi, S., 2013. The Role of Type 1 Interferon in Systemic Sclerosis. *Front. Immunol.* 4.

Wurm, J.P., Sprangers, R., 2019. Dcp2: an mRNA decapping enzyme that adopts many different shapes and forms. *Curr Opin Struct Biol* 59, 115-123.

Xie, L., Wartchow, C., Shia, S., Uehara, K., Steffek, M., Warne, R., Sutton, J., Muiru, G.T., Leonard, V.H.J., Bussiere, D.E., Ma, X., 2016. Molecular Basis of mRNA Cap Recognition by Influenza B Polymerase PB2 Subunit. *J Biol Chem* 291, 363-370.

- Xie, Y., Ren, Y., 2019. Mechanisms of nuclear mRNA export: a structural perspective. *Traffic* 20, 829-840.
- Xu, W., Jing, L., Wang, Q., Lin, C.-C., Chen, X., Diao, J., Liu, Y., Sun, X., 2015. Bax-PGAM5L-Drp1 complex is required for intrinsic apoptosis execution. *Oncotarget* 6, 30017-30034.
- Xu, Y., Song, Q., Pascal, L.E., Zhong, M., Zhou, Y., Zhou, J., Deng, F.-M., Huang, J., Wang, Z., 2019. DHX15 is up-regulated in castration-resistant prostate cancer and required for androgen receptor sensitivity to low DHT concentrations. *Prostate* 79, 657-666.
- Xue, L., Chang, T., Li, Z., Wang, C., Zhao, H., Li, M., Tang, P., Wen, X., Yu, M., Wu, J., Bao, X., Wang, X., Gong, P., He, J., Chen, X., Xiong, X., 2024. Cryo-EM structures of Thogoto virus polymerase reveal unique RNA transcription and replication mechanisms among orthomyxoviruses. *Nat Commun* 15, 4620.
- Yamaguchi, A., Ishikawa, H., Furuoka, M., Yokozeki, M., Matsuda, N., Tanimura, S., Takeda, K., 2019. Cleaved PGAM5 is released from mitochondria depending on proteasome-mediated rupture of the outer mitochondrial membrane during mitophagy. *The Journal of Biochemistry* 165, 19-25.
- Yamaguchi, Y., Takagi, T., Wada, T., Yano, K., Furuya, A., Sugimoto, S., Hasegawa, J., Handa, H., 1999. NELF, a Multisubunit Complex Containing RD, Cooperates with DSIF to Repress RNA Polymerase II Elongation. *Cell* 97, 41-51.
- Yamashita, R., Suzuki, Y., Takeuchi, N., Wakaguri, H., Ueda, T., Sugano, S., Nakai, K., 2008. Comprehensive detection of human terminal oligo-pyrimidine (TOP) genes and analysis of their characteristics. *Nucleic Acids Research* 36, 3707-3715.
- Yan, B., Wang, H., Rabbani, Z.N., Zhao, Y., Li, W., Yuan, Y., Li, F., Dewhirst, M.W., Li, C.-Y., 2006. Tumor necrosis factor-alpha is a potent endogenous mutagen that promotes cellular transformation. *Cancer Res* 66, 11565-11570.

Yang, H.-B., Xu, Y.-Y., Zhao, X.-N., Zou, S.-W., Zhang, Y., Zhang, M., Li, J.-T., Ren, F., Wang, L.-Y., Lei, Q.-Y., 2015. Acetylation of MAT II α represses tumour cell growth and is decreased in human hepatocellular cancer. *Nat Commun* 6, 6973.

Yang, S., Zheng, L., Li, L., Zhang, J., Wang, J., Zhao, H., Chen, Y., Liu, X., Gan, H., Chen, J., Yan, M., He, C., Li, K., Ding, C., Li, Y., 2024. Integrative multiomics analysis identifies molecular subtypes and potential targets of hepatocellular carcinoma. *Clinical and Translational Medicine* 14, e1727.

Yoneyama, M., Kikuchi, M., Matsumoto, K., Imaizumi, T., Miyagishi, M., Taira, K., Foy, E., Loo, Y.-M., Gale, M., Jr, Akira, S., Yonehara, S., Kato, A., Fujita, T., 2005. Shared and Unique Functions of the DExD/H-Box Helicases RIG-I, MDA5, and LGP2 in Antiviral Innate Immunity¹. *The Journal of Immunology* 175, 2851-2858.

Yoneyama, M., Kikuchi, M., Natsukawa, T., Shinobu, N., Imaizumi, T., Miyagishi, M., Taira, K., Akira, S., Fujita, T., 2004. The RNA helicase RIG-I has an essential function in double-stranded RNA-induced innate antiviral responses. *Nat Immunol* 5, 730-737.

You, A. -bin, Yang, H., Lai, C., Lei, W., Yang, L., Lin, J., Liu, S., Ding, N., Ye, F., 2023. CMTR1 promotes colorectal cancer cell growth and immune evasion by transcriptionally regulating STAT3. *Cell Death Dis* 14, 1-11.

Yu, B., Ma, J., Li, J., Wang, D., Wang, Z., Wang, S., 2020. Mitochondrial phosphatase PGAM5 modulates cellular senescence by regulating mitochondrial dynamics. *Nat Commun* 11, 2549.

Yu, L.-X., Ling, Y., Wang, H.-Y., 2018. Role of nonresolving inflammation in hepatocellular carcinoma development and progression. *npj Precision Onc* 2, 1-10.

Yu, Y., Zielinska, M., Li, W., Bernkopf, D.B., Heilingloh, C.S., Neurath, M.F., Becker, C., 2020. PGAM5-MAVS interaction regulates TBK1/ IRF3 dependent antiviral responses. *Sci Rep* 10, 8323.

Zeb, A., Choubey, V., Gupta, R., Kuum, M., Safiulina, D., Vaarmann, A., Gogichaishvili, N., Liiv, M., Ilves, I., Tämm, K., Veksler, V., Kaasik, A., 2021. A novel role of KEAP1/PGAM5 complex: ROS sensor for inducing mitophagy. *Redox Biol* 48, 102186.

Zehir, A., Benayed, R., Shah, R.H., Syed, A., Middha, S., Kim, H.R., Srinivasan, P., Gao, J., Chakravarty, D., Devlin, S.M., Hellmann, M.D., Barron, D.A., Schram, A.M., Hameed, M., Dogan, S., Ross, D.S., Hechtman, J.F., DeLair, D.F., Yao, J., Mandelker, D.L., Cheng, D.T., Chandramohan, R., Mohanty, A.S., Ptashkin, R.N., Jayakumaran, G., Prasad, M., Syed, M.H., Rema, A.B., Liu, Z.Y., Nafa, K., Borsu, L., Sadowska, J., Casanova, J., Bacares, R., Kiecka, I.J., Razumova, A., Son, J.B., Stewart, L., Baldi, T., Mullaney, K.A., Al-Ahmadie, H., Vakiani, E., Abeshouse, A.A., Penson, A.V., Jonsson, P., Camacho, N., Chang, M.T., Won, H.H., Gross, B.E., Kundra, R., Heins, Z.J., Chen, H.-W., Phillips, S., Zhang, H., Wang, J., Ochoa, A., Wills, J., Eubank, M., Thomas, S.B., Gardos, S.M., Reales, D.N., Galle, J., Durany, R., Cambria, R., Abida, W., Cercek, A., Feldman, D.R., Gounder, M.M., Hakimi, A.A., Harding, J.J., Iyer, G., Janjigian, Y.Y., Jordan, E.J., Kelly, C.M., Lowery, M.A., Morris, L.G.T., Omuro, A.M., Raj, N., Razavi, P., Shoushtari, A.N., Shukla, N., Soumerai, T.E., Varghese, A.M., Yaeger, R., Coleman, J., Bochner, B., Riely, G.J., Saltz, L.B., Scher, H.I., Sabbatini, P.J., Robson, M.E., Klimstra, D.S., Taylor, B.S., Baselga, J., Schultz, N., Hyman, D.M., Arcila, M.E., Solit, D.B., Ladanyi, M., Berger, M.F., 2017. Mutational landscape of metastatic cancer revealed from prospective clinical sequencing of 10,000 patients. *Nat Med* 23, 703-713.

Zhao, M., Ying, L., Wang, R., Yao, J., Zhu, L., Zheng, M., Chen, Z., Yang, Z., 2021. DHX15 Inhibits Autophagy and the Proliferation of Hepatoma Cells. *Front. Med.* 7.

Zhao, S., Jiang, J., Jing, Y., Liu, W., Yang, X., Hou, X., Gao, L., Wei, L., 2020. The concentration of tumor necrosis factor- α determines its protective or damaging effect on liver injury by regulating Yap activity. *Cell Death Dis* 11, 1-13.

Zheng, J., Yong, H.Y., Panutdaporn, N., Liu, C., Tang, K., Luo, D., 2015. High-resolution HDX-MS reveals distinct mechanisms of RNA recognition and activation by RIG-I and MDA5. *Nucleic Acids Research* 43, 1216-1230.

Zhou, M., Deng, L., Kashanchi, F., Brady, J.N., Shatkin, A.J., Kumar, A., 2003. The Tat/TAR-dependent phosphorylation of RNA polymerase II C-terminal domain stimulates cotranscriptional capping of HIV-1 mRNA. *Proc Natl Acad Sci U S A* 100, 12666-12671.

Zhuang, M., Guan, S., Wang, H., Burlingame, A.L., Wells, J.A., 2013. Substrates of IAP Ubiquitin Ligases Identified with a Designed Orthogonal E3 Ligase, the NEDDylator. *Molecular Cell* 49, 273-282.

Züst, R., Cervantes-Barragan, L., Habjan, M., Maier, R., Neuman, B.W., Ziebuhr, J., Szretter, K.J., Baker, S.C., Barchet, W., Diamond, M.S., Siddell, S.G., Ludewig, B., Thiel, V., 2011. Ribose 2'-O-methylation provides a molecular signature for the distinction of self and non-self mRNA dependent on the RNA sensor Mda5. *Nat Immunol* 12, 137-143.